

**REACTIVITY OF ANODICALLY-GENERATED  
METHOXYSTILBENE CATION RADICALS: THE EFFECT  
OF ORTHO'-SUBSTITUTION**

**CHONG KAM WENG**

**FACULTY OF SCIENCE  
UNIVERSITY OF MALAYA  
KUALA LUMPUR**

**2019**

**REACTIVITY OF ANODICALLY-GENERATED  
METHOXYSTILBENE CATION RADICALS: THE  
EFFECT OF ORTHO'-SUBSTITUTION**

**CHONG KAM WENG**

**THESIS SUBMITTED IN FULFILMENT OF THE  
REQUIREMENTS FOR THE DEGREE OF DOCTOR OF  
PHILOSOPHY**

**DEPARTMENT OF CHEMISTRY  
FACULTY OF SCIENCE  
UNIVERSITY OF MALAYA  
KUALA LUMPUR**

**2019**

**UNIVERSITY OF MALAYA**  
**ORIGINAL LITERARY WORK DECLARATION**

Name of Candidate: **CHONG KAM WENG**

Matric No: **SHC140109**

Name of Degree: **DOCTOR OF PHILOSOPHY**

Title of Project Paper/Research Report/Dissertation/Thesis ("this Work"):

**REACTIVITY OF ANODICALLY-GENERATED METHOXYSTILBENE  
CATION RADICALS: THE EFFECT OF ORTHO'-SUBSTITUTION**

Field of Study:

**ORGANIC CHEMISTRY**

I do solemnly and sincerely declare that:

- (1) I am the sole author/writer of this Work;
- (2) This Work is original;
- (3) Any use of any work in which copyright exists was done by way of fair dealing and for permitted purposes and any excerpt or extract from, or reference to or reproduction of any copyright work has been disclosed expressly and sufficiently and the title of the Work and its authorship have been acknowledged in this Work;
- (4) I do not have any actual knowledge nor do I ought reasonably to know that the making of this work constitutes an infringement of any copyright work;
- (5) I hereby assign all and every rights in the copyright to this Work to the University of Malaya ("UM"), who henceforth shall be owner of the copyright in this Work and that any reproduction or use in any form or by any means whatsoever is prohibited without the written consent of UM having been first had and obtained;
- (6) I am fully aware that if in the course of making this Work I have infringed any copyright whether intentionally or otherwise, I may be subject to legal action or any other action as may be determined by UM.

Candidate's Signature

Date:

Subscribed and solemnly declared before,

Witness's Signature

Date:

Name:

Designation:

**REACTIVITY OF ANODICALLY-GENERATED METHOXYSTILBENE  
CATION RADICALS: THE EFFECT OF ORTHO'-SUBSTITUTION**

**ABSTRACT**

A systematic study was undertaken to determine the influence of ortho'-substituted nucleophilic (OH, NH<sub>2</sub>, CH<sub>2</sub>OH, CH<sub>2</sub>NHR, CO<sub>2</sub>H, CH=CH<sub>2</sub>) and non-nucleophilic (OMe, OAc, CN, NO<sub>2</sub>, CF<sub>3</sub>, CO<sub>2</sub>Me, CONH<sub>2</sub>, CHO) groups on the reactivity of anodically generated 4-methoxy- and 3,4-dimethoxystilbene cation radicals. The results showed that when ortho'-substituted nucleophilic groups such as OH or NHR are directly attached to the aromatic ring, both direct and crossover intramolecular cation-nucleophile reactions occur to give bisbenzofurans/bisindoles or fused bisbenzopyrans/bisquinolines, respectively. When the ortho'-substituted side chains have been extended to include an intervening CH<sub>2</sub> group (-CH<sub>2</sub>OH, -CH<sub>2</sub>NHR), only direct intramolecular cation-nucleophile reactions occur to give bisbenzopyrans or bisisoquinolines. Crossover products (previously obtained when the ortho' substituents were OH and NH<sub>2</sub>) such as the fused benzoxepanes/fused benzoazepanes were not formed. When the ortho' substituents are CO<sub>2</sub>H and vinyl groups, direct intramolecular cation-nucleophile reaction occur to give the corresponding bis- $\delta$ -lactones and bisdihydronaphthalene, respectively. An unusual doubly-bridged, dibenzofused cyclononane derivative is also obtained in the oxidation of the ortho'-vinyl-substituted stilbene. When the ortho' substituents are non-nucleophilic groups such as OMe, OAc, CN, NO<sub>2</sub>, CF<sub>3</sub>, or CO<sub>2</sub>Me, the products are the tetraaryltetrahydrofurans and dehydrotetralin derivatives. In the case of an ortho'-amide substituent, the major products are the tetraaryltetrahydrofurans, accompanied by a minor product incorporating an isocoumarin moiety. When the ortho' substituent is a formyl group, the products include fused indanylnaphthalenes, indanylbenzopyran aldehydes, and indenyl

benzaldehyde. Where an additional 3-methoxy substituent is present, additional products are formed as a result of competing aromatic substitution/Friedel Crafts reactions. Mechanistic rationalization for the formation of the various products is presented and discussed.

**Keywords:** anodic oxidation, methoxystilbene cation radicals, effect of ortho'-substitution.

University of Malaya

## KEREAKTIFAN KATION RADIKAL METOKSISTILBEN HASILAN

### PENGOKSIDAAN ANODIK: KESAN PENGGANTIAN-ORTHO'

#### ABSTRAK

Suatu kajian terperinci telah dijakankan untuk menentu kesan penggantian-ortho' atas kereaktifan kation radikal 4-metoksi dan 3,4-dimetoksistilben yang dihasilkan melalui pengoksidaan anodik. Kumpulan pengganti-ortho' termasuk kumpulan nukleofilik seperti OH, NH<sub>2</sub>, CH<sub>2</sub>OH, CH<sub>2</sub>NH<sub>2</sub>, CO<sub>2</sub>H, CH=CH<sub>2</sub>, dan kumpulan bukan nukleofilik seperti OMe, OAc, CN, NO<sub>2</sub>, CF<sub>3</sub>, CO<sub>2</sub>Me, CONH<sub>2</sub>, CHO. Keputusan yang didapati menunjukkan bahawa apabila penggantian ortho' adalah kumpulan nukleofilik seperti OH atau NHR yang terikat secara terus pada gelang aromatik, hasil yang didapati adalah daripada tindak balas kation-nukleofil intramolekul secara terus (bisbenzofuran/bisindol) serta daripada tindak balas kation-nukleofil intramolekul secara bersilang (bisbenzopyran/bisquinolin). Apabila rantai sisi dipanjangkan dengan memasuki suatu kumpulan perantara seperti metilen (-CH<sub>2</sub>OH, -CH<sub>2</sub>NHR), cuma produk yang terdiri daripada tindak balas kation-nukleofil intramolekul secara terus (bisbenzopyran/bisisoquinolin) terdapat, produk daripada tindak balas kation-nukleofil intramolekul secara bersilang (bisbenzoxepan/benzoazepan) tidak dikesankan. Apabila pengganti ortho' adalah kumpulan CO<sub>2</sub>H, hasil yang terdapat adalah bis- $\delta$ -lakton yang merupakan produk daripada tindak balas kation-nukleofil intramolekul secara terus. Begitu juga bagi pengganti ortho' vinil, dimana hasil adalah bisdihidronaftalena daripada tindak balas kation-nukleofil intramolekul secara terus. Bagi kes ini, satu hasil tambahan, iaitu, cyclononan yang berstruktur kompleks dan luar biasa, juga diperolehi. Produk pengoksidaan bagi penggantian ortho' bukan nukleofilik seperti OMe, OAc, CN, NO<sub>2</sub>, CF<sub>3</sub>, CO<sub>2</sub>Me, terdiri daripada tetraariltetrahidrofuran dan dehidrotetralin. Apabila kumpulan penggantian ortho' adalah kumpulan formil, hasil pengoksidaan adalah

indanilnaftalena, indanilbenzopyran aldehyd, dan indenil benzaldehyd. Bagi kes dimana kumpulan metoksi tambahan hadir di kedudukan meta, hasilan terdiri daripada tindak balas penukargantian aromatik/tindak balas Fridel-Crafts yang bersaing dengan tindak balas kation-nukleofil intramolekul. Mekanisme-mekanisme bagi pembentukan produk-produk bagi semua tindak balas dibentangkan dan dibincangkan.

**Kata kunci:** pengoksidaan anodik, kation radikal metoksisilben, kesan penggantian-ortho'

University of Malaya

## ACKNOWLEDGEMENTS

First and foremost, I would like to express my sincere gratitude to my research supervisors Professor Dr. Kam Toh Seok and Dr. Low Yun Yee for their valuable and constructive suggestions during the planning and execution of this research work. I would like to express my very great appreciation to Professor Kam who gave me the golden opportunity to work on this wonderful yet challenging project. His willingness to give of his time so generously throughout my study and research is very much appreciated. His motivation, patience, and immense knowledge helped me throughout the research as well as during the preparation of this thesis. I could not have imagined having a better advisor and mentor for my Ph. D. research. I would also like to express my special thanks to Dr. Low for his continuous support and guidance. I learnt many new skills and techniques from him. Without both their assistance and dedicated involvement, this project could not have been successfully accomplished and for this, I am really thankful to them both.

My sincere thanks also go to Professor Dr. Noel F. Thomas for his enthusiastic encouragement, insightful comments, and useful critique of this research work.

I would also like to extend my thanks to my former and present colleagues in lab C100 including, Siew Huah, Choy Eng, Fong Jiao, Suet Pick, Joanne, Kuan Hon, Chew Yan, Jun Lee, Dawn, Augustus, Zoe Yi, Jia Yin, and Mr. Siew, for their unwavering personal and professional support during the time I spent in the lab.

Most important, none of this could have happened without my family and friends who gave me encouragement and emotional support throughout my study. Getting through my thesis required more than professional academic support. I have many, many people to thank for their support and tolerance over these past few years. I cannot begin to express my gratitude and appreciation for their friendship. This thesis stands as a testament of their unconditional love and encouragement.

## TABLE OF CONTENTS

Abstract .....	iii
Abstrak .....	v
Acknowledgements .....	vii
Table of Contents .....	viii
List of Figures .....	xii
List of Tables.....	xv
List of Schemes .....	xvi
List of Symbols and Abbreviations.....	xx
List of Appendices .....	xxiv
<b>CHAPTER 1: INTRODUCTION.....</b>	<b>1</b>
1.1 General .....	1
1.2 Some Basic Principles of Electroorganic Synthesis.....	5
1.3 Apparatus and Conditions for Electrochemical Studies.....	10
1.4 A Brief Survey of Electrochemically-Mediated Transformations in Organic Chemistry .....	15
1.5 Electrochemical Oxidation of Stilbenes (1,2-Diarylalkenes) – Anodically- Generated Stilbene Cation Radicals.....	25
1.6 Objective of Present Study .....	32
<b>CHAPTER 2: RESULTS AND DISCUSSION .....</b>	<b>33</b>
2.1 Synthesis of Stilbenes .....	33
2.2 Anodic Oxidation of 4-Methoxy- and 3,4-Dimethoxystilbenes Substituted with 2'-Hydroxy and 2'-Amino Groups .....	41

2.3	Anodic Oxidation of 4-Methoxy- and 3,4-Dimethoxystilbenes Substituted with 2'-Hydoxymethyl, 2'-Aminomethyl, 2'-Carboxylic Acid, and 2'-Vinyl Groups.....	66
2.4	Anodic Oxidation of 4-Methoxy- and 3,4-Dimethoxystilbenes where the Ortho'-Substituents are Non-Nucleophilic Groups .....	94
2.5	Conclusion .....	109
<b>CHAPTER 3: EXPERIMENTAL .....</b>		<b>114</b>
3.1	General .....	114
3.2	Single Crystal X-ray Diffraction Analysis.....	114
3.3	Computational Methods .....	115
3.4	Chromatographic Methods.....	115
3.4.1	Normal Phase Chromatography .....	115
3.4.2	High Performance Liquid Chromatography .....	116
3.4.3	Gel Permeation Chromatography.....	116
3.5	Microwave Irradiation Experiments .....	119
3.6	Synthesis of Stilbenes .....	119
3.7	Cyclic Voltammetry .....	141
3.8	General Procedures for Electrochemical Oxidation (Controlled Potential Electrolysis).....	141
3.8.1	Anodic oxidation of <b>1</b> in MeCN/ 0.2 M LiClO <sub>4</sub> .....	142
3.8.2	Anodic oxidation of <b>2</b> in MeCN/ 0.2 M LiClO <sub>4</sub> .....	145
3.8.3	Anodic oxidation of <b>3</b> in MeCN/ 0.2 M LiClO <sub>4</sub> .....	145
3.8.4	Anodic oxidation of <b>4</b> in MeCN/ 0.2 M LiClO <sub>4</sub> .....	148
3.8.5	Anodic oxidation of <b>7</b> in MeCN/ 0.2 M LiClO <sub>4</sub> .....	148
3.8.6	Anodic oxidation of <b>8</b> in MeCN/ 0.2 M LiClO <sub>4</sub> .....	149

3.8.7	Anodic oxidation of <b>9</b> in MeCN/ 0.2 M LiClO <sub>4</sub> .....	151
3.8.8	Anodic oxidation of <b>10</b> in MeCN/ 0.2 M LiClO <sub>4</sub> .....	152
3.8.9	Anodic oxidation of <b>11</b> in MeCN/ 0.2 M LiClO <sub>4</sub> .....	154
3.8.10	Anodic oxidation of <b>12</b> in MeCN/ 0.2 M LiClO <sub>4</sub> .....	156
3.8.11	Anodic oxidation of <b>13</b> in MeCN/ 0.2 M LiClO <sub>4</sub> .....	158
3.8.12	Anodic oxidation of <b>14</b> in MeCN/ 0.2 M LiClO <sub>4</sub> .....	160
3.8.13	Anodic oxidation of <b>15</b> in MeCN/ 0.2 M LiClO <sub>4</sub> .....	162
3.8.14	Anodic oxidation of <b>16</b> in MeCN/ 0.2 M LiClO <sub>4</sub> .....	164
3.8.15	Anodic oxidation of <b>17</b> in MeCN/ 0.2 M LiClO <sub>4</sub> .....	165
3.8.16	Anodic oxidation of <b>18</b> in MeCN/ 0.2 M LiClO <sub>4</sub> .....	165
3.8.17	Anodic oxidation of <b>19</b> in MeCN/ 0.2 M LiClO <sub>4</sub> .....	168
3.8.18	Anodic oxidation of <b>20</b> in MeCN/ 0.2 M LiClO <sub>4</sub> .....	168
3.8.19	Anodic oxidation of <b>21</b> in MeCN/ 0.2 M LiClO <sub>4</sub> .....	172
3.8.20	Anodic oxidation of <b>22</b> in MeCN/ 0.2 M LiClO <sub>4</sub> .....	173
3.8.21	Anodic oxidation of <b>23</b> in MeCN/ 0.2 M LiClO <sub>4</sub> .....	175
3.8.22	Anodic oxidation of <b>24</b> in MeCN/ 0.2 M LiClO <sub>4</sub> .....	176
3.8.23	Anodic oxidation of <b>25, 26, and 27</b> in MeCN/ 0.2 M LiClO <sub>4</sub> .....	177
3.8.24	Anodic oxidation of <b>28</b> in MeCN/ 0.2 M LiClO <sub>4</sub> .....	177
3.8.25	Anodic oxidation of <b>29</b> in MeCN/ 0.2 M LiClO <sub>4</sub> .....	179
3.8.26	Anodic oxidation of <b>30</b> in MeCN/ 0.2 M LiClO <sub>4</sub> .....	182
3.8.27	Anodic oxidation of <b>31</b> in MeCN/ 0.2 M LiClO <sub>4</sub> .....	185
3.8.28	Anodic oxidation of <b>32</b> in MeCN/ 0.2 M LiClO <sub>4</sub> .....	186
3.8.29	Anodic oxidation of <b>33</b> in MeCN/ 0.2 M LiClO <sub>4</sub> .....	187
3.8.30	Anodic oxidation of <b>34</b> in MeCN/ 0.2 M LiClO <sub>4</sub> .....	189
3.8.31	Anodic oxidation of <b>35</b> in MeCN/ 0.2 M LiClO <sub>4</sub> .....	191
3.8.32	Anodic oxidation of <b>36</b> in MeCN/ 0.2 M LiClO <sub>4</sub> .....	192

3.8.33	Anodic oxidation of <b>37</b> in MeCN/ 0.2 M LiClO <sub>4</sub> .....	194
3.8.34	Anodic oxidation of <b>38</b> in MeCN/ 0.2 M LiClO <sub>4</sub> .....	196
3.8.35	Anodic oxidation of <b>39</b> in MeCN/ 0.2 M LiClO <sub>4</sub> .....	199
3.8.36	Anodic oxidation of <b>40</b> in MeCN/ 0.2 M LiClO <sub>4</sub> .....	200
3.8.37	Anodic oxidation of <b>41</b> in MeCN/ 0.2 M LiClO <sub>4</sub> .....	201
3.8.38	Anodic oxidation of <b>42</b> in MeCN/ 0.2 M LiClO <sub>4</sub> .....	204
3.8.39	Anodic oxidation of <b>43</b> in MeCN/ 0.2 M LiClO <sub>4</sub> .....	205
3.8.40	Anodic oxidation of <b>44</b> in MeCN/ 0.2 M LiClO <sub>4</sub> .....	206
3.8.41	Anodic oxidation of <b>45</b> in MeCN/ 0.2 M LiClO <sub>4</sub> .....	207
References .....		213
List of Publications and Papers Presented .....		225
Appendix .....		229

## LIST OF FIGURES

Figure 1.1:	Correlations of organic electrosynthesis to the 12 principles of green chemistry .....	3
Figure 1.2:	General principle of direct and indirect (mediated) electrolyses .....	6
Figure 1.3:	General principle of mediated redox .....	7
Figure 1.4:	<b>A:</b> undivided <b>B:</b> divided electrochemical cells .....	11
Figure 1.5:	Basic setup of three electrode system .....	12
Figure 1.6:	Effect of silicon and sulfur electroauxiliaries on the anodic potentials .....	18
Figure 1.7:	Stabilized cations generated for various electrosynthetic applications .....	19
Figure 1.8:	Reversal of polarity in enol ethers upon one-electron oxidation .....	21
Figure 2.1:	List of synthesized stilbenes <b>1–50</b> .....	34
Figure 2.2:	COSY and selected HMBCs of <b>1aa</b> and <b>1ac</b> , <sup>13</sup> C shifts of the α and β methine carbons of model benzopyran and benzofuran, and X-ray structures of <b>1aa</b> and <b>1ac</b> .....	44
Figure 2.3:	COSY, selected HMBCs, selected NOEs and X-ray crystal structure of <b>1ab</b> .....	44
Figure 2.4:	COSY, selected HMBCs, selected NOEs, and X-ray crystal structure of <b>1ae</b> .....	45
Figure 2.5:	Diastereomers of bisbenzofurans with formula C <sub>32</sub> H <sub>30</sub> O <sub>6</sub> .....	47
Figure 2.6:	Structures of <b>3ad</b> , <b>3ad'</b> , and X-ray crystal structure of <b>7ad</b> .....	47
Figure 2.7:	COSY, selected HMBCs, and selected NOEs of <b>3af</b> , and X-ray crystal structure of <b>14af</b> .....	49
Figure 2.8:	COSY, selected HMBCs of <b>8ac</b> and <b>8ag</b> , comparison of the <sup>13</sup> C shifts of the α and β methine carbons with model bisindole and quinolone and X-ray crystal structures of <b>10ac</b> and <b>8ag</b> .....	52
Figure 2.9:	X-ray crystal structures of <b>10ag</b> , <b>11ag</b> , and <b>13ag</b> .....	53

Figure 2.10:	Origin of the fused benzopyrans <b>1aa</b> , <b>1ab</b> , and bisbenzofuran <b>1ac</b> from the <i>threo</i> and <i>meso</i> dications .....	58
Figure 2.11:	COSY, selected HMBCs, and X-ray structure of <b>16ba</b> .....	67
Figure 2.12:	COSY, selected HMBCs, and selected NOEs of <b>16bd</b> .....	68
Figure 2.13:	COSY and selected HMBCs of <b>18be</b> , <b>18bf</b> , and <b>18bg</b> .....	72
Figure 2.14:	Selected NOEs of <b>18be</b> , <b>18bf</b> , and <b>18bg</b> .....	72
Figure 2.15:	COSY and selected HMBCs of <b>20be</b> , <b>20bh</b> , and <b>22bb</b> .....	75
Figure 2.16:	Selected NOEs of <b>20be</b> , <b>20bh</b> , and <b>22bb</b> .....	75
Figure 2.17:	X-ray structures of <b>20bi</b> and <b>22bi</b> .....	75
Figure 2.18:	X-ray structures of <b>28ba</b> , <b>28bb</b> , and <b>28bc</b> .....	76
Figure 2.19:	COSY and selected HMBCs of <b>30ba</b> .....	78
Figure 2.20:	COSY, selected HMBCs, and selected NOEs of <b>30bk</b> .....	80
Figure 2.21:	COSY, selected HMBCs, and selected NOEs of <b>31bp</b> .....	82
Figure 2.22:	COSY, selected HMBCs, and selected NOEs of <b>31bq</b> .....	82
Figure 2.23:	X-ray structures of <b>33bn</b> , <b>36bm</b> , <b>37ca</b> , and <b>38cd</b> .....	99
Figure 2.24:	COSY, selected HMBCs, selected NOEs, and X-ray crystal structure of <b>41ce</b> .....	102
Figure 2.25:	COSY, selected HMBCs, selected NOEs, and X-ray crystal structure of <b>41cf</b> .....	103
Figure 2.26:	Selected NOEs of <b>41cg</b> and <b>42cf</b> .....	103
Figure 2.27:	COSY, selected HMBCs, and selected NOEs of <b>43ch</b> .....	104
Figure 2.28:	COSY, selected HMBCs, and X-ray crystal structure of <b>44ci</b> .....	105
Figure 2.29:	Reactivity of anodically generated 4-methoxy and 3,4-dimethoxystilbene cation radicals: effect of ortho'-substituted OH and NHR groups.....	110
Figure 2.30:	Reactivity of anodically generated 4-methoxy and 3,4-dimethoxystilbene cation radicals: effect of ortho'-substituted CH <sub>2</sub> OH, CH <sub>2</sub> NHR, CO <sub>2</sub> H, and CH=CH <sub>2</sub> groups.....	111

Figure 2.31: Reactivity of anodically generated 4-methoxy and 3,4-dimethoxystilbene cation radicals: effect of ortho'-substituted CHO, CO<sub>2</sub>Me, CONHR, and other non-nucleophilic groups ..... 112

University of Malaya

## LIST OF TABLES

Table 1.1:	Important primary reactions in radical cation chemistry of $\pi$ -A-B <sup>+</sup> .....	9
Table 1.2:	Important primary reactions in radical anion chemistry of $\pi$ -A-B <sup>-</sup> .....	10
Table 1.3:	Approximate potential ranges of some solvent-electrolyte systems .....	14
Table 2.1:	Yield, melting point, and anodic half-peak potential of stilbenes (1-50).....	35

University of Malaya

## LIST OF SCHEMES

Scheme 1.1:	Kolbe electrolysis.....	1
Scheme 1.2:	Tafel Rearrangement.....	2
Scheme 1.3:	Simons fluorination.....	2
Scheme 1.4:	Monsanto adiponitrile process .....	2
Scheme 1.5:	Intermediate species formed during the anodic oxidation or cathodic reduction .....	5
Scheme 1.6:	Mediated selective deprotection of PMB ethers .....	8
Scheme 1.7:	Synthesis of $\alpha$ -onoceradiene and pentacyclosqualene.....	15
Scheme 1.8:	Synthesis of perhydroazulenes via mixed-Kolbe electrolysis.....	16
Scheme 1.9:	Synthesis of (-)-dihydropertusaric acid via mixed-Kolbe electrolysis.....	16
Scheme 1.10:	Mediated electrosynthesis of a key intermediate in the synthesis of daucene.....	17
Scheme 1.11:	Shono oxidation of alkyl amide in methanol .....	17
Scheme 1.12:	Shono oxidation of amides, carbamates, and cyanoamines .....	18
Scheme 1.13:	Regioselective methoxylation of silyl-substituted carbamates .....	18
Scheme 1.14:	The cation-pool method and various downstream functionalization .....	19
Scheme 1.15:	Oxidative cyclization between an alkene cation radical and an alcohol nucleophile .....	21
Scheme 1.16:	Anodic olefin coupling reaction as key steps in the syntheses of (-)-alliacol A, (+)-nemorensic acid, (-)-crobarbatic acid, and the arteannuin ring skeleton .....	22
Scheme 1.17:	Anodic olefin coupling reaction as the key step in the synthesis of (-)-heptemerone B and (-)-guanacastepene E.....	23
Scheme 1.18:	Anodic olefin coupling reactions as key steps in the syntheses of hamigeran and cyathin ring skeletons .....	24

Scheme 1.19: Total synthesis of dixiamycin via an electrochemical N,N-dimerization.....	24
Scheme 1.20: Products from anodic oxidation of 4,4'-dimethoxystilbene as reported by Steckhan and Ebersson.....	25
Scheme 1.21: Formation of tetraanisyltetrahydrofuran via cation radical electrophilic addition to native stilbene .....	27
Scheme 1.22: Formation of tetraanisyltetrahydrofuran via cation radical dimerization.....	27
Scheme 1.23: Formation of the dimethoxylated open-chain dimer.....	28
Scheme 1.24: Formation of the acetylated tetralin .....	28
Scheme 1.25: Products from anodic oxidation of 4,4'-dimethoxystilbene as reported by Hong.....	29
Scheme 1.26: Effect of aromatic substitution on the nature and distribution of the products.....	31
Scheme 2.1: Synthesis of stilbenes <b>1, 3, 5, 6, 8, 32, 34, 35, 36, 37, 38, 39, 41, 44, 46, 47, and 48</b> by Heck coupling.....	33
Scheme 2.2: Synthesis of stilbenes <b>2, 4, 33, and 40</b> from stilbenes <b>1 and 3</b> .....	36
Scheme 2.3: Synthesis of stilbenes <b>11, 13–19</b> from stilbenes <b>5 and 6</b> .....	37
Scheme 2.4: Synthesis of stilbenes <b>16–19, 28–29</b> from stilbenes <b>37 and 46</b> .....	38
Scheme 2.5: Synthesis of stilbenes <b>20–27, 49–50</b> from stilbenes <b>47 and 48</b> .....	39
Scheme 2.6: Synthesis of stilbenes <b>30–31, 42–43, and 45</b> from stilbenes <b>41 and 44</b> .....	40
Scheme 2.7: Products from the anodic oxidation of stilbenes <b>1 and 2</b> .....	42
Scheme 2.8: Products from the anodic oxidation of stilbenes <b>3 and 4</b> .....	42
Scheme 2.9: Products from the anodic oxidation of stilbenes <b>7–9</b> .....	50
Scheme 2.10: Products from the anodic oxidation of stilbenes <b>10 and 11</b> .....	54
Scheme 2.11: Products from the anodic oxidation of stilbenes <b>12 and 13</b> .....	54
Scheme 2.12: Products from the anodic oxidation of stilbenes <b>14 and 15</b> .....	55

Scheme 2.13: Proposed mechanism for the formation of products in the anodic oxidation of stilbenes ( <b>1</b> , <b>7–11</b> ) in MeCN/LiClO <sub>4</sub> .....	56
Scheme 2.14: Proposed mechanism for the formation of <b>1ae</b> in the anodic oxidation of <b>1</b> in MeCN/LiClO <sub>4</sub> .....	59
Scheme 2.15: Proposed mechanism for the formation of products in the anodic oxidation of stilbenes ( <b>3</b> , <b>12–15</b> ) in MeCN/LiClO <sub>4</sub> .....	61
Scheme 2.16: Pathway showing the formation of <b>3aa</b> and <b>3af</b> (or <b>14af</b> ) instead of <b>3ab</b> (or <b>14ag</b> ) and the <i>trans</i> -bridged oxocine/azocine.....	62
Scheme 2.17: Proposed mechanism for the formation of the rearranged monomeric indoles <b>10ah</b> , <b>13ah</b> and dihydroindole <b>12ai</b> .....	65
Scheme 2.18: Products from the anodic oxidation of stilbenes <b>16</b> and <b>17</b> .....	67
Scheme 2.19: Products from the anodic oxidation of stilbenes <b>18</b> and <b>19</b> .....	70
Scheme 2.20: Products from the anodic oxidation of stilbenes <b>20–27</b> .....	74
Scheme 2.21: Products from the anodic oxidation of stilbenes <b>28</b> and <b>29</b> .....	77
Scheme 2.22: Products from the anodic oxidation of stilbene <b>30</b> .....	77
Scheme 2.23: Products from the anodic oxidation of stilbene <b>31</b> .....	80
Scheme 2.24: Proposed mechanism for the formation of products in the anodic oxidation of stilbene <b>16</b> in MeCN/LiClO <sub>4</sub> .....	84
Scheme 2.25: Proposed mechanism for the formation of products in the anodic oxidation of stilbene <b>18</b> in MeCN/LiClO <sub>4</sub> .....	85
Scheme 2.26: Proposed mechanism for the formation of products in the anodic oxidation of stilbenes <b>20–23</b> and <b>25</b> in MeCN/LiClO <sub>4</sub> .....	88
Scheme 2.27: Proposed mechanism for the formation of products in the anodic oxidation of stilbenes <b>28–29</b> in MeCN/LiClO <sub>4</sub> .....	90
Scheme 2.28: Proposed mechanism for the formation of products in the anodic oxidation of stilbene <b>30</b> in MeCN/LiClO <sub>4</sub> .....	92
Scheme 2.29: Proposed mechanism for the formation of products in the anodic oxidation of stilbene <b>31</b> in MeCN/LiClO <sub>4</sub> .....	93
Scheme 2.30: Products from the anodic oxidation of stilbenes <b>32–40</b> .....	95

Scheme 2.31: Proposed mechanism for the formation of products in the anodic oxidation of stilbenes <b>32–37</b> in MeCN/LiClO <sub>4</sub> .....	97
Scheme 2.32: Proposed mechanism for the formation of products in the anodic oxidation of stilbene <b>38</b> in MeCN/LiClO <sub>4</sub> .....	98
Scheme 2.33: Products from the anodic oxidation of stilbenes <b>41–43</b> .....	100
Scheme 2.34: Products from the anodic oxidation of stilbenes <b>44–45</b> .....	100
Scheme 2.35: Proposed mechanism for the formation of products in the anodic oxidation of stilbenes <b>41–43</b> in MeCN/LiClO <sub>4</sub> .....	107
Scheme 2.36: Proposed mechanism for the formation of products in the anodic oxidation of stilbenes <b>44–45</b> in MeCN/LiClO <sub>4</sub> .....	109

University of Malaya

## LIST OF SYMBOLS AND ABBREVIATIONS

°C	:	Degree Celsius
μL	:	Microlitre
<sup>13</sup> C NMR	:	Carbon-13 nuclear magnetic resonance
<sup>1</sup> H NMR	:	Proton nuclear magnetic resonance
A	:	Ampere
Å	:	Angstrom
Ac	:	Acetyl
Ac <sub>2</sub> O	:	Acetic anhydride
AcOH	:	Acetic acid
Ag	:	Silver
AgNO <sub>3</sub>	:	Silver nitrate
AM1	:	Austin model 1
Ar	:	Aryl
B3LYP	:	Becke, three-parameter, Lee-Yang-Parr
Bn	:	Benzyl
Boc	:	tert-Butyloxycarbonyl
br	:	Broad
Bu	:	Butyl
CCDC	:	Cambridge crystallographic data centre
CDCl <sub>3</sub>	:	Deuterated chloroform
CH <sub>2</sub> Cl <sub>2</sub>	:	Dichloromethane
CHCl <sub>3</sub>	:	Chloroform
cm <sup>2</sup>	:	Square centimetre
cm <sup>-1</sup>	:	Wavenumber
COSY	:	Correlation spectroscopy
CPE	:	Constant potential electrolysis
d	:	Doublet
DART	:	Direct analysis in real time
dd	:	Doublet of doublets
ddd	:	Doublet of doublet of doublets
DFT	:	Density functional theory
DMF	:	Dimethylformamide
dt	:	Doublet of triplets

e	:	Electron
$E_p$	:	Peak potential
$E_{p/2}$	:	Half-peak potential
ESI	:	Electrospray ionization
Et	:	Ethyl
Et <sub>3</sub> N	:	Triethylamine
EtOAc	:	Ethyl acetate
EWG	:	Electron withdrawing group
F/mol	:	Faraday per mole
FT	:	Fourier transform
g	:	Gram
h	:	Hour
HMBC	:	Heteronuclear Multiple Bond Correlation
HMDS	:	Hexamethyldisilazane
HPLC	:	High performance liquid chromatography
HRMS	:	High resolution mass spectrometry
$h\nu$	:	Light
<i>i</i> -PrOH	:	Iso-propanol
IR	:	Infrared
$J$	:	Coupling constant
K	:	Kelvin
kg	:	Kilogram
LAH	:	Lithium aluminium hydride
LiClO <sub>4</sub>	:	Lithium perchlorate
<i>m</i>	:	Meta
M	:	Molarity
m	:	Multiplet
$m/z$	:	Mass-to-charge ration
mA	:	Miliampere
Me	:	Methyl
MeCN	:	Acetonitrile
med	:	Mediator
MeOH	:	Methanol
MHz	:	Megahertz
min	:	Minute

mL	:	Mililitre
mmol	:	Milimole
MS	:	Mass spectrometry
NaOAc	:	Sodium Acetate
NOE	:	Nuclear overhauser effect
NOESY	:	Nuclear overhauser effect spectroscopy
Ns	:	Nosyl
Nu	:	Nucleophile
<i>o</i>	:	Ortho
OH	:	Hydroxy
OMe	:	Methoxy
ox	:	Oxidation
<i>p</i>	:	Para
Pd( <i>t</i> -Bu <sub>3</sub> P) <sub>2</sub>	:	Bis(tri- <i>tert</i> -butylphosphine)palladium(0)
Pd <sub>2</sub> (dba) <sub>3</sub>	:	Tris(dibenzylideneacetone)dipalladium(0)
Ph	:	Phenyl
PMB	:	<i>p</i> -Methoxybenzyl
ppm	:	Parts per million
Pr	:	Propyl
Pt	:	Platinum
PTSA	:	<i>p</i> -Toluenesulfonic acid
red	:	Reduction
rt	:	Room temperature
RVC	:	Reticulated vitreous carbon
s	:	Singlet
SiMe <sub>3</sub>	:	Trimethylsilyl
t	:	Triplet
TBDPS	:	Tert-butyldiphenylsilyl
TBS	:	Tert-butyldimethylsilyl
td	:	Triplet of doublets
TEAP	:	Tetraethylammonium perchlorate
THF	:	Tetrahydrofuran
TLC	:	Thin layer chromatography
TMS	:	Tetramethylsilane
TOF	:	Time of flight

Ts	:	Tosyl
UV	:	Ultraviolet
V	:	Volt
V/s	:	Volt per second
$\alpha$	:	Alpha
$\beta$	:	Beta
$\delta$	:	Delta
$\varepsilon$	:	Epsilon
$\gamma$	:	Gamma
$\lambda$	:	Lambda

University of Malaya

## LIST OF APPENDICES

Figure A1:	$^1\text{H}$ NMR ( $\text{CDCl}_3$ , 400 MHz) spectrum of stilbene <b>1</b> .....	229
Figure A2:	$^1\text{H}$ NMR ( $\text{CDCl}_3$ , 400 MHz) spectrum of stilbene <b>2</b> .....	229
Figure A3:	$^1\text{H}$ NMR ( $\text{CDCl}_3$ , 400 MHz) spectrum of stilbene <b>3</b> .....	230
Figure A4:	$^1\text{H}$ NMR ( $\text{CDCl}_3$ , 400 MHz) spectrum of stilbene <b>4</b> .....	230
Figure A5:	$^1\text{H}$ NMR ( $\text{CDCl}_3$ , 400 MHz) spectrum of stilbene <b>5</b> .....	231
Figure A6:	$^1\text{H}$ NMR ( $\text{CDCl}_3$ , 400 MHz) spectrum of stilbene <b>6</b> .....	231
Figure A7:	$^1\text{H}$ NMR ( $\text{CDCl}_3$ , 400 MHz) spectrum of stilbene <b>7</b> .....	232
Figure A8:	$^1\text{H}$ NMR ( $\text{CDCl}_3$ , 400 MHz) spectrum of stilbene <b>8</b> .....	232
Figure A9:	$^1\text{H}$ NMR ( $\text{CDCl}_3$ , 400 MHz) spectrum of stilbene <b>9</b> .....	233
Figure A10:	$^1\text{H}$ NMR ( $\text{CDCl}_3$ , 400 MHz) spectrum of stilbene <b>10</b> .....	233
Figure A11:	$^1\text{H}$ NMR ( $\text{CDCl}_3$ , 400 MHz) spectrum of stilbene <b>11</b> .....	234
Figure A12:	$^1\text{H}$ NMR ( $\text{CDCl}_3$ , 400 MHz) spectrum of stilbene <b>12</b> .....	234
Figure A13:	$^1\text{H}$ NMR ( $\text{CDCl}_3$ , 400 MHz) spectrum of stilbene <b>13</b> .....	235
Figure A14:	$^1\text{H}$ NMR ( $\text{CDCl}_3$ , 400 MHz) spectrum of stilbene <b>14</b> .....	235
Figure A15:	$^1\text{H}$ NMR ( $\text{CDCl}_3$ , 400 MHz) spectrum of stilbene <b>15</b> .....	236
Figure A16:	$^1\text{H}$ NMR ( $\text{CDCl}_3$ , 400 MHz) spectrum of stilbene <b>16</b> .....	236
Figure A17:	$^1\text{H}$ NMR ( $\text{CDCl}_3$ , 400 MHz) spectrum of stilbene <b>17</b> .....	237
Figure A18:	$^1\text{H}$ NMR ( $\text{CDCl}_3$ , 400 MHz) spectrum of stilbene <b>18</b> .....	237
Figure A19:	$^1\text{H}$ NMR ( $\text{CDCl}_3$ , 400 MHz) spectrum of stilbene <b>19</b> .....	238
Figure A20:	$^1\text{H}$ NMR ( $\text{CDCl}_3$ , 400 MHz) spectrum of stilbene <b>20</b> .....	238
Figure A21:	$^1\text{H}$ NMR ( $\text{CDCl}_3$ , 400 MHz) spectrum of stilbene <b>21</b> .....	239
Figure A22:	$^1\text{H}$ NMR ( $\text{CDCl}_3$ , 400 MHz) spectrum of stilbene <b>22</b> .....	239
Figure A23:	$^1\text{H}$ NMR ( $\text{CDCl}_3$ , 400 MHz) spectrum of stilbene <b>23</b> .....	240

Figure A24:	<sup>1</sup> H NMR (CDCl <sub>3</sub> , 400 MHz) spectrum of stilbene <b>24</b> .....	240
Figure A25:	<sup>1</sup> H NMR (CDCl <sub>3</sub> , 400 MHz) spectrum of stilbene <b>25</b> .....	241
Figure A26:	<sup>1</sup> H NMR (CDCl <sub>3</sub> , 400 MHz) spectrum of stilbene <b>26</b> .....	241
Figure A27:	<sup>1</sup> H NMR (CDCl <sub>3</sub> , 400 MHz) spectrum of stilbene <b>27</b> .....	242
Figure A28:	<sup>1</sup> H NMR (CDCl <sub>3</sub> , 400 MHz) spectrum of stilbene <b>28</b> .....	242
Figure A29:	<sup>1</sup> H NMR (CDCl <sub>3</sub> , 400 MHz) spectrum of stilbene <b>29</b> .....	243
Figure A30:	<sup>1</sup> H NMR (CDCl <sub>3</sub> , 400 MHz) spectrum of stilbene <b>30</b> .....	243
Figure A31:	<sup>1</sup> H NMR (CDCl <sub>3</sub> , 400 MHz) spectrum of stilbene <b>31</b> .....	244
Figure A32:	<sup>1</sup> H NMR (CDCl <sub>3</sub> , 400 MHz) spectrum of stilbene <b>33</b> .....	244
Figure A33:	<sup>1</sup> H NMR (CDCl <sub>3</sub> , 400 MHz) spectrum of stilbene <b>34</b> .....	245
Figure A34:	<sup>1</sup> H NMR (CDCl <sub>3</sub> , 400 MHz) spectrum of stilbene <b>35</b> .....	245
Figure A35:	<sup>1</sup> H NMR (CDCl <sub>3</sub> , 400 MHz) spectrum of stilbene <b>36</b> .....	246
Figure A36:	<sup>1</sup> H NMR (CDCl <sub>3</sub> , 400 MHz) spectrum of stilbene <b>37</b> .....	246
Figure A37:	<sup>1</sup> H NMR (CDCl <sub>3</sub> , 400 MHz) spectrum of stilbene <b>38</b> .....	247
Figure A38:	<sup>1</sup> H NMR (CDCl <sub>3</sub> , 400 MHz) spectrum of stilbene <b>39</b> .....	247
Figure A39:	<sup>1</sup> H NMR (CDCl <sub>3</sub> , 400 MHz) spectrum of stilbene <b>40</b> .....	248
Figure A40:	<sup>1</sup> H NMR (CDCl <sub>3</sub> , 400 MHz) spectrum of stilbene <b>41</b> .....	248
Figure A41:	<sup>1</sup> H NMR (CDCl <sub>3</sub> , 400 MHz) spectrum of stilbene <b>42</b> .....	249
Figure A42:	<sup>1</sup> H NMR (CDCl <sub>3</sub> , 400 MHz) spectrum of stilbene <b>43</b> .....	249
Figure A43:	<sup>1</sup> H NMR (CDCl <sub>3</sub> , 400 MHz) spectrum of stilbene <b>44</b> .....	250
Figure A44:	<sup>1</sup> H NMR (CDCl <sub>3</sub> , 400 MHz) spectrum of stilbene <b>45</b> .....	250
Figure A45:	<sup>1</sup> H NMR (CDCl <sub>3</sub> , 400 MHz) spectrum of stilbene <b>46</b> .....	251
Figure A46:	<sup>1</sup> H NMR (CDCl <sub>3</sub> , 400 MHz) spectrum of stilbene <b>47</b> .....	251
Figure A47:	<sup>1</sup> H NMR (CDCl <sub>3</sub> , 400 MHz) spectrum of stilbene <b>48</b> .....	252

Figure A48:	$^1\text{H}$ NMR ( $\text{CDCl}_3$ , 400 MHz) spectrum of stilbene <b>49</b> .....	252
Figure A49:	$^1\text{H}$ NMR ( $\text{CDCl}_3$ , 400 MHz) spectrum of stilbene <b>50</b> .....	253
Figure A50:	$^1\text{H}$ NMR ( $\text{CDCl}_3$ , 400 MHz) spectrum of compound <b>1aa</b> .....	253
Figure A51:	$^1\text{H}$ NMR ( $\text{CDCl}_3$ , 400 MHz) spectrum of compound <b>1ab</b> .....	254
Figure A52:	$^1\text{H}$ NMR ( $\text{CDCl}_3$ , 400 MHz) spectrum of compound <b>1ac</b> .....	254
Figure A53:	$^1\text{H}$ NMR ( $\text{CDCl}_3$ , 400 MHz) spectrum of compound <b>1ae</b> .....	255
Figure A54:	$^1\text{H}$ NMR ( $\text{CDCl}_3$ , 400 MHz) spectrum of compound <b>3aa</b> .....	255
Figure A55:	$^1\text{H}$ NMR ( $\text{CDCl}_3$ , 400 MHz) spectrum of compound <b>3ac</b> .....	256
Figure A56:	$^1\text{H}$ NMR ( $\text{CDCl}_3$ , 400 MHz) spectrum of compound <b>3ad</b> .....	256
Figure A57:	$^1\text{H}$ NMR ( $\text{CDCl}_3$ , 400 MHz) spectrum of compound <b>3af</b> .....	257
Figure A58:	$^1\text{H}$ NMR ( $\text{CDCl}_3$ , 400 MHz) spectrum of compound <b>7ac</b> .....	257
Figure A59:	$^1\text{H}$ NMR ( $\text{CDCl}_3$ , 400 MHz) spectrum of compound <b>7ad</b> .....	258
Figure A60:	$^1\text{H}$ NMR ( $\text{CDCl}_3$ , 400 MHz) spectrum of compound <b>8ac</b> .....	258
Figure A61:	$^1\text{H}$ NMR ( $\text{CDCl}_3$ , 400 MHz) spectrum of compound <b>8ag</b> .....	259
Figure A62:	$^1\text{H}$ NMR ( $\text{CDCl}_3$ , 400 MHz) spectrum of compound <b>9ac</b> .....	259
Figure A63:	$^1\text{H}$ NMR ( $\text{CDCl}_3$ , 400 MHz) spectrum of compound <b>9ag</b> .....	260
Figure A64:	$^1\text{H}$ NMR ( $\text{CDCl}_3$ , 400 MHz) spectrum of compound <b>10ac</b> .....	260
Figure A65:	$^1\text{H}$ NMR ( $\text{CDCl}_3$ , 400 MHz) spectrum of compound <b>10ag</b> .....	261
Figure A66:	$^1\text{H}$ NMR ( $\text{CDCl}_3$ , 400 MHz) spectrum of compound <b>10ah</b> .....	261
Figure A67:	$^1\text{H}$ NMR ( $\text{CDCl}_3$ , 400 MHz) spectrum of compound <b>11ac</b> .....	262
Figure A68:	$^1\text{H}$ NMR ( $\text{CDCl}_3$ , 400 MHz) spectrum of compound <b>11ad</b> .....	262
Figure A69:	$^1\text{H}$ NMR ( $\text{CDCl}_3$ , 400 MHz) spectrum of compound <b>11ag</b> .....	263
Figure A70:	$^1\text{H}$ NMR ( $\text{CDCl}_3$ , 400 MHz) spectrum of compound <b>12ac</b> .....	263
Figure A71:	$^1\text{H}$ NMR ( $\text{CDCl}_3$ , 400 MHz) spectrum of compound <b>12ai</b> .....	264

Figure A72:	$^1\text{H}$ NMR ( $\text{CDCl}_3$ , 400 MHz) spectrum of compound <b>13ac</b> .....	264
Figure A73:	$^1\text{H}$ NMR ( $\text{CDCl}_3$ , 400 MHz) spectrum of compound <b>13ag</b> .....	265
Figure A74:	$^1\text{H}$ NMR ( $\text{CDCl}_3$ , 400 MHz) spectrum of compound <b>13ah</b> .....	265
Figure A75:	$^1\text{H}$ NMR ( $\text{CDCl}_3$ , 400 MHz) spectrum of compound <b>14ac</b> .....	266
Figure A76:	$^1\text{H}$ NMR ( $\text{CDCl}_3$ , 400 MHz) spectrum of compound <b>14af</b> .....	266
Figure A77:	$^1\text{H}$ NMR ( $\text{CDCl}_3$ , 400 MHz) spectrum of compound <b>15ac</b> .....	267
Figure A78:	$^1\text{H}$ NMR ( $\text{CDCl}_3$ , 400 MHz) spectrum of compound <b>15af</b> .....	267
Figure A79:	$^1\text{H}$ NMR ( $\text{CDCl}_3$ , 400 MHz) spectrum of compound <b>16ba</b> .....	268
Figure A80:	$^1\text{H}$ NMR ( $\text{CDCl}_3$ , 400 MHz) spectrum of compound <b>16bd</b> .....	268
Figure A81:	$^1\text{H}$ NMR ( $\text{CDCl}_3$ , 400 MHz) spectrum of compound <b>18be</b> .....	269
Figure A82:	$^1\text{H}$ NMR ( $\text{CDCl}_3$ , 400 MHz) spectrum of compound <b>18bf</b> .....	269
Figure A83:	$^1\text{H}$ NMR ( $\text{CDCl}_3$ , 400 MHz) spectrum of compound <b>18bg</b> .....	270
Figure A84:	$^1\text{H}$ NMR ( $\text{CDCl}_3$ , 400 MHz) spectrum of compound <b>20ba</b> .....	270
Figure A85:	$^1\text{H}$ NMR ( $\text{CDCl}_3$ , 400 MHz) spectrum of compound <b>20be</b> .....	271
Figure A86:	$^1\text{H}$ NMR ( $\text{CDCl}_3$ , 400 MHz) spectrum of compound <b>20bh</b> .....	271
Figure A87:	$^1\text{H}$ NMR ( $\text{CDCl}_3$ , 400 MHz) spectrum of compound <b>20bi</b> .....	272
Figure A88:	$^1\text{H}$ NMR ( $\text{CDCl}_3$ , 400 MHz) spectrum of compound <b>21ba</b> .....	272
Figure A89:	$^1\text{H}$ NMR ( $\text{CDCl}_3$ , 400 MHz) spectrum of compound <b>21bi</b> .....	273
Figure A90:	$^1\text{H}$ NMR ( $\text{CDCl}_3$ , 400 MHz) spectrum of compound <b>22bb</b> .....	273
Figure A91:	$^1\text{H}$ NMR ( $\text{CDCl}_3$ , 400 MHz) spectrum of compound <b>22bi</b> .....	274
Figure A92:	$^1\text{H}$ NMR ( $\text{CDCl}_3$ , 400 MHz) spectrum of compound <b>23bi</b> .....	274
Figure A93:	$^1\text{H}$ NMR ( $\text{CDCl}_3$ , 400 MHz) spectrum of compound <b>24ba</b> .....	275
Figure A94:	$^1\text{H}$ NMR ( $\text{CDCl}_3$ , 400 MHz) spectrum of compound <b>28ba</b> .....	275
Figure A95:	$^1\text{H}$ NMR ( $\text{CDCl}_3$ , 400 MHz) spectrum of compound <b>28bb</b> .....	276

Figure A96:	<sup>1</sup> H NMR (CDCl <sub>3</sub> , 400 MHz) spectrum of compound <b>28bc</b> .....	276
Figure A97:	<sup>1</sup> H NMR (CDCl <sub>3</sub> , 400 MHz) spectrum of compound <b>29ba</b> .....	277
Figure A98:	<sup>1</sup> H NMR (CDCl <sub>3</sub> , 400 MHz) spectrum of compound <b>29bb</b> .....	277
Figure A99:	<sup>1</sup> H NMR (CDCl <sub>3</sub> , 400 MHz) spectrum of compound <b>29bc</b> .....	278
Figure A100:	<sup>1</sup> H NMR (CDCl <sub>3</sub> , 400 MHz) spectrum of compound <b>29bj</b> .....	278
Figure A101:	<sup>1</sup> H NMR (CDCl <sub>3</sub> , 400 MHz) spectrum of compound <b>30ba</b> .....	279
Figure A102:	<sup>1</sup> H NMR (CDCl <sub>3</sub> , 400 MHz) spectrum of compound <b>30bk</b> .....	279
Figure A103:	<sup>1</sup> H NMR (CDCl <sub>3</sub> , 400 MHz) spectrum of compound <b>30bm</b> .....	280
Figure A104:	<sup>1</sup> H NMR (CDCl <sub>3</sub> , 400 MHz) spectrum of compound <b>30bn</b> .....	280
Figure A105:	<sup>1</sup> H NMR (CDCl <sub>3</sub> , 400 MHz) spectrum of compound <b>31bp</b> .....	281
Figure A106:	<sup>1</sup> H NMR (CDCl <sub>3</sub> , 400 MHz) spectrum of compound <b>31bq</b> .....	281
Figure A107:	<sup>1</sup> H NMR (CDCl <sub>3</sub> , 400 MHz) spectrum of compound <b>33bm</b> .....	282
Figure A108:	<sup>1</sup> H NMR (CDCl <sub>3</sub> , 400 MHz) spectrum of compound <b>33bn</b> .....	282
Figure A109:	<sup>1</sup> H NMR (CDCl <sub>3</sub> , 400 MHz) spectrum of compound <b>33ca</b> .....	283
Figure A110:	<sup>1</sup> H NMR (CDCl <sub>3</sub> , 400 MHz) spectrum of compound <b>34bm</b> .....	283
Figure A111:	<sup>1</sup> H NMR (CDCl <sub>3</sub> , 400 MHz) spectrum of compound <b>34bn</b> .....	284
Figure A112:	<sup>1</sup> H NMR (CDCl <sub>3</sub> , 400 MHz) spectrum of compound <b>34ca</b> .....	284
Figure A113:	<sup>1</sup> H NMR (CDCl <sub>3</sub> , 400 MHz) spectrum of compound <b>35bm</b> .....	285
Figure A114:	<sup>1</sup> H NMR (CDCl <sub>3</sub> , 400 MHz) spectrum of compound <b>35bn</b> .....	285
Figure A115:	<sup>1</sup> H NMR (CDCl <sub>3</sub> , 400 MHz) spectrum of compound <b>36bm</b> .....	286
Figure A116:	<sup>1</sup> H NMR (CDCl <sub>3</sub> , 400 MHz) spectrum of compound <b>36bn</b> .....	286
Figure A117:	<sup>1</sup> H NMR (CDCl <sub>3</sub> , 400 MHz) spectrum of compound <b>36ca</b> .....	287
Figure A118:	<sup>1</sup> H NMR (CDCl <sub>3</sub> , 400 MHz) spectrum of compound <b>37bn</b> .....	287
Figure A119:	<sup>1</sup> H NMR (CDCl <sub>3</sub> , 400 MHz) spectrum of compound <b>37ca</b> .....	288

Figure A120:	<sup>1</sup> H NMR (CDCl <sub>3</sub> , 400 MHz) spectrum of compound <b>37cc</b> .....	288
Figure A121:	<sup>1</sup> H NMR (CDCl <sub>3</sub> , 400 MHz) spectrum of compound <b>38bm</b> .....	289
Figure A122:	<sup>1</sup> H NMR (CDCl <sub>3</sub> , 400 MHz) spectrum of compounds <b>38bm</b> and <b>38bn</b> .....	289
Figure A123:	<sup>1</sup> H NMR (CDCl <sub>3</sub> , 400 MHz) spectrum of compound <b>38cd</b> .....	290
Figure A124:	<sup>1</sup> H NMR (CDCl <sub>3</sub> , 400 MHz) spectrum of compound <b>39ca</b> .....	290
Figure A125:	<sup>1</sup> H NMR (CDCl <sub>3</sub> , 400 MHz) spectrum of compound <b>40ca</b> .....	291
Figure A126:	<sup>1</sup> H NMR (CDCl <sub>3</sub> , 400 MHz) spectrum of compound <b>41ce</b> .....	291
Figure A127:	<sup>1</sup> H NMR (CDCl <sub>3</sub> , 400 MHz) spectrum of compound <b>41cf</b> .....	292
Figure A128:	<sup>1</sup> H NMR (CDCl <sub>3</sub> , 400 MHz) spectrum of compound <b>41cg</b> .....	292
Figure A129:	<sup>1</sup> H NMR (CDCl <sub>3</sub> , 400 MHz) spectrum of compound <b>41bm</b> .....	293
Figure A130:	<sup>1</sup> H NMR (CDCl <sub>3</sub> , 400 MHz) spectrum of compound <b>42cf</b> .....	293
Figure A131:	<sup>1</sup> H NMR (CDCl <sub>3</sub> , 400 MHz) spectrum of compound <b>43ch</b> .....	294
Figure A132:	<sup>1</sup> H NMR (CDCl <sub>3</sub> , 400 MHz) spectrum of compound <b>44ci</b> .....	294
Figure A133:	<sup>1</sup> H NMR (CDCl <sub>3</sub> , 400 MHz) spectrum of compound <b>103</b> .....	295
Figure A134:	<sup>1</sup> H NMR (CDCl <sub>3</sub> , 400 MHz) spectrum of compound <b>104</b> .....	295
Figure A135:	<sup>1</sup> H NMR (CDCl <sub>3</sub> , 400 MHz) spectrum of compound <b>105</b> .....	296
Figure A136:	<sup>1</sup> H NMR (CDCl <sub>3</sub> , 400 MHz) spectrum of compound <b>106</b> .....	296
Figure A137:	<sup>1</sup> H NMR (CDCl <sub>3</sub> , 400 MHz) spectrum of compound <b>107</b> .....	297
Figure A138:	X-ray crystal structure of <b>1aa</b> . Thermal ellipsoids are shown at the 50% probability level .....	298
Table A1:	Crystal data and structure refinement for compound <b>1aa</b> .....	298
Figure A139:	X-ray crystal structure of <b>1ab</b> . Thermal ellipsoids are shown at the 50% probability level .....	299
Table A2:	Crystal data and structure refinement for compound <b>1ab</b> .....	299

Figure A140:	X-ray crystal structure of <b>1ac</b> . Thermal ellipsoids are shown at the 50% probability level .....	300
Table A3:	Crystal data and structure refinement for compound <b>1ac</b> .....	300
Figure A141:	X-ray crystal structure of <b>1ae</b> . Thermal ellipsoids are shown at the 50% probability level .....	301
Table A4:	Crystal data and structure refinement for compound <b>1ae</b> .....	301
Figure A142:	X-ray crystal structure of <b>3aa</b> . Thermal ellipsoids are shown at the 50% probability level .....	302
Table A5:	Crystal data and structure refinement for compound <b>3aa</b> .....	302
Figure A143:	X-ray crystal structure of <b>7ad</b> . Thermal ellipsoids are shown at the 50% probability level .....	303
Table A6:	Crystal data and structure refinement for compound <b>7ad</b> .....	303
Figure A144:	X-ray crystal structure of <b>9ag</b> . Thermal ellipsoids are shown at the 50% probability level .....	304
Table A7:	Crystal data and structure refinement for compound <b>9ag</b> .....	304
Figure A145:	X-ray crystal structure of <b>10ac</b> . Thermal ellipsoids are shown at the 50% probability level .....	305
Table A8:	Crystal data and structure refinement for compound <b>10ac</b> .....	305
Figure A146:	X-ray crystal structure of <b>10ag</b> . Thermal ellipsoids are shown at the 50% probability level .....	306
Table A9:	Crystal data and structure refinement for compound <b>10ag</b> .....	306
Figure A147:	X-ray crystal structure of <b>11ag</b> . Thermal ellipsoids are shown at the 50% probability level .....	307
Table A10:	Crystal data and structure refinement for compound <b>11ag</b> .....	307
Figure A148:	X-ray crystal structure of <b>13ac</b> . Thermal ellipsoids are shown at the 50% probability level .....	308
Table A11:	Crystal data and structure refinement for compound <b>13ac</b> .....	308
Figure A149:	X-ray crystal structure of <b>13ag</b> . Thermal ellipsoids are shown at the 50% probability level .....	309

Table A12:	Crystal data and structure refinement for compound <b>13ag</b> .....	309
Figure A150:	X-ray crystal structure of <b>14ac</b> . Thermal ellipsoids are shown at the 50% probability level .....	310
Table A13:	Crystal data and structure refinement for compound <b>14ac</b> .....	310
Figure A151:	X-ray crystal structure of <b>14af</b> . Thermal ellipsoids are shown at the 50% probability level .....	311
Table A14:	Crystal data and structure refinement for compound <b>14af</b> .....	311
Figure A152:	X-ray crystal structure of <b>16ba</b> . Thermal ellipsoids are shown at the 50% probability level .....	312
Table A15:	Crystal data and structure refinement for compound <b>16ba</b> .....	312
Figure A153:	X-ray crystal structure of <b>20bi</b> . Thermal ellipsoids are shown at the 50% probability level .....	313
Table A16:	Crystal data and structure refinement for compound <b>20bi</b> .....	313
Figure A154:	X-ray crystal structure of <b>22bi</b> . Thermal ellipsoids are shown at the 50% probability level .....	314
Table A17:	Crystal data and structure refinement for compound <b>22bi</b> .....	314
Figure A155:	X-ray crystal structure of <b>28ba</b> . Thermal ellipsoids are shown at the 50% probability level .....	315
Table A18:	Crystal data and structure refinement for compound <b>28ba</b> .....	315
Figure A156:	X-ray crystal structure of <b>28bb</b> . Thermal ellipsoids are shown at the 50% probability level .....	316
Table A19:	Crystal data and structure refinement for compound <b>28bb</b> .....	316
Figure A157:	X-ray crystal structure of <b>28bc</b> . Thermal ellipsoids are shown at the 50% probability level .....	317
Table A20:	Crystal data and structure refinement for compound <b>28bc</b> .....	317
Figure A158:	X-ray crystal structure of <b>33bn</b> . Thermal ellipsoids are shown at the 50% probability level .....	318
Table A21:	Crystal data and structure refinement for compound <b>33bn</b> .....	318

Figure A159: X-ray crystal structure of <b>36bm</b> . Thermal ellipsoids are shown at the 50% probability level .....	319
Table A22: Crystal data and structure refinement for compound <b>36bm</b> .....	319
Figure A160: X-ray crystal structure of <b>37ca</b> . Thermal ellipsoids are shown at the 50% probability level .....	320
Table A23: Crystal data and structure refinement for compound <b>37ca</b> .....	320
Figure A161: X-ray crystal structure of <b>38cd</b> . Thermal ellipsoids are shown at the 50% probability level .....	321
Table A24: Crystal data and structure refinement for compound <b>38cd</b> .....	321
Figure A162: X-ray crystal structure of <b>41ce</b> . Thermal ellipsoids are shown at the 50% probability level .....	322
Table A25: Crystal data and structure refinement for compound <b>41ce</b> .....	322
Figure A163: X-ray crystal structure of <b>41cf</b> . Thermal ellipsoids are shown at the 50% probability level .....	323
Table A26: Crystal data and structure refinement for compound <b>41cf</b> .....	323
Figure A164: X-ray crystal structure of <b>44ci</b> . Thermal ellipsoids are shown at the 50% probability level .....	324
Table A27: Crystal data and structure refinement for compound <b>44ci</b> .....	324
Figure A165: Cyclic voltammogram of <b>1</b> at Pt electrode in MeCN/0.2 M LiClO <sub>4</sub> . E/V versus Ag/AgNO <sub>3</sub> , sweep rate = 0.2 V/s .....	325
Figure A166: Cyclic voltammogram of <b>2</b> at Pt electrode in MeCN/0.2 M LiClO <sub>4</sub> . E/V versus Ag/AgNO <sub>3</sub> , sweep rate = 0.2 V/s .....	325
Figure A167: Cyclic voltammogram of <b>3</b> at Pt electrode in MeCN/0.2 M LiClO <sub>4</sub> . E/3 versus Ag/AgNO <sub>3</sub> , sweep rate = 0.2 V/s .....	325
Figure A168: Cyclic voltammogram of <b>4</b> at Pt electrode in MeCN/0.2 M LiClO <sub>4</sub> . E/V versus Ag/AgNO <sub>3</sub> , sweep rate = 0.2 V/s .....	326
Figure A169: Cyclic voltammogram of <b>5</b> at Pt electrode in MeCN/0.2 M LiClO <sub>4</sub> . E/V versus Ag/AgNO <sub>3</sub> , sweep rate = 0.2 V/s .....	326
Figure A170: Cyclic voltammogram of <b>7</b> at Pt electrode in MeCN/0.2 M LiClO <sub>4</sub> . E/V versus Ag/AgNO <sub>3</sub> , sweep rate = 0.2 V/s .....	326

Figure A171: Cyclic voltammogram of <b>8</b> at Pt electrode in MeCN/0.2 M LiClO <sub>4</sub> . E/V versus Ag/AgNO <sub>3</sub> , sweep rate = 0.2 V/s .....	327
Figure A172: Cyclic voltammogram of <b>9</b> at Pt electrode in MeCN/0.2 M LiClO <sub>4</sub> . E/V versus Ag/AgNO <sub>3</sub> , sweep rate = 0.2 V/s .....	327
Figure A173: Cyclic voltammogram of <b>10</b> at Pt electrode in MeCN/0.2 M LiClO <sub>4</sub> . E/V versus Ag/AgNO <sub>3</sub> , sweep rate = 0.2 V/s.....	327
Figure A174: Cyclic voltammogram of <b>11</b> at Pt electrode in MeCN/0.2 M LiClO <sub>4</sub> . E/V versus Ag/AgNO <sub>3</sub> , sweep rate = 0.2 V/s.....	328
Figure A175: Cyclic voltammogram of <b>12</b> at Pt electrode in MeCN/0.2 M LiClO <sub>4</sub> . E/V versus Ag/AgNO <sub>3</sub> , sweep rate = 0.2 V/s.....	328
Figure A176: Cyclic voltammogram of <b>13</b> at Pt electrode in MeCN/0.2 M LiClO <sub>4</sub> . E/V versus Ag/AgNO <sub>3</sub> , sweep rate = 0.2 V/s.....	328
Figure A177: Cyclic voltammogram of <b>14</b> at Pt electrode in MeCN/0.2 M LiClO <sub>4</sub> . E/V versus Ag/AgNO <sub>3</sub> , sweep rate = 0.2 V/s.....	329
Figure A178: Cyclic voltammogram of <b>15</b> at Pt electrode in MeCN/0.2 M LiClO <sub>4</sub> . E/V versus Ag/AgNO <sub>3</sub> , sweep rate = 0.2 V/s.....	329
Figure A179: Cyclic voltammogram of <b>16</b> at Pt electrode in MeCN/0.2 M LiClO <sub>4</sub> . E/V versus Ag/AgNO <sub>3</sub> , sweep rate = 0.2 V/s.....	329
Figure A180: Cyclic voltammogram of <b>17</b> at Pt electrode in MeCN/0.2 M LiClO <sub>4</sub> . E/V versus Ag/AgNO <sub>3</sub> , sweep rate = 0.2 V/s.....	330
Figure A181: Cyclic voltammogram of <b>18</b> at Pt electrode in MeCN/0.2 M LiClO <sub>4</sub> . E/V versus Ag/AgNO <sub>3</sub> , sweep rate = 0.2 V/s.....	330
Figure A182: Cyclic voltammogram of <b>19</b> at Pt electrode in MeCN/0.2 M LiClO <sub>4</sub> . E/V versus Ag/AgNO <sub>3</sub> , sweep rate = 0.2 V/s.....	330
Figure A183: Cyclic voltammogram of <b>20</b> at Pt electrode in MeCN/0.2 M LiClO <sub>4</sub> . E/V versus Ag/AgNO <sub>3</sub> , sweep rate = 0.2 V/s.....	331
Figure A184: Cyclic voltammogram of <b>21</b> at Pt electrode in MeCN/0.2 M LiClO <sub>4</sub> . E/V versus Ag/AgNO <sub>3</sub> , sweep rate = 0.2 V/s.....	331
Figure A185: Cyclic voltammogram of <b>22</b> at Pt electrode in MeCN/0.2 M LiClO <sub>4</sub> . E/V versus Ag/AgNO <sub>3</sub> , sweep rate = 0.2 V/s.....	331
Figure A186: Cyclic voltammogram of <b>23</b> at Pt electrode in MeCN/0.2 M LiClO <sub>4</sub> . E/V versus Ag/AgNO <sub>3</sub> , sweep rate = 0.2 V/s.....	332

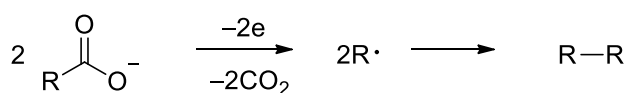
Figure A187: Cyclic voltammogram of <b>24</b> at Pt electrode in MeCN/0.2 M LiClO <sub>4</sub> . E/V versus Ag/AgNO <sub>3</sub> , sweep rate = 0.2 V/s.....	332
Figure A188: Cyclic voltammogram of <b>25</b> at Pt electrode in MeCN/0.2 M LiClO <sub>4</sub> . E/V versus Ag/AgNO <sub>3</sub> , sweep rate = 0.2 V/s.....	332
Figure A189: Cyclic voltammogram of <b>26</b> at Pt electrode in MeCN/0.2 M LiClO <sub>4</sub> . E/V versus Ag/AgNO <sub>3</sub> , sweep rate = 0.2 V/s.....	333
Figure A190: Cyclic voltammogram of <b>27</b> at Pt electrode in MeCN/0.2 M LiClO <sub>4</sub> . E/V versus Ag/AgNO <sub>3</sub> , sweep rate = 0.2 V/s.....	333
Figure A191: Cyclic voltammogram of <b>28</b> at Pt electrode in MeCN/0.2 M LiClO <sub>4</sub> . E/V versus Ag/AgNO <sub>3</sub> , sweep rate = 0.2 V/s.....	333
Figure A192: Cyclic voltammogram of <b>29</b> at Pt electrode in MeCN/0.2 M LiClO <sub>4</sub> . E/V versus Ag/AgNO <sub>3</sub> , sweep rate = 0.2 V/s.....	334
Figure A193: Cyclic voltammogram of <b>30</b> at Pt electrode in MeCN/0.2 M LiClO <sub>4</sub> . E/V versus Ag/AgNO <sub>3</sub> , sweep rate = 0.2 V/s.....	334
Figure A194: Cyclic voltammogram of <b>31</b> at Pt electrode in MeCN/0.2 M LiClO <sub>4</sub> . E/V versus Ag/AgNO <sub>3</sub> , sweep rate = 0.2 V/s.....	334
Figure A195: Cyclic voltammogram of <b>33</b> at Pt electrode in MeCN/0.2 M LiClO <sub>4</sub> . E/V versus Ag/AgNO <sub>3</sub> , sweep rate = 0.2 V/s.....	335
Figure A196: Cyclic voltammogram of <b>34</b> at Pt electrode in MeCN/0.2 M LiClO <sub>4</sub> . E/V versus Ag/AgNO <sub>3</sub> , sweep rate = 0.2 V/s.....	335
Figure A197: Cyclic voltammogram of <b>35</b> at Pt electrode in MeCN/0.2 M LiClO <sub>4</sub> . E/V versus Ag/AgNO <sub>3</sub> , sweep rate = 0.2 V/s.....	335
Figure A198: Cyclic voltammogram of <b>36</b> at Pt electrode in MeCN/0.2 M LiClO <sub>4</sub> . E/V versus Ag/AgNO <sub>3</sub> , sweep rate = 0.2 V/s.....	336
Figure A199: Cyclic voltammogram of <b>37</b> at Pt electrode in MeCN/0.2 M LiClO <sub>4</sub> . E/V versus Ag/AgNO <sub>3</sub> , sweep rate = 0.2 V/s.....	336
Figure A200: Cyclic voltammogram of <b>38</b> at Pt electrode in MeCN/0.2 M LiClO <sub>4</sub> . E/V versus Ag/AgNO <sub>3</sub> , sweep rate = 0.2 V/s.....	336
Figure A201: Cyclic voltammogram of <b>39</b> at Pt electrode in MeCN/0.2 M LiClO <sub>4</sub> . E/V versus Ag/AgNO <sub>3</sub> , sweep rate = 0.2 V/s.....	337
Figure A202: Cyclic voltammogram of <b>40</b> at Pt electrode in MeCN/0.2 M LiClO <sub>4</sub> . E/V versus Ag/AgNO <sub>3</sub> , sweep rate = 0.2 V/s.....	337

Figure A203: Cyclic voltammogram of <b>41</b> at Pt electrode in MeCN/0.2 M LiClO <sub>4</sub> . E/V versus Ag/AgNO <sub>3</sub> , sweep rate = 0.2 V/s.....	337
Figure A204: Cyclic voltammogram of <b>42</b> at Pt electrode in MeCN/0.2 M LiClO <sub>4</sub> . E/V versus Ag/AgNO <sub>3</sub> , sweep rate = 0.2 V/s.....	338
Figure A205: Cyclic voltammogram of <b>43</b> at Pt electrode in MeCN/0.2 M LiClO <sub>4</sub> . E/V versus Ag/AgNO <sub>3</sub> , sweep rate = 0.2 V/s.....	338
Figure A206: Cyclic voltammogram of <b>44</b> at Pt electrode in MeCN/0.2 M LiClO <sub>4</sub> . E/V versus Ag/AgNO <sub>3</sub> , sweep rate = 0.2 V/s.....	338
Figure A207: Cyclic voltammogram of <b>45</b> at Pt electrode in MeCN/0.2 M LiClO <sub>4</sub> . E/V versus Ag/AgNO <sub>3</sub> , sweep rate = 0.2 V/s.....	339
Figure A208: Cyclic voltammogram of <b>46</b> at Pt electrode in MeCN/0.2 M LiClO <sub>4</sub> . E/V versus Ag/AgNO <sub>3</sub> , sweep rate = 0.2 V/s.....	339

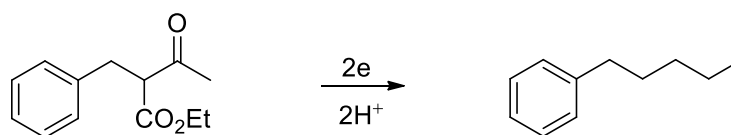
## CHAPTER 1: INTRODUCTION

### 1.1 General

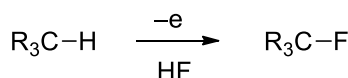
Most organic chemists tend to regard electrosynthesis as an unfamiliar tool, involving the use of complicated procedures which are more suited for applications in industry for the production of bulk chemicals.<sup>1</sup> Although under exploited in the field of organic synthesis, electroorganic synthesis has a long history dating back almost 220 years and can be traced to 1800 with the invention of the first electric battery, the Volta Pile that allowed electric current to be continuously provided to a circuit. Over the past few decades, many reviews<sup>2-10</sup> and scientific reports<sup>11-17</sup> have consistently lauded the diverse applications of electrochemically mediated organic transformations as a convenient and alternative tool for the preparation of organic compounds. The use of electrosynthesis in organic chemistry began in the early 19th century when Michael Faraday first performed the electrolysis of acetic acid under preparative conditions.<sup>4,9</sup> This was followed by the development of other reactions such as the well-known Kolbe electrolysis (Scheme 1.1) which offered a means to access alkyl radicals through the anodic oxidation of various carboxylic acids,<sup>18</sup> the Tafel rearrangement (Scheme 1.2) which allowed the reduction of various alkylated ethyl acetoacetates to give different hydrocarbons.<sup>19</sup> Mid-twentieth century developments include impressive applications in Industry such as the Simons fluorination process<sup>20</sup> (Scheme 1.3) and the Monsanto adiponitrile process<sup>21</sup> (Scheme 1.4).



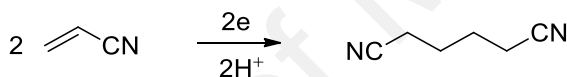
**Scheme 1.1:** Kolbe electrolysis



**Scheme 1.2:** Tafel Rearrangement



**Scheme 1.3:** Simons fluorination



**Scheme 1.4:** Monsanto adiponitrile process

Since then, the use of electrochemistry as a synthetic tool in organic chemistry has increased remarkably over the past decade. This classical technology has also been recently recognized as a potentially green methodology (involving the development of environmentally compatible processes) for organic synthesis. Over the years, the need for the development of green industrial processes is becoming more and more urgent and energy from renewable resources has been increasingly exploited all over the world to reduce pollution, carbon dioxide emission, and waste generation.<sup>5</sup> Electrochemistry has reemerged as a potential green methodology, providing tools for the development of cleaner synthetic procedures and the evolution of green chemistry. This “green aspect”

of organic electrosynthesis relates to at least 9 of the 12 principles of sustainable or green chemistry (Figure 1.1) as stated below.<sup>22</sup>

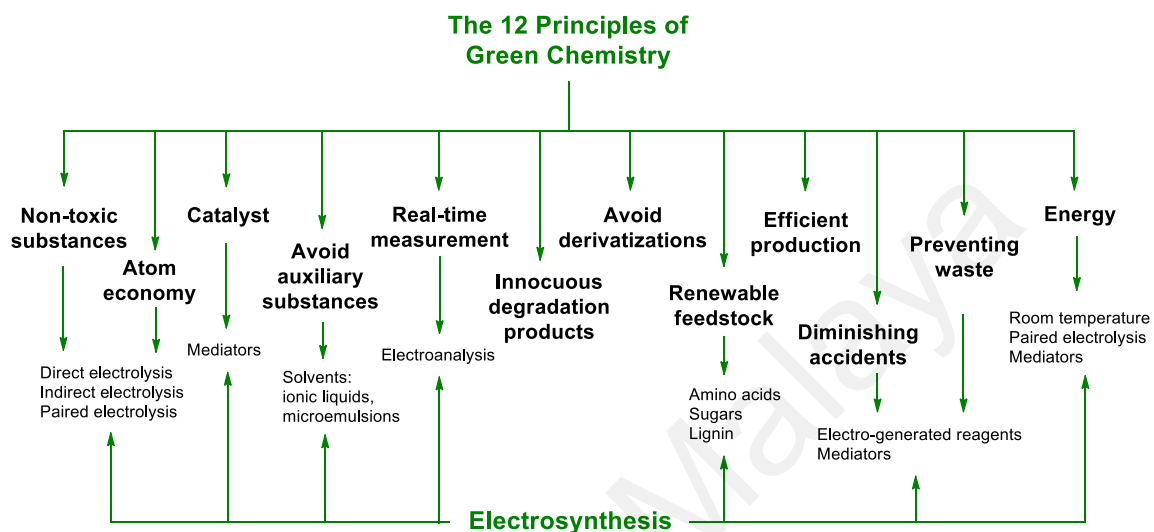


**Figure 1.1:** Correlations of organic electrosynthesis to the 12 principles of green chemistry<sup>22</sup>

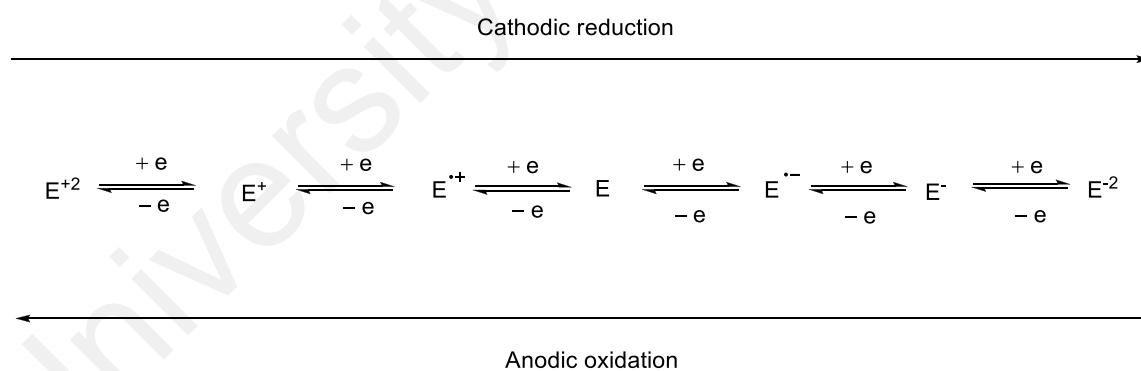
- Environmentally friendly, since green solvents such as ionic liquids or microemulsions are used in electrosynthesis.
- Mediators act as catalysts in synthetic processes to reduce chemical waste and decrease energy consumption.
- The possibility to improve atom economy when conducting direct, indirect, or paired electrolysis.
- Use of renewable starting materials such as amino acids, sugars and lignins.
- Improvements in energy efficiency in cases where electrosyntheses are performed at room temperature, or when mediators are used, or when paired electrosynthesis is conducted.

- The coupling of electroanalytical control methods for real-time monitoring during the electrolysis.
- *In situ* electrogenerated or recycled reactive species, intermediates, or reactants, can reduce chances of accidents.
- Waste production can be reduced since reagents are electrogenerated in the electrochemical cell.
- Toxic reagents or chemicals are avoided during the electrochemical-mediated processes.

In view of the intrinsic “greenness” of the reaction processes, organic electrosynthesis has experienced a renaissance in the field of preparative organic methods since stoichiometric oxidizing or reducing agents are being replaced by electric current as an inexpensive, renewable, and inherently safe reagent.<sup>5,6</sup> Apart from this “green” aspect, electrochemical reactions are efficient by enabling shortening of conventional multi-step reaction sequences since the reactivity of each reaction can be tuned by changing the applied potential, circumventing the limitations in the redox potential associated with every chemical reagent. The application of electrochemical methodologies to organic synthesis is receiving significant attention from industry and research centers worldwide, and it is an important prospect in the solution of current and future challenges.<sup>5,22</sup>

## 1.2 Some Basic Principles of Electroorganic Synthesis

Electrochemistry involves the addition or removal of electrons from a substrate through the direct application of an electrical potential. Conventional organic reactions require reagents (oxidants or reductants) in the conversion of the substrate which is in contrast with electroorganic reactions, where no reagent is required since the role of the reagent has been replaced by the electrodes. When a potential is set at the electrode and under the conditions of direct electrolysis, substrate molecules undergo electron transfer with the electrode surface and active species are generated at the surface of the electrodes (the double layer).<sup>23</sup> These high energy species include radical ions, ions and radicals (derived from the radical ions), depending on whether the substrate loses (anodic oxidation) or receives (cathodic reduction) electrons from the anode (positive electrode) or cathode (negative electrode), respectively (Scheme 1.5).



**Scheme 1.5:** Intermediate species formed during the anodic oxidation or cathodic reduction

For electrochemically-mediated reactions, there are mainly three types of reactions involved, viz., anodic oxidation, cathodic reduction, and paired electrolysis (where both oxidation and reduction occur in the same vessel) using different electrochemical techniques such as direct electrolysis or indirect (or mediated) electrolysis (Figure 1.2).<sup>4,8</sup> The classical technique for electroorganic reactions is the direct electrolysis where electro-conversion occurs at an inert or at an electrocatalytically active surface (heterogeneous electron transfer) and by preselecting the desirable electrode potential during the electrolysis process.

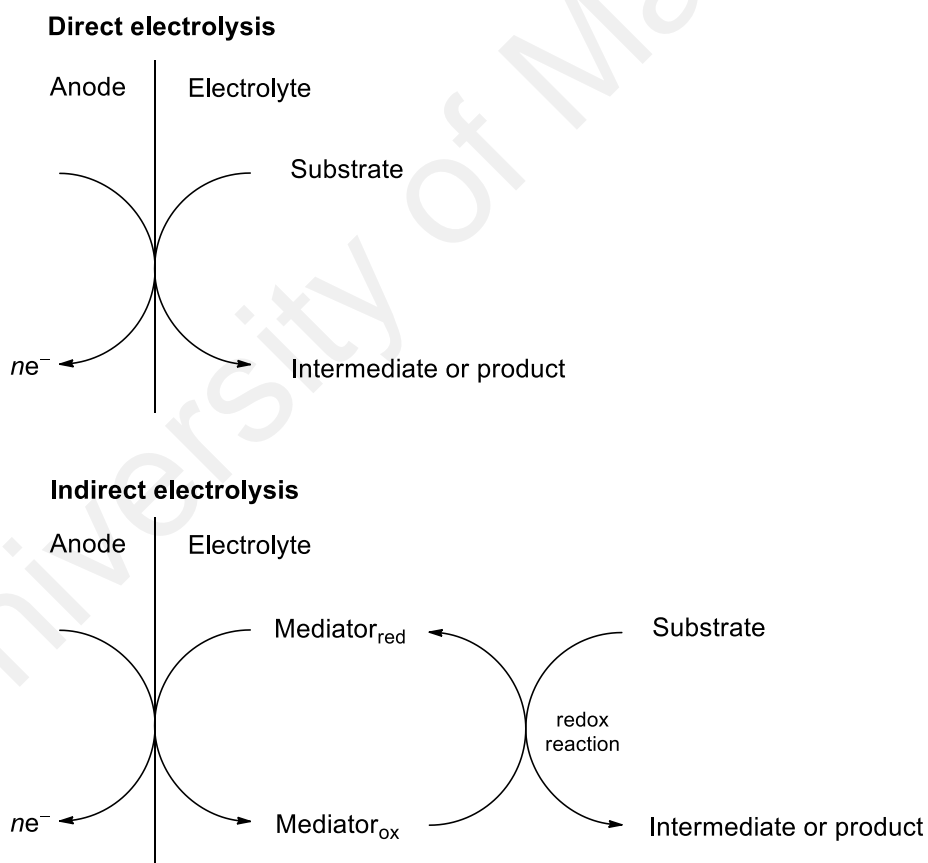


**Figure 1.2:** General principle of direct and indirect (mediated) electrolyses<sup>7,8</sup>

Although direct electrolysis is the most commonly used electrochemical technique, there are several drawbacks associated with electrochemical synthesis using the direct electron transfer method. Firstly, electroorganic synthesis often requires longer reaction times and together with the use of polar solvents for the required conductivity, can sometimes cause undesirable competing side reactions.<sup>24</sup> Furthermore, some of the reactive intermediates can diffuse back into the bulk solution for downstream functionalization while others decompose and adsorb on the electrode surface causing electrode deactivation (known as passivation), impeding further reactions, if the electrochemical reaction is not completely halted.<sup>4</sup> These problems can be circumvented by using a mediator (or redox catalyst) that undergoes heterogeneous electron transfer with the electrode surface to form a stabilized intermediate.<sup>4,7</sup> This reactive intermediate can then oxidize or reduce a substrate molecule homogenously in an indirect electrolytic process. Organic redox mediators consisting of extended  $\pi$ -electron systems such as triarylamine are among the most frequently employed for indirect electroorganic synthesis. The triarylamine cation radicals represent the active species in the catalytic cycle and are only stable when a substituent in the para position (such as *tris*(*p*-bromophenyl)amine) is present to block dimerization or attack by nucleophiles.<sup>7,25</sup>

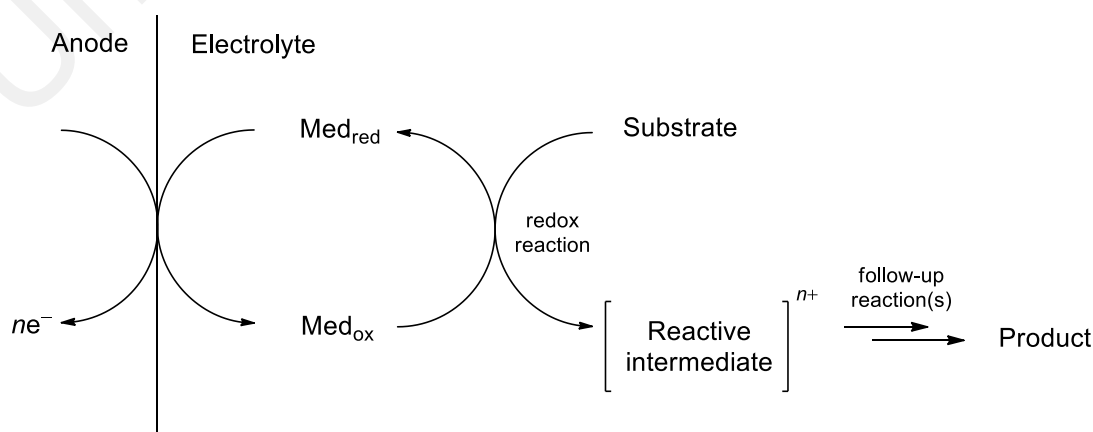
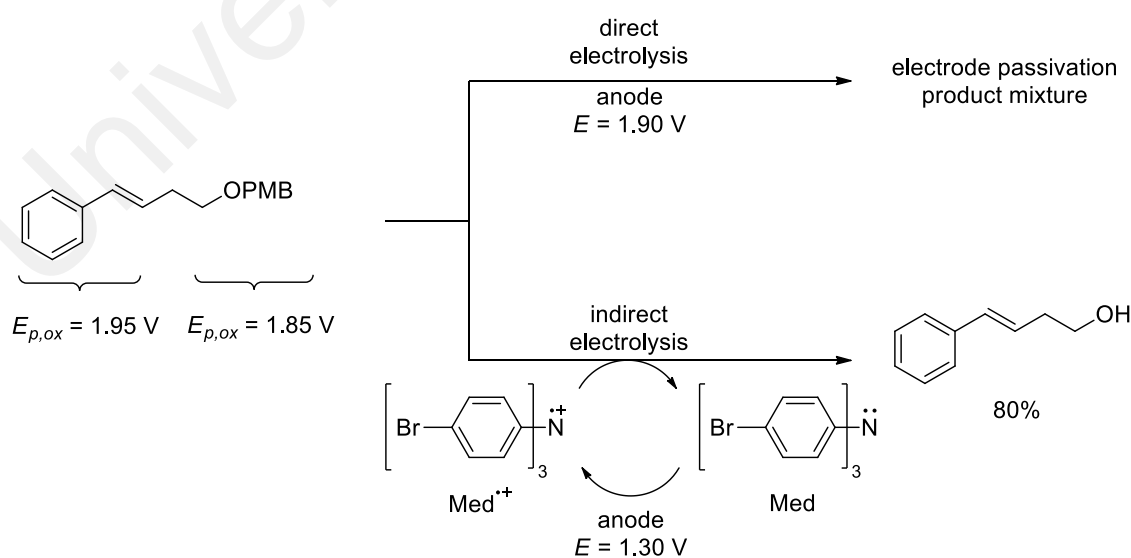


**Figure 1.3:** General principle of mediated redox<sup>7</sup>

In cases where direct electrochemical conversion causes passivation of the electrode, the employment of a mediator can be helpful, since direct interaction of the substrate with the electrode surface is avoided and since the electrolysis is conducted at potentials lower than the redox potential of the starting material, the reaction can be carried out under milder conditions and side reactions can be avoided.<sup>7</sup> This is exemplified in Scheme 1.6 where the *p*-methoxybenzyl ether (PMB) protecting group was removed from 4-phenyl-3-butenol by mediated anodic oxidation.<sup>26</sup> The substrate contains two electrophores whose potentials differ only by 100 mV. The indirect electrolysis of the substrate proceeded efficiently to selectively remove the PMB group, in contrast to direct electrolysis where electrode passivation occurs, resulting in the formation of a mixture of undesirable products.

Highly reactive intermediates such as cation radicals and anion radicals can therefore be generated electrochemically and these reactive intermediates often undergo subsequent chemical reactions as classified in Tables 1.1 and 1.2.<sup>27</sup>



**Scheme 1.6:** Mediated selective deprotection of PMB ethers<sup>26</sup>

**Table 1.1:** Important primary reactions in radical cation chemistry of  $\pi$ -A-B<sup>+</sup>

Classification	Primary Reaction	A	B
C–H deprotonation	$\pi$ -C-H <sup>+</sup> → $\pi$ -C <sup>•</sup> + H <sup>+</sup>	C	H
A–H deprotonation	$\pi$ -A-H <sup>+</sup> → $\pi$ -A <sup>•</sup> + H <sup>+</sup>	O, N, S, X	H
A–B bond cleavage	$\pi$ -A-B <sup>+</sup> → $\pi$ -A <sup>•</sup> + B <sup>+</sup> or $\pi$ -A <sup>+</sup> + B <sup>•</sup>	A	B
C–C bond cleavage	$\pi$ -C-C <sup>+</sup> → $\pi$ -C <sup>•</sup> + C <sup>+</sup>	C	C
C–X bond cleavage	$\pi$ -C-X <sup>+</sup> → $\pi$ -C <sup>•</sup> + X <sup>+</sup>	C	Si, Sn
Nu attack	Nu + $\pi$ -A-B <sup>+</sup> → Nu- $\pi$ -A-B <sup>+</sup>	A	B
cycloaddition	cycloaddition	A	B
rearrangement	rearrangement	A	B
electron-transfer	$\pi$ -A-B <sup>+</sup> ± e <sup>−</sup> → $\pi$ -A-B or $\pi$ -A-B <sup>2+</sup>	A	B
radical attack	R <sup>•</sup> + $\pi$ -A-B <sup>+</sup> → R- $\pi$ -A-B <sup>+</sup>	A	B
radical anion attack	RA <sup>•−</sup> + $\pi$ -A-B <sup>+</sup> → RA- $\pi$ -A-B	A	B
dimerization	2 $\pi$ -A-B <sup>+</sup> → ( $\pi$ -A-B) <sub>2</sub> <sup>2+</sup>	A	B
hydrogen transfer	H <sup>•</sup> + $\pi$ -A-B <sup>+</sup> → H- $\pi$ -A-B <sup>+</sup>	A	B

The same patterns are observed for n-A-B<sup>+</sup>

**Table 1.2:** Important primary reactions in radical anion chemistry of  $\pi\text{-A-B}^{\cdot-}$ 

Classification	Primary Reaction	A	B
protonation	$\text{H}^+ + \pi\text{-A-B}^{\cdot-} \rightarrow \text{H-}\pi\text{-A-B}^{\cdot}$	A	B
electron-transfer	$\pi\text{-A-B}^{\cdot-} \pm e^- \rightarrow$ $\pi\text{-A-B}$ or $\pi\text{-A-B}^{2-}$	A	B
radical attack	$\text{R}^{\cdot} + \pi\text{-A-B}^{\cdot+} \rightarrow \text{R-}\pi\text{-A-B}^+$	A	B
radical anion attack	$\text{RC}^{\cdot+} + \pi\text{-A-B}^{\cdot-} \rightarrow \text{RC-}\pi\text{-A-B}$	A	B
dimerization	$2\pi\text{-A-B}^{\cdot-} \rightarrow (\pi\text{-A-B})_2^{2-}$	A	B
hydrogen transfer	$\text{H}^{\cdot} + \pi\text{-A-B}^{\cdot-} \rightarrow \text{H-}\pi\text{-A-B}^{\cdot}$	A	B

### 1.3 Apparatus and Conditions for Electrochemical Studies

The electrochemical cell always consists of at least two electrodes as it is part of a closed electric circuit (Figure 1.4). It is the principle of electrochemistry to replace the direct electron transfer between atoms and molecules in conventional redox reactions by the separated electron release (oxidation) at the anode and the electron consumption (reduction) at the cathode (both processes described with respect to the chemical species in the electrolyte). In most electrochemical reactions, only one of these processes (oxidation/reduction) may be intended at the working electrode while the other one has to be carried out in the counter electrode to complete the redox reaction with the exception for paired electrolysis where two desirable half-reactions are allowed to be performed simultaneously.<sup>28,29</sup>

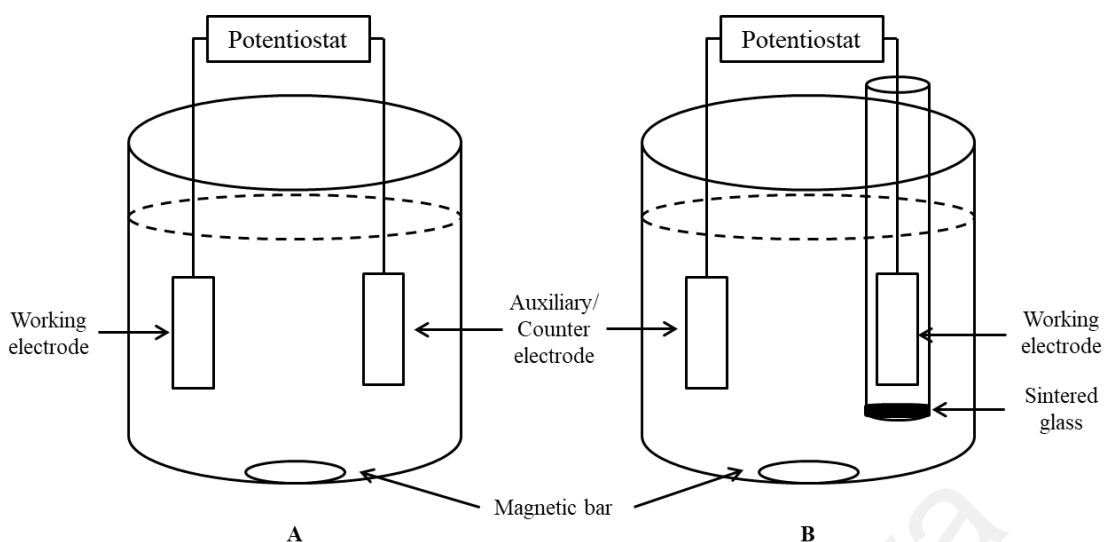


**Figure 1.4: A: undivided B: divided electrochemical cells**

In general, simple electrochemical cells such as the undivided cells (Figure 1.4A) are strongly preferred in order to minimize the laboratory effort since they are easier to set up compared to the divided cells (Figure 1.4B). However, scenarios can arise where high energy intermediates generated at the working anode are prematurely reduced at the cathode and vice versa. This can be overcome with divided electrochemical cells where the anodic and cathodic chambers are separated by a partially permeable membrane or a salt bridge.<sup>4,30</sup> Ion transfer between the electrodes is necessary in a closed electric circuit where the electrodes are connected to an electrical power supply. Thus, an electrolyte of sufficient ion conductivity is needed. Usually, this is a solution containing minimal concentration of an acid, a base, or a salt as supporting electrolyte, which normally has to be separated after the reaction.<sup>28</sup>

The basic setup of a three-electrode system for electrochemical reaction (anodic oxidation) consists of a working electrode, a counter electrode and a reference electrode (Figure 1.5). The materials used for the electrodes must be mechanically stable and

chemically inert. Generally, the most common materials for the anode are platinum and carbon (carbon paste, carbon felt, and vitreous carbon or glassy carbon), nickel (NiOOH), and lead (PbO<sub>2</sub>). On the other hand, materials for the cathode have a wider variety of selection mainly, platinum, iron (mild steel, stainless steel), carbon, mercury, lead, cadmium, tin, copper, silver, nickel, aluminium and titanium.<sup>28,31-35</sup> A number of modern electrodes have been developed and employed in the industries and in synthetic laboratories recently. The conductive ceramic, Ebonex<sup>®</sup> is an electrode material suitable if low electrocatalytic activity, high corrosion resistance, and high overpotentials for oxygen and hydrogen is required.<sup>36</sup> Dimensionally stable anodes (DSA<sup>®</sup>) are the most used anodes in industry<sup>37</sup> where in this case, TiO<sub>2</sub> passivation layer on the titanium is replaced by a conductive coating based on titanium and ruthenium oxides, with optimal electrocatalytic activity for chlorine evolution from aqueous chloride solutions. Boron doped diamond (BDD) electrodes have relatively low catalytic activity, high overpotential for oxygen, and high hydrogen evolution in aqueous solution, hence offering an extraordinarily high potential range and electrochemical power for oxidation and reduction.<sup>38</sup> Besides the working electrode (where the electrochemical reaction, oxidation or reduction, takes place), a reference electrode with known electrode potential is required as it allows the measurement of the working electrode potential without the need of current passing through it. In addition, a counter electrode allows for the flow of the same magnitude of current so as to ensure that there is no current flow between the working and reference electrodes during an electrochemical reaction. For instance, if oxidation occurs at the working electrode, reduction involving the same magnitude of current is sustained at the counter electrode. This is not possible in a two electrode system. A sintered glass can also be used to separate the working electrode from the counter electrode to prevent contamination (reaction at the counter electrode) of the main test solution (Figure 1.5).

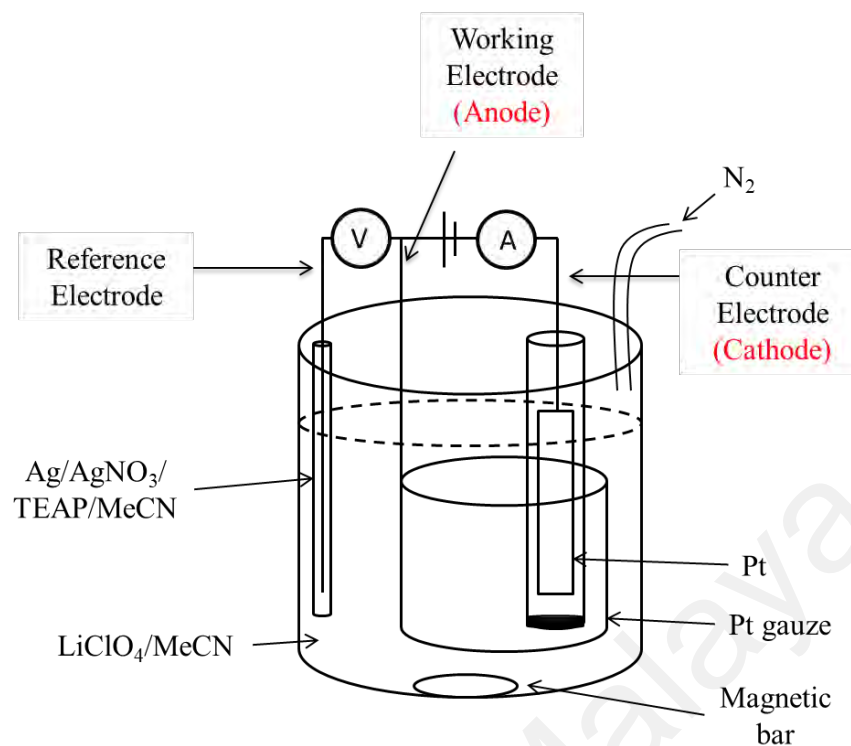


**Figure 1.5:** Basic setup of three electrode system

Electrolysis occurs in the space near the electrode surface and the medium that conducts the electric current, and the nature of the solvent is important for the course of electrochemical reactions. Such factor as usable potential range, proton activity, dielectric constant, ion pair formation, ability to dissolve electrolytes and substrates, accessible temperature range, viscosity, toxicity, vapour pressure, and price must be taken into consideration when selecting the solvent for electrolysis.<sup>39</sup> On the other hand, the supporting electrolyte is to maintain high conductivity of the current in the solution during electrochemical reaction. Common electrolytes used in electrochemical reactions are mainly made up of ammonium ( $\text{Et}_4\text{N}^+$  or  $n\text{-Bu}_4\text{N}^+$ ) or alkali metal ( $\text{Li}^+$  or  $\text{Na}^+$ ) cations, and anions such as halide ions,  $\text{ClO}_4^-$ ,  $\text{BF}_4^-$ ,  $\text{PF}_6^-$ ,  $\text{OTs}^-$ , and  $\text{RO}^-$ . The decomposition potential of the solvent-electrolyte system is important since the range of the working potential is limited by decomposition potentials of the selected solvent-

electrolyte system. Examples of the accessible potential ranges of some solvent-electrolyte systems are shown in Table 1.3.

**Table 1.3:** Approximate potential ranges of some solvent-electrolyte systems<sup>a</sup>

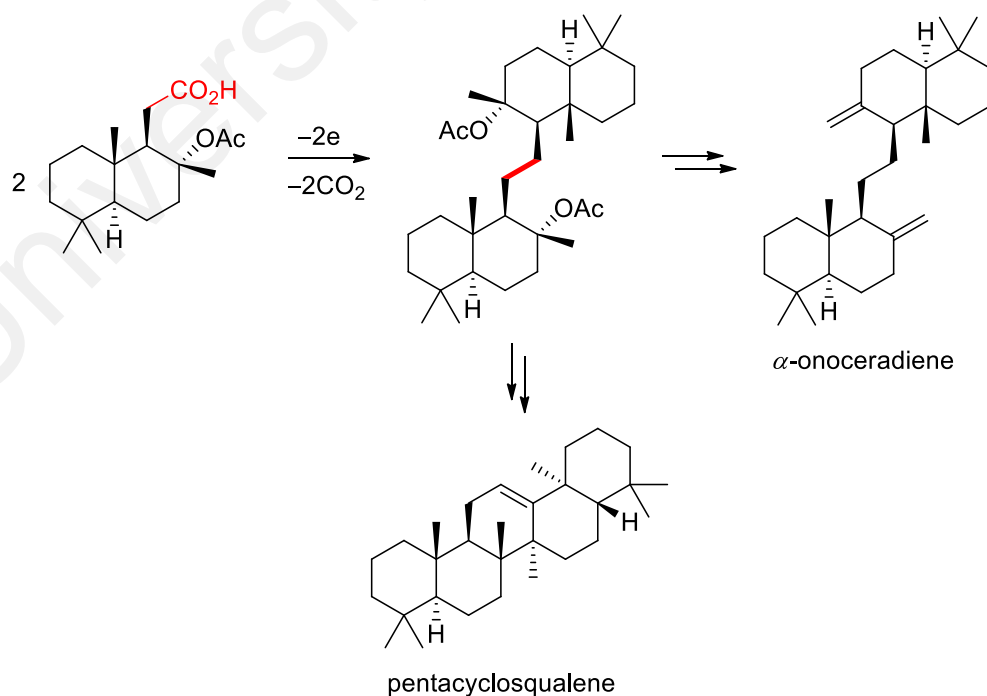
Solvent	Electrolyte	Anodic limit (V)	Cathodic limit (V)
Acetic acid	NaOAc	+2.0	-1.0
Acetone	Bu <sub>4</sub> NClO <sub>4</sub>	+1.6	-1.0
Acetonitrile	LiClO <sub>4</sub>	+2.6	-3.2
	NaClO <sub>4</sub>	+2.6	-1.6
	Bu <sub>4</sub> NClO <sub>4</sub>	+2.6	-2.7
	Et <sub>4</sub> NClO <sub>4</sub>	+3.5	-2.8
	Et <sub>4</sub> NBF <sub>4</sub>	+3.2	-1.8
1,2-dimethoxyethane	Bu <sub>4</sub> NClO <sub>4</sub>	+0.7 <sup>b</sup>	-3.0 <sup>b</sup>
Dimethylacetamide	Bu <sub>4</sub> NClO <sub>4</sub>	+1.6	-2.7
Dimethylformamide	Bu <sub>4</sub> NClO <sub>4</sub>	+1.6	-2.8
	Et <sub>4</sub> NClO <sub>4</sub>	+1.9	-2.8
Dimethylsulphoxide	LiClO <sub>4</sub>	+1.3	-3.4
	Et <sub>4</sub> NClO <sub>4</sub>	+2.1	-2.7
Hexamethylphosphoramide	LiClO <sub>4</sub>	+1.0	-3.3
Methanol	KOH	+0.6	-1.0
	LiClO <sub>4</sub>	+1.3	-1.0
Methylene chloride	Bu <sub>4</sub> NClO <sub>4</sub>	+1.8	-1.7
Nitrobenzene	Pr <sub>4</sub> NClO <sub>4</sub>	+1.6	-0.7
Nitromethane	LiClO <sub>4</sub>	+3.0	-2.4
Propylene carbonate	Et <sub>4</sub> NClO <sub>4</sub>	+1.7	-1.9
Pyridine	Et <sub>4</sub> NClO <sub>4</sub>	+3.3	-2.2
Sulfolane	Et <sub>4</sub> NClO <sub>4</sub>	+3.0	-2.2
Tetrahydrofuran	LiClO <sub>4</sub>	+1.6	-3.2

<sup>a</sup>Working electrode, Pt; V *versus* SCE

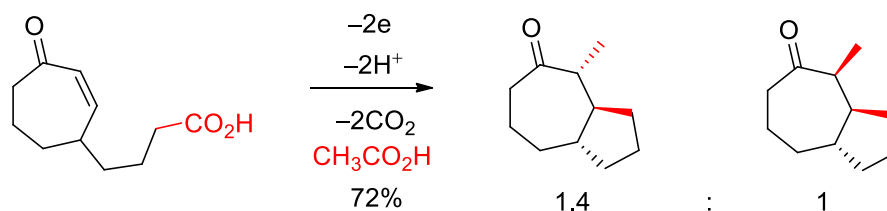
<sup>b</sup>Working electrode, Hg

## 1.4 A Brief Survey of Electrochemically-Mediated Transformations in Organic Chemistry

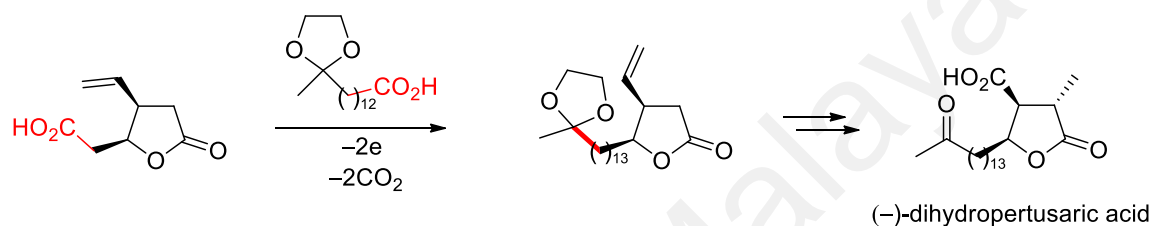
The Kolbe electrolysis is one of the oldest and well-known electrochemical transformations first performed by Faraday in 1834 and further developed by Kolbe in 1849. In the Kolbe reaction, anodic oxidation of alkyl carboxylates followed by oxidative decarboxylation, gives the alkyl radicals whereupon dimerization forges a new C–C bond (Scheme 1.1, *vide supra*). Corey's synthesis of  $\alpha$ -onoceradiene and pentacyclosqualene represent one of the earlier examples employing the Kolbe electrolysis methodology (Scheme 1.7).<sup>40</sup> Schäfer and co-workers reported the synthesis of perhydroazulenes involving a cascade of reactions initiated by the Kolbe electrolysis (Scheme 1.8).<sup>41</sup> Renaud and co-workers on the other hand reported the synthesis of (–)-phaseolinic, (–)-nephromopsinic, and (–)-dihydropertusaric acids using a mixed Kolbe electrolysis (Scheme 1.9).<sup>42</sup>



**Scheme 1.7:** Synthesis of  $\alpha$ -onoceradiene and pentacyclosqualene

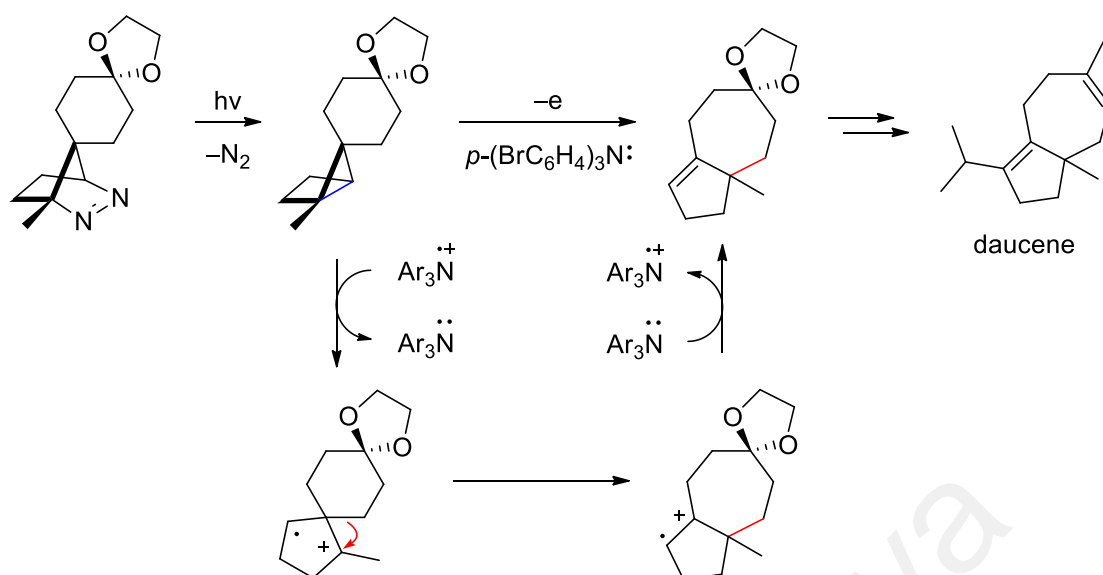


**Scheme 1.8:** Synthesis of perhydroazulenes via mixed-Kolbe electrolysis



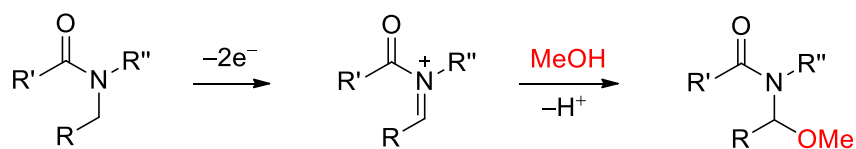
**Scheme 1.9:** Synthesis of (-)-dihydropertusaric acid via mixed-Kolbe electrolysis

Early examples of indirect electrolysis using chromium salts as mediators to facilitate the electrosynthesis of quinones were reported as early as 1900.<sup>43</sup> The 1970s and 1980s saw the introduction of triaryl amines<sup>25</sup> and nitroxyl radicals<sup>44</sup> as mediators in indirect electrolysis. The principles of indirect electrolysis (*vide supra*) were also formalized by Steckhan in the 1980s.<sup>26,45</sup> A recent example includes the mediated electrosynthesis of a key intermediate in the total synthesis daucene by Park and Little using *tris*(4-bromophenyl)amine as a redox mediator (Scheme 1.10).<sup>46</sup>

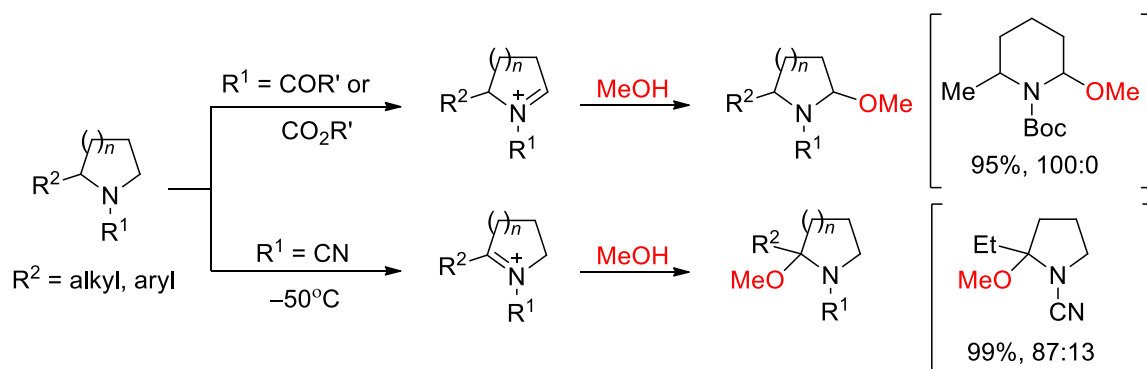


**Scheme 1.10:** Mediated electrocatalysis of a key intermediate in the synthesis of daucene

The development of the Shono oxidation (functionalization of the  $\alpha$ -carbon of alkyl amides in an undivided cell) in 1975<sup>47,48</sup> represents one of the most widely studied and utilized electroorganic transformations to this day (Scheme 1.11). Recent reports by Onomura and co-workers demonstrated reversal of the regioselectivity of the Shono oxidation with cyanoamines where methoxylation at a more substituted position is favored (Scheme 1.12).<sup>49,50</sup>



**Scheme 1.11:** Shono oxidation of alkyl amide in methanol



**Scheme 1.12:** Shono oxidation of amides, carbamates, and cyanoamines

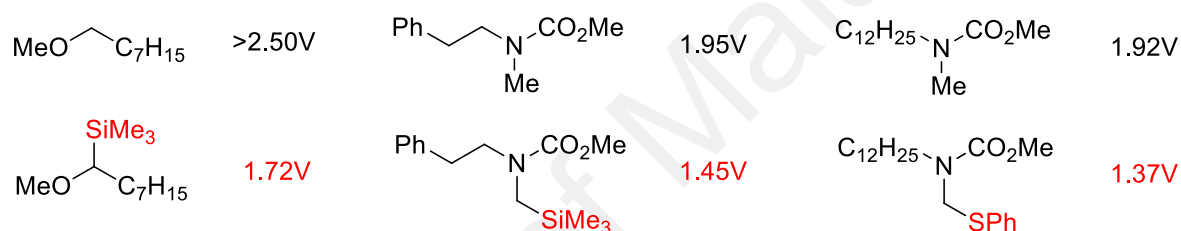
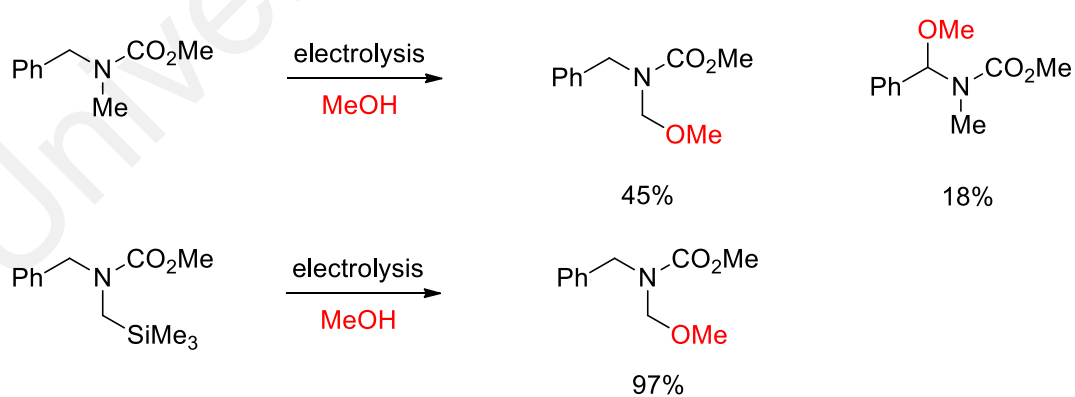
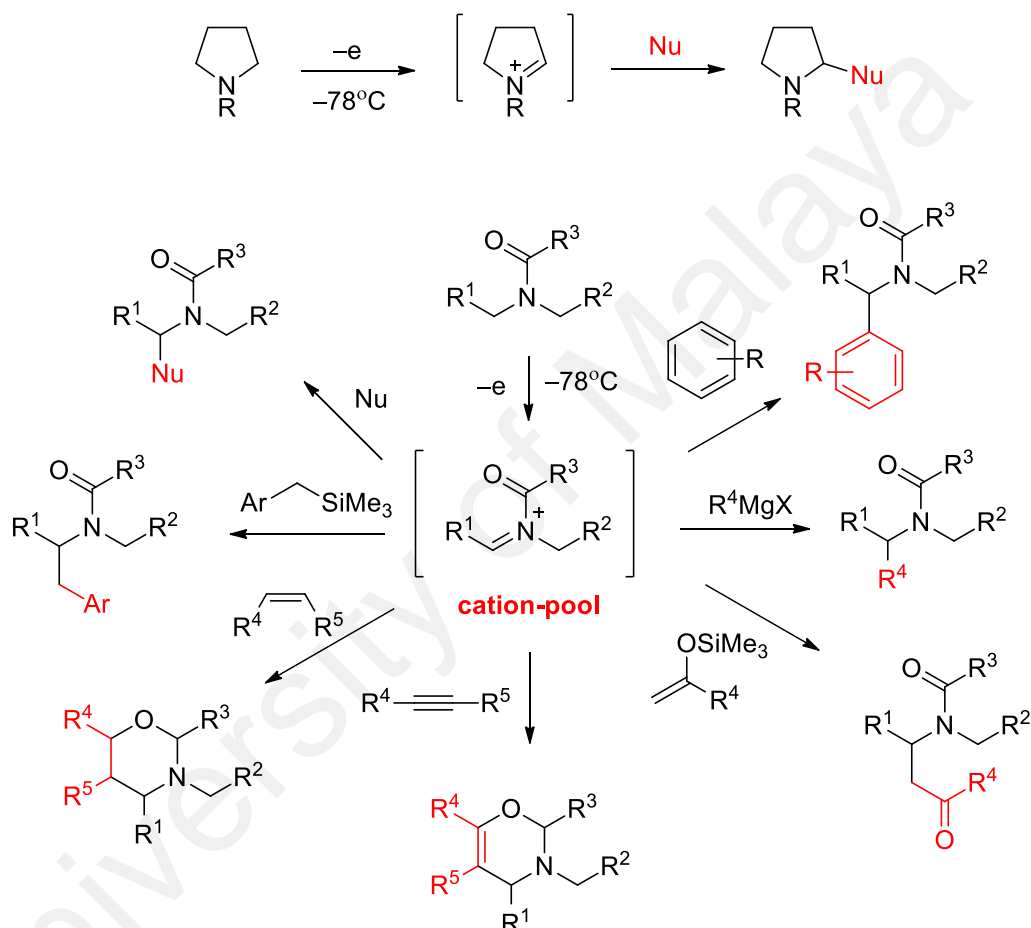


**Figure 1.6:** Effect of silicon and sulfur electroauxiliaries on the anodic potentials



**Scheme 1.13:** Regioselective methoxylation of silyl-substituted carbamates

Yoshida introduced the concept of electroauxiliaries in 1986 to lower the electrochemical potentials of substrate molecules by incorporating silicon- and sulfur-containing functional groups (Figure 1.6), thus allowing controls over regio- and chemoselectivities (Scheme 1.13).<sup>3,51</sup>



**Scheme 1.14:** The cation-pool method and various downstream functionalization

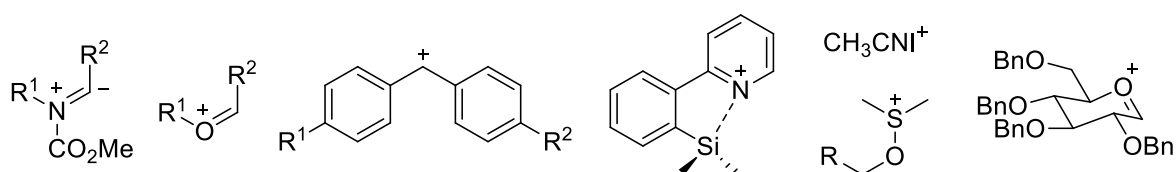
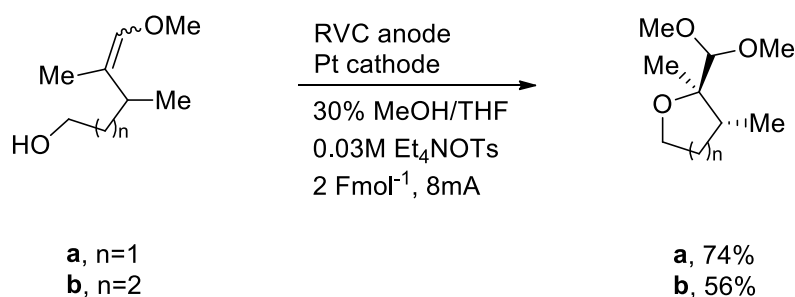


**Figure 1.7:** Stabilized cations generated for various electrochemical applications

Yoshida's cation pool concept has evolved into a versatile and valuable tool in electrosynthesis, allowing stabilized cations to engage nucleophilic species in various downstream functionalization (Scheme 1.14).<sup>3</sup> The generated cations such as the *N*-acyliminium,<sup>52–57</sup> alkoxy-carbenium,<sup>58</sup> diarylcarbenium,<sup>59–62</sup> silyl<sup>63</sup>, iodine<sup>64,65</sup> alkoxy-sulfonium,<sup>66,67</sup> and glycosyl cations,<sup>68–70</sup> (Figure 1.7), have enhanced lifetimes by carrying out the anodic oxidation under cryogenic conditions which allows accumulation of the reactive cations and creation of a pool of stabilized cations.<sup>57,71</sup>

Moeller's studies of anodic olefin coupling based on the polarity of the generated cation radicals have led to numerous modern electrosynthetic applications.<sup>2</sup> The polarity inversion of a substrate (umpolung) as a result of electron transfer has enabled reactions between electrophile and electrophile, or nucleophile with nucleophile to be carried out in a single step.<sup>2,24,28,72</sup> Moeller and co-workers reported systematic studies of intramolecular cyclization that arises from the attack on alkene cation radicals with nucleophiles (Scheme 1.15) such as oxygen,<sup>73</sup> nitrogen,<sup>14</sup> and carbon<sup>74</sup> by transforming a relatively electron-rich, essentially nucleophilic compound, into an electron-deficient cation radical that tends to be electrophilic, as exemplified by the cation radicals generated from enol ethers (Figure 1.8).<sup>75,76</sup> Furthermore the ability to change the polarity and/or the potential of the electrode easily means that a given function can be converted selectively, provided the reduction or oxidation potential differs by only *ca.* 200 mV from those of the other electroactive groups, in compounds with complex skeletons and multiple functional groups.<sup>24</sup>



**Scheme 1.15:** Oxidative cyclization between an alkene cation radical and an alcohol nucleophile<sup>73</sup>

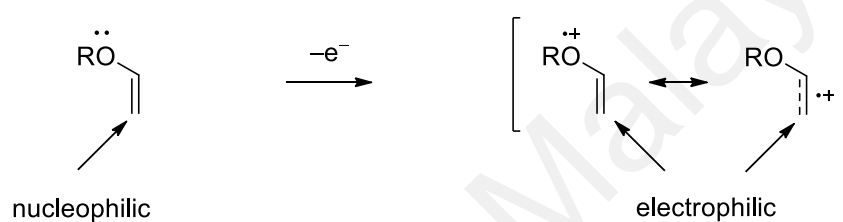
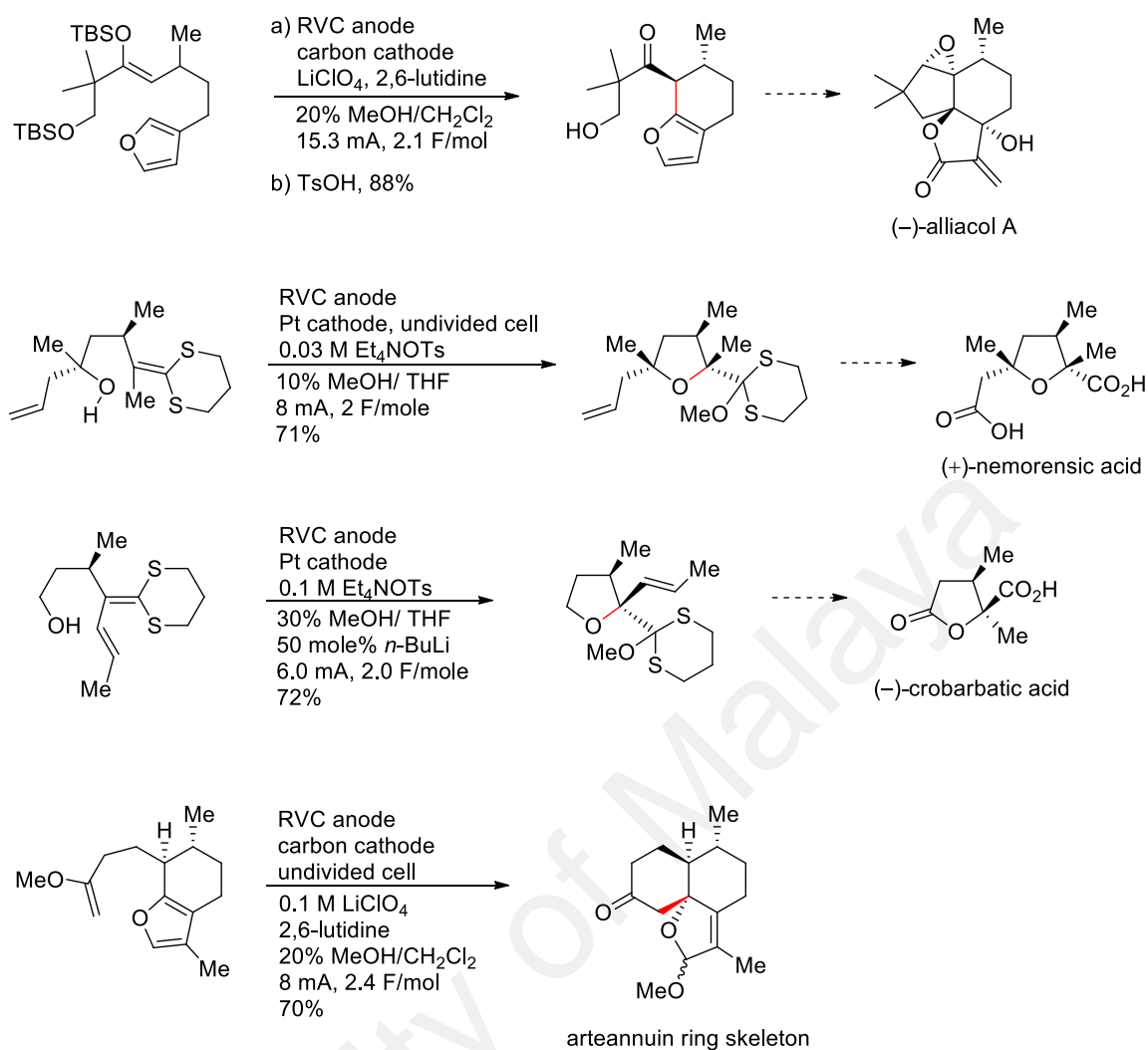


**Figure 1.8:** Reversal of polarity in enol ethers upon one-electron oxidation

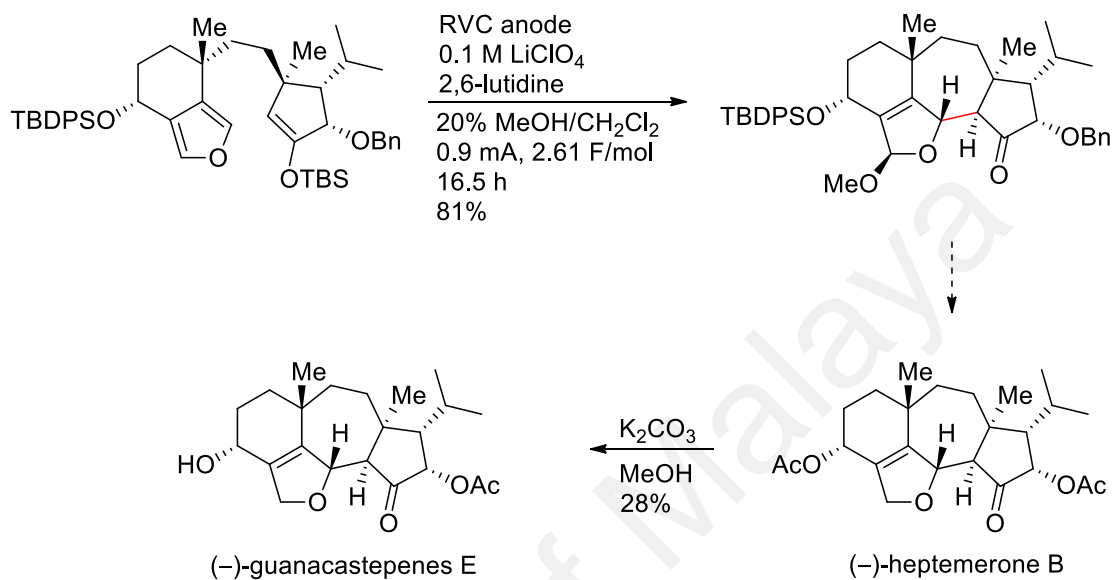
The tremendous structural diversity of natural products, coupled with their useful biological activities, continues to attract the attention of synthetic chemists. Many synthetic targets incorporate cyclic moieties where cyclizations are usually achieved with chemical reagents but where increasingly electrochemistry offers a viable option. A large variety of different natural products were synthesized by including an intramolecular anodic olefin coupling reaction as a key step. Examples from the Moeller group include the synthesis of (-)-alliacol A,<sup>77</sup> (+)-nemorensic acid,<sup>78</sup> (-)-crobarbatic acid,<sup>79</sup> and the arteannuin ring skeleton<sup>74</sup> (Scheme 1.16).



**Scheme 1.16:** Anodic olefin coupling reaction as key steps in the syntheses of (-)-alliacol A, (+)-nemorensic acid, (-)-crobarbatic acid, and the arteannuin ring skeleton

In his synthesis of (-)-heptemerone B and (-)-guanacastepenes E, Trauner et al. prepared a challenging seven-membered ring intermediate compound by adopting the anodically-mediated silyl enol ether/furan coupling in the key step of the cyclization<sup>80,81</sup> (Scheme 1.17). Wright et al. on the other hand, reported the synthesis of the hemigeran ring skeleton by utilizing the anodic coupling of the trimethylsilyl enol ether with the phenyl group to give the tricyclic hamigeran skeleton<sup>82</sup> (Scheme 1.18). Wright and co-workers also reported the synthesis of the cyathin ring skeleton by the oxidative

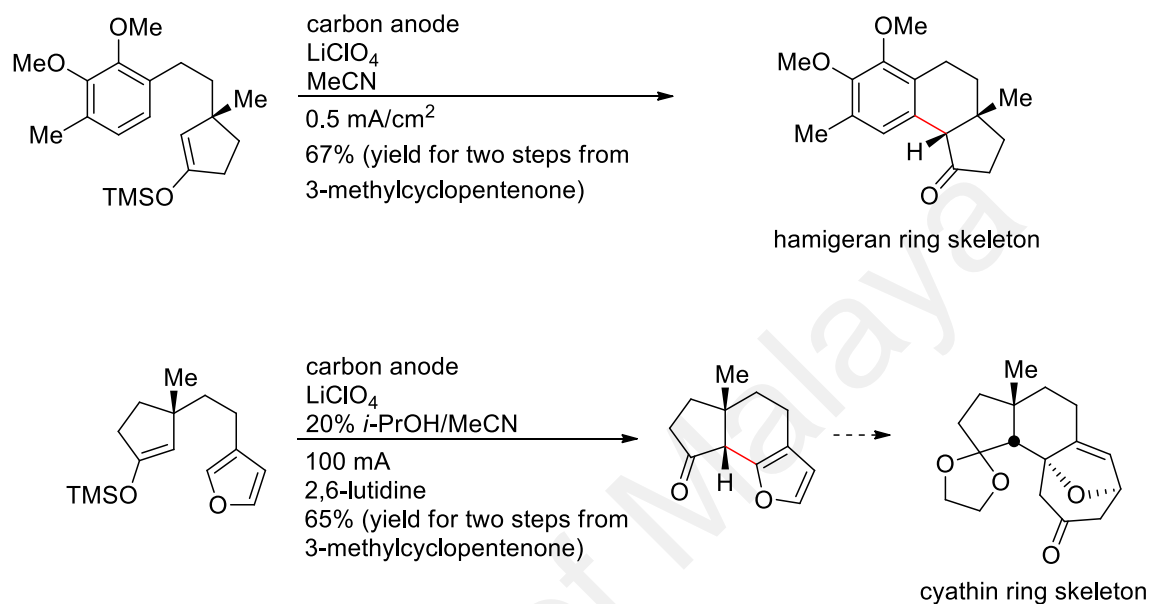
coupling of the silyl enol ether with the furan ring to give the tricyclic ketone<sup>83</sup> (Scheme 1.18).



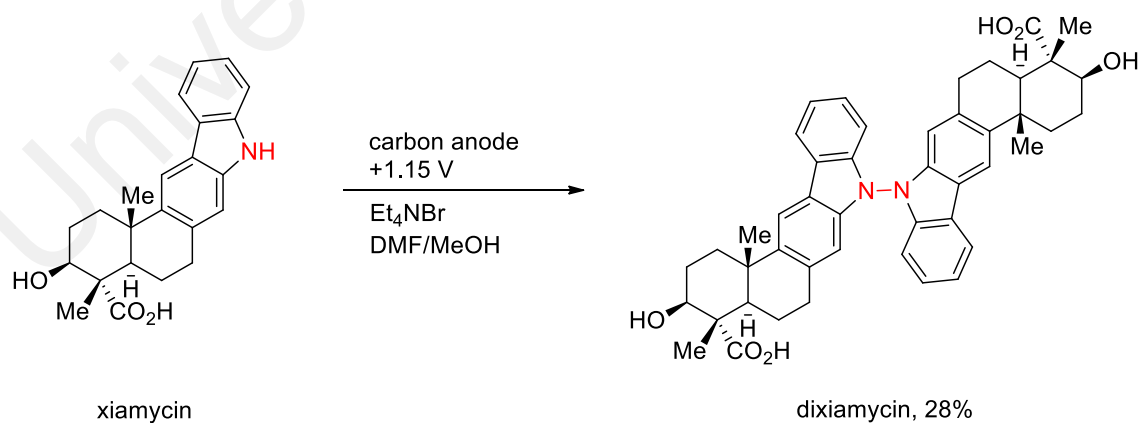
**Scheme 1.17:** Anodic olefin coupling reaction as the key step in the synthesis of (-)-heptemerone B and (-)-guanacastepene E

The role of electrochemistry in the design and synthesis of natural products is increasing, as are the increasing number of organic chemists who realize the importance and utility of electrochemical tools. It is increasingly apparent that the important advances that continue to be made by electrochemists are attracting the attention of organic chemists who have previously not embraced the field. Additionally, electrochemical transformations can lead to superior results in situations where conventional methods fail. Examples include the synthesis of the central seven-membered ring of guanacastepene (Scheme 1.17) where conventional transformations using rhodium-catalyzed cyclopropanation/rearrangement or diazotization reactions did not deliver the desired compound,<sup>80</sup> and Baran's synthesis of dixiamycin, where the use of controlled potential anodic oxidation (in the face of a singular lack of success using

chemical oxidants) facilitated the N,N-dimerization of the carbazole monomers in the presence of carboxylic acid and alcohol groups (Scheme 1.19).<sup>84</sup>

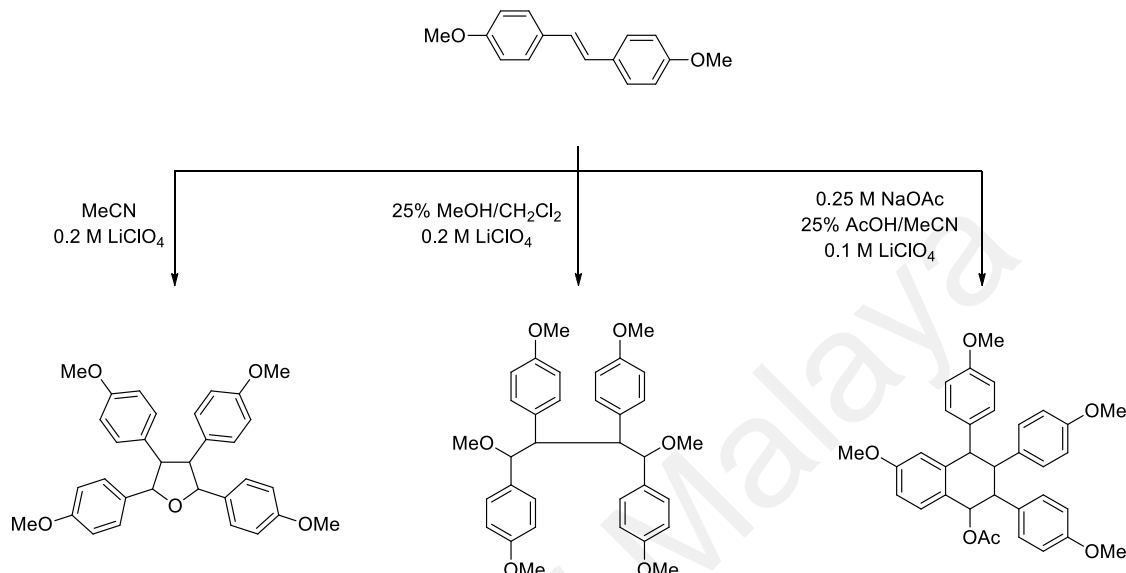


**Scheme 1.18:** Anodic olefin coupling reactions as key steps in the syntheses of hamigeran and cyathin ring skeletons



**Scheme 1.19:** Total synthesis of dixiamycin via an electrochemical N,N-dimerization

## 1.5 Electrochemical Oxidation of Stilbenes (1,2-Diarylalkenes) – Anodically-Generated Stilbene Cation Radicals



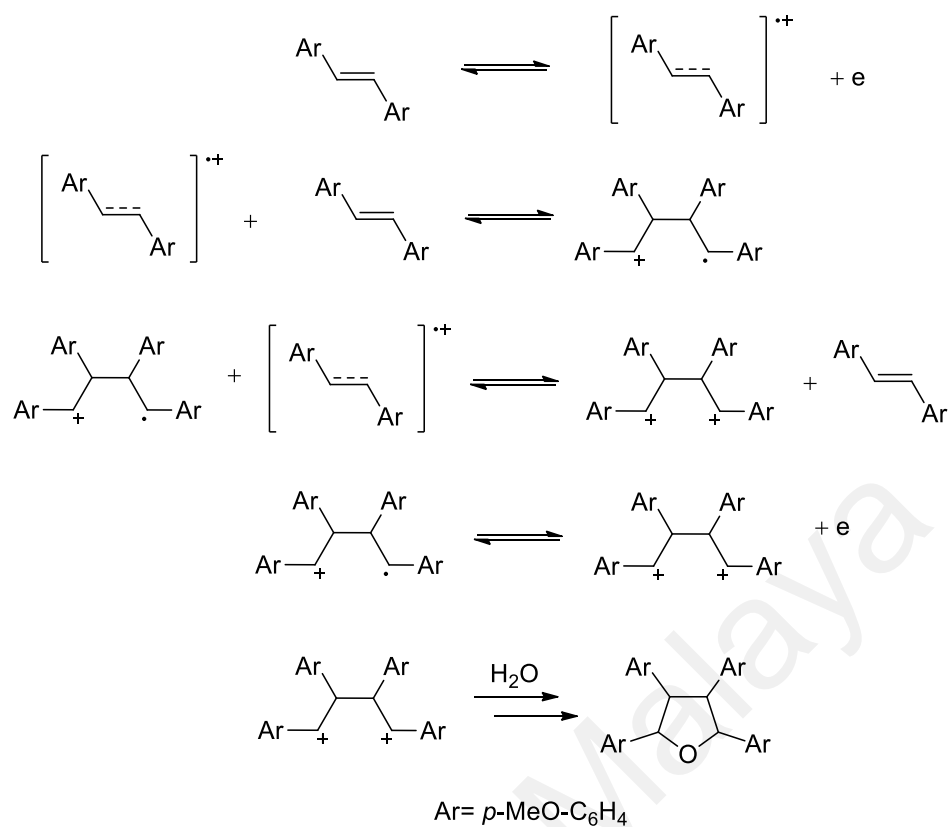
**Scheme 1.20:** Products from anodic oxidation of 4,4'-dimethoxystilbene as reported by Steckhan<sup>35</sup> and Ebersson<sup>32</sup>

Another aspect of electroorganic chemistry, besides applications in synthesis, is the study of the reactive intermediates (cation and anion radicals) that are the first formed intermediates in the oxidation or reduction process. An example is the stilbene cation radical generated by anodic oxidation of stilbenes or 1,2-diarylalkenes, which forms the subject of interest of the present study. Steckhan carried out a thorough kinetic and product study of the anodic oxidation of 4,4'-dimethoxystilbene under different conditions. He reported the quantitative formation of 2,3,4,5-tetraanisyltetrahydrofuran (without stereochemical assignment) as the sole product when the anodic oxidation of 4,4'-dimethoxystilbene was carried out in acetonitrile followed by aqueous workup (Scheme 1.20). When the electrooxidation was carried out in 25% MeOH/CH<sub>2</sub>Cl<sub>2</sub>, the main product was the dimethoxylated open-chain dimer<sup>35</sup> (Scheme 1.20). Ebersson, on

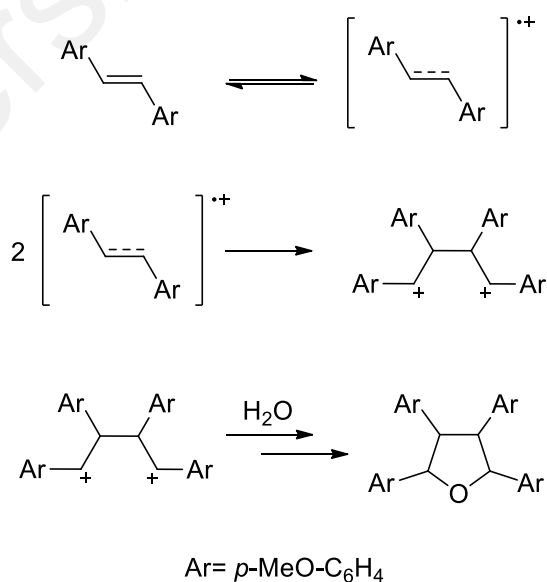
the other hand, reported the isolation of an acetylated tetralin when the reaction was carried out in 25% AcOH/MeCN/0.10 M LiClO<sub>4</sub> in the presence of 0.25 M NaOAc, but did not furnish full characterization details or a mechanism to explain the formation of the tetralin product<sup>32</sup> (Scheme 1.20).

Steckhan proposed that the formation of the tetraanisyltetrahydrofuran product involved nucleophilic capture of the dicationic species, formed as a result of either electrophilic addition to the native stilbene by the stilbene cation radical followed by a second electron transfer (Scheme 1.21), or through cation radical dimerization (Scheme 1.22). The kinetic studies concluded that in the absence of a nucleophile, the two pathways take place simultaneously, however, Steckhan added that under the conditions of preparative electrolysis of 4,4'-dimethoxystilbene in acetonitrile under diffusion controlled conditions, the cation radical dimerization mechanism should by far be the dominant reaction<sup>35</sup> (Scheme 1.22).

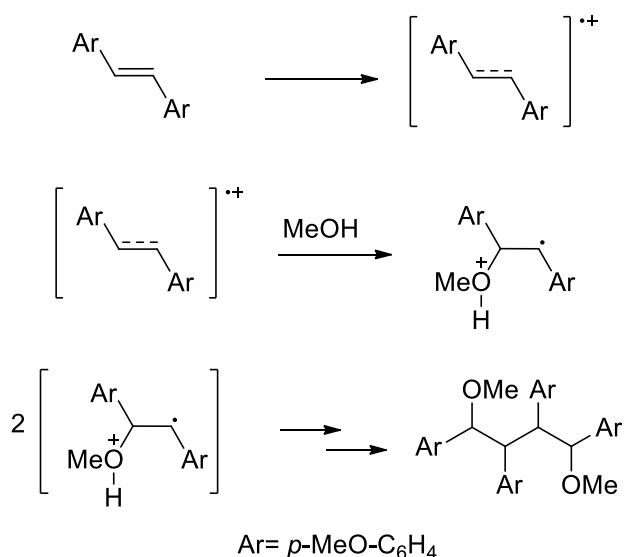
In addition, it was also noted that during preparative electrolysis of 4,4'-dimethoxystilbene, in 25% MeOH/CH<sub>2</sub>Cl<sub>2</sub>, reaction of the stilbene cation radical with methanol was clearly favored, since in the presence of high methanol concentrations, the cation radical dimerization step cannot compete with nucleophilic attack of the cation radical by methanol<sup>35</sup> (Scheme 1.23). On the other hand, formation of the acetylated tetralin in Ebersson's study on the anodic oxidation of 4,4'-dimethoxystilbene, only a limited mechanism was provided involving initial cation radical coupling followed by addition of the acetate nucleophile en route to the tetralin product<sup>32</sup> (Scheme 1.24).



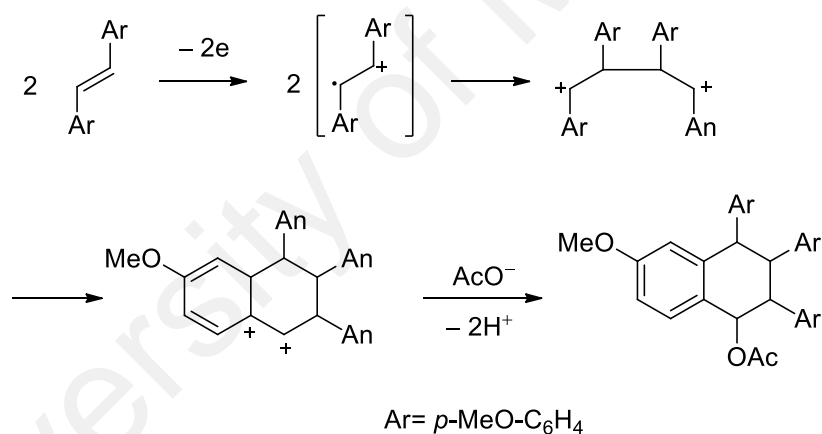
**Scheme 1.21:** Formation of tetraanisyltetrahydrofuran via cation radical electrophilic addition to native stilbene<sup>35</sup>



**Scheme 1.22:** Formation of tetraanisyltetrahydrofuran via cation radical dimerization<sup>35</sup>



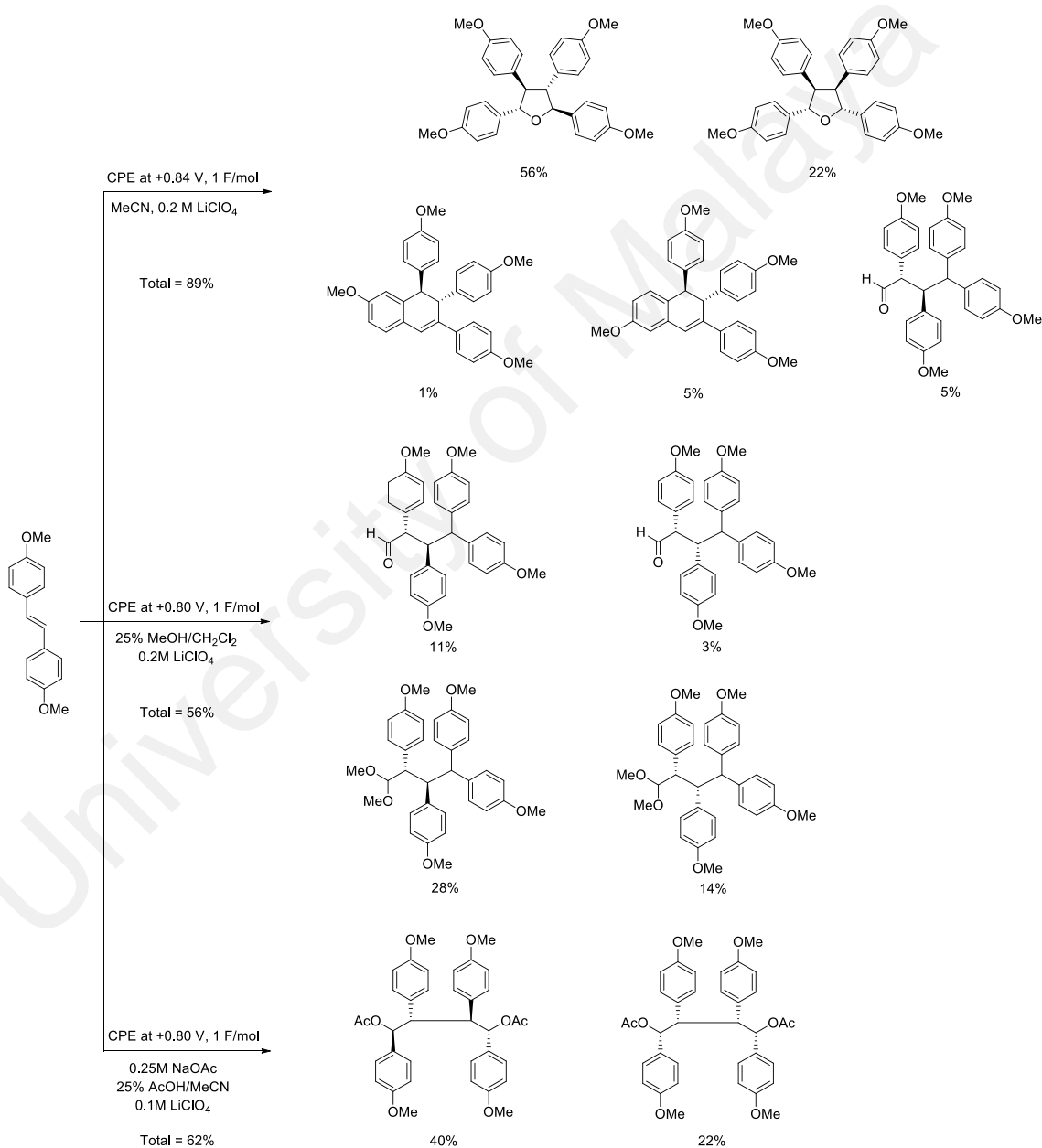
**Scheme 1.23:** Formation of the dimethoxylated open-chain dimer<sup>35</sup>



**Scheme 1.24:** Formation of the acetylated tetralin<sup>32</sup>

A detailed reinvestigation of the electrochemical oxidation of 4,4'-dimethoxystilbene under different conditions was recently reported by Hong and co-workers<sup>85</sup> (Scheme 1.25). Anodic oxidation of 4,4'-dimethoxystilbene in MeCN/0.2 M LiClO<sub>4</sub> followed by aqueous workup, gave a product mixture comprising the stereoisomeric 2,3,4,5-tetraanisyl-tetrahydrofurans as the major product, accompanied by the regioisomeric dehydrotetralins and an aldehyde as minor products, whereas anodic oxidation of 4,4'-

dimethoxystilbene in 25% MeOH/CH<sub>2</sub>Cl<sub>2</sub>/0.2 M LiClO<sub>4</sub> followed by aqueous workup, gave a product mixture comprising the diastereoisomeric aldehydes and the corresponding acetals. Anodic oxidation of 4,4'-dimethoxystilbene in 25% AcOH/MeCN/0.1 M LiClO<sub>4</sub> in the presence of NaOAc (0.25 M) (Ebersson's conditions) on the other hand, gave the diastereoisomeric diacetate products (Scheme 1.25).

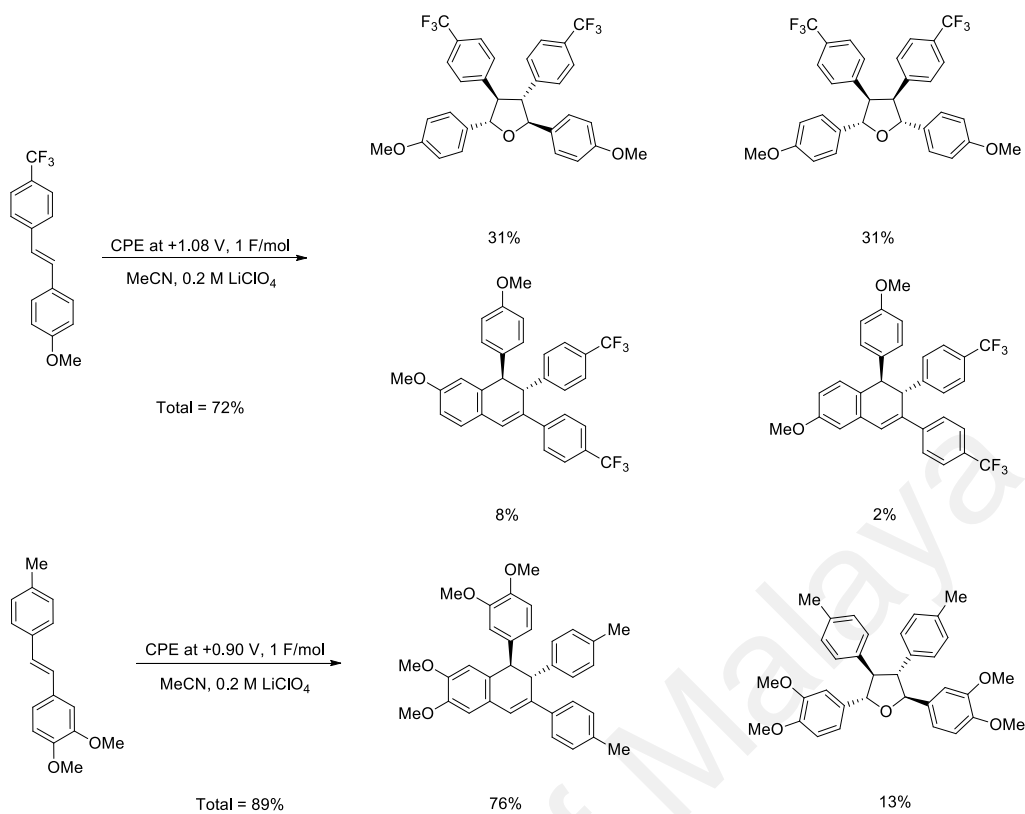


**Scheme 1.25:** Products from anodic oxidation of 4,4'-dimethoxystilbene as reported by Hong<sup>85</sup>

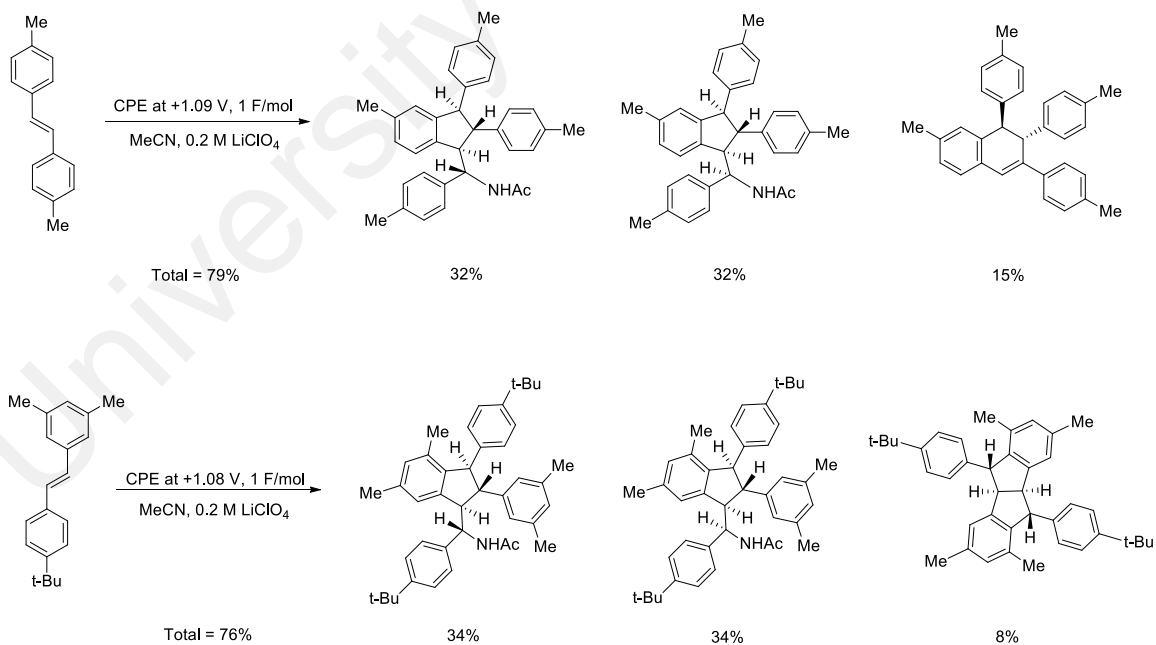
Following the thorough reinvestigation of the products formed from the anodic oxidation of 4,4'-dimethoxystilbene, a series of differentially disubstituted stilbenes were investigated to determine the effect of aromatic substitution on the course of the electrooxidation. These oxidations were carried out in MeCN/0.2 M LiClO<sub>4</sub> with standard aqueous workup. From the viewpoint of product type, the aromatic substituents appear to fall into three main categories (Scheme 1.26), viz.:

- i) Substrates in which the nature and position of the aromatic substituents give rise to essentially the same products as 4,4'-dimethoxystilbene, for example, tetraaryltetrahydrofurans, dehydrotetalins, and aldehydes (*p*-OMe or *p*-NMe<sub>2</sub> on one ring and X on the other ring, where X = *o*-OMe or *p*-alkyl, or *m*- or *p*-EWG; e.g., 4-methoxy-4'-trifluoromethylstilbene);
- ii) Substrates that give rise to a mixture of indanyl (or tetralinyl) acetamides and dehydrotetalins (or pallidols) (both or one ring substituted by alkyl groups, e.g., 4,4'-dimethylstilbene);
- iii) Substrates where strategic placement of donor groups, such as OMe and OH, leads to the formation of ampelopsin F and pallidol-type carbon skeletons (e.g., 4,3',4'-trimethoxystilbene).

Group 1

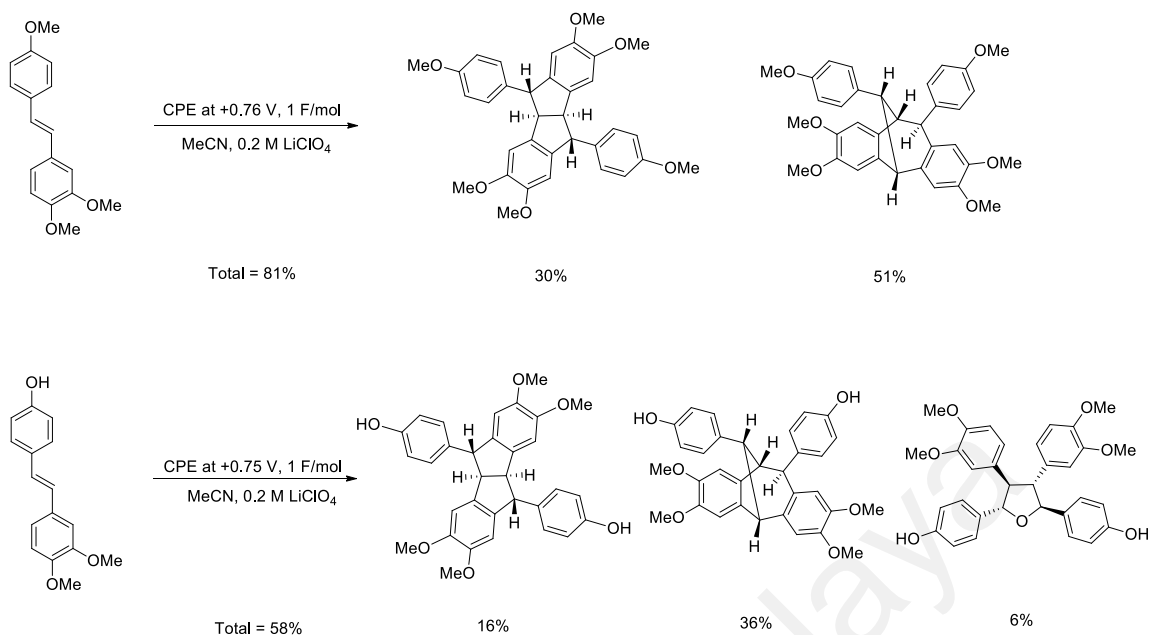


Group 2



**Scheme 1.26:** Effect of aromatic substitution on the nature and distribution of the products

### Group 3



Scheme 1.26, continued

## 1.6 Objective of Present Study

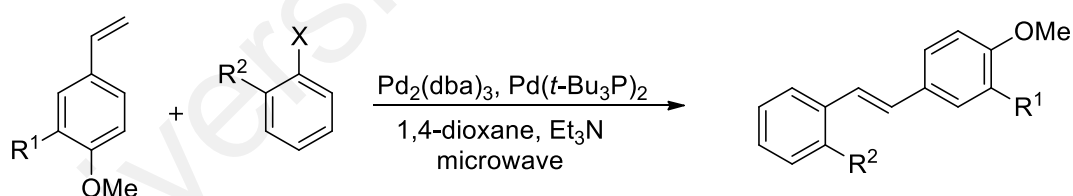
The objective of the present study is to extend the systematic studies of the chemistry of anodically generated 4-methoxystilbene cation radicals, with the primary focus on the effect of ortho'-substituted nucleophilic groups such as OH, NH<sub>2</sub> (or NHR), CH<sub>2</sub>OH, CH<sub>2</sub>NH<sub>2</sub> (or CH<sub>2</sub>NHR), CO<sub>2</sub>H, and CH=CH<sub>2</sub>, as well as non-nucleophilic groups such as CONH<sub>2</sub> and CH=O, on the nature and distribution of products formed during anodic oxidation, in order to gain a deeper understanding of stilbene cation radical reactivity.

## CHAPTER 2: RESULTS AND DISCUSSION

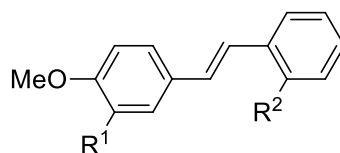
### 2.1 Synthesis of Stilbenes

A series of ortho'-substituted methoxystilbenes (total of 50) were selected and prepared for the purpose of the present study (Schemes 2.1–2.6, Figure 2.1, and Table 2.1). The required stilbenes were synthesized by Heck coupling of the appropriate styrene and aryl halide precursors.<sup>85–88</sup>

Cyclic voltammograms were first obtained to determine the appropriate potential for carrying out controlled potential electrolysis (CPE). Preparative electrolyses were carried out at the first anodic wave until consumption of *ca.* 0.9–1.0 F, after which the products were separated by preparative radial chromatography (Chromatotron) and/or HPLC.



**Scheme 2.1:** Synthesis of stilbenes **1**, **3**, **5**, **6**, **8**, **32**, **34**, **35**, **36**, **37**, **38**, **39**, **41**, **44**, **46**, **47**, and **48** by Heck coupling



- |   |   |
|---|---|
| 1: R <sup>1</sup> = H; R <sup>2</sup> = OH                                    | 26: R <sup>1</sup> = OMe; R <sup>2</sup> = CH <sub>2</sub> NHAc                 |
| 2: R <sup>1</sup> = H; R <sup>2</sup> = OSiMe <sub>3</sub>                    | 27: R <sup>1</sup> = OMe; R <sup>2</sup> = CH <sub>2</sub> NHCO <sub>2</sub> Me |
| 3: R <sup>1</sup> = OMe; R <sup>2</sup> = OH                                  | 28: R <sup>1</sup> = H; R <sup>2</sup> = CO <sub>2</sub> H                      |
| 4: R <sup>1</sup> = OMe; R <sup>2</sup> = OSiMe <sub>3</sub>                  | 29: R <sup>1</sup> = OMe; R <sup>2</sup> = CO <sub>2</sub> H                    |
| 5: R <sup>1</sup> = H; R <sup>2</sup> = NH <sub>2</sub>                       | 30: R <sup>1</sup> = H; R <sup>2</sup> = CH=CH <sub>2</sub>                     |
| 6: R <sup>1</sup> = OMe; R <sup>2</sup> = NH <sub>2</sub>                     | 31: R <sup>1</sup> = OMe; R <sup>2</sup> = CH=CH <sub>2</sub>                   |
| 7: R <sup>1</sup> = H; R <sup>2</sup> = NHAc                                  | 32: R <sup>1</sup> = H; R <sup>2</sup> = OMe                                    |
| 8: R <sup>1</sup> = H; R <sup>2</sup> = NHBoc                                 | 33: R <sup>1</sup> = H; R <sup>2</sup> = OAc                                    |
| 9: R <sup>1</sup> = H; R <sup>2</sup> = NHCO <sub>2</sub> Me                  | 34: R <sup>1</sup> = H; R <sup>2</sup> = CN                                     |
| 10: R <sup>1</sup> = H; R <sup>2</sup> = NHTs                                 | 35: R <sup>1</sup> = H; R <sup>2</sup> = NO <sub>2</sub>                        |
| 11: R <sup>1</sup> = H; R <sup>2</sup> = NHNs                                 | 36: R <sup>1</sup> = H; R <sup>2</sup> = CF <sub>3</sub>                        |
| 12: R <sup>1</sup> = OMe; R <sup>2</sup> = NHAc                               | 37: R <sup>1</sup> = H; R <sup>2</sup> = CO <sub>2</sub> Me                     |
| 13: R <sup>1</sup> = OMe; R <sup>2</sup> = NHCO <sub>2</sub> Me               | 38: R <sup>1</sup> = H; R <sup>2</sup> = CONHAc                                 |
| 14: R <sup>1</sup> = OMe; R <sup>2</sup> = NHTs                               | 39: R <sup>1</sup> = OMe; R <sup>2</sup> = OMe                                  |
| 15: R <sup>1</sup> = OMe; R <sup>2</sup> = NHNs                               | 40: R <sup>1</sup> = OMe; R <sup>2</sup> = OAc                                  |
| 16: R <sup>1</sup> = H; R <sup>2</sup> = CH <sub>2</sub> OH                   | 41: R <sup>1</sup> = H; R <sup>2</sup> = CHO                                    |
| 17: R <sup>1</sup> = H; R <sup>2</sup> = CH <sub>2</sub> OSiMe <sub>3</sub>   | 42: R <sup>1</sup> = H; R <sup>2</sup> = CH(OMe) <sub>2</sub>                   |
| 18: R <sup>1</sup> = OMe; R <sup>2</sup> = CH <sub>2</sub> OH                 | 43: R <sup>1</sup> = H; R <sup>2</sup> = CH(OCH <sub>2</sub> CH <sub>2</sub> O) |
| 19: R <sup>1</sup> = OMe; R <sup>2</sup> = CH <sub>2</sub> OSiMe <sub>3</sub> | 44: R <sup>1</sup> = OMe; R <sup>2</sup> = CHO                                  |
| 20: R <sup>1</sup> = H; R <sup>2</sup> = CH <sub>2</sub> NHNs                 | 45: R <sup>1</sup> = OMe; R <sup>2</sup> = CH(OMe) <sub>2</sub>                 |
| 21: R <sup>1</sup> = H; R <sup>2</sup> = CH <sub>2</sub> NHTs                 | 46: R <sup>1</sup> = OMe; R <sup>2</sup> = CO <sub>2</sub> Me                   |
| 22: R <sup>1</sup> = H; R <sup>2</sup> = CH <sub>2</sub> NHAc                 | 47: R <sup>1</sup> = H; R <sup>2</sup> = CONH <sub>2</sub>                      |
| 23: R <sup>1</sup> = H; R <sup>2</sup> = CH <sub>2</sub> NHCO <sub>2</sub> Me | 48: R <sup>1</sup> = OMe; R <sup>2</sup> = CONH <sub>2</sub>                    |
| 24: R <sup>1</sup> = OMe; R <sup>2</sup> = CH <sub>2</sub> NHTs               | 49: R <sup>1</sup> = H; R <sup>2</sup> = CH <sub>2</sub> NH <sub>2</sub>        |
| 25: R <sup>1</sup> = OMe; R <sup>2</sup> = CH <sub>2</sub> NHNs               | 50: R <sup>1</sup> = OMe; R <sup>2</sup> = CH <sub>2</sub> NH <sub>2</sub>      |

**Figure 2.1:** List of synthesized stilbenes 1–50

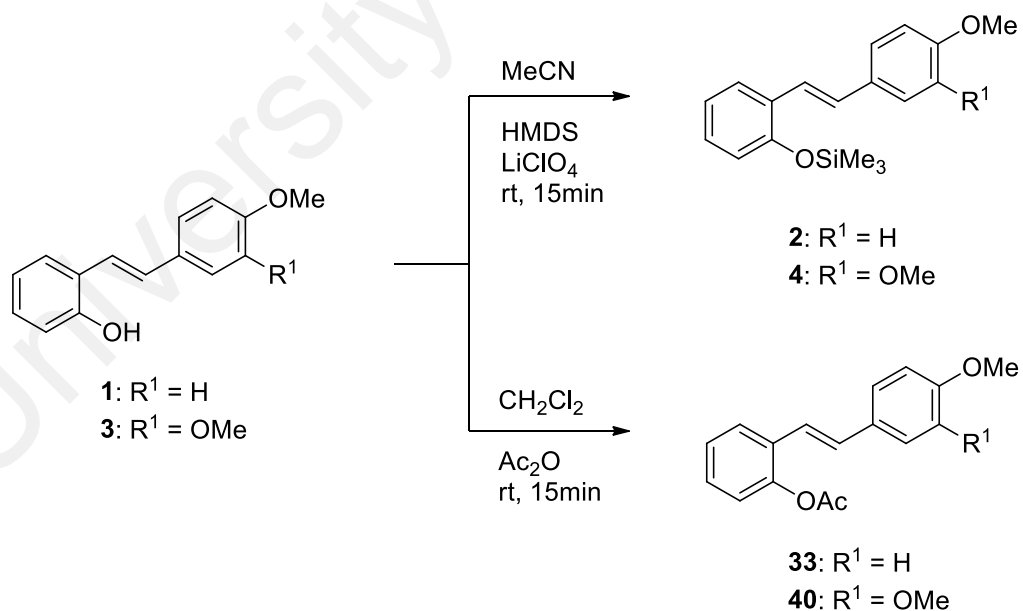
**Table 2.1:** Yield, melting point, and anodic half-peak potential of stilbenes (**1–50**)

Entry	Stilbene	% Yield	Melting Point (°C)	$E_{p/2}$ (V) <sup>a</sup>
1	<b>1</b>	85	120–122	+0.81
2	<b>2</b>	89	68–70	+0.84
3	<b>3</b>	90	–	+0.79
4	<b>4</b>	87	73–75	+0.83
5	<b>5</b>	70	108–110	+0.91
6	<b>6</b>	89	117–120	– <sup>b</sup>
7	<b>7</b>	70	123–125	+0.90
8	<b>8</b>	82	109–111	+0.99
9	<b>9</b>	86	118–120	+0.93
10	<b>10</b>	75	–	+0.91
11	<b>11</b>	90	–	+0.93
12	<b>12</b>	90	108–110	+1.00
13	<b>13</b>	70	–	+0.94
14	<b>14</b>	83	153–155	+0.83
15	<b>15</b>	71	–	+0.88
16	<b>16</b>	76	142–143	+0.93
17	<b>17</b>	76	–	+0.86
18	<b>18</b>	79	–	+0.82
19	<b>19</b>	75	–	+0.82
20	<b>20</b>	62	–	+0.88
21	<b>21</b>	61	–	+0.85
22	<b>22</b>	86	130–133	+0.87
23	<b>23</b>	72	122–124	+0.84
24	<b>24</b>	62	–	+0.75
25	<b>25</b>	60	–	+0.87
26	<b>26</b>	67	–	+0.87
27	<b>27</b>	64	113–115	+0.73
28	<b>28</b>	96	–	+0.90
29	<b>29</b>	98	–	+0.85
30	<b>30</b>	57	–	+0.84
31	<b>31</b>	62	–	+0.73
32	<b>32</b>	89	80–82	+0.72
33	<b>33</b>	61	70–71	+0.94
34	<b>34</b>	79	84–86	+0.97
35	<b>35</b>	73	66–68	+1.00
36	<b>36</b>	71	40–41	+1.06
37	<b>37</b>	97	77–78	+0.95

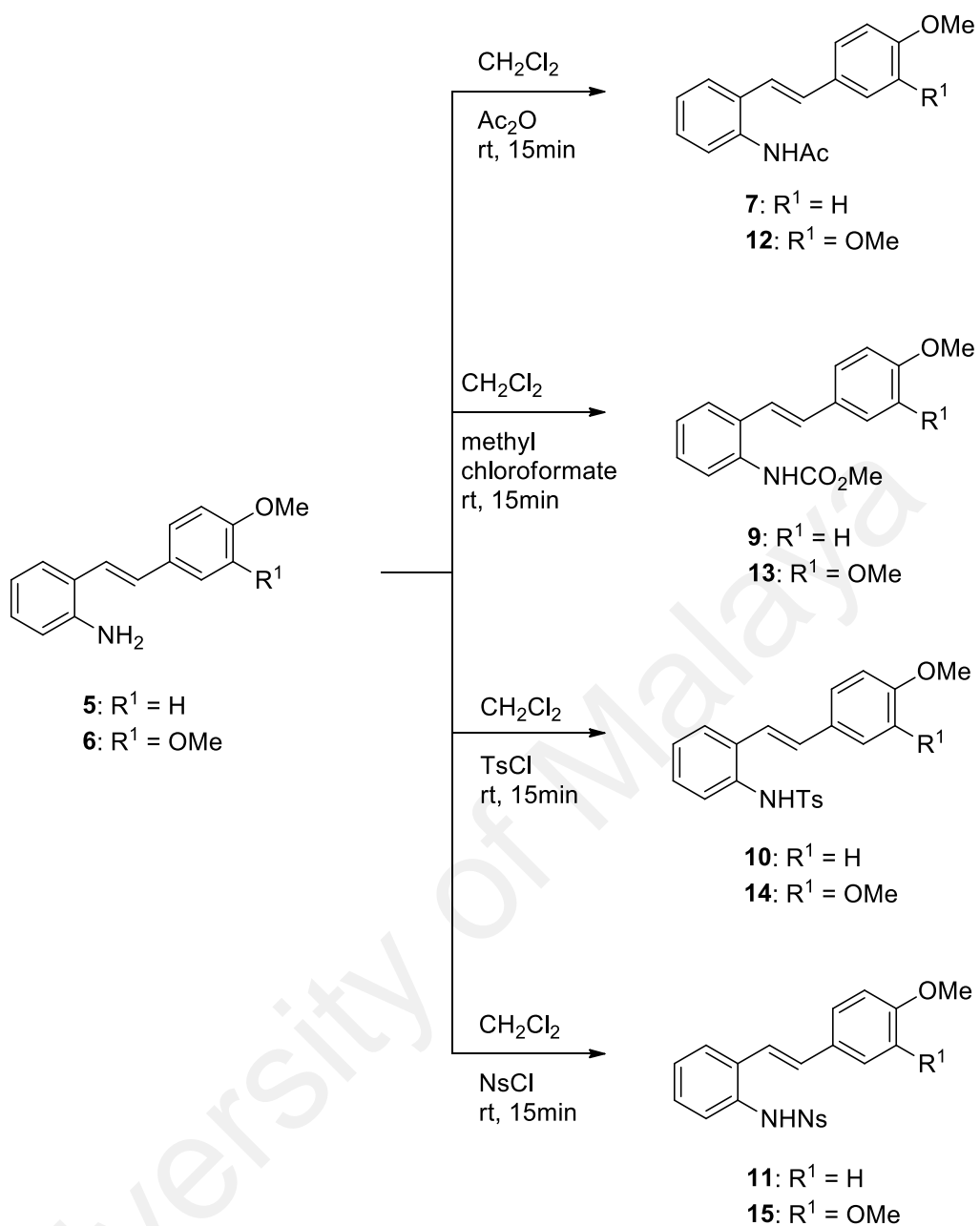
**Table 2.1, continued**

38	<b>38</b>	70	149–151	+0.96
39	<b>39</b>	91	102–104	+0.76
40	<b>40</b>	65	80–82	+0.85
41	<b>41</b>	90	116–118	+0.94
42	<b>42</b>	96	–	+0.92
43	<b>43</b>	80	–	+0.93
44	<b>44</b>	95	125–127	+1.05
45	<b>45</b>	94	–	+0.97
46	<b>46</b>	92	–	+1.03
47	<b>47</b>	81	150–153	– <sup>b</sup>
48	<b>48</b>	79	180–182	– <sup>b</sup>
49	<b>49</b>	75	90–92	– <sup>b</sup>
50	<b>50</b>	50	108–110	– <sup>b</sup>

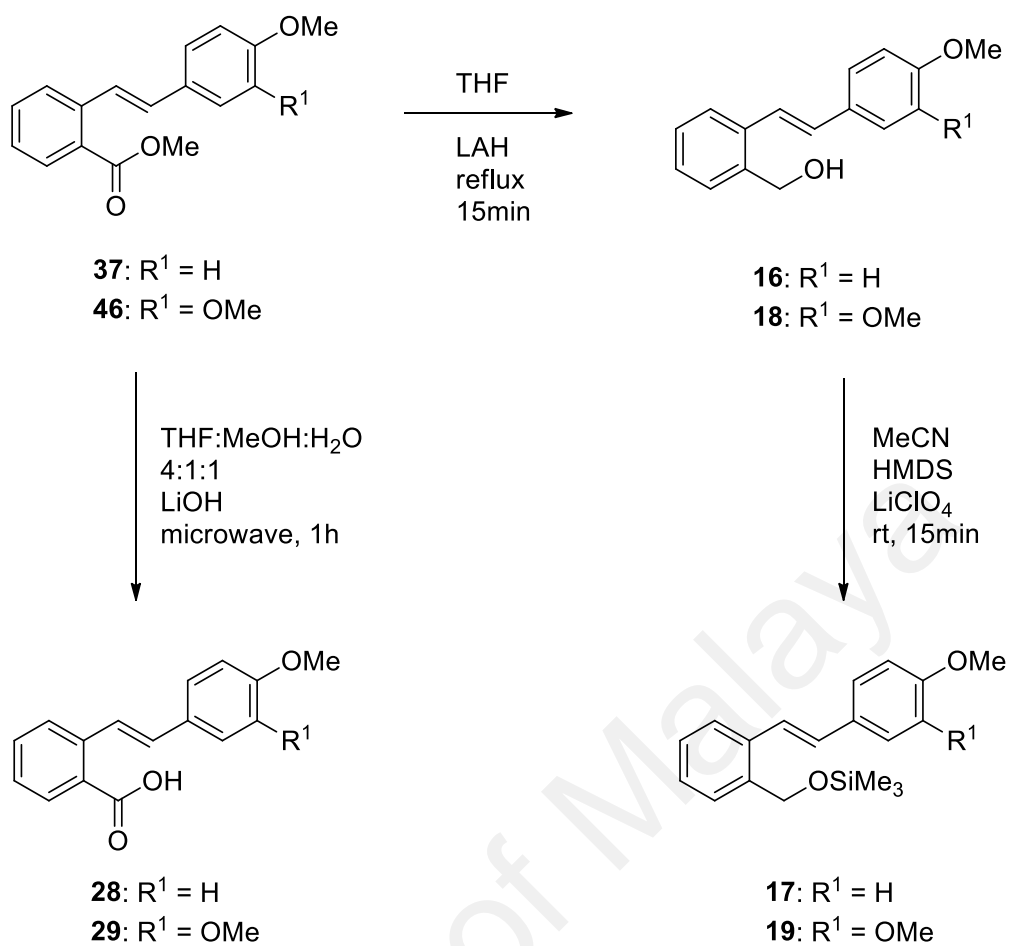
<sup>a</sup> $E_{p/2}$  (V) = anodic half-peak potential (Pt anode, Pt cathode, versus Ag/AgNO<sub>3</sub> in MeCN/0.2 M LiClO<sub>4</sub>), <sup>b</sup>Not analyzed.



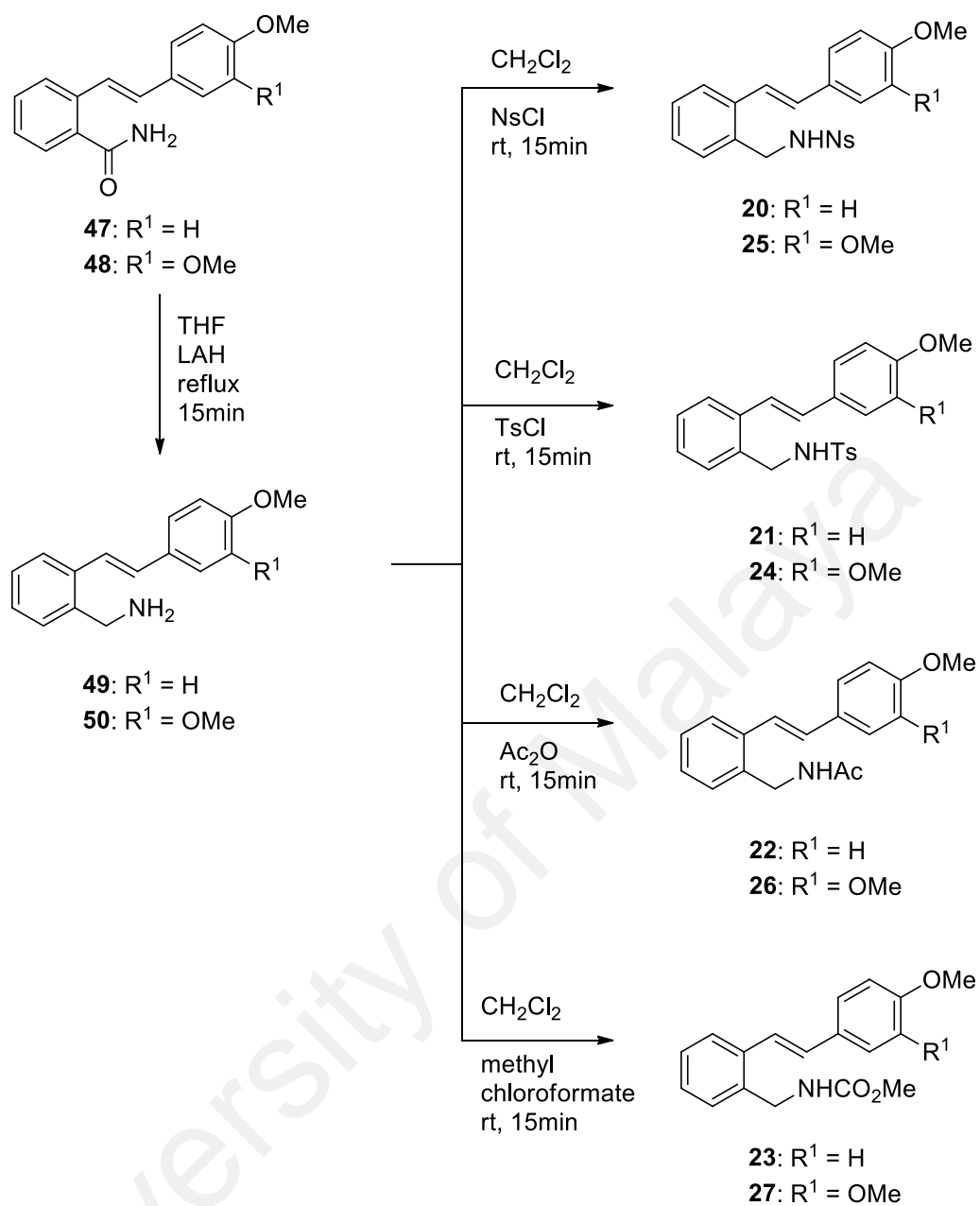
**Scheme 2.2:** Synthesis of stilbenes **2**, **4**, **33**, and **40** from stilbenes **1** and **3**



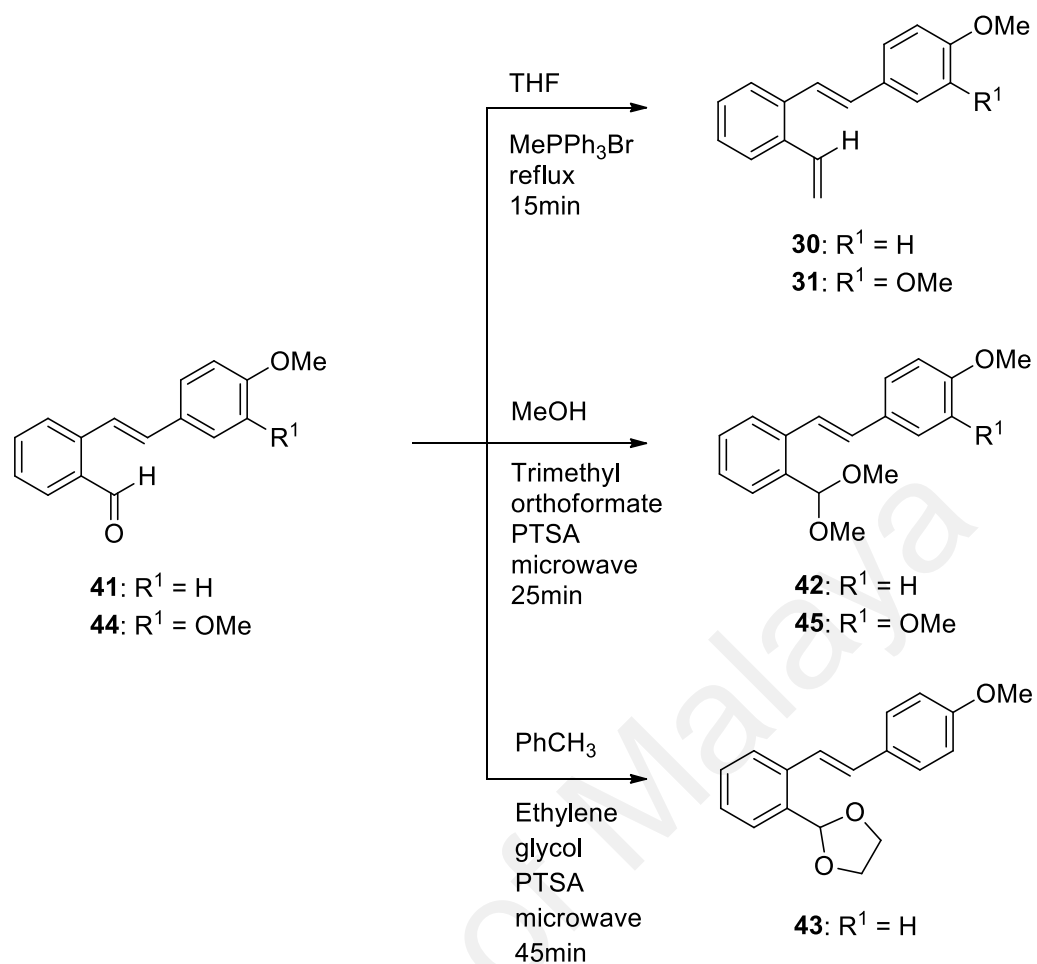
**Scheme 2.3:** Synthesis of stilbenes 11, 13–19 from stilbenes 5 and 6



**Scheme 2.4:** Synthesis of stilbenes **16–19**, **28–29** from stilbenes **37** and **46**



**Scheme 2.5:** Synthesis of stilbenes **20–27**, **49–50** from stilbenes **47** and **48**

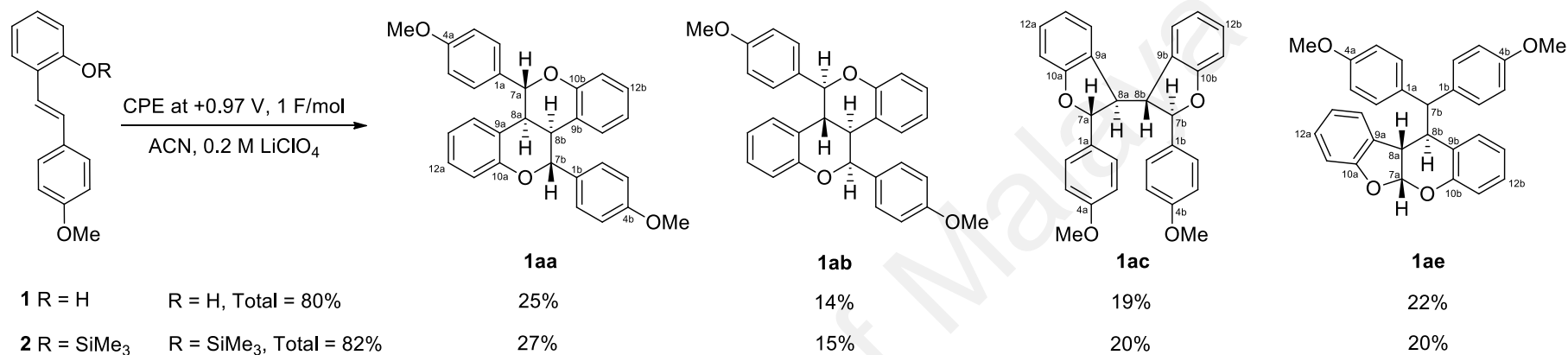


**Scheme 2.6:** Synthesis of stilbenes **30–31**, **42–43**, and **45** from stilbenes **41** and **44**

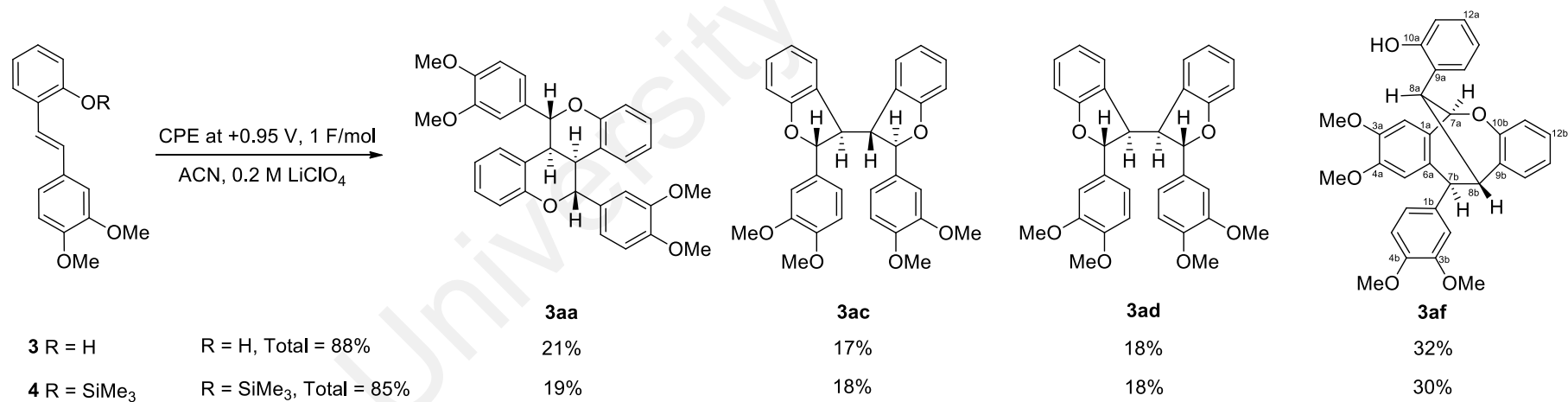
## 2.2 Anodic Oxidation of 4-Methoxy- and 3,4-Dimethoxystilbenes Substituted with 2'-Hydroxy and 2'-Amino groups

The first stilbene investigated was 4-methoxy-2'-hydroxystilbene (**1**), which has an *o*-hydroxy group present in one ring and a *p*-methoxy group in the other ring. Anodic oxidation of **1** (Pt anode, MeCN/0.2M LiClO<sub>4</sub>) showed the presence of one irreversible wave at +0.87 V versus Ag/AgNO<sub>3</sub> in the potential range investigated, as revealed by cyclic voltammetry. Controlled-potential electrolysis (Pt-gauze anode, Pt cathode; MeCN/0.2 M LiClO<sub>4</sub>) at the anodic wave (+0.97 V) was allowed to proceed until about 1.0 F of charge had been transferred. A mixture of products was obtained in a total yield of about 80%, comprising the stereoisomeric fused bisbenzopyrans (as the major products in a combined yield of ca. 40% (**1aa**, 25%; **1ab**, 14%), the bisbenzofuran **1ac** (19%), and the fused benzofuranobenzopyran **1ae** (22%) (Scheme 2.7). The product mixture was separated by a combination of preparative radial chromatography on SiO<sub>2</sub> (Chromatotron), reverse phase HPLC, and Sephadex LH20, and the products were characterized by their spectroscopic data (HRMS, <sup>1</sup>H and <sup>13</sup>C NMR), as well as by X-ray analysis.

HRMS measurements of compound **1aa** established the molecular formula as C<sub>30</sub>H<sub>26</sub>O<sub>4</sub>, indicating that it is a dimerization product from the oxidation stilbene **1** (C<sub>15</sub>H<sub>14</sub>O<sub>2</sub>). However, the <sup>1</sup>H and <sup>13</sup>C NMR data showed only resonances due to half of the molecule, indicating the presence of an element of symmetry. Aside from the readily recognizable aromatic and methoxy resonances, the <sup>1</sup>H NMR spectrum showed two mutually coupled methine hydrogens at δ 5.28 (H-7a) and 3.33 (H-8a) with a coupling constant of ca. 10 Hz. The former resonance corresponds to an oxymethine, while the latter is likely a benzylic methine. Analysis of the 2-D NMR data (COSY, HSQC, HMBC) led to two possible structures: one a fused bisbenzopyran, and the other a bisbenzofuran (Figure 2.2).



**Scheme 2.7:** Products from the anodic oxidation of stilbenes **1** and **2**



**Scheme 2.8:** Products from the anodic oxidation of stilbenes **3** and **4**

Differentiation between the two structures was made possible by comparison of the  $^{13}\text{C}$  shifts of the  $\alpha$  and  $\beta$  methine carbons with model benzopyran<sup>89</sup> and benzofuran<sup>90</sup> compounds from the literature (Figure 2.2), which allowed **1aa** to be assigned the fused bisbenzopyran structure (and compound **1ac** the bisbenzofuran structure; vide infra). Assignment of the stereochemistry was based on the observed H-7a/H-8a coupling of ca. 10 Hz in the  $^1\text{H}$  NMR spectrum of **1aa**, indicating that these hydrogens are trans-diaxially oriented in the six-membered pyran ring, leading to a fused bisbenzopyran with a  $C_2$  axis. These conclusions were confirmed by X-ray analysis, which also revealed the cis fusion of the pyran rings (Figure 2.2).

Examination of the HRMS,  $^1\text{H}$  and  $^{13}\text{C}$  NMR data of compound **1ab** ( $\text{C}_{30}\text{H}_{26}\text{O}_4$ , isomeric with **1aa**) revealed that unlike the previous compound **1aa**, compound **1ab** is devoid of any symmetry and in addition, was shown to possess a similar fused bisbenzopyran structure, based on comparison of the observed  $^{13}\text{C}$  shifts of the  $\alpha$  and  $\beta$  carbons as before. In the  $^1\text{H}$  NMR spectrum, H-8a was observed as a triplet with a coupling constant of 10.8 Hz, indicating that both of the adjacent hydrogens (H-7a and H-8b) were in a *trans* relationship with H-8a (a *trans*-fused bisbenzopyran). H-8b on the other hand was observed as a doublet of doublets with coupling constants of 10.8 and 3.9 Hz, indicating that H-7b and H-8b were *cis* to each other. These conclusions were also confirmed by X-ray analysis (Figure 2.3).

Compound **1ac** ( $\text{C}_{30}\text{H}_{26}\text{O}_4$ ) was deduced to be a bisbenzofuran possessing an element of symmetry, based on the  $^1\text{H}$  and  $^{13}\text{C}$  NMR data (vide supra). In this instance (five-membered furan rings), the observed H-7a/H-8a coupling of 3.6 Hz was insufficient for definitive assignment of the relative configurations at C-7a and C-8a. Fortunately suitable crystals were obtained, and X-ray analysis revealed a *trans*-disposition between H-7a and H-8a, resulting in the presence of a  $C_2$  axis (Figure 2.2).

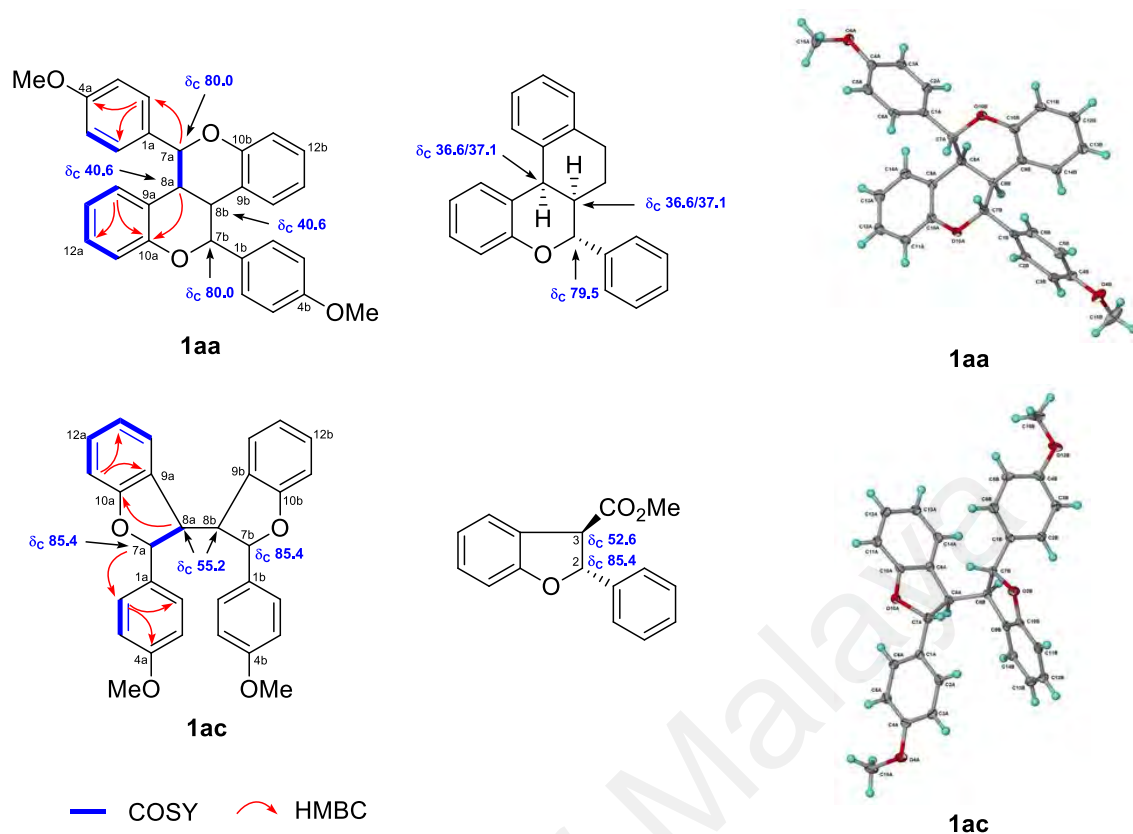


**Figure 2.2:** COSY and selected HMBCs of **1aa** and **1ac**,  $^{13}\text{C}$  shifts of the  $\alpha$  and  $\beta$  methine carbons of model benzopyran<sup>89</sup> and benzofuran<sup>90</sup>, and X-ray structures of **1aa** and **1ac**

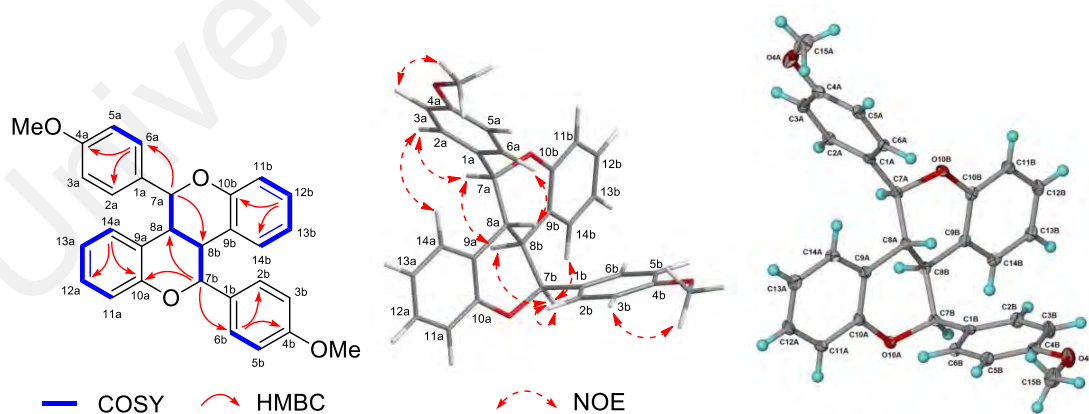


**Figure 2.3:** COSY, selected HMBCs, selected NOEs and X-ray crystal structure of **1ab**

The  $^1\text{H}$  NMR data of compound **1ae** ( $\text{C}_{30}\text{H}_{26}\text{O}_4$ ) showed the presence of 16 aromatic resonances, 4 methine protons, and 2 methoxy groups. The resonance at  $\delta_{\text{H}}$  6.36 ( $\delta_{\text{C}}$  104.2) was assigned to a methine (H-7a) linked to two oxygen atoms, while the resonance at  $\delta_{\text{H}}$  4.04 ( $\delta_{\text{C}}$  44.8), which was coupled to H-7a ( $J = 7.8$  Hz), was assigned to the adjacent benzylic methine (H-8a). The COSY spectrum (Figure 2.4) showed the presence of OCH(O)–CH and CH–CH partial structures. The latter fragment is assigned to C-8b–C-7b ( $\delta_{\text{C}}$  45.7,  $\delta_{\text{H}}$  3.74;  $\delta_{\text{C}}$  53.6,  $\delta_{\text{H}}$  4.23), while the former is assigned to C-7a–C-8a ( $\delta_{\text{C}}$  104.2,  $\delta_{\text{H}}$  6.36;  $\delta_{\text{C}}$  44.8,  $\delta_{\text{H}}$  4.04), with C-8b linked to C-8a to form the C-7a–C-8a–C-8b–C-7b fragment from the observed three bond correlation from H-8a to C-7b in the HMBC spectrum (Figure 2.4). Assembly of the rest of the molecule based on the HMBC data (Figure 2.4) leads to the fused benzofuranobenzopyran as shown in **1ae**, with the acetal carbon (C-7a) shared between two rings. Cis-fusion of the furan and pyran rings was based on the  $J_{7a-8a}$  vicinal coupling of 7.8 Hz and from the H-7a/H-8a NOE (Figure 2.4). The resonance for H-8b was observed as a doublet with  $J = 11.8$  Hz, consistent with the cis-fused geometry, which results in H-8a and H-8b being orthogonal to each other. The  $\alpha$ -orientation of H-8b is also in agreement with the observed H-8b/H-14a, H-8b/H-14b, and H-8b/H-2a,H-6a NOEs (Figure 2.4). The structure and relative configuration were also confirmed by X-ray diffraction (Figure 2.4).

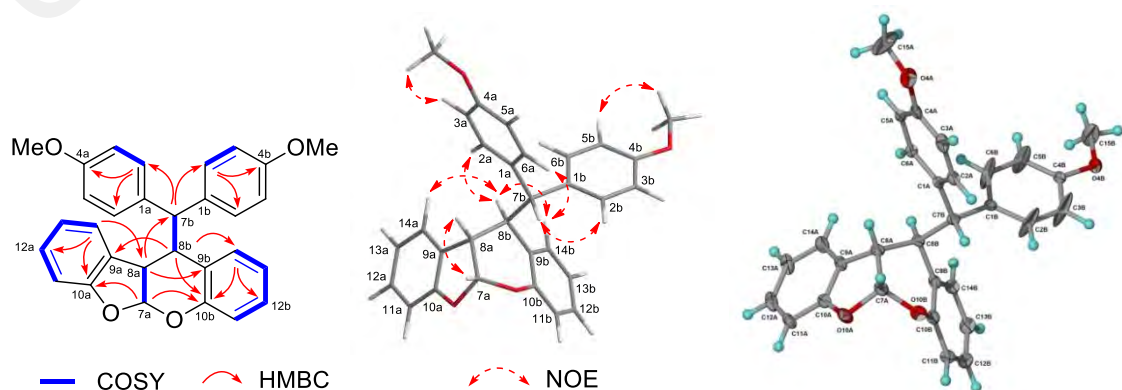


**Figure 2.4:** COSY, selected HMBCs, selected NOEs, and X-ray crystal structure of **1ae**

Anodic oxidation of the TMS-protected 4-methoxy-2'-hydroxystilbene **2** resulted the same four products (**1aa**, **1ab**, **1ac**, and **1ae**), and although there were minor variations in the product distribution, the overall yield was essentially unchanged (Scheme 2.7).

We next investigated the anodic oxidation of 3,4-dimethoxy-2'-hydroxystilbene (**3**), which has an additional methoxy substituent at the meta position in the *p*-methoxy-substituted ring. Anodic oxidation of **3** (+0.95 V, Pt gauze anode, Pt cathode; MeCN/0.2 M LiClO<sub>4</sub>, 1.0 F/mol) gave a mixture comprising four isomeric products: the C<sub>2</sub>-symmetric fused bisbenzopyran **3aa** (analogous to **1aa**), the C<sub>2</sub>-symmetric bisbenzofuran **3ac** (analogous to **1ac**), another symmetric bisbenzofuran **3ad**, and the bridged oxocine **3af** (Scheme 2.8). The structures of **3aa** and **3ac** were readily assigned based on their <sup>1</sup>H and <sup>13</sup>C NMR data and by analogy to **1aa** and **1ac**, respectively (which have been thoroughly characterized by MS, NMR, and X-ray diffraction analysis, *vide supra*; the structure of **3aa** was also confirmed by X-ray analysis).

Compound **3ad** (C<sub>32</sub>H<sub>30</sub>O<sub>6</sub>) was a symmetric bisbenzofuran, as indicated by the HRMS and NMR data. For the bisbenzofurans, after discounting enantiomeric partners, there are a total of eight possible diastereomers (four symmetric and four nonsymmetric stereoisomers). Of the symmetric arrangements, two have a C<sub>2</sub> axis and two are *meso* structures characterized by the presence of a mirror plane  $\sigma$  (Figure 2.5). Compound **3ac** (C<sub>2</sub>) showed the presence of two enantiomers on chiral phase HPLC analysis. On the other hand, compound **3ad** showed only one peak on chiral phase HPLC analysis (tested on two different chiral stationary phases). Compound **3ad** must therefore correspond to either one of two *meso*-bisbenzofurans (**3ad** and **3ad'**; Figure 2.6).

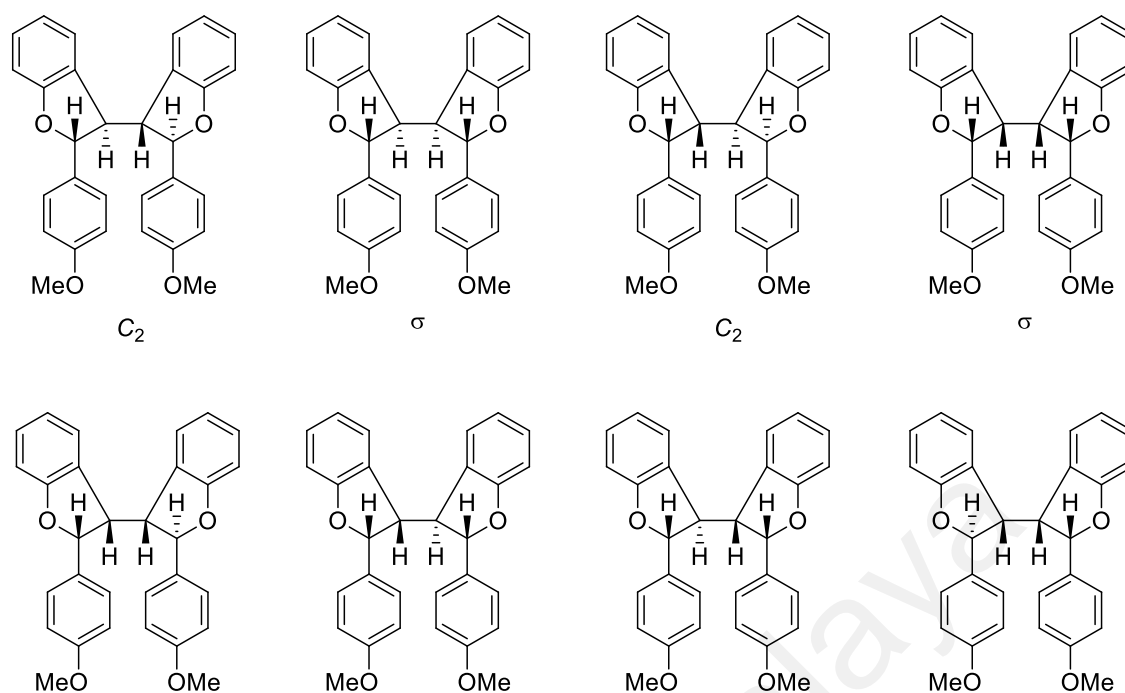


**Figure 2.5:** Diastereomers of bisbenzofurans with formula  $C_{32}H_{30}O_6$

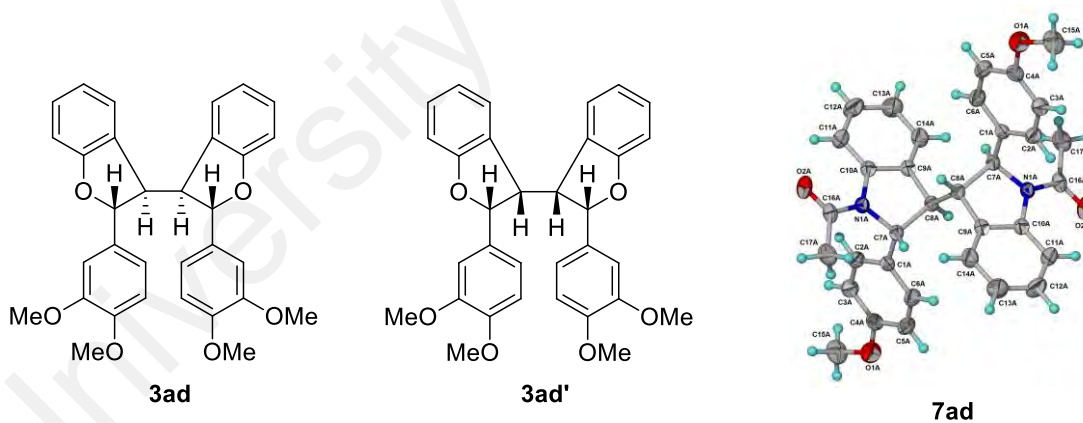


**Figure 2.6:** Structures of **3ad**, **3ad'**, and X-ray crystal structure of **7ad**

Examination of models showed that **3ad'** with an all-cis configuration of the methine hydrogens should suffer from appreciable steric congestion (hence less stable) in comparison to **3ad** (**3ad** is estimated to be more stable than **3ad'** by ca. 14.74 kcal

mol<sup>-1</sup>). The structure of this compound is probably **3ad**, which received further confirmation by analogy to the corresponding nitrogen analogue (**7ad**, *vide infra*), whose structure was verified by X-ray analysis (Figure 2.6) (Chiral phase HPLC of **7ad** also showed the presence of a single peak as in the case of **3ad**).

HRMS measurements of compound **3af** established the molecular formula as C<sub>32</sub>H<sub>30</sub>O<sub>6</sub>, indicating that it is isomeric with compounds **3aa**, **3ac**, and **3ad**. The <sup>1</sup>H NMR spectrum showed the presence of 13 aromatic resonances, 4 methoxy groups, 4 methine protons ( $\delta$  5.60, 4.48, 3.81, 3.35), and an OH group ( $\delta$  5.40, exchanged with D<sub>2</sub>O). The low-field resonance at  $\delta$  5.60 ( $\delta_C$  73.5) was due to an oxymethine (H-7a), while the resonance at  $\delta$  4.48 ( $\delta_C$  56.1) can be attributed to the doubly benzylic H-7b by analogy to H-7b in compound **1ae**. The COSY spectrum (Figure 2.7) showed the presence of an OCH-CH-CH-CH fragment, corresponding to C-7a-C-8a-C-8b-C-7b, based on the observed three-bond correlations from H-7b to C-8a and from H-8b to C-7a in the HMBC spectrum (Figure 2.7). In addition, the <sup>1</sup>H NMR spectrum of **3af** showed two of the aromatic hydrogens of one ring as singlets (H-2a,  $\delta$  6.99; H-5a,  $\delta$  6.43), indicating that one aromatic moiety was 1,2,4,5-tetrasubstituted. The observed three-bond correlations (<sup>3</sup>*J*) for H-7a/C-2a, C-6a and H-7b/C-1a, C-5a, in the HMBC spectrum indicated the attachment of C-7a to the aromatic C-1a and of C-7b to C-6a. This accounted for the 1,2-substitution of a 4,5-dimethoxyaryl moiety by the four-carbon CHCHCHCH unit. The HMBC data (Figure 2.7) also showed that the oxygen linked to C-7a is attached to the aromatic C-10b (<sup>3</sup>*J* for H-7a/C-10b), while the adjacent aromatic C-9b is linked to the methine C-8b (<sup>3</sup>*J* for H-8b/C-10b, H-14b/C-8b), thus forging the bridged oxocine core. Attachment of the remaining aryl units at C-7b (<sup>3</sup>*J* for H-7b/C-6b, H-2b/C-7b) and C-8a (<sup>3</sup>*J* for H-14a/C-8a) completed the assembly of the structure of **3af**, which was also consistent with the NOE data. In addition, the IR

spectrum of **3af** showed a sharp band due to an OH function at  $3441\text{ cm}^{-1}$ , indicating the presence of a free OH that remained intact throughout the reaction.

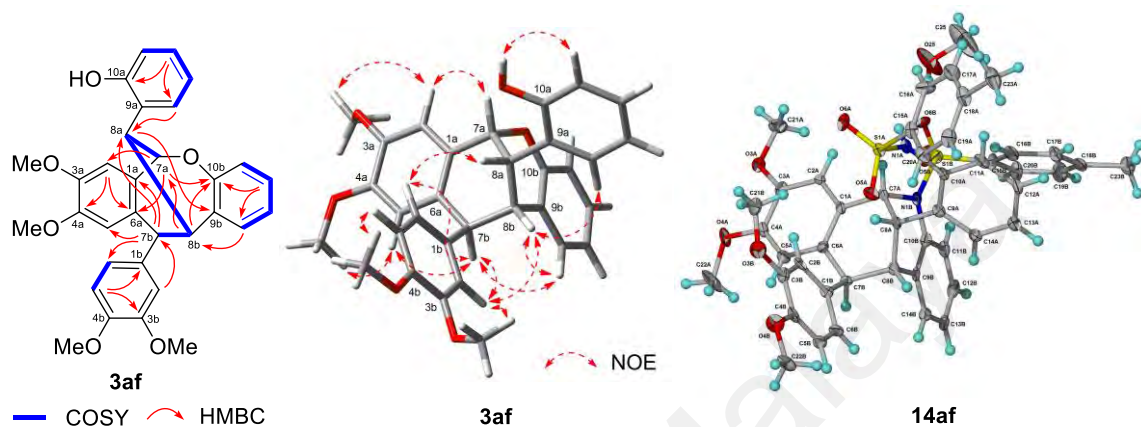
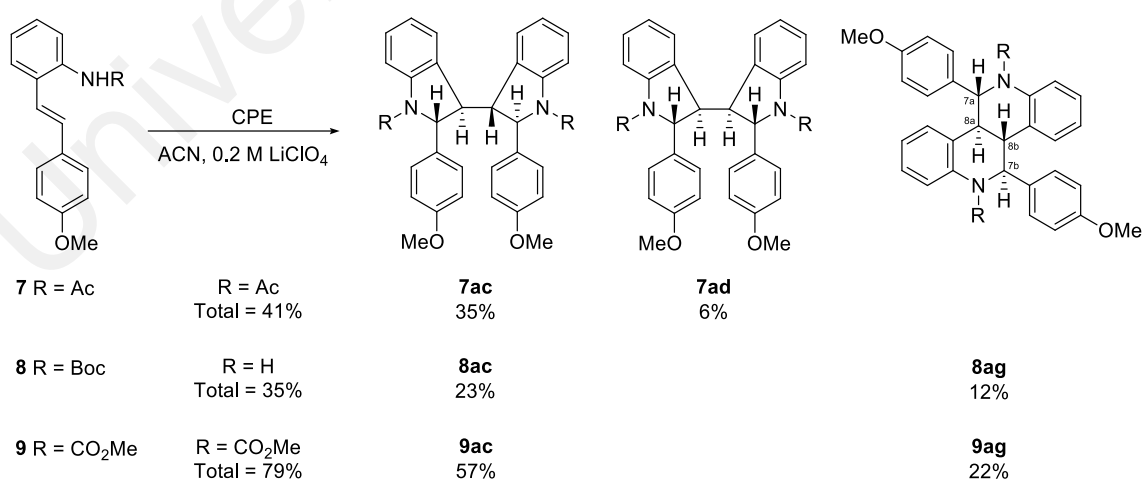


**Figure 2.7:** COSY, selected HMBCs, and selected NOEs of **3af**, and X-ray crystal structure of **14af**

Of the four stereogenic centers in **3af**, the relative configurations of two, C-7a and C-8b, are fixed by the geometry of their attachment to the methine bridge (C-8a). The NOEs observed for H-6b/H-8a required H-8a to be directed toward ring A, while the substitution of ring A' at C-7b is deduced to be  $\beta$  from the observed H-6b/H-8a and H-7b/H-14b NOEs. Attempts to obtain suitable crystals of **3af** and its derivatives (tosylate, acetate, *p*-bromobenzoate) were unsuccessful. However, the nitrogen analogue of **3af** (**14af**) furnished suitable crystals, which allowed X-ray analysis to be carried out (Figure 2.7), providing verification of the structure of **14af** and support for the structure proposed for **3af**.

Anodic oxidation of the TMS-protected 3,4-dimethoxy-2'-hydroxystilbene **4** gave the same four products (**3aa**, **3ac**, **3ad**, and **3af**) and although there were minor variations in the product distribution, the overall yield was essentially unchanged (Scheme 2.8).

We next investigated the effect of an *ortho*-substituted amino group. Anodic oxidation of 4-methoxy-2'-aminostilbene **5** and 3,4-dimethoxy-2'-aminostilbene **6** were unsuccessful due to significant electrode fouling (passivation) which was not unanticipated in the light of our previous experience.<sup>85,91–95</sup> Hence, a series of *N*-protecting groups was introduced to overcome the deactivation of the electrode. Anodic oxidation of the *N*-acetylated derivative **7** gave two dimeric products in total yield of *ca.* 40%: the  $C_2$  symmetric bisindole **7ac** (35%) and the *meso* bisindole **7ad** (6%) (Scheme 2.9). The structure of **7ac** can be assigned based on their MS and NMR data and by analogy to **1ac** and **10ac** (X-ray structures available for both), while the structure of **7ad** was confirmed by X-ray analysis (Figure 2.6) (chiral phase HPLC of **7ad** also showed the presence of a single peak as in the case of **3ad**).



**Scheme 2.9:** Products from the anodic oxidation of stilbenes **7–9**

Since only a moderate yield was obtained for the acetylated derivative, it was of interest to investigate the dependence of both the product distribution and the yields on the nature of the protecting group. Anodic oxidation of the *N*-Boc derivative **8** gave two products in combined yield of only 35%, viz., the  $C_2$  symmetric bisindole **8ac** (23%) and the symmetric fused bisquinoline **8ag** (12%) (Scheme 2.9). In this instance both products have lost their respective protecting groups during electrolysis and a substantial quantity (*ca.* 40%) of deprotected starting material was also recovered. The fused bisquinoline structure of **8ag** was indicated by the characteristic carbon shifts of the non-aromatic carbons (C-7a, C-8a), which were different from those of the bisindoles, corresponding to quinoline as opposed to indoline units (Figure 2.8). The  $^1\text{H}$  NMR spectrum showed resonances due to only one half of the molecule, including a pair of doublet of doublets at  $\delta$  4.60 (H-7a) and 3.39 (H-8a) with  $J = 6.9, 2.8$  Hz (attributed to a pair of mutually coupled methine hydrogens), in addition to the aromatic and methoxy resonances. The NMR data other than indicating the presence of an element of symmetry was insufficient for complete stereochemical assignment of the structure of this bisquinolinic compound.

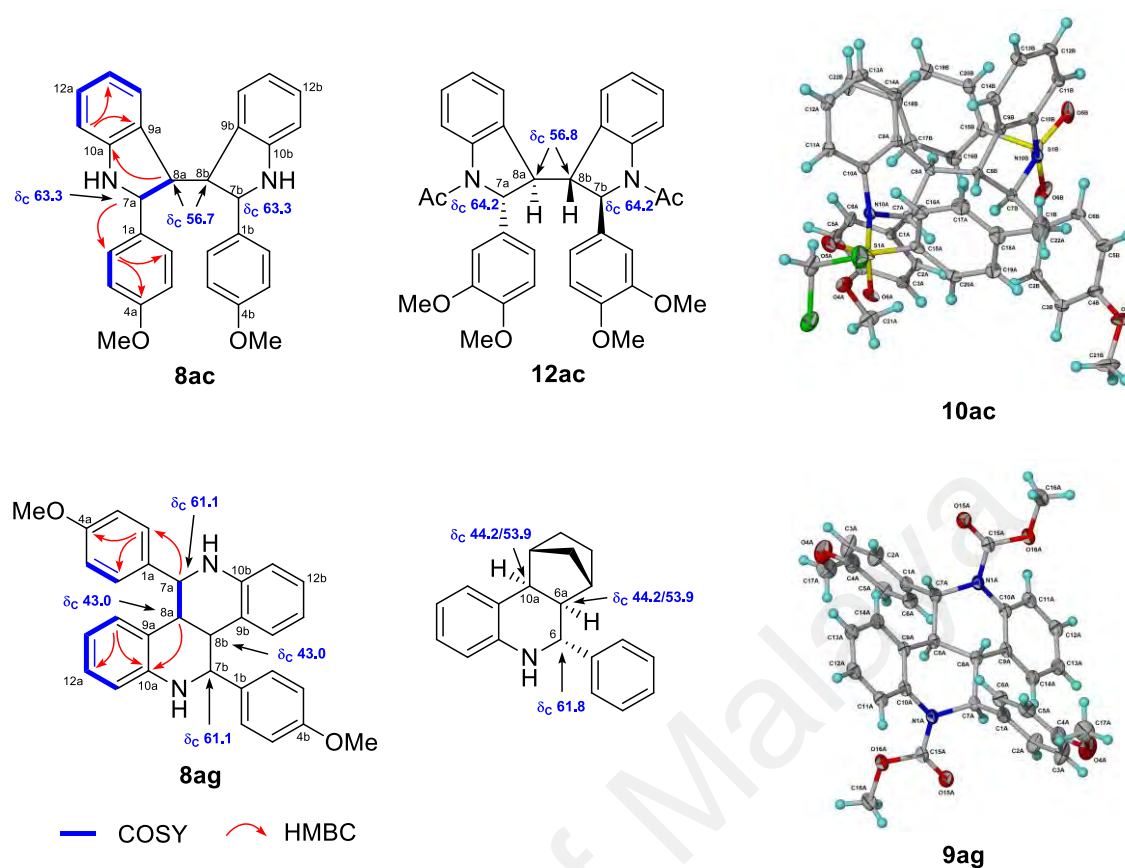


**Figure 2.8:** COSY, selected HMBCs of **8ac** and **8ag**, comparison of the  $^{13}\text{C}$  shifts of the  $\alpha$  and  $\beta$  methine carbons with model bisindole<sup>96</sup> and quinolone<sup>97</sup> and X-ray crystal structures of **10ac** and **8ag**

In view of this finding, as well as the poor yields obtained for the *N*-Boc derivative, we next investigated the oxidation of the carbamate **9**. Anodic oxidation proceeded smoothly in this case and gave a mixture of products comprising the bisindole **9ac** (57%) and the fused bisquinoline **9ag** (22%) in combined yield of ca. 80% (Scheme 2.9). In this case, the bisquinoline **9ag** provided suitable crystals for X-ray analysis (Figure 2.8), which confirmed its structure as well as that for the previous amide analog **8ag**. The X-ray structure also showed that the element of symmetry present in **8ag** and **9ag** was a center of inversion (*i*).

Anodic oxidation of the *N*-tosyl aminostilbene **10** gave a mixture comprising the bisindole **10ac** (52%) and the fused bisquinoline **10ag** (25%). In addition, the rearranged monomeric indole **10ah** was also isolated as a minor product (6%) (Scheme 2.10). X-ray structures were available for both **10ac** (Figure 2.8) and **10ag** (Figure 2.9). In the case of the *N*-nosyl protected stilbene, anodic oxidation gave the symmetric bisindoles **11ac** ( $C_2$ , 49%) and **11ad** ( $\sigma$ , 21%), the symmetric fused bisquinoline **11ag** (*i*, 13%), and a trace of the monomer, **11ah** (Scheme 2.10). An X-ray structure was available for **11ag** (Figure 2.9).

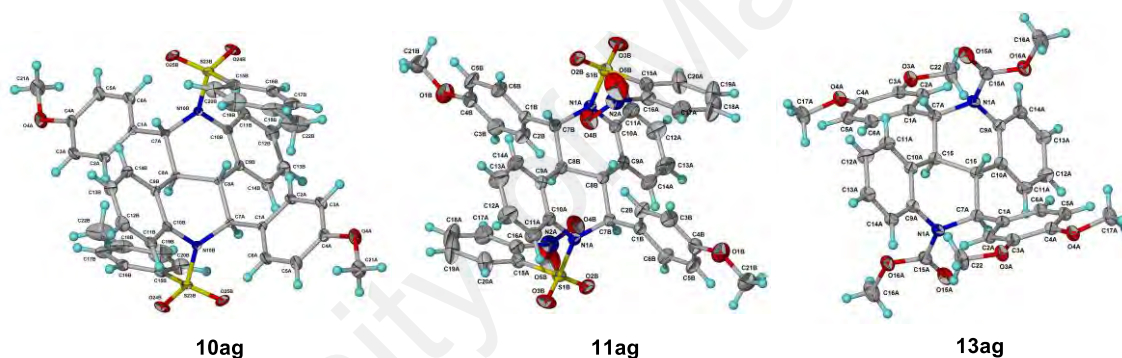
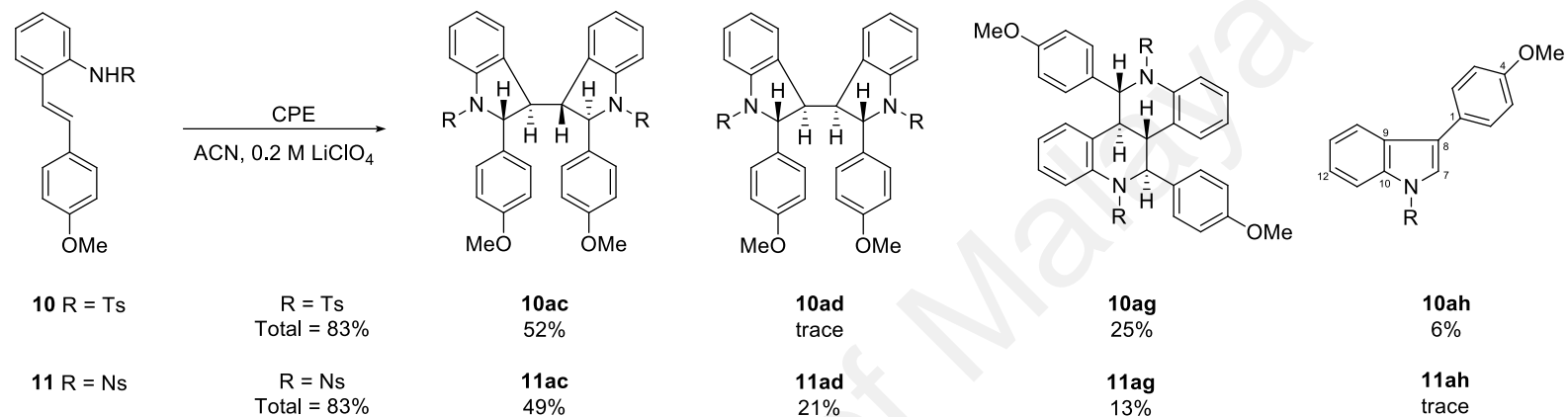
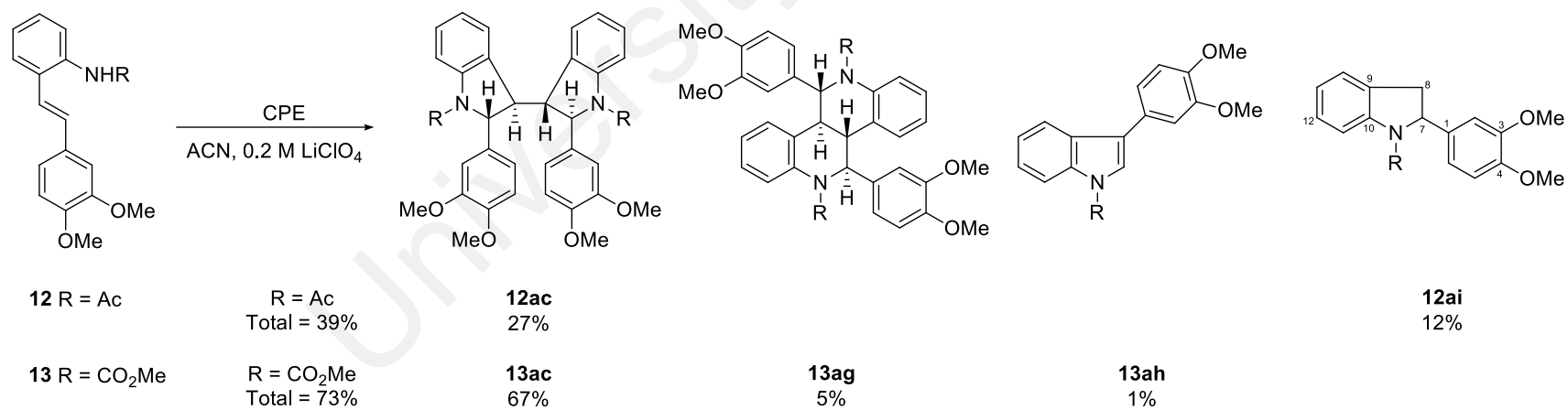


**Figure 2.9:** X-ray crystal structures of **10ag**, **11ag**, and **13ag**

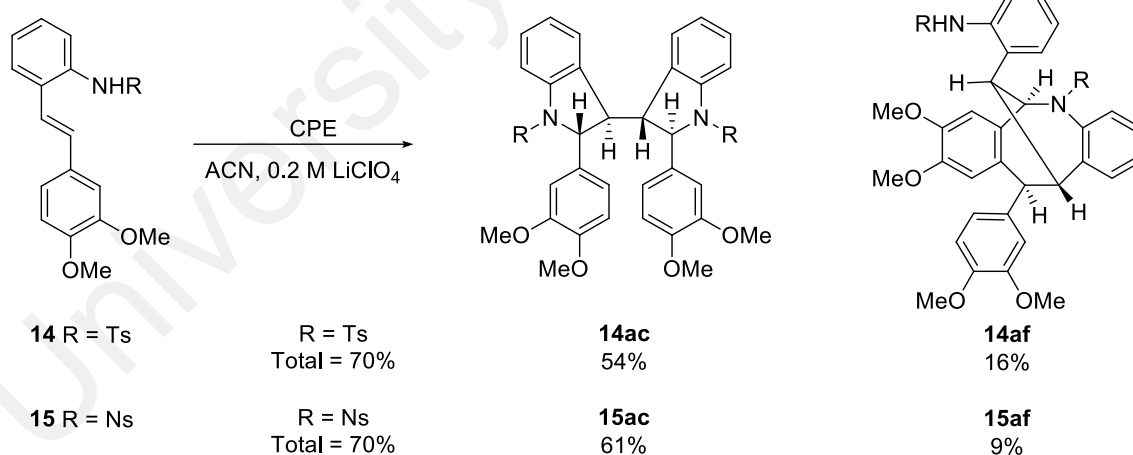


**Scheme 2.10:** Products from the anodic oxidation of stilbenes **10** and **11**

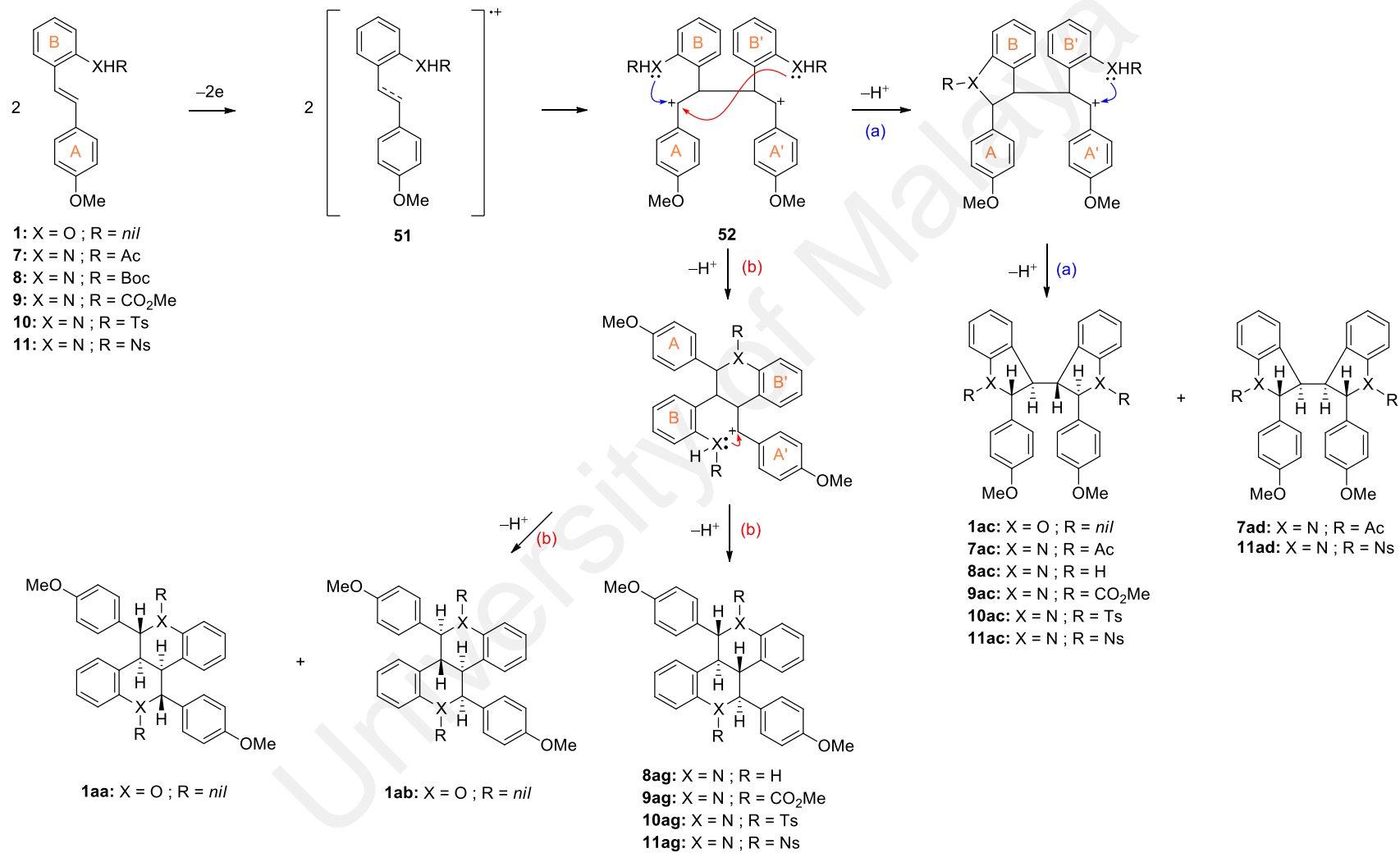


**Scheme 2.11:** Products from the anodic oxidation of stilbenes **12** and **13**

In the case of the 3,4-dimethoxysubstituted aminostilbenes, some variation in the product type and distribution were noted. The acetylated derivative **12** gave only the bisindole **12ac** and the monomeric indole **12ai** in a total yield of only 39% (Scheme 2.11). As before, in view of the poor yields for the acetylated derivative, anodic oxidation of the carbamate derivative **13** was next attempted which gave the bisindole **13ac** as the major product in 67% yield, the bisquinoline **13ag** (5%), and the rearranged monomeric indole **13ah** as a very minor product (1%) (Scheme 2.11). The tosyl and nosyl derivatives **14** and **15**, respectively, gave only two products, the bisindoles **14ac** and **15ac**, and the bridged azocines **14af** and **15af** (Scheme 2.12). The structures of **13ac**, **13ag** (Figure 2.9), **14ac**, and **14af** (Figure 2.7) were also confirmed by X-ray analysis. The X-ray structure of the azocine **14af** provides additional support for the structure proposed for the oxocine analogue, **3af** (vide supra).



**Scheme 2.12:** Products from the anodic oxidation of stilbenes **14** and **15**



**Scheme 2.13:** Proposed mechanism for the formation of products in the anodic oxidation of stilbenes (**1**, **7–11**) in MeCN/LiClO<sub>4</sub>

The current investigation was carried out to address several questions regarding stilbene cation radical reactivity. First, will the proximate ortho'-substituted nucleophilic groups (OH, NH<sub>2</sub>) engage the cation radical in an intramolecular reaction? Second, if intramolecular cation trapping occurs, does it precede bimolecular dimerization of the first formed cation radical, or does trapping by the internal nucleophile take place subsequent to cation radical dimerization? Additionally, can 'crossover trapping' occur to provide six-membered ring products (pyrans/quinolines) in addition to five-membered ring products (furans/indoles) from direct trapping? The formation of the fused bisbenzopyrans/ bisquinolines (a result of crossover trapping), in addition to the bisbenzofurans/bisindoles clearly showed that the ortho'-substituted OH (and NHR) groups do react with cationic groups, and that such engagements occur subsequent to cation radical dimerization. We propose the following mechanism to rationalize the formation of the products in the oxidation of the 4-methoxy-2'-hydroxy(or 2'-amino)stilbenes, **1**, **2**, **7–11**.

One-electron oxidation of the starting stilbene gave the cation radical **51**, which under the conditions of preparative electrolysis undergoes facile cation radical dimerization to give the dicationic intermediate **52** as the dominant step, as demonstrated by previous studies.<sup>85</sup> Formation of the fused bisbenzopyrans (**1aa**, **1ab**) or bisquinolines (**7ag–11ag**) is a result of "crossover trapping" by the ortho'-substituted nucleophiles, i.e., *o*-OH (or *o*-NHR) in ring B of one stilbene half attacks the benzylic cation associated with ring A' of the other stilbene half, while, *o*-OH (or *o*-NHR) in ring B' attacks the benzylic cation of ring A (Scheme 2.13, path b). On the other hand, the formation of the bisbenzofuran (**1ac**) or bisindoles (**7ac–11ac**, **7ad**, **11ad**) is a consequence of the respective direct trapping of the cation by the ortho'-substituted nucleophiles belonging to the same stilbene half, i.e., *o*-OH (or *o*-NHR) belonging to

ring B of one stilbene half reacts with the benzylic cation of ring A of the same stilbene half, while, *o*-OH (or *o*-NHR) in ring B' reacts with the benzylic cation of ring A', as shown in Scheme 2.13, path a. The occurrence of crossover trapping represents firm evidence for intramolecular cation trapping by the internal nucleophile taking place subsequent to cation radical dimerization.

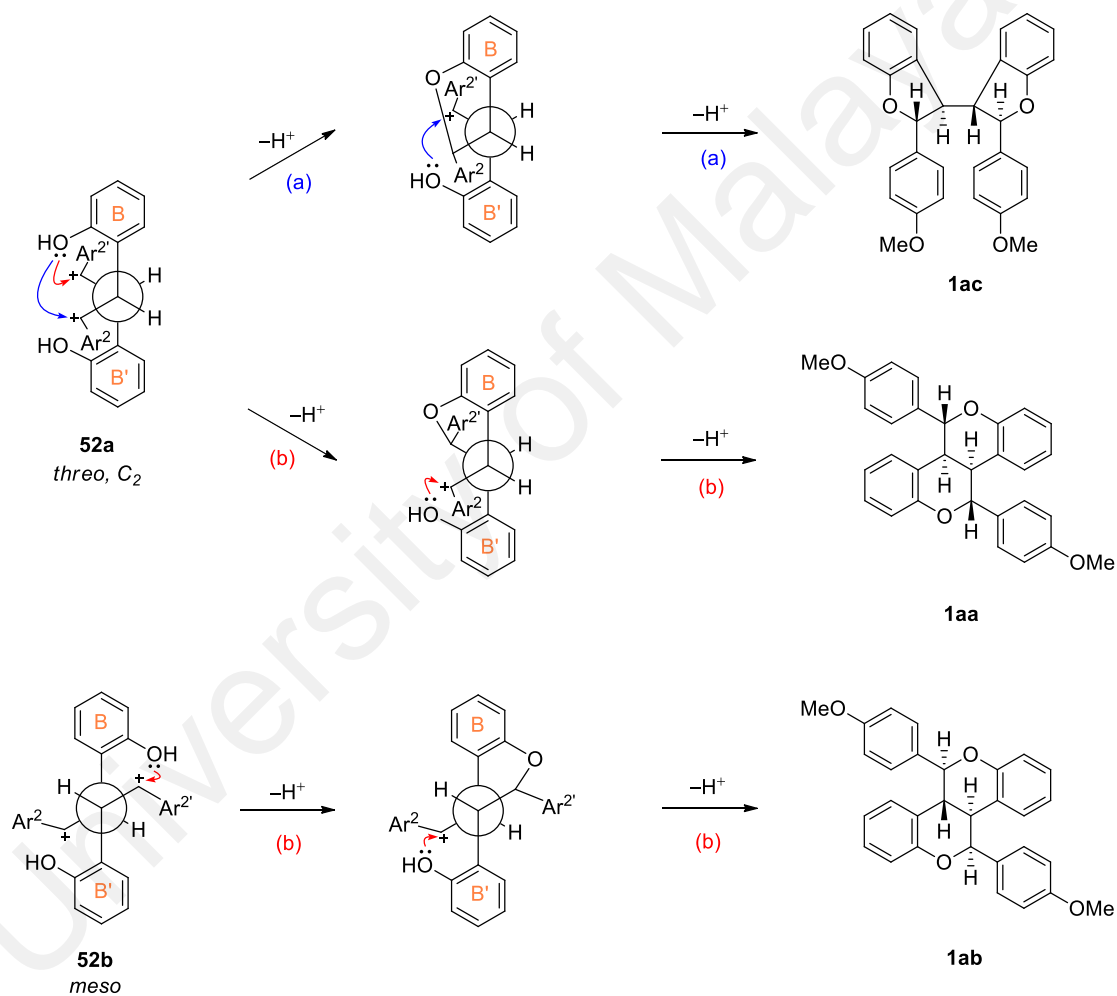
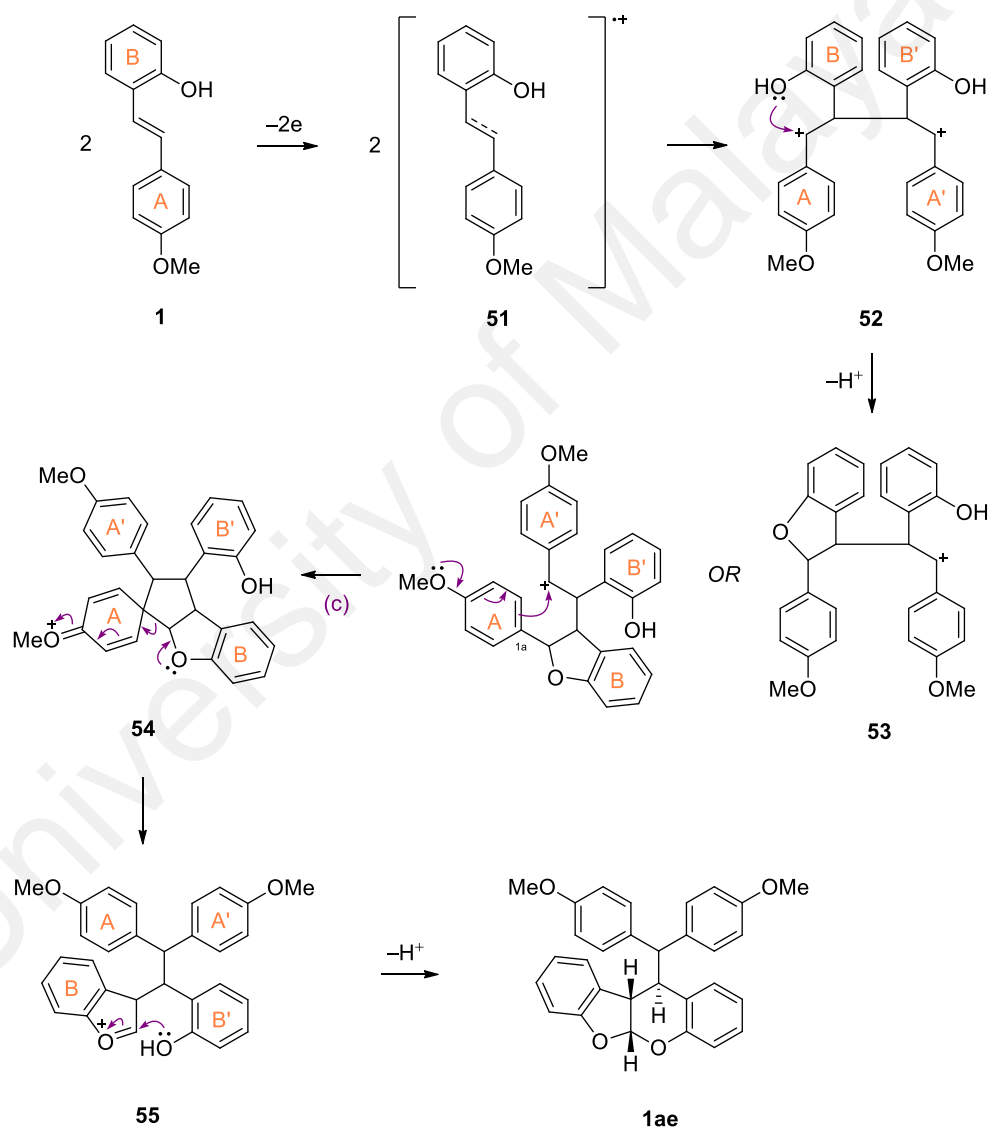


**Figure 2.10:** Origin of the fused benzopyrans **1aa**, **1ab**, and bisbenzofuran **1ac** from the *threo* and *meso* dications

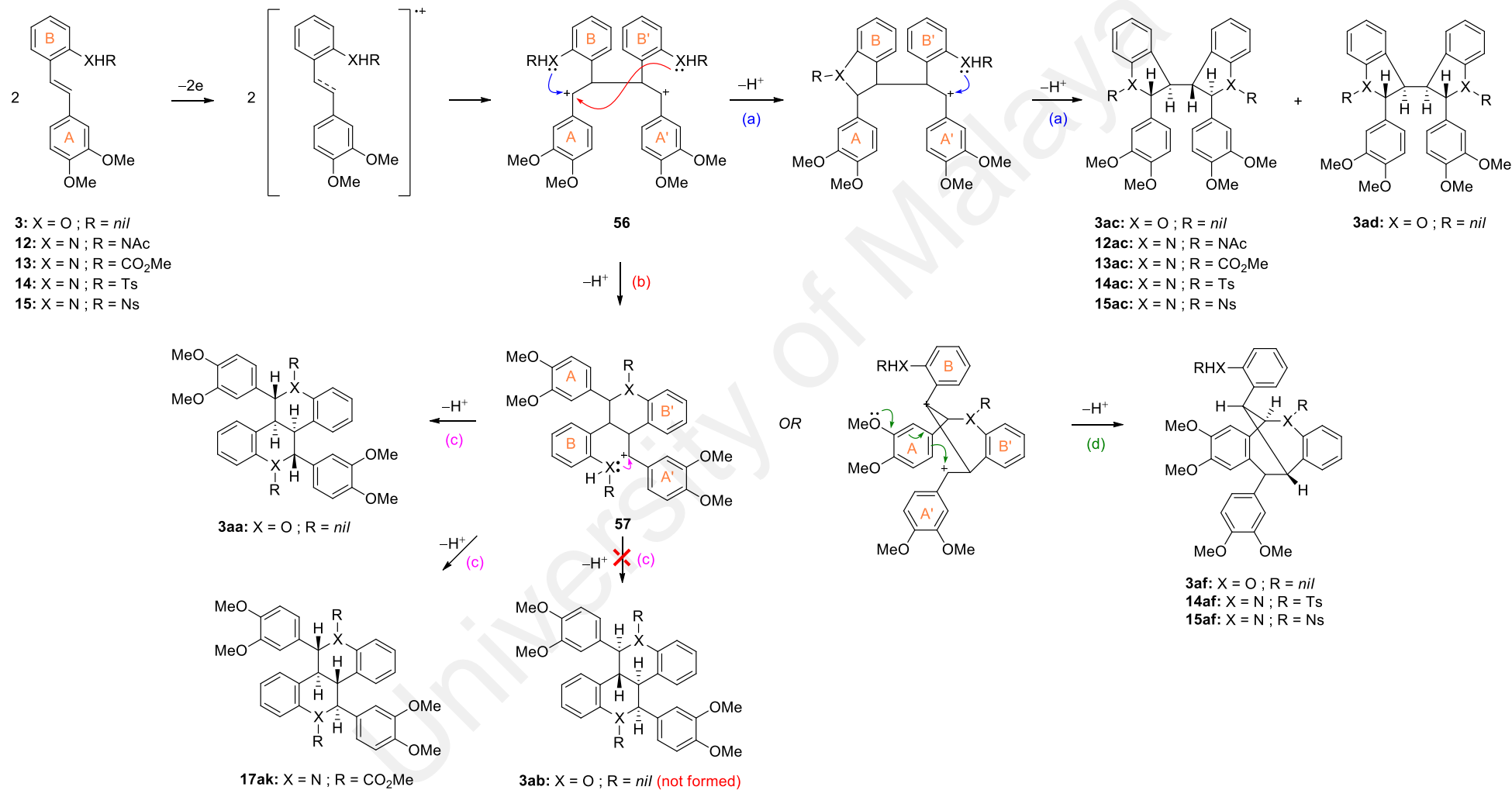
There are two possible modes for the initial cation radical coupling to give the dication **52**, from which all the products are derived.<sup>85</sup> The two regioisomers **1aa** and **1ac** formed in the oxidation of **1** originate from the *threo*-dication **52a**, which is characterized by the presence of a  $C_2$  axis. On the other hand, the fused benzopyran **1b** originates from the *meso*-dication **52b**, as shown in Figure 2.10.



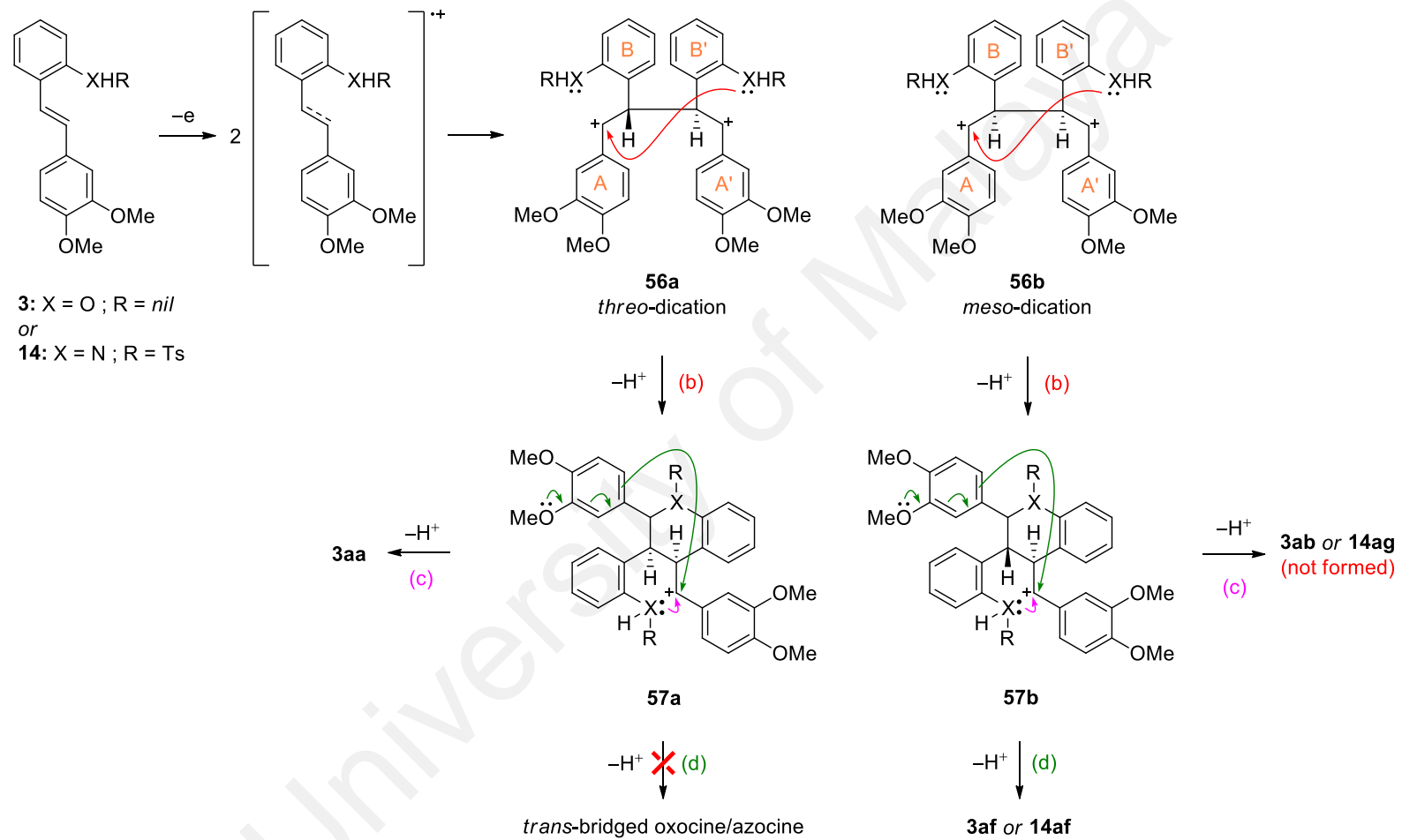
**Scheme 2.14:** Proposed mechanism for the formation of **1ae** in the anodic oxidation of **1** in MeCN/LiClO<sub>4</sub>

The fused benzofuranobenzopyran **1ae** formed in the anodic oxidation of stilbene **1**, appeared at first sight to be an unusual product. It possesses an acetal function shared between two rings and in addition showed evidence of aryl migration, features which had been noted previously.<sup>85</sup> Cation radical dimerization followed by the first direct trapping of the dication **52** by one of the OH groups gave the cationic intermediate **53**. Subsequent electrophilic aromatic substitution or Friedel-Crafts reaction as a result of activation of C-1a (ring A) by the 4-methoxy group leads to the spirocyclic intermediate **54** (path c, Scheme 2.14). Ring opening of the spirocyclic intermediate assisted by the lone pair of electrons in the oxygen atom (benzofuran ring) gave the oxycarbenium ion **55** which on subsequent nucleophilic attack by the remaining OH group gave the fused benzofurano-benzopyran **1ae**.

Anodic oxidation of the 3,4-dimethoxysubstituted 2'-hydroxystilbene **3** (and the corresponding aminostilbenes **12–15**) were also investigated, since it has been shown in the previous study that the presence of a *m*-methoxy group in addition to a *p*-methoxy substituent, enhances the nucleophilicity of the aromatic carbon para to the *m*-OMe group (C-6), and this had an effect on the product distribution.<sup>85</sup> Indeed, oxidation of **3** (as a representative example) gave in addition to the expected bisbenzopyran **3aa**, bisbenzofurans **3ac** and **3ad**, the unexpected bridged oxocine **3af**. The latter product was formed as a result of 3,4-dimethoxy substitution in the starting 2'-hydroxystilbene and was also obtained in the oxidation of the corresponding 3,4-dimethoxy-, tosyl- and nosyl- protected 2'-amino analogues, **14** and **15**, respectively. We propose the following mechanism (Scheme 2.15) to rationalize the formation of these products. Direct trapping of the dication **56** from the initial cation radical dimerization leads to the isomeric fused bisbenzofurans **3ac** and **3ad**. Two successive crossover trapping reactions lead to the formation of one of the expected bisbenzopyrans, **3aa**.



**Scheme 2.15:** Proposed mechanism for the formation of products in the anodic oxidation of stilbenes (**3**, **12–15**) in MeCN/LiClO<sub>4</sub>



**Scheme 2.16:** Pathway showing the formation of **3aa** and **3af** (or **14af**) instead of **3ab** (or **14ag**) and the *trans*-bridged oxocine/azocine

The other bisbenzopyran **3ab** however was not formed, instead the bridged oxocine was isolated in 32% yield. The cationic intermediate **57** formed after the first crossover trapping instead of undergoing a second crossover trapping to **3ab**, undergoes electrophilic substitution (Friedel-Crafts alkylation) via attack of the benzylic cation (associated with ring A') on the activated C-6 of ring A.<sup>85,98</sup> This aromatic substitution is facilitated by the activation of ring A due to the appropriately placed *m*-OMe group, and as a result is able to compete favorably with the second crossover trapping by *o*-OH.

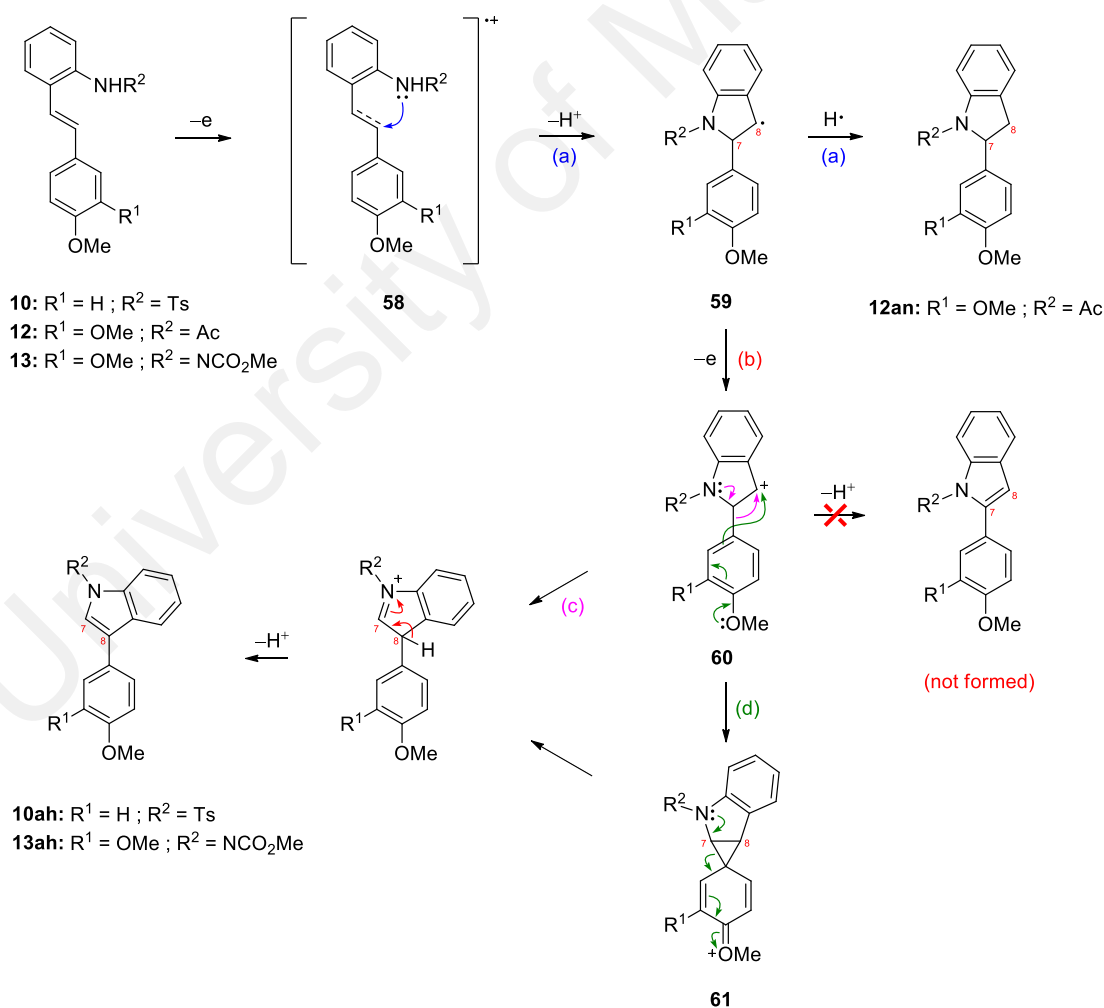
From the above observations, one could ask why **3aa** was formed while **3ab** was not, instead the oxocine **3af** was formed in its place, and not *vice versa* (i.e., formation of **3ab** and the corresponding oxocine in place of **3aa**). The bisbenzopyrans **3aa** and **3ab** originate from different dications arising from the initial cation radical coupling. Bisbenzopyran **3aa** results from two successive crossover trapping reactions from the *threo*-dication. Bisbenzopyran **3ab** on the other hand is a result of two successive crossover trapping reactions from the *meso*-dication (Scheme 2.16). Examination of models showed that while the second crossover reaction from the cationic intermediate **57b** (from the *meso*-dication) to give **3ab** is feasible, the alternative electrophilic substitution reaction was able to compete effectively, resulting instead in the formation of the bridged oxocine product at the expense of **3ab**. In the case of the cation **57a** (from the *threo*-dication), examination of models showed that while a second cyclization from **57a** to **3aa** is feasible, the alternative aromatic substitution to the bridged oxocine product is highly unlikely for geometric reasons, as it will result in formation of a *trans*-bridged oxocine. A similar explanation applies in the case of the ortho'-NHR-substituted dimethoxystilbenes (e.g., **14** and **15** in Scheme 2.16) (in the case of stilbene **13** (carbamate), the corresponding bridged azocine product was not detected; instead, the *meso* dication derived bisquinoline **13ag** was obtained in 5% yield).

Another notable difference in the oxidation of **1** versus **3** was the absence of the acetal product (analogous to **1ae**) in the reaction of the 3,4-dimethoxy-substituted stilbene **3**. A possible explanation for this is that activation of the aromatic ring A (at C-6) towards aromatic substitution (Friedel-Crafts reaction) by the appositely substituted 3-OMe group in **3** has resulted in intramolecular reactions leading to the bridged oxocine being overwhelmingly favored over competing pathways leading to the spirocyclic cationic intermediate. The same observation was noted when comparing the results for the reactions of the *o'*-aminostilbenes (**7–11**) versus the reaction of the *o'*-hydroxystilbene **1**, where the amino acetal (or aminal) analogue of **1ae** was not detected among the products in the reactions of **7–11**, which may be attributed to the greater nucleophilicity of nitrogen versus oxygen, resulting in the predominance of the more facile intramolecular cation trapping reactions over other pathways.

Another departure when comparing the products of the ortho'-OH- versus those of the ortho'-NHR-substituted 4-methoxystilbenes (for which we were unable to formulate a convincing explanation), was the formation of the crossover trapping derived bisquinolines of the **ag** series (from the *meso*-dication, and characterized by presence of a center of inversion, (*i*) for the ortho'-NHR-substituted stilbenes, whereas this type of product was absent for the reaction of the ortho'-OH-substituted stilbenes, where *meso*-dication derived crossover bisbenzopyran products of the **ab** type were formed instead (Such a comparison may not be entirely valid, since it is not between a free -OH versus a free -NH<sub>2</sub> but against a protected NH<sub>2</sub> instead. In addition, based on the DFT-calculated energies, **9ag** is more stable than **9ab** by 1.66 kcal mol<sup>-1</sup>, while **13ag** is more stable than **17ab** by 1.71 kcal mol<sup>-1</sup>).

The monomeric indoles (**10ah**, **13ah**) and dihydroindole (**12ai**) were minor products and were detected only in the oxidation of the ortho'-amino substrates (**10**, **12**, **13**).

Their formation is shown in Scheme 2.17. The rearranged structure of the indoles **10ah** and **13ah** versus the non-rearranged structure for the dihydroindole **12ai** was not immediately apparent on a cursory inspection of the NMR data. Examination of the HMBC data however showed that the correct structures of the indoles correspond to **10ah** and **13ah**, while that of the dihydroindole to **12ai**. The dihydroindole (**12ai**) derives from hydrogen abstraction by the radical **59** formed after direct trapping of the cation radical **58**, and subsequent deprotonation (path a). The rearranged indoles (**10ah** and **13ah**) can be rationalized by two alternative pathways, either via a lone-pair assisted 1,2-aryl shift of the cation **60**, followed by deprotonation (Scheme 2.17, path c), or via involvement of the phenonium ion intermediate **61** (Scheme 2.17, path d).



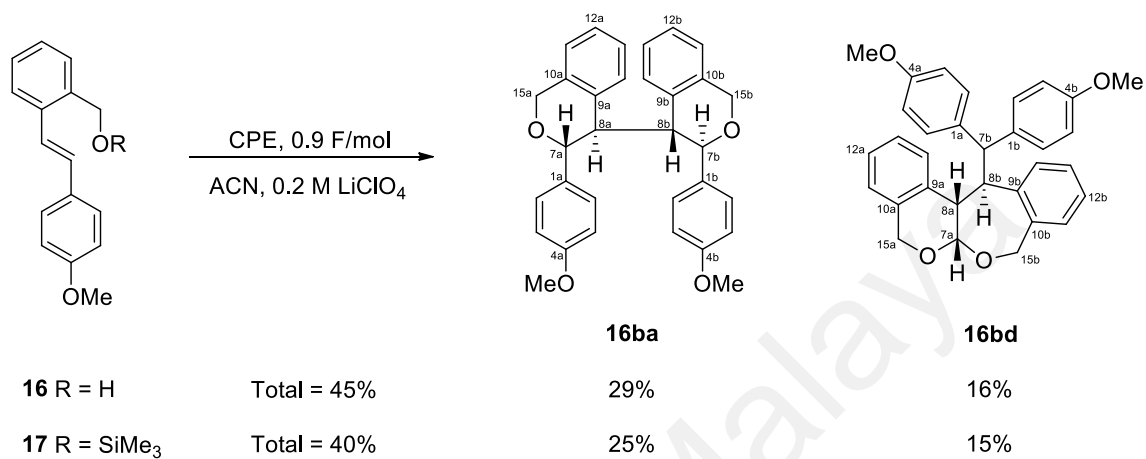
**Scheme 2.17:** Proposed mechanism for the formation of the rearranged monomeric indoles **10ah**, **13ah** and dihydroindole **12ai**

### 2.3 Anodic Oxidation of 4-Methoxy- and 3,4-Dimethoxystilbenes Substituted with 2'-Hydroxymethyl, 2'-Aminomethyl, 2'-Carboxylic Acid, and 2'-Vinyl Groups

As a logical extension of the above studies, we next investigated the effect of ortho'-substituted side chains bearing nucleophilic groups such as  $-\text{CH}_2\text{OH}$ ,  $-\text{CH}_2\text{NHR}$ ,  $-\text{CO}_2\text{H}$ , and  $-\text{CH}=\text{CH}_2$  on the reactivity of anodically-generated 4-methoxy- and 3,4-dimethoxystilbene cation radicals, in order to gain further insight into the reactivity of stilbene cation radicals, as well as to compare the results with those of substrates where the nucleophilic groups such as  $-\text{OH}$  and  $-\text{NHR}$  are directly attached to the aromatic ring.

Anodic oxidation of 4-methoxy-2'-hydroxymethylstilbene (**16**) gave two isomeric products (with molecular formula  $\text{C}_{32}\text{H}_{30}\text{O}_4$  as shown by HRMS), the bisbenzopyran (**16ba**, 29%) and the fused benzopyranobenzoxepane (**16bd**, 16%) in a combined yield of about 45% as shown in Scheme 2.18. The structure of the bisbenzopyran (**16ba**) was established based on the MS and NMR data and confirmed by X-ray analysis. The  $^1\text{H}$  and  $^{13}\text{C}$  NMR data of **16ba** showed only resonances due to half of the molecule, indicating the presence of an element of symmetry. In addition to the aromatic and methoxy resonances, the  $^1\text{H}$  NMR spectrum showed two methine hydrogens as singlets at  $\delta$  5.17 (H-7a) and 3.80 (H-8a), indicating that H-7a and H-8a were orthogonal, which was also shown in the X-ray structure of **16ba** (Figure 2.11). Since the other half is related by the symmetry element present, the resulting molecule is a bisbenzopyran with a  $C_2$  axis (the possibility of a *meso* compound is ruled out by chiral phase HPLC). Compound **16ba** was similar to that of the previously observed  $C_2$  symmetric bisbenzofuran (**1ac**, see Figure 2.2) obtained in the anodic oxidation of 4-methoxy-2'-hydroxystilbene (**1**),<sup>99</sup> except for the additional methylene groups in compound **16ba**. The observed H-15a to C-7a, C-9a, and C-11a three-bond correlations in the HMBC

spectrum confirmed the insertion of a methylene group to give a  $C_2$  symmetric bisbenzopyran **16ba** (Figure 2.11).



**Scheme 2.18:** Products from the anodic oxidation of stilbenes **16** and **17**

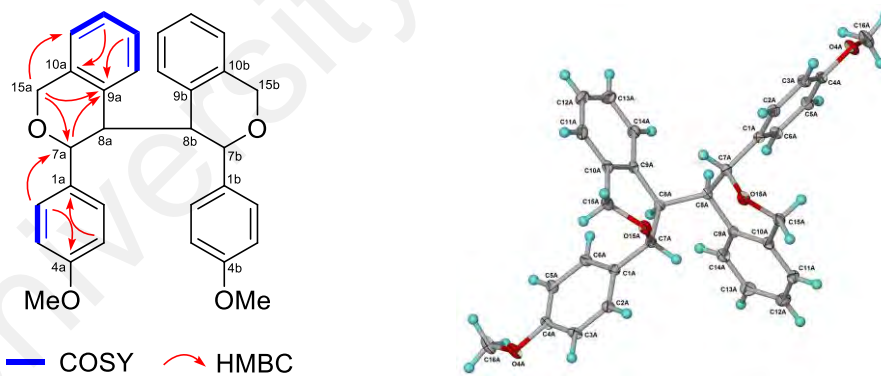


**Figure 2.11:** COSY, selected HMBCs, and X-ray structure of **16ba**

The structure of the fused benzopyranobenzoxepane (**16bd** C<sub>32</sub>H<sub>30</sub>O<sub>4</sub>) was deduced based on the MS and NMR spectroscopic data (Figure 2.12) and by analogy with the corresponding product, the fused benzofuranobenzopyran (**1ae**, see Figure 2.4) previously obtained in the oxidation of the ortho'-hydroxy-4-methoxystilbene (**1**) and for which the structure was confirmed by X-ray analysis<sup>99</sup>. The main difference in the <sup>1</sup>H and <sup>13</sup>C NMR spectra is the appearance of additional resonances due to the two sets of benzylic oxymethylenes in **16bd**, corresponding to C-15a ( $\delta_{\text{H}}$  4.60, 4.94;  $\delta_{\text{C}}$  63.5; pyran ring) and C-15b ( $\delta_{\text{H}}$  4.69, 5.15;  $\delta_{\text{C}}$  70.1; oxepane ring), based on the observed three-bond correlations from H-15a to C-7a, C-9a, C-11a, and from H-15b to C-7b, C-9b, C-11b, in the HMBC spectrum (Figure 2.12).

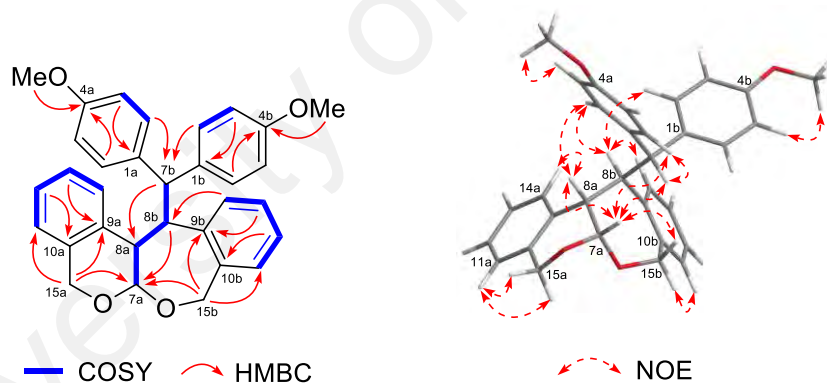
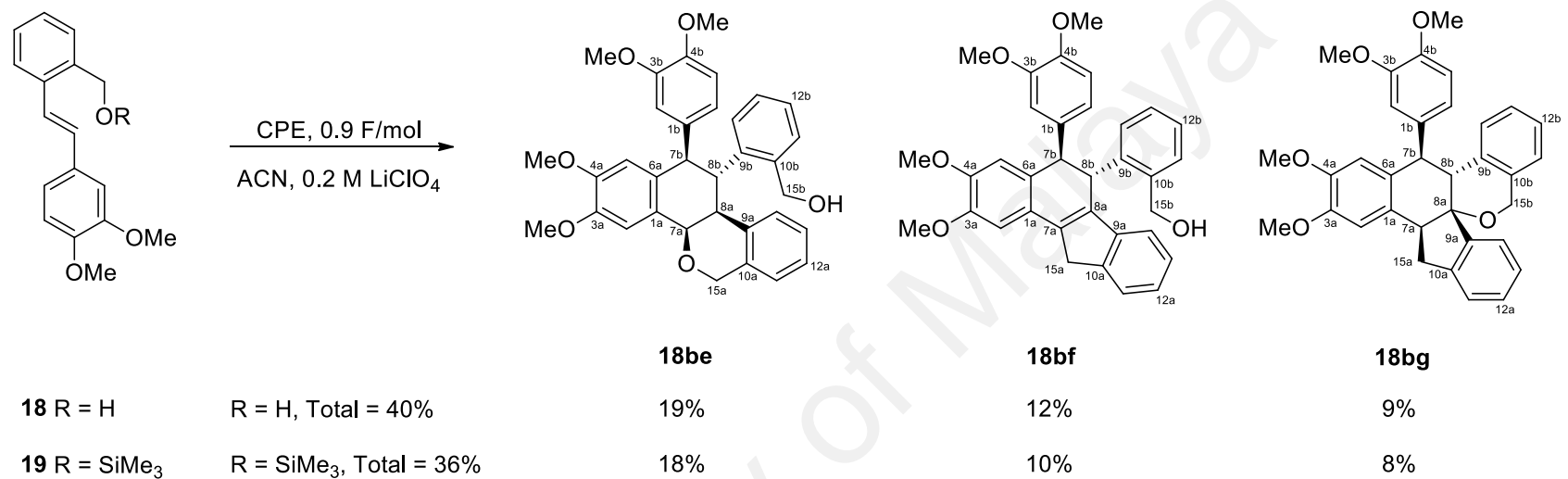


**Figure 2.12:** COSY, selected HMBCs, and selected NOEs of **16bd**

We next investigated the anodic oxidation of the TMS-protected 4-methoxy-2'-hydroxymethylstilbene **17**. The results showed that the same products (**16ba** and **16bd**) were obtained, and although there were minor variations in the product distribution, the overall yield was essentially unchanged (Scheme 2.18).

Anodic oxidation (0.96 V) of the 3,4-dimethoxy-substituted derivative (**18**) gave three products, the fused tetralinylbenzopyran (**18be**, 19%), the fused indanyltetralin (**18bf**, 12%), and the fused benzopyranoindanyltetralin (a hexacyclic spiroether, **18bg**, 9%), in combined yield of about 40% (Scheme 2.19). As in the previous case, all three were dimerization products as indicated by the HRMS data. Anodic oxidation of the TMS-protected 3,4-dimethoxy-2'-hydroxymethylstilbene **19** gave the same products (**18be**, **18bf**, and **18bg**) as in the anodic oxidation of stilbene **18** (Scheme 2.19).

The  $^1\text{H}$  NMR spectrum of **18be** ( $\text{C}_{34}\text{H}_{34}\text{O}_6$ ) showed the presence of 13 aromatic resonances, 4 methoxy groups, 4 methine hydrogens, and 2 sets of benzylic oxymethylenes. The COSY data (Figure 2.13) showed that the four methines are linked to form a CH-CH-CH-CH-O fragment corresponding to C-7b-C-8b-C-8a-C-7a-O from the 2-D HMBC data ( $^3J$  H-2a/C-7a, H-7b/C-1a, Figure 2.13). This is also consistent with two of the aromatic resonances from the same ring being seen as singlets ( $\delta$  6.37, H-5a; 6.93, H-2a) in agreement with the presence of a 1,2,4,5-tetrasubstituted aromatic ring. Of the two benzylic oxymethylene singlets, one is assigned to a hydroxymethyl ( $\delta$  3.76, H-15b; IR:  $3500\text{ cm}^{-1}$ ) while the other at lower field ( $\delta$  5.13, H-15a) is part of a 2-benzopyran ring. The relative configuration is readily assigned based on analysis of the vicinal coupling constants as well as the 2-D NOESY data. The observed  $J_{7b-8b}$  and  $J_{8b-8a}$  coupling of 11.6 Hz requires H-7b/H-8b and H-8a/H-8b to be in a trans arrangement while the  $J_{7a-8a}$  coupling of 2.2 Hz indicates H-7a/H-8a to be cis. These conclusions are also in agreement with the NOESY data (Figure 2.14).



**Scheme 2.19:** Products from the anodic oxidation of stilbenes **18** and **19**

The HRMS data of the indanyltetralin **18bf** (C<sub>34</sub>H<sub>32</sub>O<sub>5</sub>) indicated that it differs from compound **18be** by loss of H<sub>2</sub>O. Examination of the NMR data indicated that the oxygen atom lost corresponds to that belonging to the pyran ring since the benzylic hydroxymethyl moiety is still present in **18bf** ( $\delta$  4.89, H-15b; IR: 3500 cm<sup>-1</sup>; HMBC: <sup>3</sup>J H-15b/C-11b, Figure 2.13), while C-15a is an isolated benzylic methylene ( $\delta_{\text{H}}$  3.78, 3.94;  $\delta_{\text{C}}$  36.3) in **18bf**. Comparison of the <sup>1</sup>H and <sup>13</sup>C NMR data also indicated that the loss of 2H in **18bf** corresponds to the loss of two methine hydrogens (H-7a and H-8a), with the concomitant appearance of a tetrasubstituted double bond corresponding to C7a=C8a ( $\delta_{\text{C}}$  139.7, 137.5). The relative configuration was deduced from the NOESY data (Figure 2.14), which indicated H-7b and H-8b to be  $\alpha$ - and  $\beta$ -oriented, respectively.<sup>85</sup> The benzopyranoindanyltetralin or spiroether **18bg** (C<sub>34</sub>H<sub>32</sub>O<sub>5</sub>) is isomeric with **18bf** as shown by HRMS. The <sup>1</sup>H and <sup>13</sup>C NMR data of **18bg** showed a number of similarities with that of **18bf**. The presence of the same 1,2,4,5-substituted aromatic moiety is indicated by the two aromatic singlets at  $\delta$  6.29 (H-5a) and 6.81 (H-2a), while the non-equivalent benzylic hydrogens associated with the indane moiety is seen as a pair of doublet of doublets ( $\delta$  2.99, *J* 15.6, 11.2 Hz, H-15a; 3.59, *J* 15.6, 9.2 Hz, H-15a'), as a consequence of coupling to the vicinal H-7a. The remaining CHCH fragment shown by the COSY data (Figure 2.13) corresponds to C-7b–C-8b, while C-8a is an oxygenated tertiary carbon ( $\delta_{\text{C}}$  83.2) as a consequence of the linking of the C-15b–O to C-8a to forge a 2-benzopyran moiety in **18bg**. The structure is in full agreement with the HMBC data (Figure 2.13), while the relative configuration is assigned based on the NOESY data (Figure 2.13).

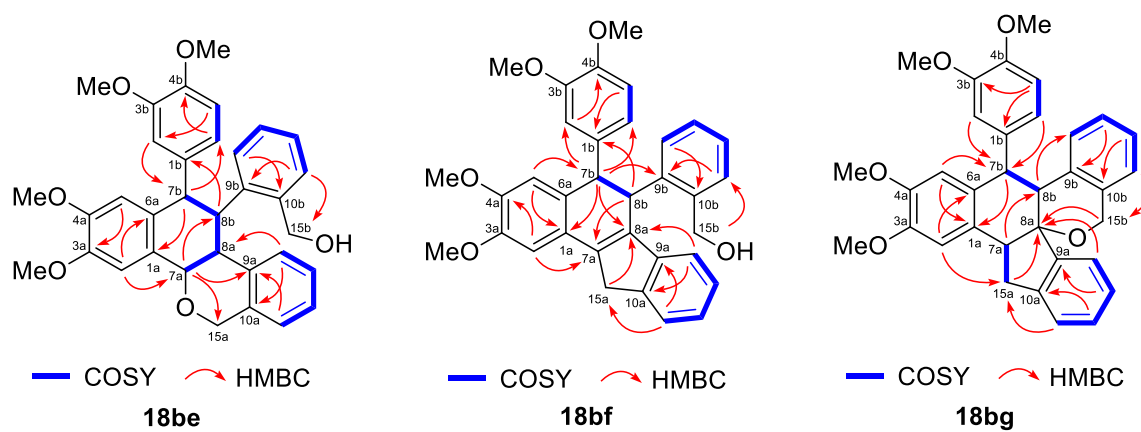


**Figure 2.13:** COSY and selected HMBCs of **18be**, **18bf**, and **18bg**

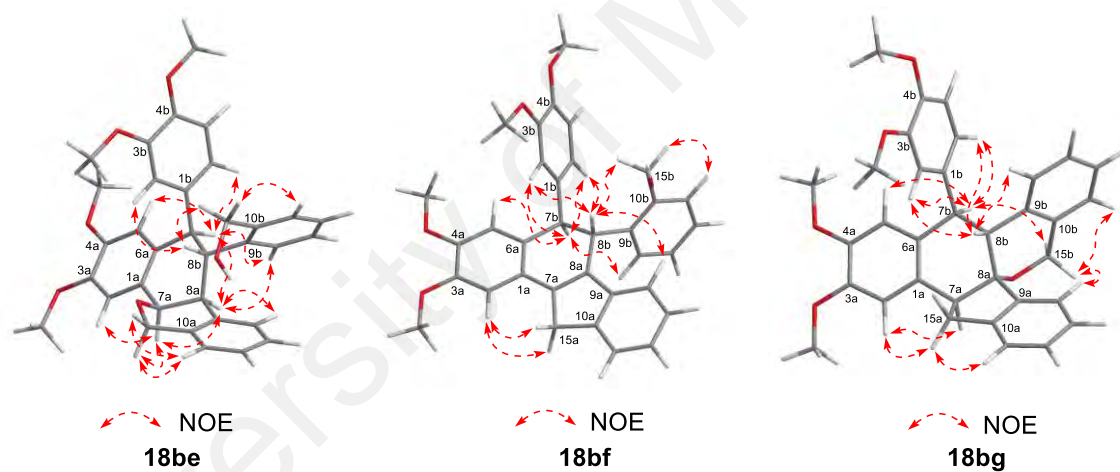
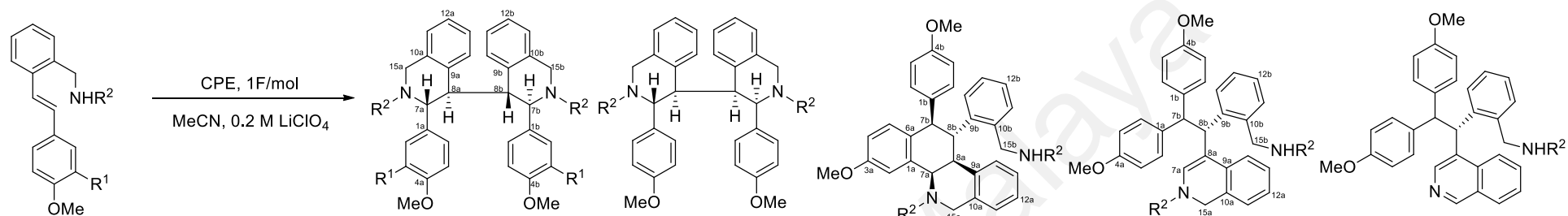


**Figure 2.14:** Selected NOEs of **18be**, **18bf**, and **18bg**

The next series of compounds investigated were the nitrogen analogues of **16** and **18**, i.e., where the ortho'-substituents are aminomethyl instead of hydroxymethyl. As in the previous study,<sup>99</sup> protection of the free amino function was necessary to avoid electrode passivation and the results are shown in Scheme 2.20. The nosyl-protected stilbene **20** gave the highest overall yield (ca. 70%) of a product mixture comprising the  $C_2$  symmetric bisisoquinoline (**20ba** 25%), the fused tetralinylisoquinoline (**20be** 10%), the dihydroisoquinoline (**20bh** 20%), and the isoquinoline (**20bi** 12%). The tosyl-protected stilbene **21** gave **21ba** (24%) and **21bi** (27%). The acetylated stilbene **22** gave the unsymmetrical bisisoquinoline **22bb** (17%) and **22bi** (14%), while the carbamate **23** gave only **23bi** (15%). The oxidation of stilbenes **22** and **23** were also characterized by formation of a significant quantity of insoluble polymeric products.

The structure of the  $C_2$  symmetric bisisoquinoline **20ba** is readily assigned by analogy to the oxygen analogue, the bisbenzopyran **16ba**, whose structure was confirmed by X-ray analysis (vide supra). X-ray structures were available for **20bi** and **22bi** (Figure 2.17), and furthermore **20bh** is transformed to **20bi** by reaction with thiophenol (aromatization and partial nosyl deprotection). The tetralinylisoquinoline **20be** is related to **20bh** by bond formation from C-7a to C-2a (Figure 2.15), and in addition, **20be** (NOEs in Figure 2.16) is also structurally related to the fused tetralinylbenzopyran **18be** (vide supra). Anodic oxidation of the 3,4-dimethoxy-substituted stilbenes (**24–27**) was mainly unproductive giving insoluble polymeric products except for the tosyl-protected stilbene **24** which gave the  $C_2$  symmetric bisisoquinoline **24ba** in 24% yield in addition to the polymeric products. The stereochemical assignments for the nonsymmetric bisisoquinoline **22bb** (Figure 2.15) was based on the NOESY data (H-15a/H-8b and H-8a/H-15b NOEs, Figure 2.16) as well as by analogy to the nonsymmetric bis- $\delta$ -lactone **28bb**, whose structure was also confirmed by X-ray analysis (vide infra).



**20** R<sup>1</sup> = H; R<sup>2</sup> = Ns

R<sup>1</sup> = H; R<sup>2</sup> = Ns  
Total = 67%

**20ba**  
25%

**21** R<sup>1</sup> = H; R<sup>2</sup> = Ts

R<sup>1</sup> = H; R<sup>2</sup> = Ts  
Total = 51%

**21ba**  
24%

**22** R<sup>1</sup> = H; R<sup>2</sup> = Ac

R<sup>1</sup> = H; R<sup>2</sup> = Ac  
Total = 31%

**22bb**  
17%

**23** R<sup>1</sup> = H; R<sup>2</sup> = CO<sub>2</sub>Me

R<sup>1</sup> = H; R<sup>2</sup> = CO<sub>2</sub>Me  
Total = 15%

**20bi**  
12%

**21bi**  
27%

**22bi**  
14%

**23bi**  
15%

**24** R<sup>1</sup> = OMe; R<sup>2</sup> = Ts

R<sup>1</sup> = OMe; R<sup>2</sup> = Ts  
Total = 24%

**24ba**  
24%

**25** R<sup>1</sup> = OMe; R<sup>2</sup> = Ns

R<sup>1</sup> = OMe; R<sup>2</sup> = Ns

(insoluble polymeric products)

**26** R<sup>1</sup> = OMe; R<sup>2</sup> = Ac

R<sup>1</sup> = OMe; R<sup>2</sup> = Ac

(insoluble polymeric products)

**27** R<sup>1</sup> = OMe; R<sup>2</sup> = CO<sub>2</sub>Me R<sup>1</sup> = OMe; R<sup>2</sup> = CO<sub>2</sub>Me

(insoluble polymeric products)

**Scheme 2.20:** Products from the anodic oxidation of stilbenes **20–27**

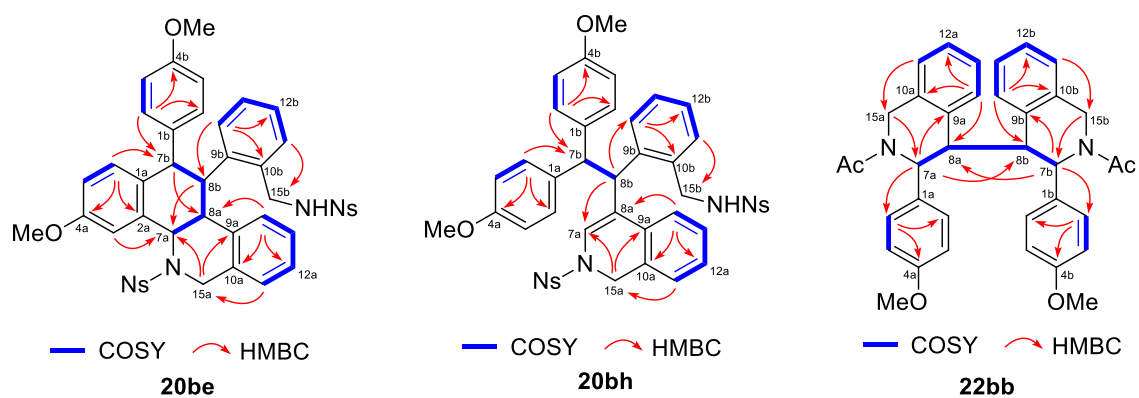


**Figure 2.15:** COSY and selected HMBCs of **20be**, **20bh**, and **22bb**

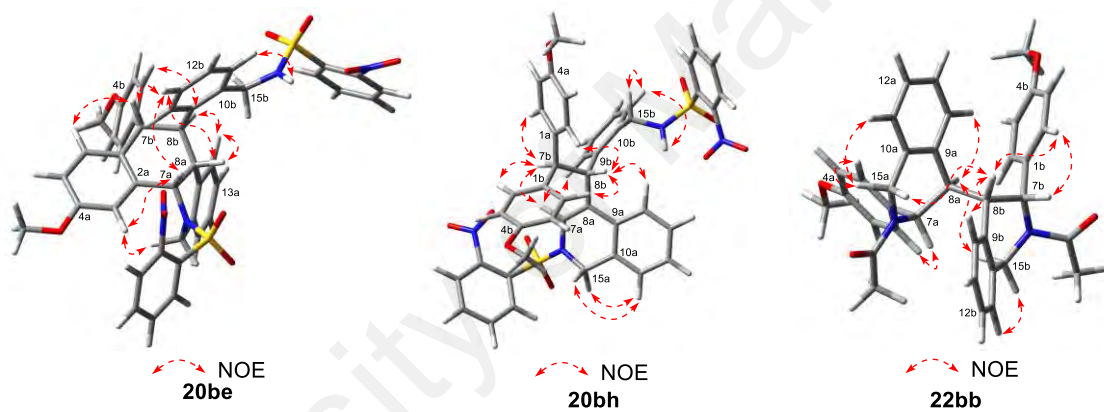


**Figure 2.16:** Selected NOEs of **20be**, **20bh**, and **22bb**

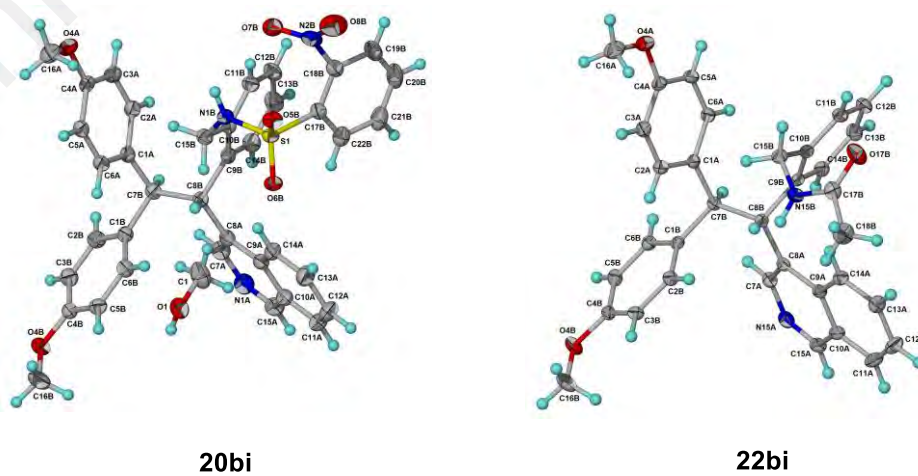


**Figure 2.17:** X-ray structures of **20bi** and **22bi**

The next 4-methoxystilbene chosen for investigation (**28**) was one substituted by an ortho'-carboxylic acid group in the other ring. Anodic oxidation of **28** gave a mixture comprising three isomeric dimerization products ( $C_{32}H_{26}O_6$ ), viz., the  $C_2$  symmetric bis- $\delta$ -lactone (**28ba**, 29%), the *meso* bis- $\delta$ -lactone (**28bc**, 18%), and the nonsymmetric bis- $\delta$ -lactone (**28bb**, 24%), in a combined yield of about 71% as shown in Scheme 2.21. The structures of the bis- $\delta$ -lactones (**28ba–28bc**) were established based on the MS and NMR data and confirmed by X-ray analysis (Figure 2.18). Anodic oxidation of the 3,4-dimethoxy-substituted compound **29** gave the corresponding three bis- $\delta$ -lactone products (**29ba**, **29bb**, **29bc**) accompanied by the monomeric  $\delta$ -lactone **29bj** as a minor product (Scheme 2.21).

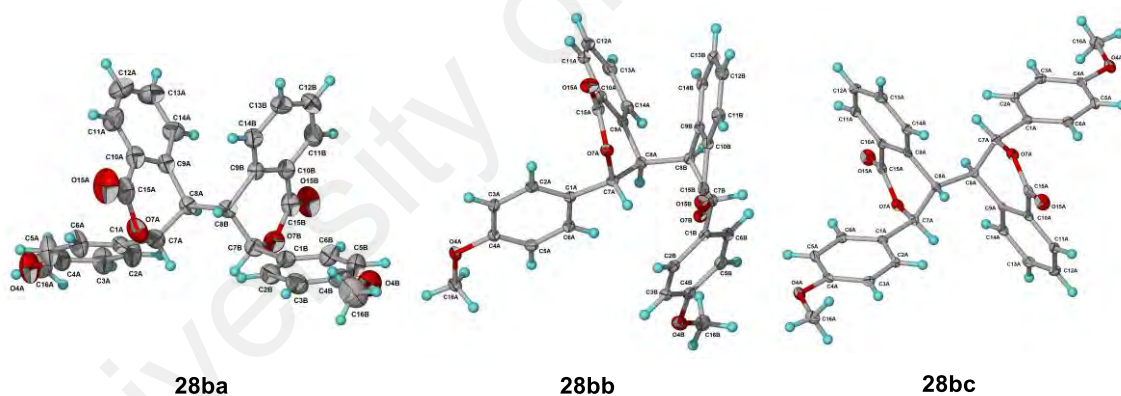
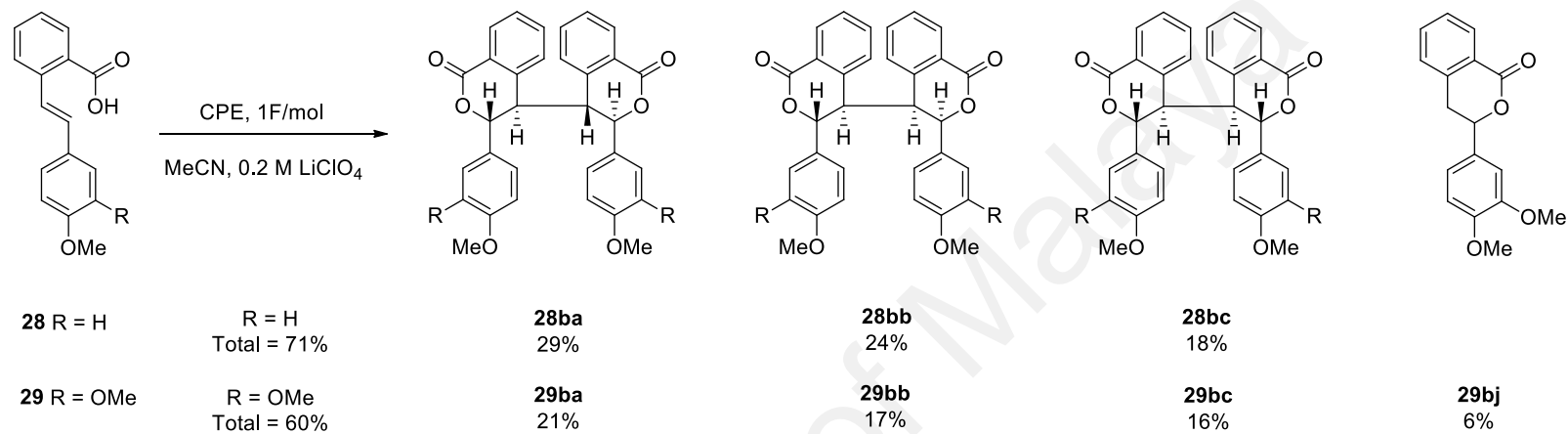
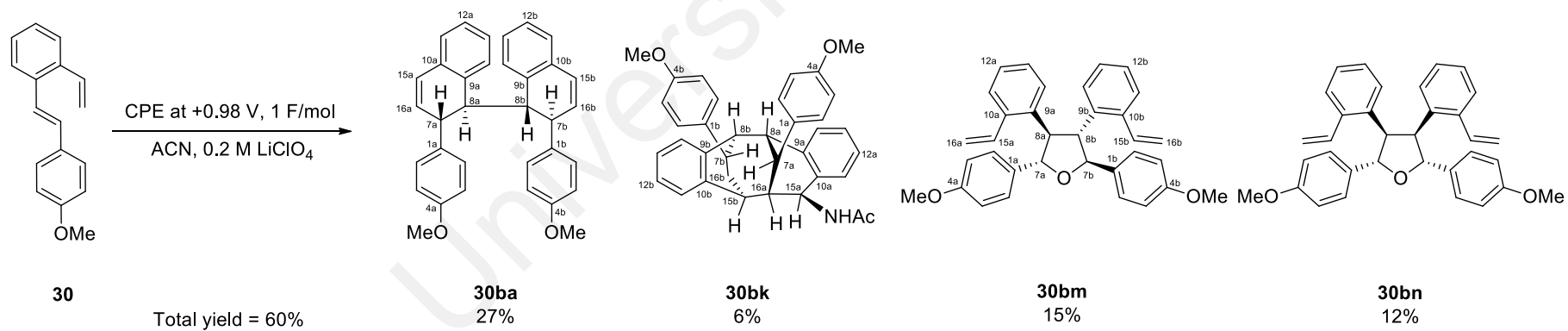


**Figure 2.18:** X-ray structures of **28ba**, **28bb**, and **28bc**



**Scheme 2.21:** Products from the anodic oxidation of stilbenes **28** and **29**



**Scheme 2.22:** Products from the anodic oxidation of stilbene **30**

The effect of a vinyl group as the ortho'-substituent was next investigated (stilbenes **30** and **31**) with a view to assess whether  $\pi$ -electrons can efficiently trap the benzylic cations. Anodic oxidation of 4-methoxy-2'-vinylstilbene **30** gave a product mixture comprising the  $C_2$  symmetric bisdihydronaphthalene **30ba** (27%), the unusual, doubly-bridged, dibenzofused cyclononane **30bk** (6%), and the stereoisomeric tetraaryltetrahydrofurans<sup>85</sup> **30bm** (15%) and **30bn** (12%) as shown in Scheme 2.22.

The structure of the bisdihydronaphthalene **30ba** is readily assigned by analogy to the related  $C_2$  symmetric compounds such as **16ba**, **20ba**, **21ba**, **24ba**, **28ba**, and **29ba** (the structures of **16ba** and **28ba** were also confirmed by X-ray analysis, vide supra, Figures 2.11 and 2.18, respectively). The presence of the C-15–C-16 double bond is indicated by the olefinic resonances at  $\delta_H$  6.68 ( $\delta_C$  130.0) and  $\delta_H$  6.01 ( $\delta_C$  130.1), respectively. The structure is in full agreement with the HMBC data (Figure 2.19).

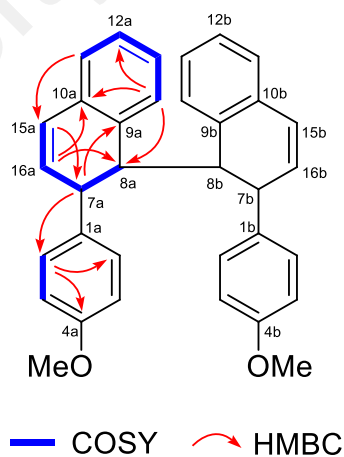


**Figure 2.19:** COSY and selected HMBCs of **30ba**

The  $^1\text{H}$  NMR data of the cyclononane derivative **30bk** ( $\text{C}_{36}\text{H}_{35}\text{NO}_3$ ) showed resonances due to 16 aromatic hydrogens, 7 methines, 2 methoxy groups, one methylene, and one methyl of an acetamide group. The NH resonance is observed as a doublet at  $\delta_{\text{H}}$  4.52 while a deshielded doublet at  $\delta_{\text{H}}$  5.31 ( $\delta_{\text{C}}$  48.1) is assigned to an aminomethine (H-15a). The presence of an amide group is also indicated by the amide carbonyl resonance at  $\delta_{\text{C}}$  168.5 as well as by the IR bands at 1655 (C=O) and 3305 (NH)  $\text{cm}^{-1}$ . The aromatic resonances are attributed to two 1,4-disubstituted (two *p*-methoxyphenyl) and two 1,2-disubstituted aromatic moieties, corresponding to rings A, A', B and B' (Figure 2.20). The COSY data (Figure 2.20) showed the presence of a  $-\text{NHCHCHCHCHCHCHCHCH}-$  partial structure, corresponding to NH-C-15a-C-16a-C-7a-C-8a-C-8b-C-7b-C-16b-C-15b, with C-15b linked to C16a to forge a substituted seven-membered ring. Examination of the HMBC data allowed complete structural assignment leading to a doubly-bridged, dibenzofused cyclononane derivative **30bk**. The acetamido side chain is linked to the cyclononane core at C-15a, based on the H-15a/C-17 three-bond correlation in the HMBC spectrum. The stereochemistry/orientation of H-8a, H-8b, H-15b, and H-16a are fixed by the geometry of the methano (C-7a) and ethano (C-7b-C-16b) bridges, which are oriented anti to each other from the NOE data (strong H-15a/H-16b NOE, the same NOE would be impossible for the alternative structure with the methano and ethano bridges oriented syn to each other). With the geometry of the methano (C-7a) and ethano (C-7b-C16b) bridges fixed, the orientation of H-8a, H-8b, H-15b, and H-16a can be accordingly assigned, while the orientations of H-7a and H-7b are assigned from the H-2a (H-6a)/H-16a and H-2b (H-6b)/H-16b NOEs (Figure 2.20). Other observations which are consistent with the structure include the observation that H-15a and H-16a are orthogonal ( $J_{15a-16a} = 0$ ) consistent with the  $\alpha$ -orientation of H-15a and the observation of long-range *W*-coupling (3.2 Hz) between H-8a and H-16a.

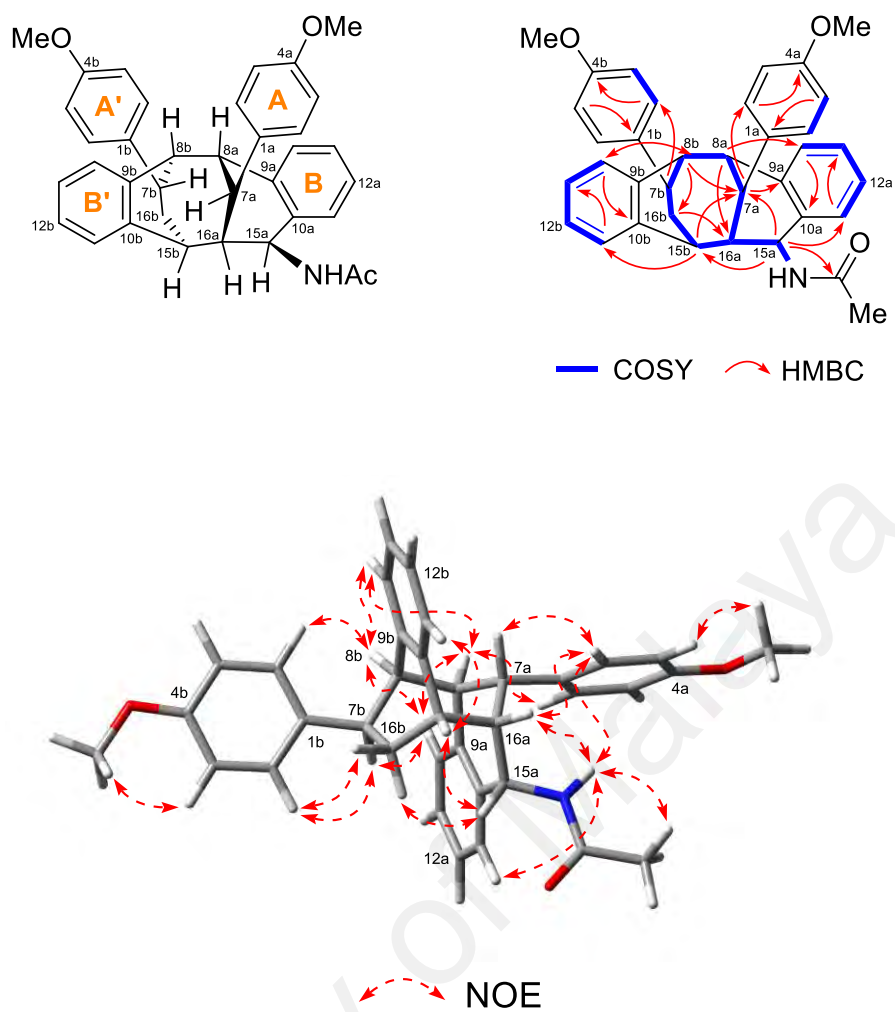
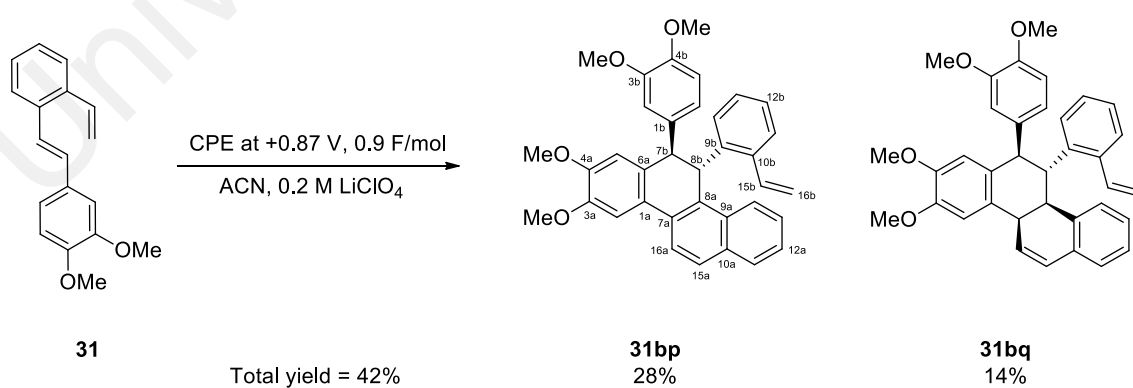
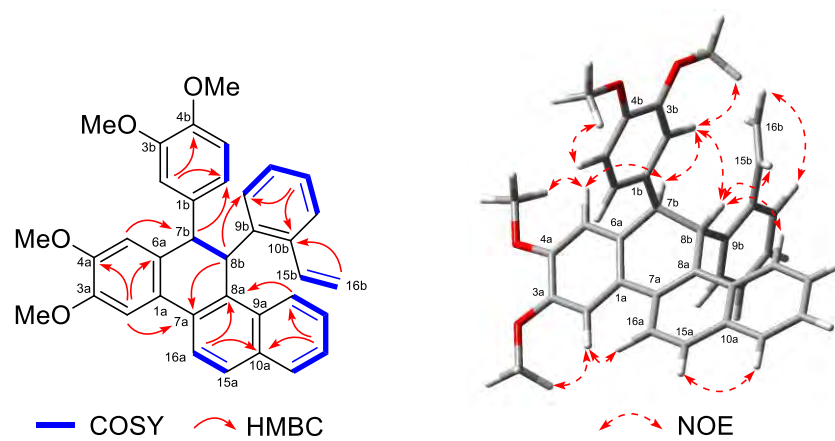


Figure 2.20: COSY, selected HMBCs, and selected NOEs of **30bk**



Scheme 2.23: Products from the anodic oxidation of stilbene **31**

Anodic oxidation of the 3,4-dimethoxy-substituted derivative **31** gave two products which are derivatives of the fused polyaromatic hydrocarbon, chrysene, the dihydrochrysene **31bp** (28%) and the tetrahydrochrysene **31bq** (14%) (Scheme 2.23). The  $^1\text{H}$  and  $^{13}\text{C}$  NMR data of **31bp** ( $\text{C}_{36}\text{H}_{32}\text{O}_4$ ) can be readily assigned with the aid of the 2-D data. The  $^1\text{H}$  resonances of H-7b and H-8b (constituting the CHCH fragment linked to C-6a) are singlets indicating that they are orthogonal, which has been noted previously in related dehydrotetralin derivatives.<sup>85,99</sup> The benzylic C-7b is linked to a 1,2-dimethoxyphenyl group while the adjacent C-8b is linked to an ortho vinyl substituted aromatic moiety based on the 2-D HMBC data ( $^3J$  H-5a/C-7b, H-8b/C-14b, Figure 2.21). The vinyl group ( $\delta_{\text{H}}$  5.65, 5.92, and 7.69) is attached to C-10b based on the three-bond H-16b/C-10b correlation, while the C-16a=C-15a fragment is linked to C-7a based on the three-bond H-16a/C-8a correlation in the HMBC spectrum (Figure 2.21). Compound **31bq** is readily identified as the dihydro derivative of **31bp** from the HRMS ( $\text{C}_{36}\text{H}_{34}\text{O}_4$ ) and the  $^1\text{H}$  and  $^{13}\text{C}$  NMR data. The  $^1\text{H}$  spectrum of **31bq** is generally similar to that of **31bp** except for the observation of a CHCHCHCH=CH fragment (in place of a CHCH and CH=CH fragment in **31bp**) corresponding to C-7b–C-8b–C-8a–C-7a–C-16a–C-15a from the COSY data (Figure 2.22). This change is also shown in the  $^{13}\text{C}$  NMR spectrum of **31bq** in which C-8a and C-7a appear as methines ( $\delta$  44.3, 41.0) instead of as quaternary olefinic carbons in **31bp** ( $\delta$  130.9, 132.5). The relative configuration is readily assigned based on analysis of the vicinal coupling constants as well as the 2-D NOESY data. The observed  $J_{7\text{b}-8\text{b}}$  and  $J_{8\text{b}-8\text{a}}$  coupling of 11.2 Hz requires H-7b/H-8b and H-8a/H-8b to be in a trans arrangement while the  $J_{7\text{a}-8\text{a}}$  coupling of 6.0 Hz indicates H-7a/H-8a to be cis. These conclusions are also in agreement with the NOESY data (Figure 2.22).



**Figure 2.21:** COSY, selected HMBCs, and selected NOEs of **31bp**

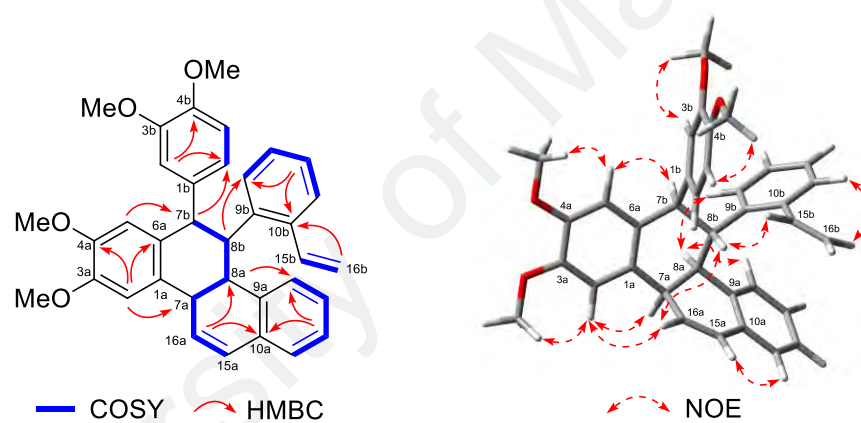
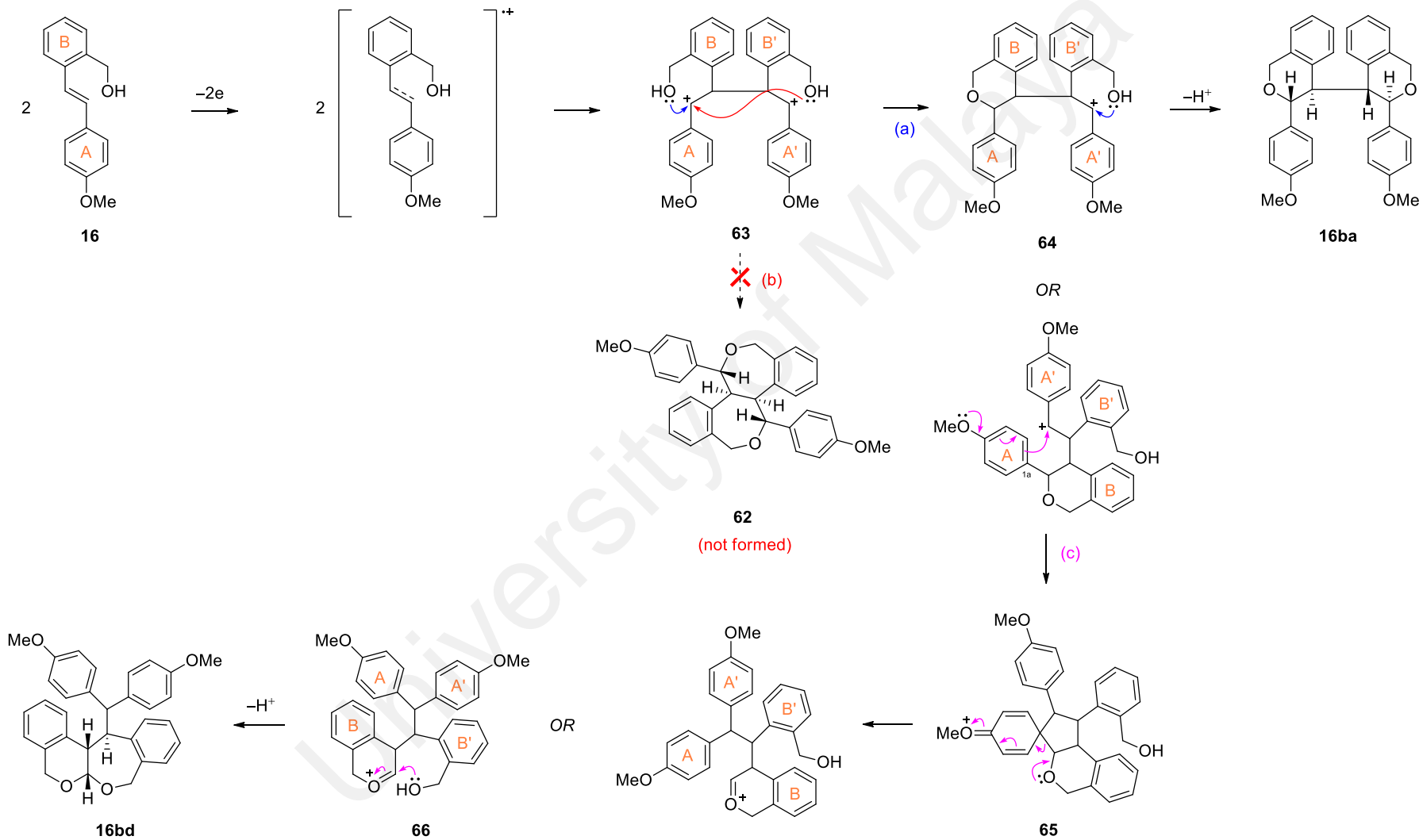


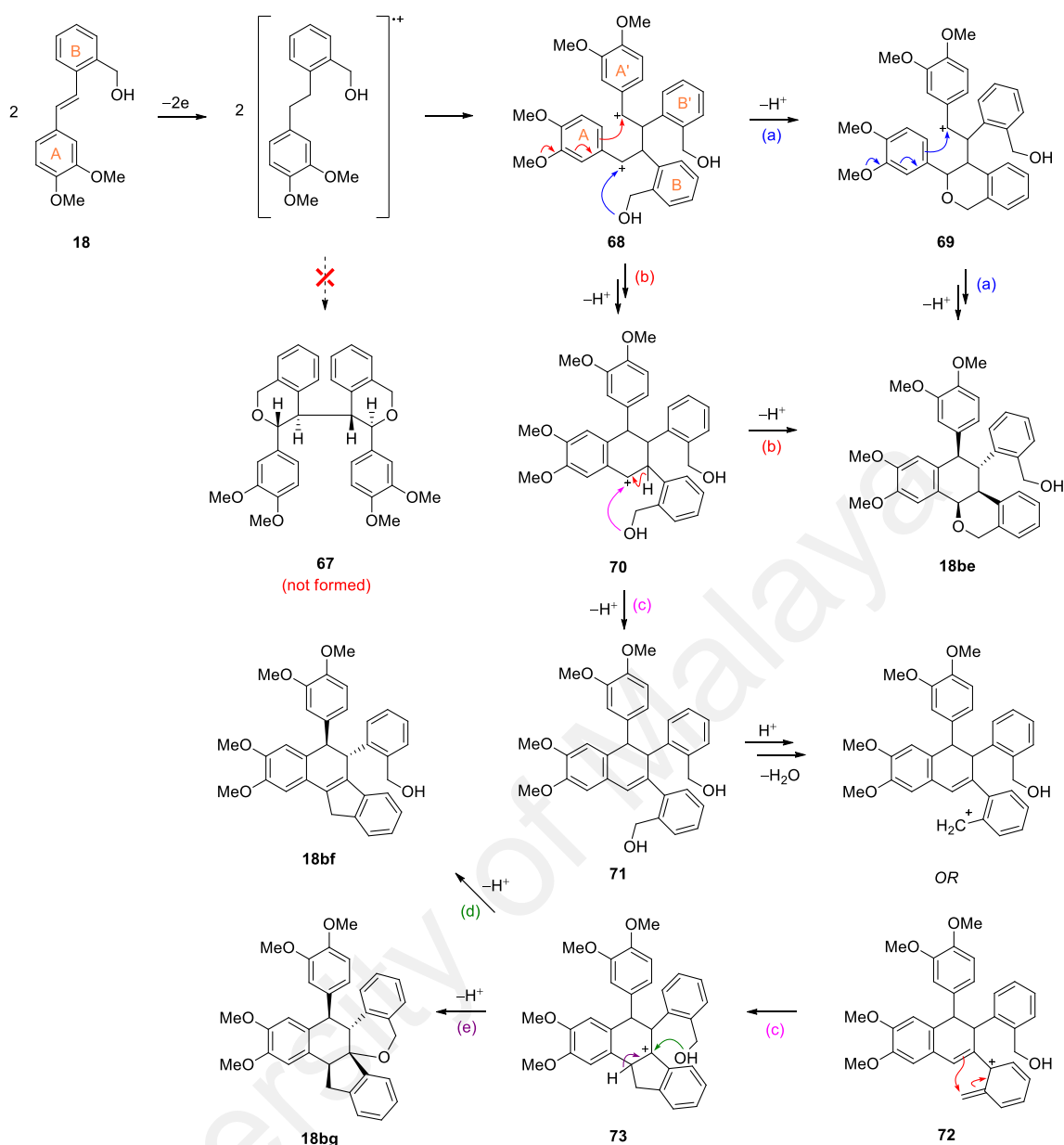
**Figure 2.22:** COSY, selected HMBCs, and selected NOEs of **31bq**

In the preceding section, the nucleophilic groups ( $-\text{OH}$  and  $-\text{NH}_2/\text{NHR}$ ) were attached directly to the aromatic ring. In the present instance, the ortho'-substituted side chains have been extended with an intervening  $\text{CH}_2$  ( $-\text{CH}_2\text{OH}$ ,  $-\text{CH}_2\text{NHR}$ ), or  $\text{C}=\text{O}$  ( $-\text{COOH}$ ) group, or where  $\pi$ -electrons of an ortho'-substituted vinyl group ( $-\text{CH}=\text{CH}_2$ ) assume the role of the nucleophile. Comparison of the oxidation of the hydroxymethylstilbene **16** with that of the hydroxystilbene **1**, showed a clear absence of the products of crossover cation trapping (e.g., **62** in Scheme 2.24, path b) in the oxidation of **16**. In contrast, in the oxidation of the hydroxystilbene **1**, the crossover cation trapping products, viz., the stereoisomeric fused bisbenzopyrans (**1aa**, **1ab**) were obtained as the major products in addition to the direct cation trapping product **1ac** (Scheme 2.13). Furthermore, the oxidation of **16** was also characterized by a reduction in the overall yield compared to that for the hydroxystilbene **1** (45% vs 80%). The products in the present instance include the bisbenzopyran **16ba** resulting from direct cation trapping, and the fused pyranooxepane **16bd**, the analogue of the fused furanopyran **1ae**, obtained in the reaction of the hydroxystilbene **1**.

The mechanism (Scheme 2.24) leading to the two products is similar to that proposed previously for the reaction of the hydroxystilbene **1** involving cation radical dimerization followed by direct trapping of the dication **63** by the ortho'-substituted OH nucleophiles leading to the bisbenzopyran **16ba** (Scheme 2.24, path a). Formation of the fused pyranooxepane **22bd** is via further reaction of the first formed cation intermediate **64** where a Friedel-Crafts reaction as a result of activation of C-1a (ring A) by the 4-methoxy group leads to the spirocyclic cation **65** (Scheme 2.24, path c) which on subsequent ring opening<sup>85,99</sup>, followed by nucleophilic attack on the oxycarbenium ion **66** gives the ketal product **16bd**.



**Scheme 2.24:** Proposed mechanism for the formation of products in the anodic oxidation of stilbene **16** in MeCN/LiClO<sub>4</sub>



**Scheme 2.25:** Proposed mechanism for the formation of products in the anodic oxidation of stilbene **18** in MeCN/LiClO<sub>4</sub>

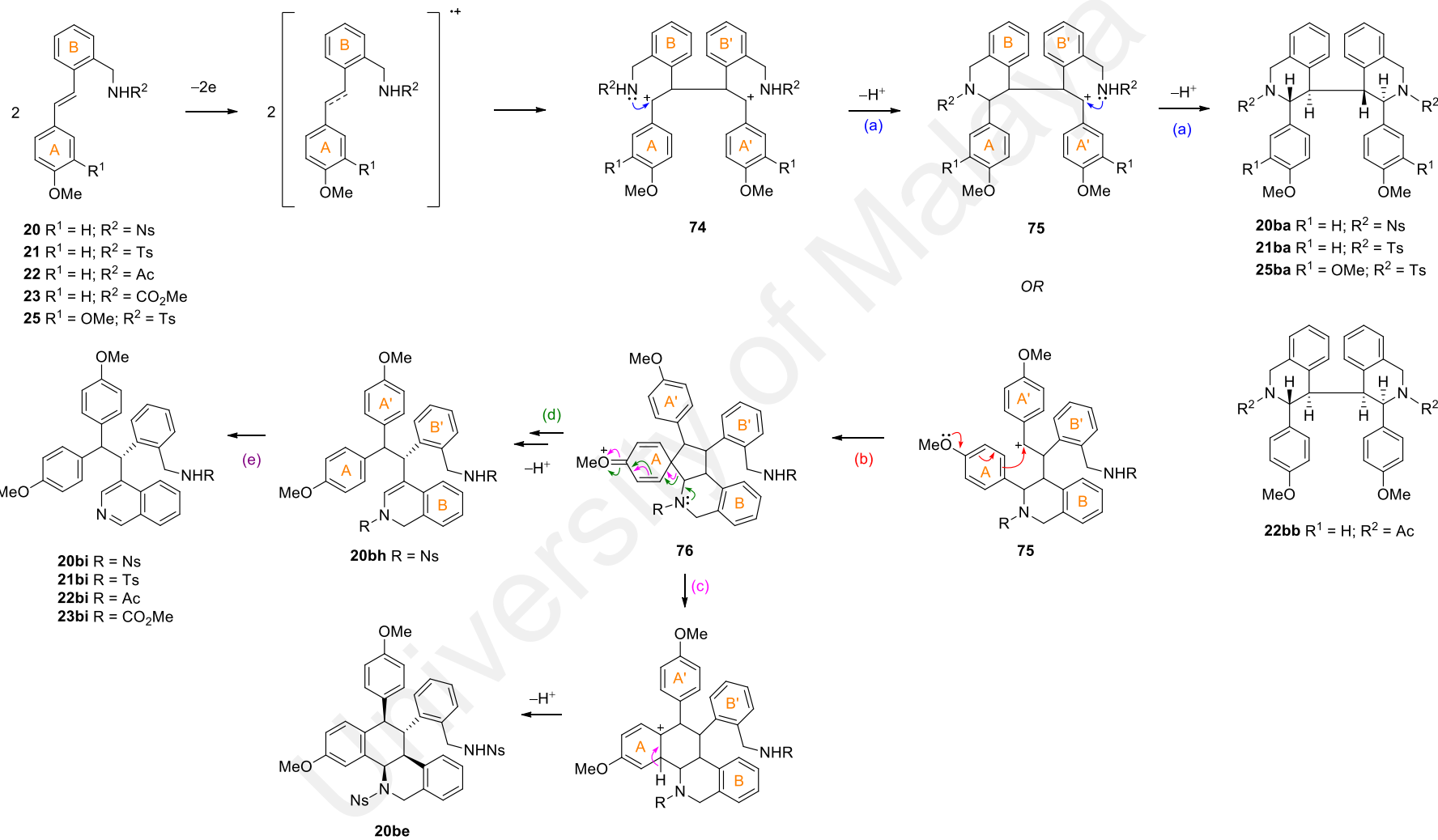
In the oxidation of the 3,4-dimethoxy-2'-hydroxystilbene **3**, the products formed include the fused bisbenzopyran (**3aa**, from crossover trapping), the stereoisomeric bisbenzofuran (**3ac** and **3ad**, from direct trapping), and the bridged oxocine (**3af**, from Friedel-Crafts reaction due to the presence of the 3-methoxy group). The anodic oxidation of the 3,4-dimethoxy-2'-hydroxymethylstilbene **18** on the other hand gave three products, all of which derived from electrophilic aromatic substitution or Friedel-Craft

reactions<sup>98</sup> as a result of activation of ring A towards electrophilic substitution by the 3-methoxy substituent. No product from direct cation trapping (e.g., bisbenzopyran **67**, see scheme 2.25) was detected. A plausible mechanism leading to the observed products is presented in Scheme 2.25. The cation **69** formed after the first cation-nucleophile reaction (Scheme 2.25, path a), undergoes cyclization via a Friedel-Crafts reaction leading to the major product, the fused tetralinylbenzopyran **18be**. Alternatively, ring-closure of the dication **68** (Scheme 2.25, path b), gave the tetralinyl cation intermediate **70** and subsequent nucleophilic attack by the OH group (ring B) also lead to the fused tetralinylbenzopyran **18be**. Deprotonation of the tetralinyl cation **70** (Scheme 2.25, path c) followed by ionization/dehydration of the tetralin **71** leads to the pentadienyl cation **72**, which on electrocyclic closure yields the tetracyclic cation **70** (Scheme 2.25, path c). Deprotonation of the tetracyclic cation **73** yields the fused indanyltetralin **18bf** (Scheme 2.25, path d) while intramolecular nucleophilic capture by OH gives the hexacyclic spiroether **18bg** (Scheme 2.25, path e).

The major difference of the oxidation of the ortho'-NHR-substituted versus the ortho'-CH<sub>2</sub>NHR-substituted stilbenes is that the latter series are characterized by poorer yields and the absence of crossover cation trapping products. In the former series where -NHR is directly attached to the aromatic ring, both the 4-methoxy- and 3,4-dimethoxy-substituted stilbenes investigated (**7–15**) gave the direct cation trapping products (bisindoles **7ac–15ac**, Schemes 2.9–2.12) in good yields. In stilbenes **8–11**, and **13**, the fused bisquinoline crossover products were also obtained (**8ag–11ag** and **13ag**, Schemes 2.9–2.11). By contrast, in the case of the aminomethyl-substituted stilbenes, only the reaction of the nosyl- (**20**) and tosyl- (**21**) protected 4-methoxystilbenes (and the tosyl-protected 3,4-dimethoxystilbene **24**) resulted in the formation of the corresponding direct cation trapping products (the bisisoquinolines, yields ca. 25%, Scheme 2.20). In addition, the nosyl- and tosyl-substituted stilbenes (**20** and **21**) also

reacted smoothly to give a mixture of well-characterized products in ca. 70% and 50% overall yields, respectively (Scheme 2.20), while the reaction of stilbenes **20–23** also resulted in the formation of the isoquinoline products (**20bi–23bi**, yields 12–27%, Scheme 2.20). In the case of the 4-methoxystilbenes **22**, **23** and the 3,4-dimethoxystilbenes **24–27**, insoluble polymeric products were also obtained in significant quantities (see Scheme 2.20). Thus in the aminomethyl-substituted stilbene series, extension of the ortho' side chain substituent by one carbon compared to where the ortho' nucleophilic group is attached directly to the aromatic ring (i.e.  $-\text{CH}_2\text{NHR}$  vs  $-\text{NHR}$ ) has also resulted in significant lowering of the yields of the oxidation product(s) as well as in the absence of crossover cation trapping products.

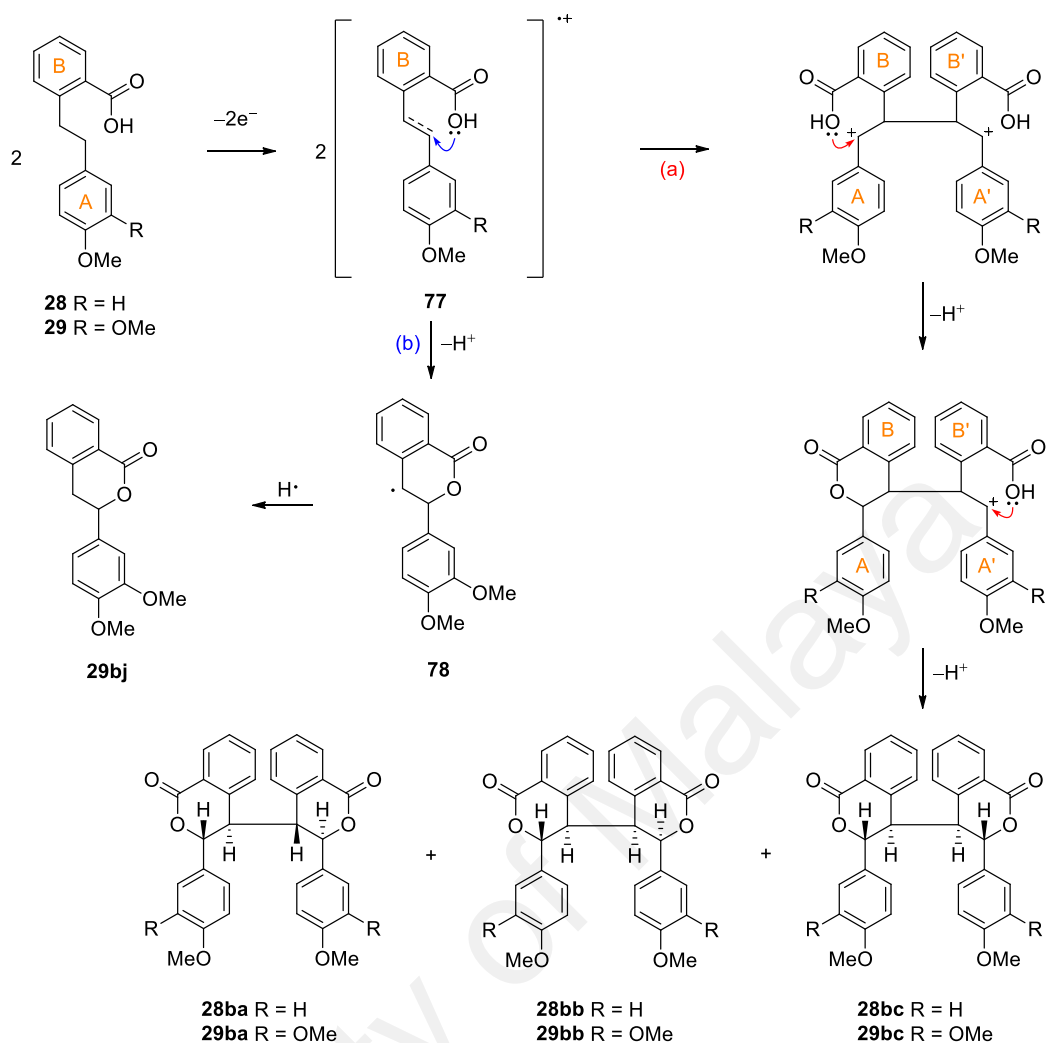
A generalized mechanism, which accounts for the formation of all the products is shown based on the nosyl protected stilbene **20** as an example (Scheme 2.26). The bisisoquinolines (**20ba**, **21ba**, **22bb**, **25ba**) are the result of direct cation trapping of the dication **74** by the respective ortho'-substituted nucleophilic groups (path a, Scheme 2.26). The benzylic cation **75** formed after the first cation-nucleophile reaction (path a, Scheme 2.26) undergoes cyclization (Friedel-Crafts reaction, path b) to the spirocyclic cation **76**, which on subsequent ring expansion gives the tetracyclic tetralinylisoquinoline **20be** (path c, Scheme 2.26). Alternatively, lone pair assisted ring opening of the spirocyclic cation **76**, gives the dihydroisoquinoline **20bh** (path d, Scheme 2.26) and under the reaction conditions, **20bh** undergoes partial deprotection and aromatization to the isoquinoline **20bi** (path e, Scheme 2.26).



**Scheme 2.26:** Proposed mechanism for the formation of products in the anodic oxidation of stilbenes **20–23** and **25** in MeCN/LiClO<sub>4</sub>

The decrease in the overall yields and the absence of crossover cation trapping products therefore constitute the two common features in the oxidation of both the hydroxymethyl- and aminomethylstilbenes, compared to the reactions of the hydroxy- and aminostilbenes. The poorer yields of the nucleophilic trapping products could be a result of a decrease in reactivity as a result of the presence of an intervening methylene group, while the absence of crossover trapping products could be a reflection of the greater difficulty in accessing 7-membered versus 6-membered rings.<sup>100–103</sup> For the 3,4-dimethoxy-substituted stilbenes (**18**, **24**), another notable difference is the absence of the oxocine/azocine products corresponding to **3af** and **14af–15af**, which is understandable since the formation of these products require the intermediacy of the cation resulting from the first crossover cation-nucleophile reaction (see scheme 2.15). The other departures are in the different products generated as a result of the shift of the dominant pathway from intramolecular cation trapping to aromatic substitution or Friedel-Crafts reaction.

When the ortho'-substituent is a carboxylic acid group, the reactions (for both 4-methoxy, **28** and 3,4-dimethoxystilbenes, **29**) proceeded smoothly to yield the three stereoisomeric ( $C_2$ , *meso*, and unsymmetric) bis- $\delta$ -lactones in good yields (ca. 70%, see scheme 2.21). This could be a result of a favored geometry for bond formation as the  $\text{CO}_2\text{H}$  group (with its  $sp^2$  carbonyl carbon) is able to be coplanar with the benzylic cation in a six-membered transition state. In common with the hydroxymethyl- and aminomethyl-substituted stilbenes however, crossover trapping products were also not formed. The mechanism for the formation of the three stereoisomeric bis- $\delta$ -lactones and the minor monomeric  $\delta$ -lactone is shown in Scheme 2.27.

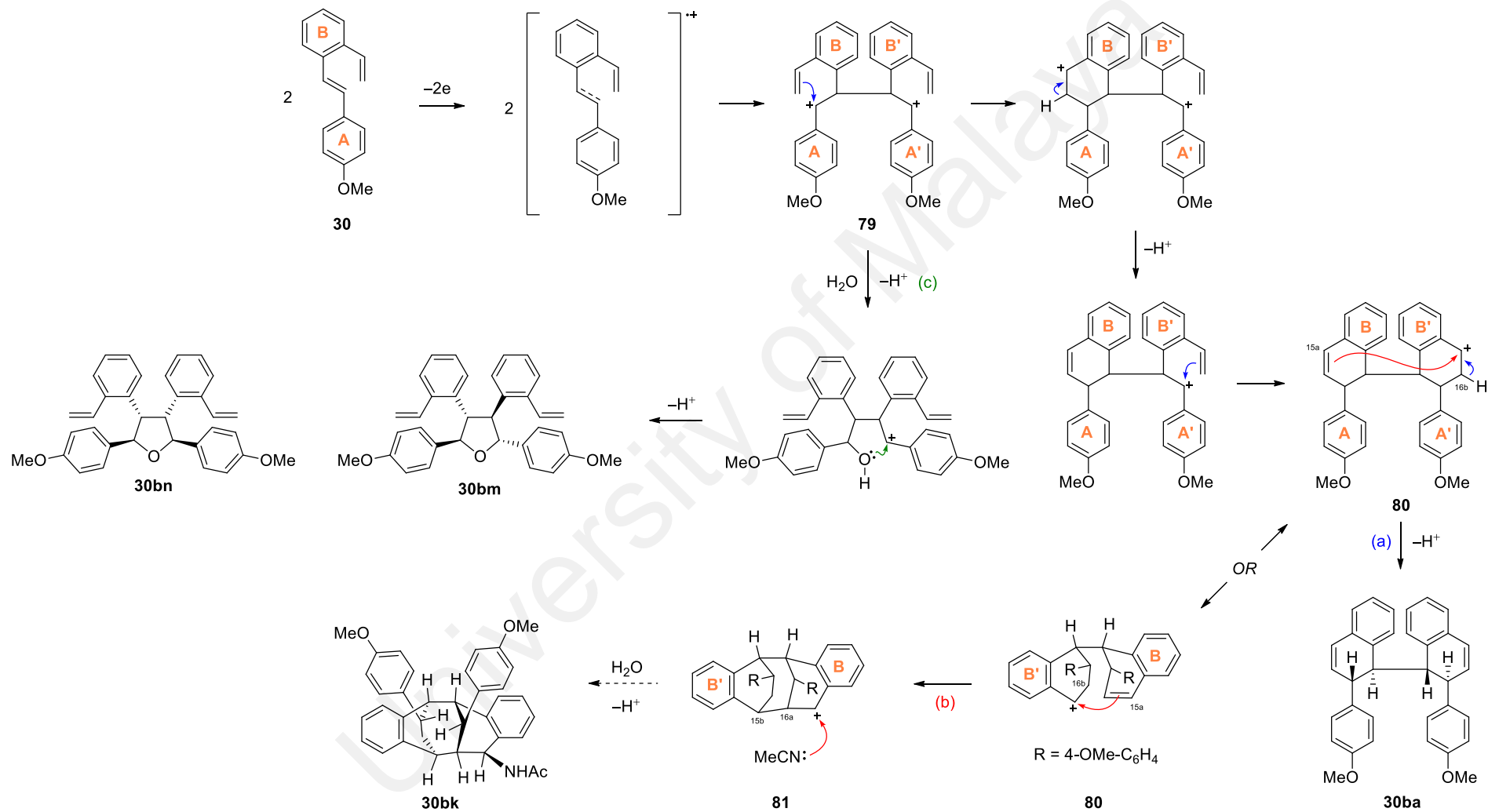


**Scheme 2.27:** Proposed mechanism for the formation of products in the anodic oxidation of stilbenes **28–29** in MeCN/LiClO<sub>4</sub>

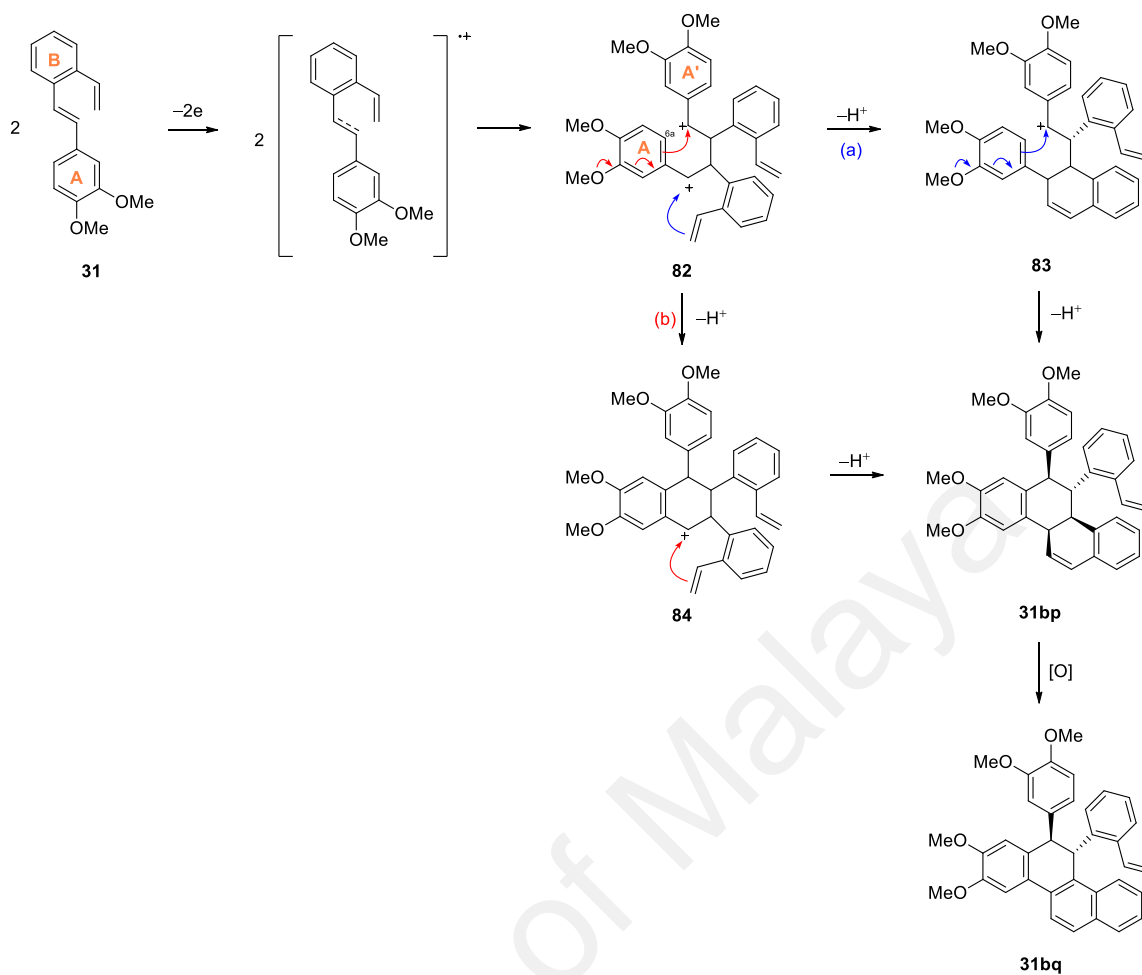
The investigation of methoxystilbene **30** (and **31**) in which the ortho'-substituent is a vinyl group, is to examine whether and how efficiently the  $\pi$ -electrons of the vinyl moiety can trap the benzylic cations. The results showed that although intramolecular cation trapping products are obtained (**30ba**, **30bk**; 33%, see Scheme 2.22), the competing intermolecular cation trapping products are also formed (**30bm**, **30bn**; 27%, see Scheme 2.22). The proposed mechanism leading to the formation of the products is shown in Scheme 2.28. The bisdihydronaphthalene **30ba** is a result of direct trapping of the dication **79** by the respective vinyl groups, followed by deprotonation (Scheme 2.28,

path a), while the doubly-bridged, dibenzofused cyclononane derivative **30bk** is a result of further reaction of the cationic intermediate **80**, formed after the second direct cation trapping step. Instead of deprotonation to the bisdihydronaphthalene **30ba** (Scheme 2.28, path a), ‘crossover trapping’ of the benzylic cation in **80** by the  $\pi$ -electrons of the conjugated double bond associated with the first formed dihydronaphthalene moiety (Scheme 2.28, path b), gives the cationic intermediate **81**. Subsequent capture of the cationic intermediate **81** by acetonitrile followed by hydrolysis (Ritter reaction) gave **30bk**. Alternatively, interception of the dicationic intermediate **79** by water and subsequent deprotonation leads to the stereoisomeric tetraaryltetrahydrofurans, **30bm** and **30bn** (Scheme 2.28, path c).

Formation of the chrysene derivatives in the oxidation of the dimethoxystilbene **31** is a consequence of additional methoxy substitution in the meta-position, promoting electrophilic aromatic substitution (Friedel-Crafts reaction) at the carbon para to the meta-substituted methoxy group (C-6a in ring A) as shown in Scheme 2.29. The cation **83** formed after the first cation-olefin reaction (Scheme 2.29, path a), undergoes cyclization via a Friedel-Crafts reaction leading to the tetrahydrochrysene **31bp**. Subsequent aromatization gave the dihydrochrysene **31bq**. Alternatively, ring-closure of the dication **82** (Scheme 2.29, path b), gave the tetralinyl cation intermediate **84** and subsequent nucleophilic attack by the vinyl group also leads to the tetrahydrochrysene **31bp**.



**Scheme 2.28:** Proposed mechanism for the formation of products in the anodic oxidation of stilbene **30** in MeCN/LiClO<sub>4</sub>

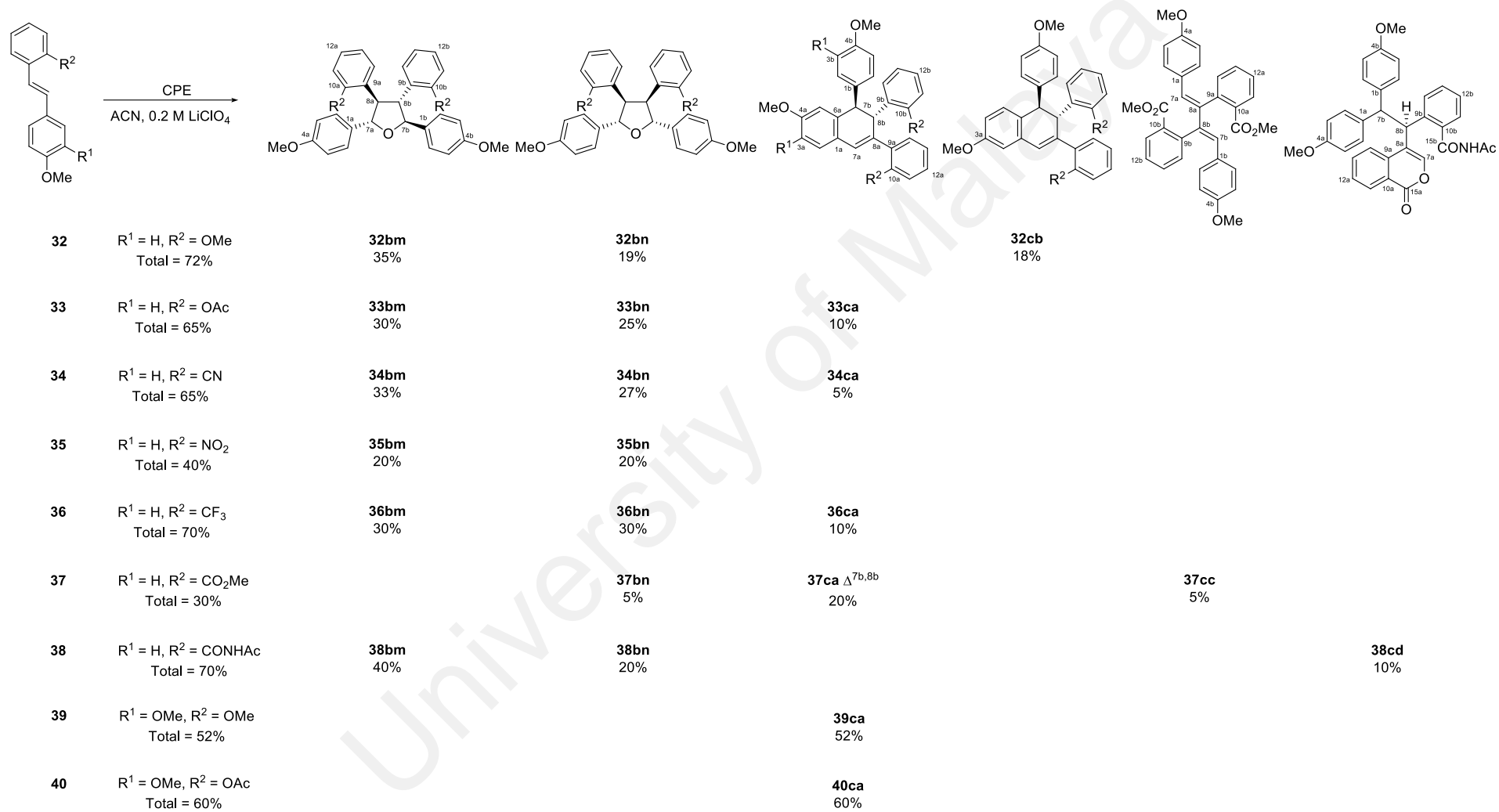


**Scheme 2.29:** Proposed mechanism for the formation of products in the anodic oxidation of stilbene **31** in MeCN/LiClO<sub>4</sub>

## 2.4 Anodic Oxidation of 4-Methoxy- and 3,4-Dimethoxystilbenes where the Ortho'-Substituents are Non-Nucleophilic Groups

In the preceding sections, the effect of various ortho'-substituted nucleophilic groups such as  $-\text{OH}$ ,  $-\text{NHR}$ ,  $-\text{CH}_2\text{OH}$ ,  $-\text{CH}_2\text{NHR}$ ,  $-\text{CO}_2\text{H}$ , and  $-\text{CH}=\text{CH}_2$  on the course of the anodic oxidation of methoxystilbenes were investigated. We now address the effect of the ortho'-substituted non-nucleophilic groups such as  $-\text{OMe}$ ,  $-\text{OAc}$ ,  $-\text{CN}$ ,  $-\text{CF}_3$ ,  $-\text{NO}_2$ , ester  $-\text{CO}_2\text{Me}$  (ester),  $-\text{CONHAc}$  (amide), and  $-\text{CH}=\text{O}$  (formyl) groups.

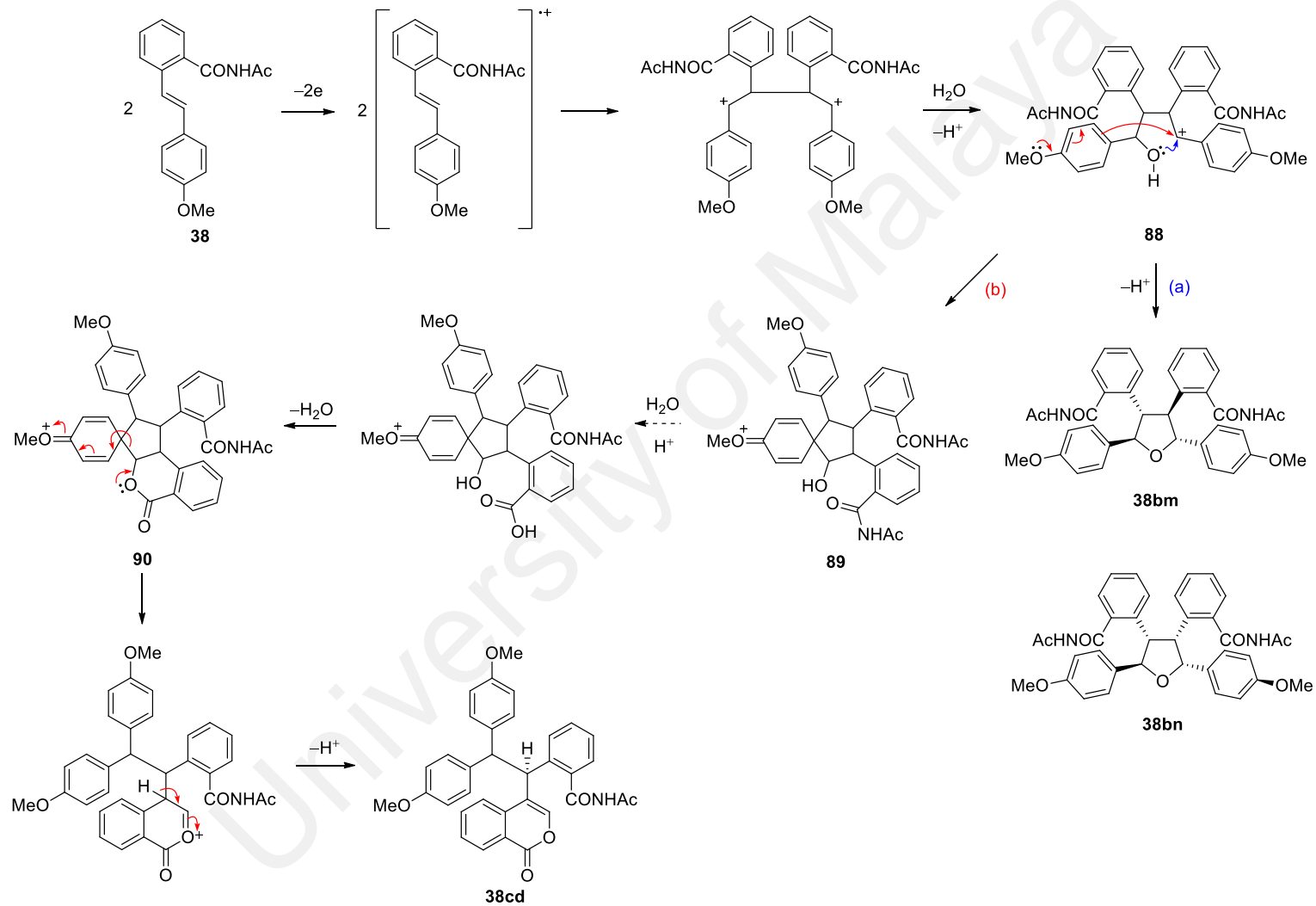
It has been previously noted by Hong that anodic oxidation of 4-methoxystilbene substituted by an *o*-methoxy group in the other ring (stilbene **32**) gave a mixture comprising the stereoisomeric tetraaryltetrahydrofurans (**32bm** and **32bm**) accompanied by the methoxy-migrated dehydrotetralin **32cb**.<sup>85</sup> In the present instance, similar results were also obtained for oxidation of 4-methoxystilbene with *o*'-OAc (**33**), *o*'-CN (**34**), *o*'-NO<sub>2</sub> (**35**), and *o*'-CF<sub>3</sub> (**36**) substituents, where the products were the tetraaryltetrahydrofurans (**bm** and **bn**) and the dehydrotetralins (**ca**) (Scheme 2.30). When the ortho'-substituent is an ester group (**37**), the products were the tetraaryltetrahydrofuran (**37bn**), dehydrotetralin (**37ca**), and a 1,3-butadiene derivative (**37cc**). When the ortho'-substituent is an amide group (**38**), the products are the tetraaryltetrahydrofurans (**38bm** and **38bn**) accompanied by a minor product, an isocoumarin *N*-acetylbenzamide **38cd** in about 10% yield. Anodic oxidation of the 3,4-dimethoxystilbenes (**39** and **40**) gave only the dehydrotetralins **39ca** and **40ca** (Scheme 2.30). X-ray structures were available for **33bn**, **36bm**, **37ca**, and **38cd** (Figure 2.23).



**Scheme 2.30:** Products from the anodic oxidation of stilbenes **32–40**

Formation of the stereoisomeric tetraaryltetrahydrofurans and the regioisomeric dehydrotetralins has been discussed in detail previously (Scheme 2.31).<sup>85</sup> Intermolecular nucleophilic capture of the dication **85** by water gives the stereoisomeric tetraarylhydrofurans (Scheme 2.31, path a). Deprotonation of the dication **85** gives the cationic intermediate **86** (Scheme 2.31, path b) which on subsequent formation of the spirocyclic cation **87** followed by ring expansion gives the dehydrotetralin **ca** (1,2-*p*-methoxybenzyl shift, Scheme 2.31, path c) and/or the migrated regioisomer **cb** (1,2-*p*-methoxystyryl shift, Scheme 2.31, path d). In the case of the stilbene **37**, further oxidation/aromatization of the dehydrotetralin yields the naphthalene derivative **37ca** (Scheme 2.31, path e). Alternatively, a second deprotonation of the cationic intermediate **86** leads to the diene derivative **37cc** (Scheme 2.31, path f). In the anodic oxidation of the 4-methoxystilbene with an ortho'-amide substituent (**38**), formation of the isocoumarin-*N*-acetylbenzamide **38cd** is also a consequence of initial intermolecular nucleophilic capture of the dication by a water molecule (Scheme 2.32). Interception of the dication by a water molecule followed by deprotonation gives the cationic intermediate **88**. Formation of the spirocyclic cationic intermediate **89** (Scheme 2.32, path b) is followed by hydrolysis to the hydroxyacid which then leads to formation of the lactone **90**. Subsequent lone pair assisted bond cleavage followed by deprotonation furnishes the isocoumarin-*N*-acetylbenzamide **38cd** (Scheme 2.32, path b).





**Scheme 2.32:** Proposed mechanism for the formation of products in the anodic oxidation of stilbene **38** in MeCN/LiClO<sub>4</sub>

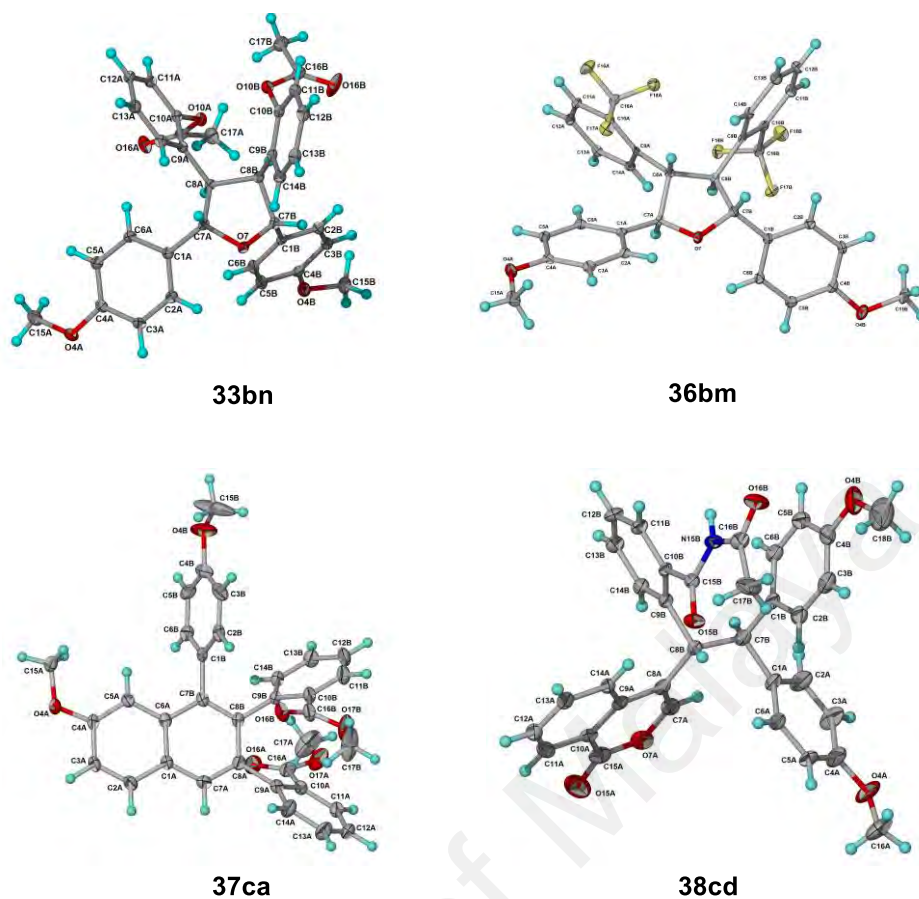
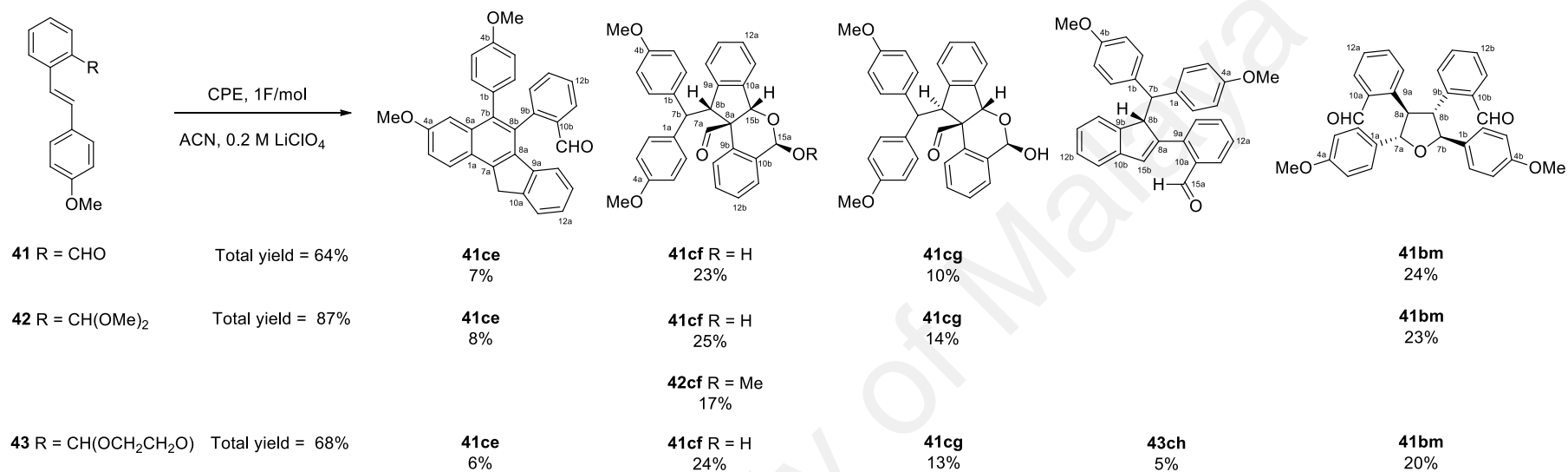
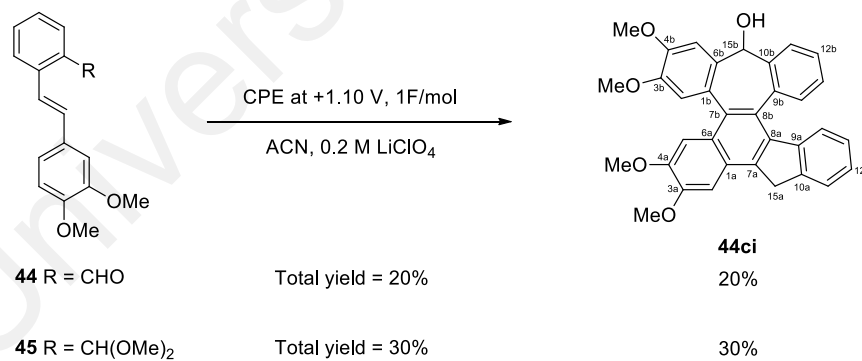


**Figure 2.23:** X-ray structures of **33bn**, **36bm**, **37ca**, and **38cd**

A notable departure was observed in the oxidation of methoxystilbenes where the ortho'-substituent is a formyl group (**41–45**). Anodic oxidation of 4-methoxy-2'-formylstilbene (**41**) gave a mixture of products comprising the fused indanylnaphthalene **41ce** (7%), the epimeric indanylbenzopyran aldehydes (**41cf** 23%, **41cg** 10%), and the tetraaryltetrahydrofuran **41bm** (24%) (Scheme 2.33). In addition to the four oxidation products formed, anodic oxidation of the formyl-protected 4-methoxy-2'-formylstilbenes **42** and **43**, each gave an additional product, viz, the acetal **42cf** in the case of **42**, and the indene aldehyde **43ch**, in the case of **43** (Scheme 2.33).



**Scheme 2.33:** Products from the anodic oxidation of stilbenes **41–43**



**Scheme 2.34:** Product from the anodic oxidation of stilbenes **44–45**

HRMS measurements of compound **41ce** established the molecular formula as  $C_{32}H_{24}O_3$  indicating loss of  $H_2O$  from the dimerization of the two starting 4-methoxy-2'-formylstilbenes (**41**). The  $^1H$  NMR data showed the presence of 2 aromatic methoxy groups, an isolated benzylic methylene ( $\delta_H$  4.28,  $\delta_C$  35.8), an aldehyde-H ( $\delta_H$  9.81,  $\delta_C$  191.8), and 15 aromatic resonances. The aromatic resonances correspond to a 1,3,4-trisubstituted aryl, a 1,2-disubstituted aryl, a 4-methoxyaryl, and a 2-formylaryl moiety. These partial structures can be linked by COSY and the HMBC data (three-bond correlations ( $^3J$ ): H-2a to C-7a; H-14a, H-15a to C-8a; H-5a, H-2b, H-6b to C-7b; H-14b to C-8b; Figure 2.24) to give the structure shown in **41ce** (further confirmation by X-ray analysis, Figure 2.24). The HRMS measurements of **41cf** ( $C_{32}H_{28}O_5$ ) showed that it is derived from dimerization of two starting stilbenes **41** with addition of  $H_2O$ . The  $^1H$  NMR spectrum showed the presence of 2 aromatic methoxy groups, 4 methine hydrogens, an aldehyde-H ( $\delta_H$  9.31,  $\delta_C$  197.6), a hemiacetal OH ( $\delta_H$  3.51, exchanged with  $D_2O$ ), and 16 aromatic resonances which correspond to two 4-methoxyaryl and two 1,2-disubstituted aryl moieties. The two 4-methoxyaryl groups are linked to the same carbon ( $\delta$  52.9, C-7b) from the HMBC data (three-bond ( $^3J$ ) correlations from H-2a, H-6a to C-7b and from H-2b, H-6b to C-7b, Figure 2.25), while the hemiacetal H and C resonances, are observed at  $\delta_H$  5.93 (H-15a) and  $\delta_C$  91.9 (C-15a), respectively. Examination of the 2-D NMR data (Figure 2.25) leads to the structure shown in **41cf**, which also received confirmation from X-ray analysis (Figure 2.25). The  $^1H$  and  $^{13}C$  NMR data of compounds **41cf** and **41cg** ( $C_{32}H_{28}O_5$ ) are very similar except for small differences in chemical shifts, suggesting a stereoisomeric relationship. Noticeable differences are seen for the resonances of H-13a, 14a, and 15b in the  $^1H$  NMR spectra and C-8b in the  $^{13}C$  NMR spectra, while the large carbon chemical shift difference of 10 ppm for C-8b suggests that C-8b could be the epimeric center, which was confirmed by the NOESY data. Comparison of the NOESY data for **41cg** (Figure 2.26) with that of

**41cf** (Figure 2.25), readily establish **41cg** as the C-8b epimer of **41cf** (H-7a/H-7b and H-15a/H-14b NOEs observed for **41cg** but not **41cf**, whereas, H-7a/H-8b and H-15a/H-8b NOEs observed for **41cf** but not **41cg**)

HRMS measurements of **42cf** ( $C_{33}H_{30}O_5$ ) showed that it differs from **41cf** (and **41cg**) by 14 mass units (replacement of H with  $CH_3$ ). Furthermore comparison of the NMR spectroscopic data of **42cf** with that of the hemiacetal **41cf**, indicated that **42cf** is the acetal derivative of **41cf**. The NMR spectroscopic data of **42cf** is similar to that of **41cf** except that the hemiacetal OH ( $\delta_H$  3.51), H-15a ( $\delta_H$  5.93), and C-15a ( $\delta_C$  91.9) resonances in **41cf** have been replaced by the acetal OMe ( $\delta_H$  3.71,  $\delta_C$  55.9), H-15a ( $\delta_H$  5.50), and C-15a ( $\delta_C$  98.5) resonances, respectively, in **42cf** (Figure 2.26).

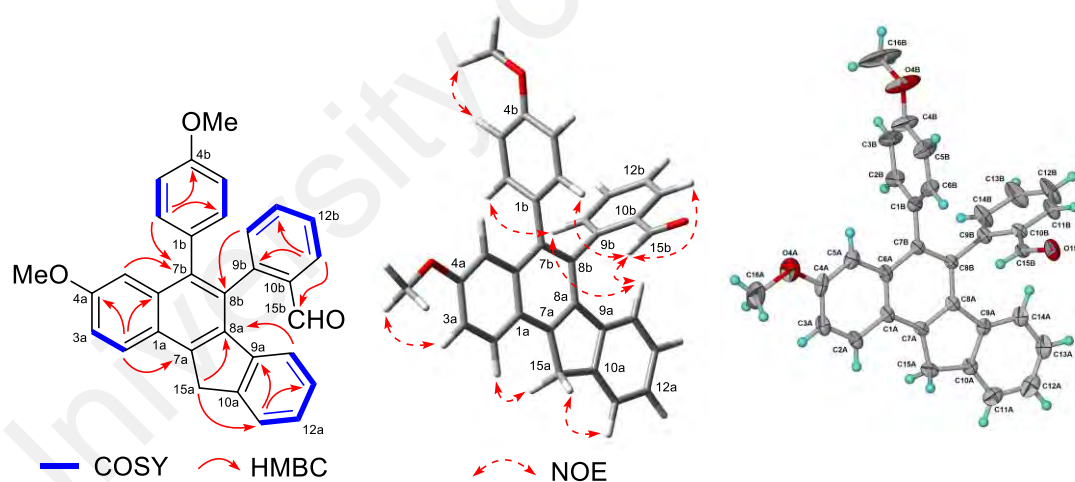


**Figure 2.24:** COSY, selected HMBCs, selected NOEs, and X-ray crystal structure of **41ce**

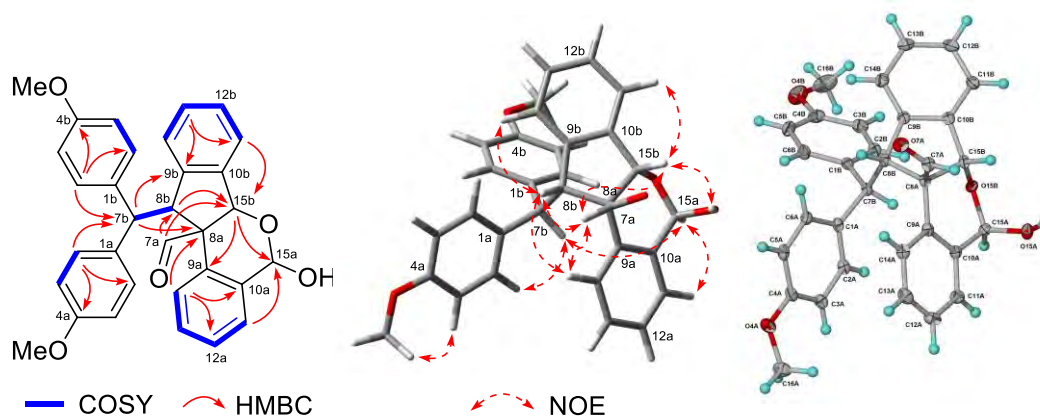


**Figure 2.25:** COSY, selected HMBCs, selected NOEs, and X-ray crystal structure of **41cf**

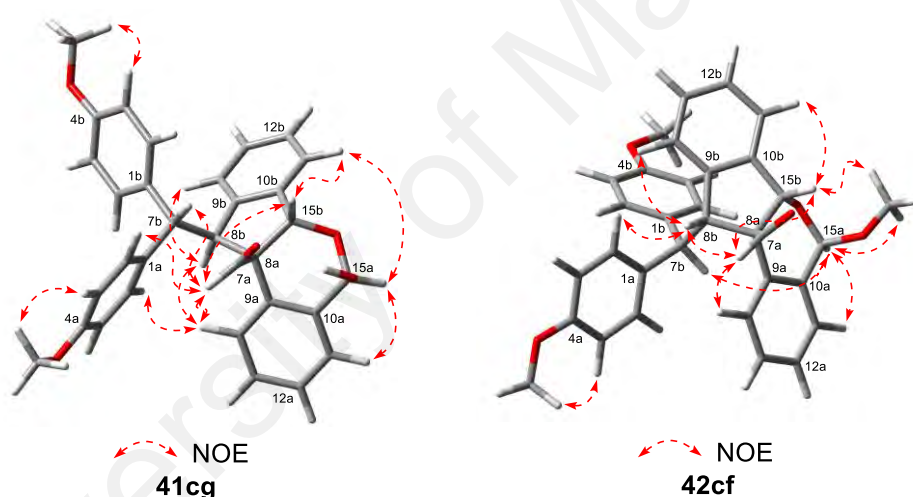


**Figure 2.26:** Selected NOEs of **41cg** and **42cf**

The HRMS data of **43ch** ( $C_{31}H_{26}O_3$ ) indicated loss of a formic acid moiety when compared to **41cf** and **41cg**. The  $^1H$  NMR data showed the presence of 2 aromatic methoxy groups, an isolated olefinic methine ( $\delta_H$  6.56,  $\delta_C$  135.8), an aldehyde-H ( $\delta_H$  8.90,  $\delta_C$  192.6), and 16 aromatic resonances which correspond to two 1,2-disubstituted aromatic moieties and two 4-methoxyaryl groups which are linked to the same carbon

( $\delta$  50.0, C-7b, HMBC, Figure 2.27). This carbon (C-7b) is linked to the benzylic methine (C-8b) of an indene moiety from the COSY data and the vicinal ( $J_{7b-8b}$ ) coupling of 6 Hz. The presence of the trisubstituted indene double bond was consistent with the observed NMR resonances at  $\delta_H$  6.56, H-15b;  $\delta_C$  135.8, C-15b; 146.1, C-8a. The NMR and IR data also indicated that in **43ch**, an aromatic aldehyde group ( $\delta_H$  8.90,  $\delta_C$  192.6; IR 1686  $\text{cm}^{-1}$ ) has replaced the formyl group present in **41cf** ( $\delta_H$  9.31,  $\delta_C$  197.6; IR 1720  $\text{cm}^{-1}$ ). This aromatic aldehyde is part of the other 1,2-disubstituted aryl group, and linking the partial structures by reference to the HMBC data (three-bond correlations ( $^3J$ ) from H-2a to C-7a; from H-8b to C-14ba; from H-15b to C-9a; from H-2a, H-2b, H-6a, H-6b to C-7b; from H-15a to C-11a; Figure 2.27) leads to the structure shown in **43ch**.

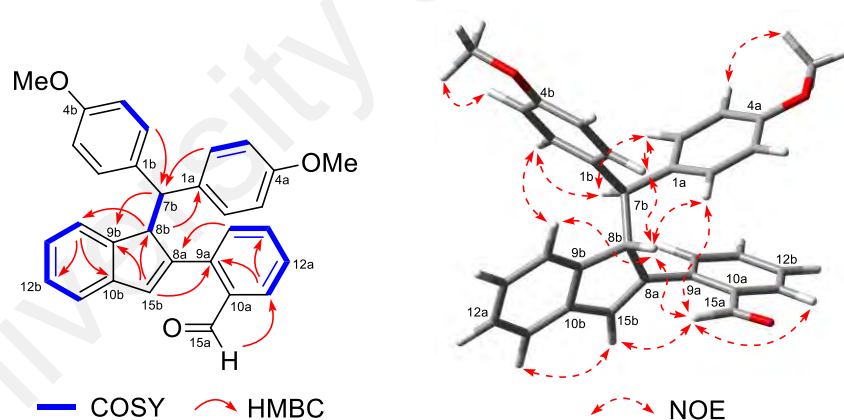


**Figure 2.27:** COSY, selected HMBCs, and selected NOEs of **43ch**

Anodic oxidation of the 3,4-dimethoxy-2'-formylstilbenes (**44** and **45**) gave only one product, viz., the fused benzofluorene-dibenzoannulene alcohol **44ci** (Scheme 2.34). The acetal protected stilbene **45** gave the better yield (30% vs 20%), although in both

cases the reactions were accompanied by formation of a significant quantity of polymeric products. HRMS measurements of **44ci** established the molecular formula as  $C_{34}H_{28}O_5$  and the  $^1H$  NMR data showed the presence of 4 methoxy groups, two hydrogens of a benzylic methylene which is part of an indene moiety ( $\delta$  4.14, 4.34), an oxymethine hydrogen ( $\delta$  5.71), an OH group ( $\delta$  2.51, exchanged with  $D_2O$ ), and 12 aromatic resonances which are due to two 1,2-disubstituted and two 1,2,4-5-tetrasubstituted aromatic moieties (each substituted by 2 aromatic OMe groups). In addition to the two quaternary olefinic carbons of the indene unit at  $\delta_C$  134.7 and 139.7, two additional quaternary carbons are seen at  $\delta_C$  130.1 and 133.3. Examination of the HMBC data (Figure 2.28) leads to the structure shown in **41ce**, which was further confirmation by X-ray analysis (Figure 2.28).

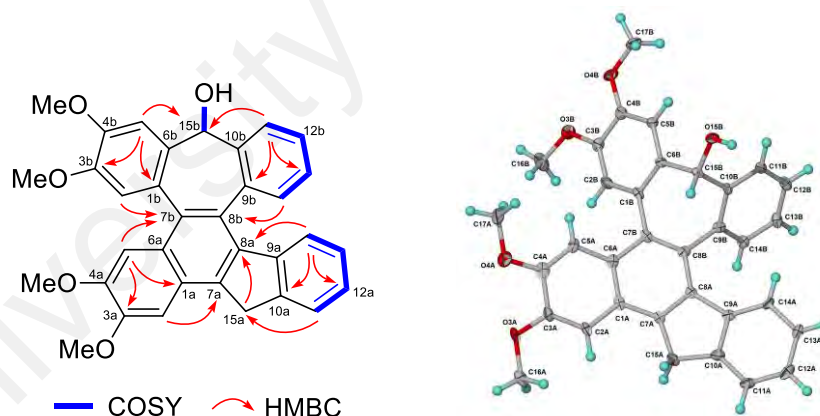
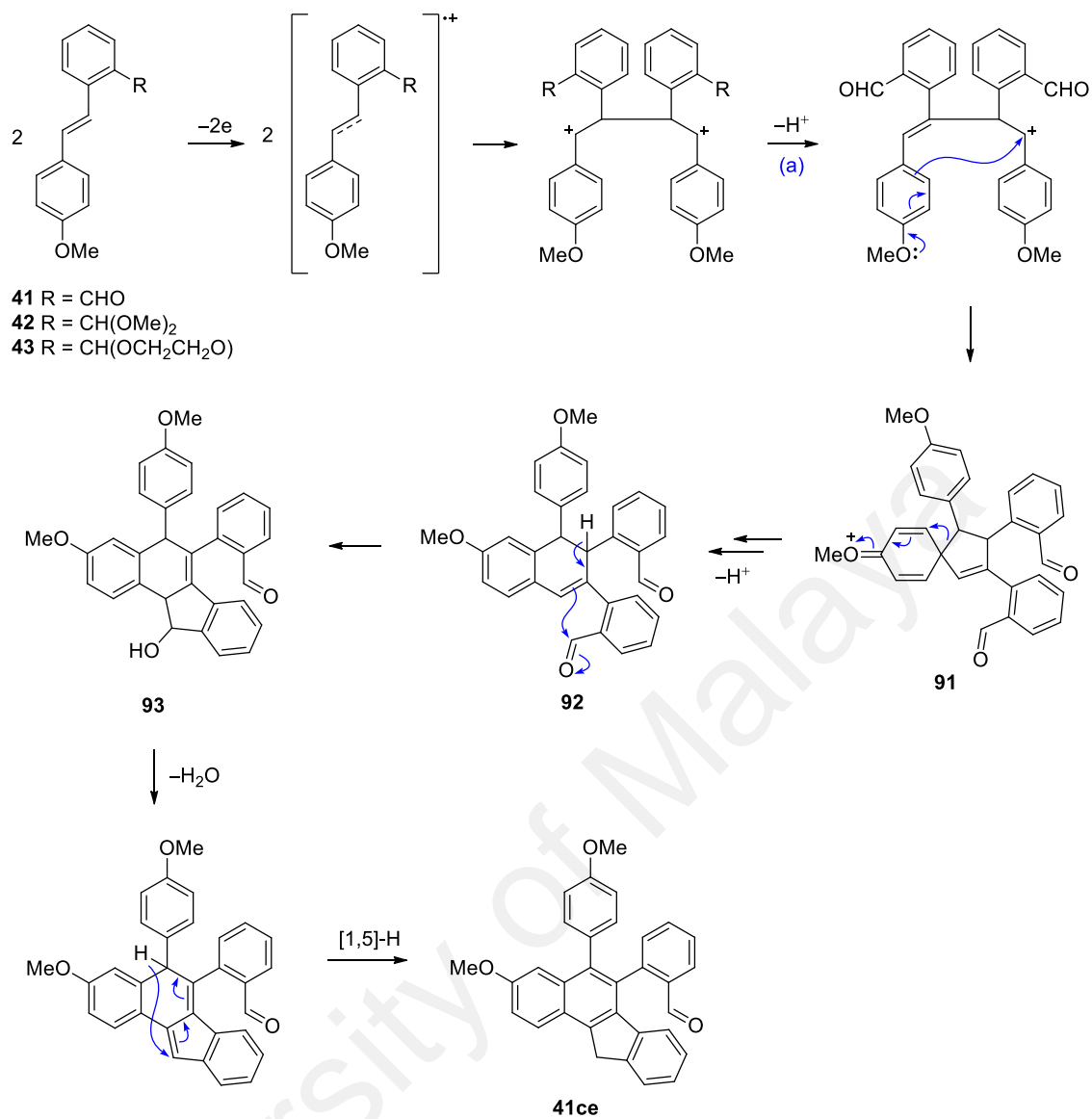


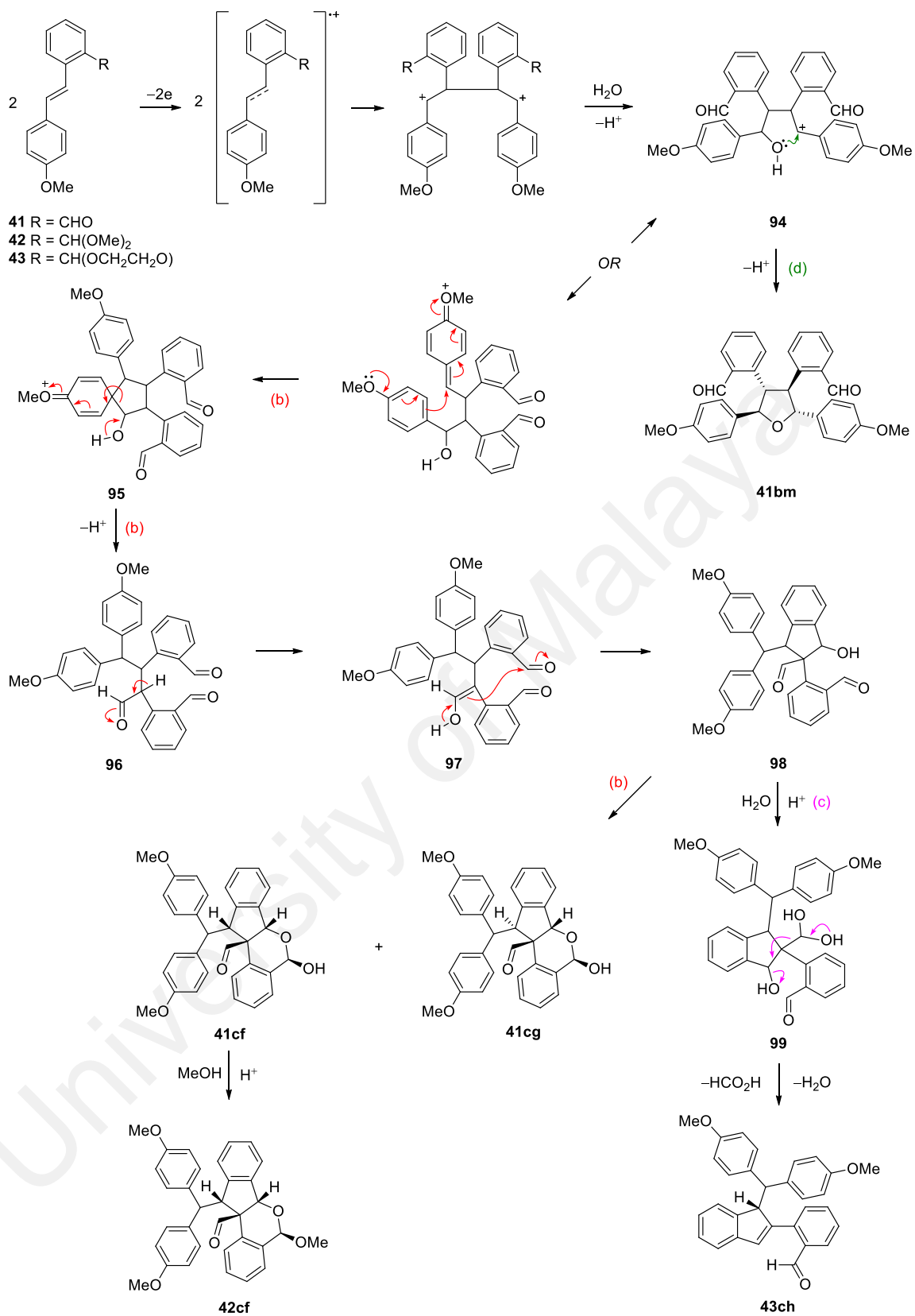
**Figure 2.28:** COSY, selected HMBCs, and X-ray crystal structure of **44ci**

Plausible pathways which account for the formation of the products from the anodic oxidation of the ortho'-substituted substituted stilbenes **41–43** are shown in Scheme 2.35. Formation of the spirocyclic cation **91** via a Friedel-Crafts reaction, followed by ring-expansion and deprotonation as described previously,<sup>85</sup> leads to the dehydrotetralin **92** (Scheme 2.35, path a). A concerted deprotonation-Prins-type cyclization gives the tetracyclic carbinol **93**, which on dehydration, followed by a [1,5] shift, leads to the indanylnaphthalene **41ce** (Scheme 2.35, path a). Friedel-Crafts cyclization of the cationic intermediate **94** on the other hand, leads to the spirocyclic alcohol **95**, which on ring opening as described previously,<sup>85</sup> gives the aldehyde **96**. Formation of the enol **97** from the aldehyde **96**, followed by an aldol addition gives the hydroxyaldehyde **98** (Scheme 2.35, path b). A Grob-like fragmentation from the aldehyde hydrate **99** with elimination of formic acid and water, gives the indene aldehyde **43ch** (Scheme 2.35, path c). Alternatively, cyclization of the hydroxyaldehyde **98** leads to the epimeric hemiacetals **41cf** and **41cg** (Scheme 2.35, path b). Further reaction of the hemiacetal **41cf** furnishes the acetal **42cf**.

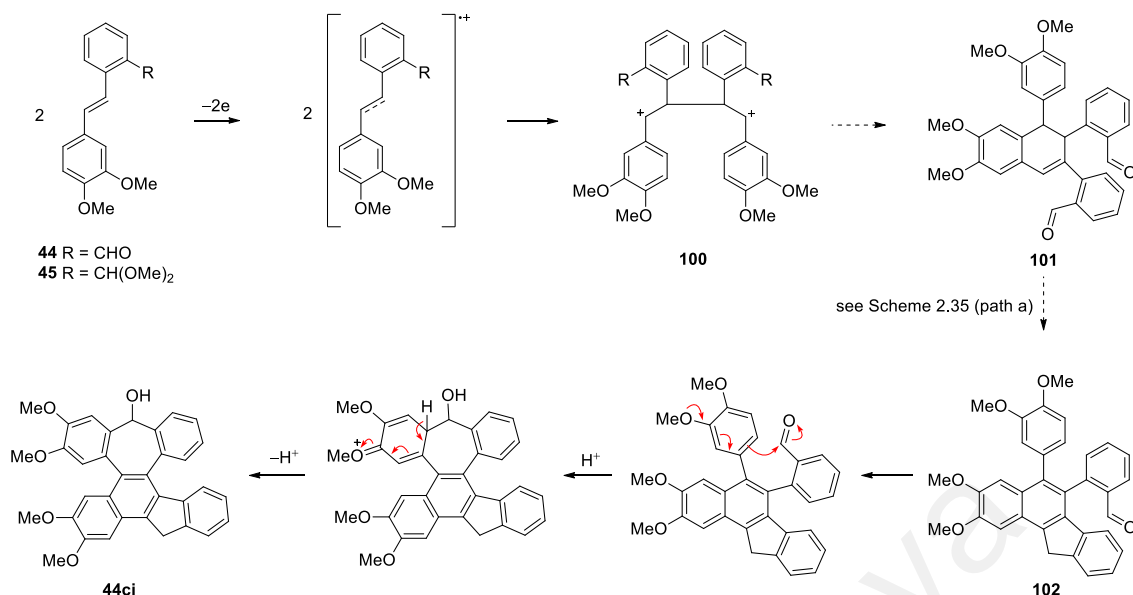
We proposed the following mechanism as shown in Scheme 2.36 to explain the formation of the fused benzofluorene-dibenzoannulene **44ci** in the oxidation of the dimethoxystilbene derivatives **44** and **45**. Formation of the fused benzofluorene-dibenzoannulene **44ci** follows essentially the same pathway as in Scheme 2.35 (path a), viz, via the dication **100** to the dehydrotetralin **101**, and finally to the indanylnaphthalene **102**. This is then followed by a further aromatic substitution or Friedel-Crafts reaction (which is possible due to the presence of the 3-methoxy substituent) which leads to the fused benzofluorene-dibenzoannulene **44ci**.



**Scheme 2.35:** Proposed mechanism for the formation of products in the anodic oxidation of stilbenes **41–43** in MeCN/LiClO<sub>4</sub>



Scheme 2.35, continued



**Scheme 2.36:** Proposed mechanism for the formation of **44ci** in the anodic oxidation of stilbenes **44–45** in MeCN/LiClO<sub>4</sub>

## 2.5 Conclusion

The primary objective of this study is to systematically investigate the effect of ortho'-substitution (in particular where the ortho'-substituents are nucleophilic groups) on the reactivity of anodically generated 4-methoxy- and 3,4-dimethoxystilbene cation radicals. This objective has been achieved and the results can be summarized in Figures 2.29, 2.30, and 2.31.

The presence of ortho'-substituted OH and NHR groups in the other ring results in both direct and crossover intramolecular cation-nucleophile reactions to give bisbenzofurans/bisindoles or bisbenzopyrans/bisquinolines, respectively. The presence of an additional 3-methoxy substituent results in the formation of bridged oxocine/azocine products in addition to the bisbenzopyrans and bisbenzofurans/bisindoles (Figure 2.31).

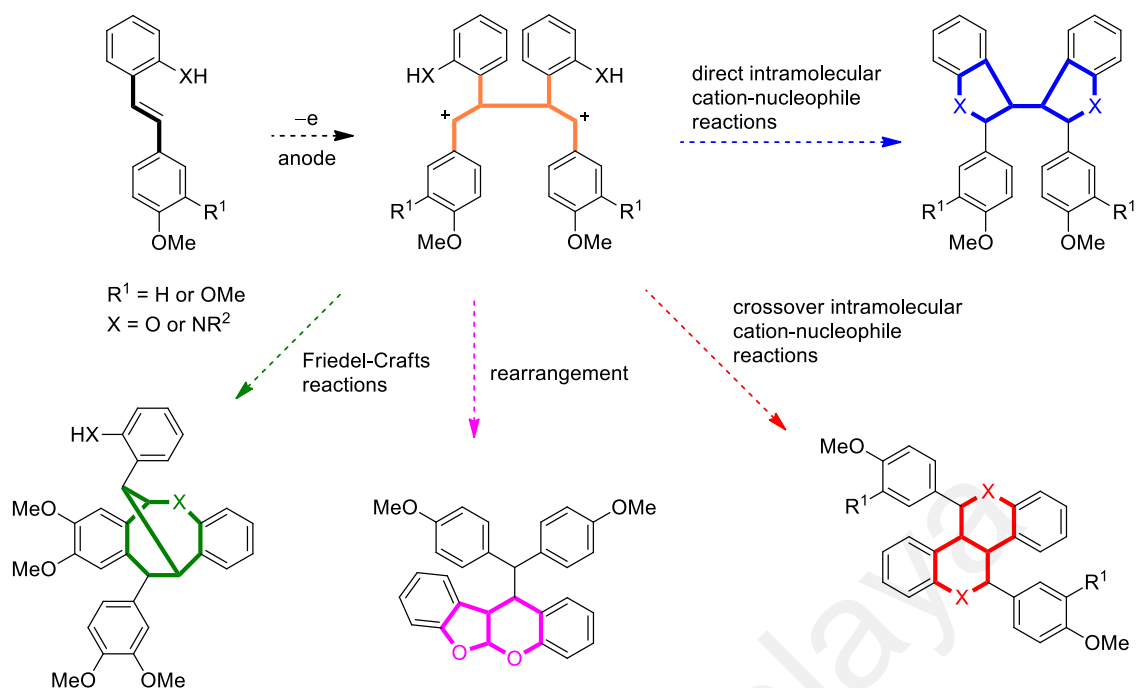


**Figure 2.29:** Reactivity of anodically generated 4-methoxy and 3,4-dimethoxystilbene cation radicals: effect of ortho'-substituted OH and NHR groups

When the ortho'-substituted side chains have been extended to include an intervening  $\text{CH}_2$  group ( $-\text{CH}_2\text{OH}$ ,  $-\text{CH}_2\text{NHR}$ ), only direct intramolecular cation-nucleophile reactions occur to give bisbenzopyrans or bisisoquinolines. Crossover products (previously obtained when the ortho' substituents were OH and  $\text{NH}_2$ ) such as the fused benzoxepanes/fused benzoazepanes are not formed. When the ortho' substituent is a  $\text{CO}_2\text{H}$  group, direct intramolecular cation-nucleophile reactions occur to give the corresponding bis- $\delta$ -lactones (three stereoisomers) in good yields. In the case of an ortho'-substituted vinyl group, direct intramolecular cation-trapping reaction leads to a bisdihydronaphthalene, in addition to an unusual doubly-bridged, dibenzofused cyclononane derivative. Oxidation of the corresponding 3,4-dimethoxystilbenes lead to formation of other polycyclic derivatives as a result of competing aromatic substitution (Figure 2.30).

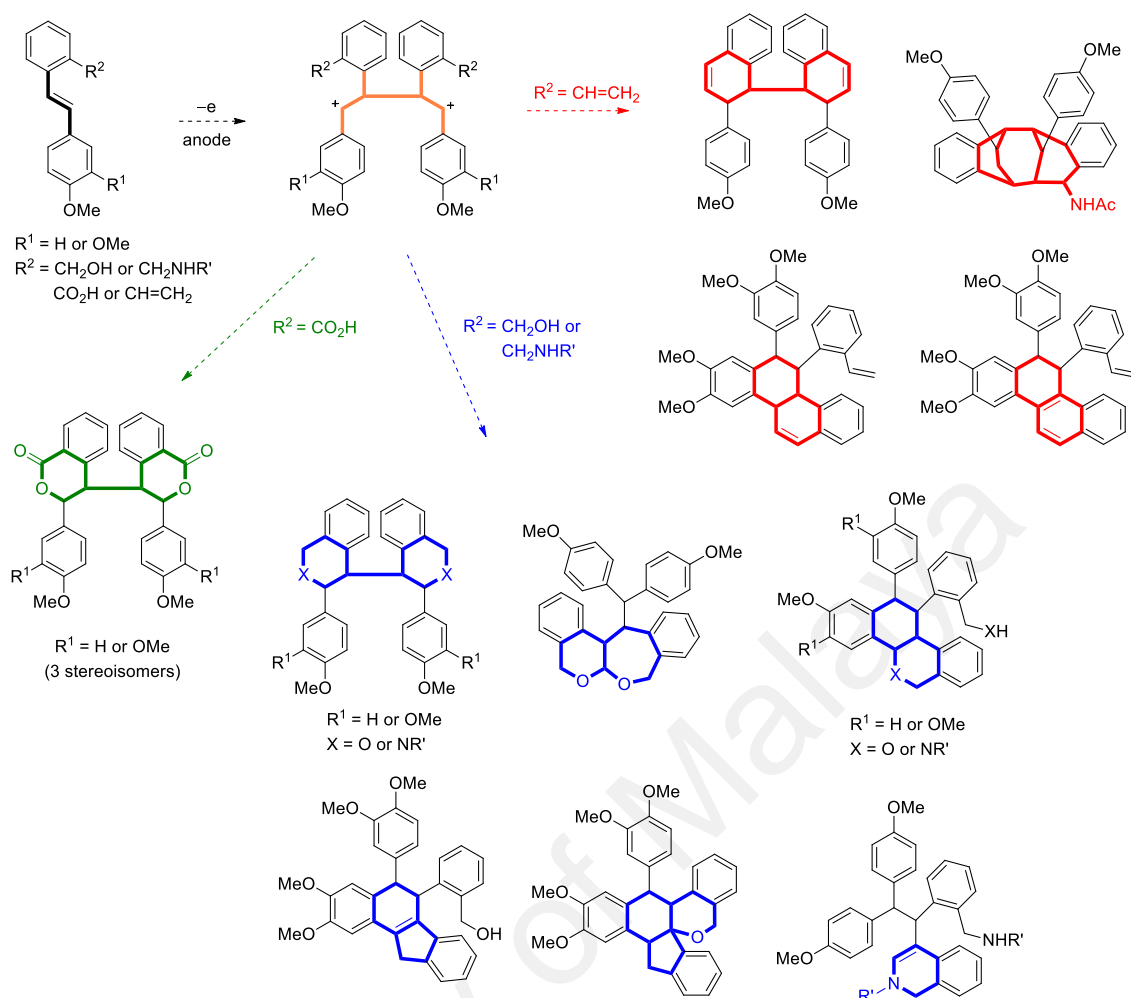


**Figure 2.30:** Reactivity of anodically generated 4-methoxy and 3,4-dimethoxystilbene cation radicals: effect of ortho'-substituted  $\text{CH}_2\text{OH}$ ,  $\text{CH}_2\text{NHR}$ ,  $\text{CO}_2\text{H}$ , and  $\text{CH=CH}_2$  groups

When the ortho' substituents are non-nucleophilic groups such as OMe, OAc, CN,  $\text{NO}_2$ ,  $\text{CF}_3$ , or  $\text{CO}_2\text{Me}$ , the products are the tetraaryltetrahydrofurans and the dehydrotetralin derivatives. In the case of an ortho'-amide substituent, the major products are the tetraaryltetrahydrofurans, accompanied by a minor product incorporating an isocoumarin moiety. When the ortho' substituent is a formyl group, the products include fused indanylnaphthalenes, indanylbenzopyran aldehydes, and indenyl benzaldehyde. When an additional 3-methoxy substituent is present, a fused benzofluorene-dibenzoannulene was the sole product obtained (Figure 2.33).

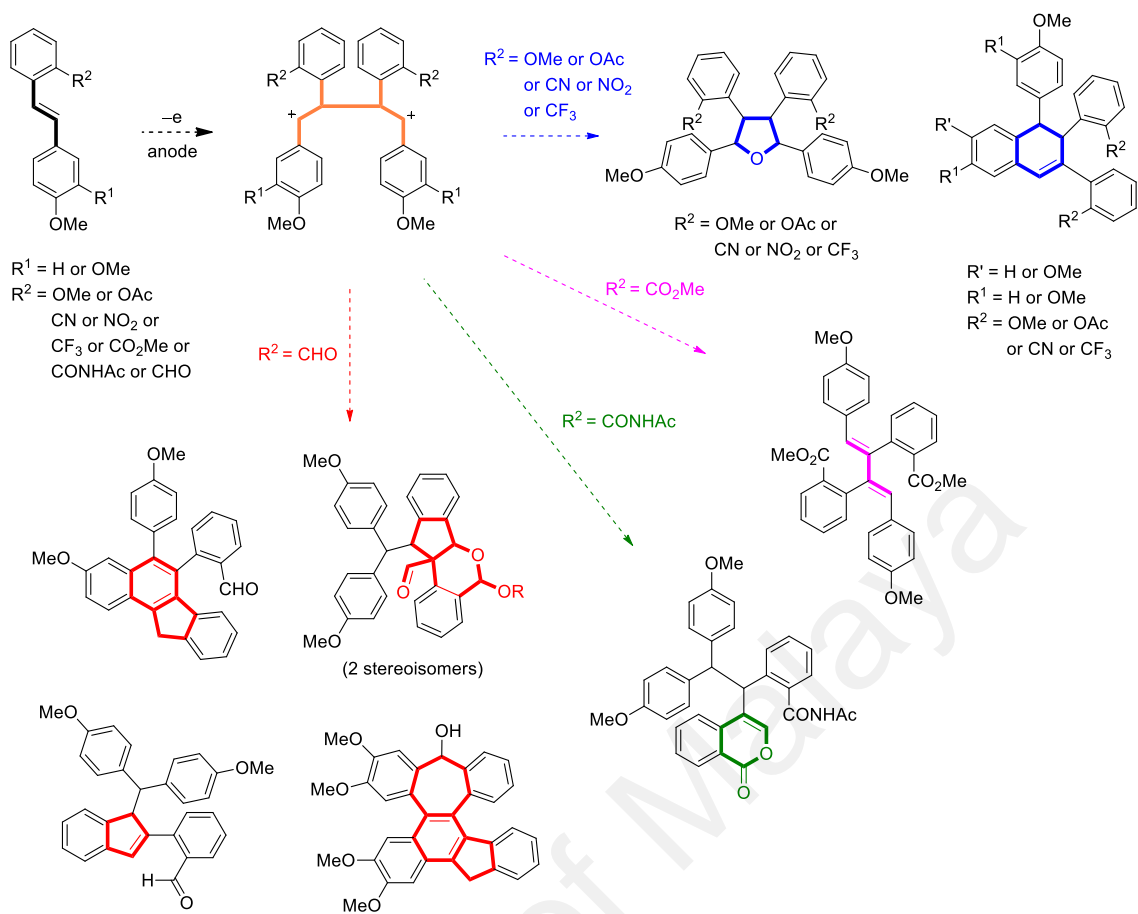


**Figure 2.33:** Reactivity of anodically generated 4-methoxy and 3,4-dimethoxystilbene cation radicals: effect of ortho'-substituted CHO, CO<sub>2</sub>Me, CONHR, and other non-nucleophilic groups

In all the instances investigated in this study where ortho'-substituted nucleophilic groups are present, the observed behavior of the anodically generated methoxystilbene cation radicals is consistent with a generalized pathway involving rapid cation radical dimerization following initial electron transfer, followed by intramolecular direct and/or crossover trapping of the dicationic intermediates by the ortho'-substituted nucleophilic groups. The presence of an additional 3-methoxy substituent results in competing Friedel-Crafts (or aromatic substitution) reactions leading to additional polycyclic products. Many of the products generated incorporate interesting structural motifs

which may be of relevance in natural products as well as organic synthesis.<sup>104,105,114-118,106-113</sup>

University of Malaya

## CHAPTER 3: EXPERIMENTAL

### 3.1 General

Melting points were measured on a Mel-Temp melting point apparatus and an Electrothermal IA9100 digital melting point apparatus and are uncorrected. UV spectra were obtained on a Shimadzu UV-3101PC and UV-2600 spectrophotometers. IR spectra were recorded on a PerkinElmer Spectrum 400 FT-IR/FT-FIR spectrophotometer.  $^1\text{H}$  and  $^{13}\text{C}$  NMR spectra were recorded in  $\text{CDCl}_3$  using TMS as internal standard on JEOL JNM-ECA 400 or Bruker Avance III 400 and 600 spectrometers. ESIMS and HRESIMS were obtained on an Agilent 6530 Q-TOF spectrometer, HRDARTMS were recorded on a JEOL Accu TOF-DART mass spectrometer. Electrochemical experiments (cyclic voltammetry and controlled potential electrolysis) were performed on a Metrohm-Autolab electrochemical workstation PGSTAT100. All reactions were carried out under Ar or  $\text{N}_2$ , in oven-dried glasswares. THF was distilled from Na/benzophenone under  $\text{N}_2$ .  $\text{CH}_2\text{Cl}_2$  and MeCN were distilled from  $\text{CaH}_2$ , while MeOH was distilled from Mg under  $\text{N}_2$ .

### 3.2 Single Crystal X-ray Diffraction Analysis

X-ray diffraction analyses were carried out on a Bruker SMART APEX II CCD diffractometer with Mo  $K\alpha$  radiation ( $\lambda = 0.71073 \text{ \AA}$ ) at 100–150 K, or on a Rigaku Oxford (formerly Agilent Technologies) SuperNova Dual diffractometers with Cu  $K\alpha$  radiation ( $\lambda = 1.54184 \text{ \AA}$ ) or Mo  $K\alpha$  radiation ( $\lambda = 0.71073 \text{ \AA}$ ) at rt or 100 K. The structures were solved by direct methods (SHELXS-97) and refined with full-matrix least-squares on  $F^2$  (SHELXL-2014/7). All non-hydrogen atoms were refined anisotropically, and all hydrogen atoms were placed in idealized positions and refined as riding atoms with the relative isotropic parameters.

### 3.3 Computational Methods

Structures corresponding to compounds **3ad** and **3ad'** were initially built using GaussView 5 and the optimized at the semi-empirical level of theory (AM1). These structures were then imported into the Gaussian 09 software for DFT-level geometry optimization and frequency calculations using the B3LYP functional with basis set of 6-31G(d) to obtain the energy minimized conformations.

### 3.4 Chromatographic Methods

#### 3.4.1 Normal Phase Chromatography

Thin layer chromatography was carried out using precoated  $2.5 \times 10$  cm aluminium plates, 0.25 mm thickness, silica gel 60 F254 (Merck 5554). Column chromatography was performed using silica gel (Merck 9385, 230-400 Mesh ASTM). The ratio of silica gel to sample was approximately 100:1. The gel was made into slurry with respective solvents with certain ratio before it was packed onto column and allowed to equilibrate for at least half an hour before use. Preparative radial chromatography was carried out using a chromatotron (Harrison Research) with 1, 2 or 4 mm thick plated 24 cm diameter of silica gel PF 254 (Merck 7749). The plate was prepared as follows. A long piece of cellophane tape was secured around the edge of the plate to form a mould. Silica gel was added to cold distilled water and the slurry formed was poured onto the circular glass plate. The circular glass plate was rotated while the gel was being poured to obtain an even setting. The plate was left to air dry before being dried in an oven at 80 °C for about 12 hours. The sample was dissolved in a minimum volume of suitable solvent and loaded at the center of the plate while the plate was rotating to form a thin band. Elution was then carried out with the appropriate solvent system. Some of the solvent systems used such as hexane,  $\text{CH}_2\text{Cl}_2$ ,  $\text{CH}_2\text{Cl}_2$ :*n*-hexane,  $\text{CH}_2\text{Cl}_2$ :MeOH,

CHCl<sub>3</sub>, CHCl<sub>3</sub>:*n*-hexane, CHCl<sub>3</sub>:MeOH, EtOAc, EtOAc:*n*-hexane, EtOAc:MeOH, Et<sub>2</sub>O, Et<sub>2</sub>O:*n*-hexane, Et<sub>2</sub>O:MeOH.

### 3.4.2 High Performance Liquid Chromatography

HPLC analysis and separation were performed using a system comprising of Waters 600 controller, Waters 600 pump, and either Waters 2489 variable-wavelength absorbance detector or Waters 996 Photodiode Absorbance Detector. All solvents were HPLC grade and filtered prior to use. All samples were dissolved in minimal amount of MeCN (for reverse phase), filtered with nylon membrane (0.45  $\mu\text{m}$ ) prior to loading into the column. The columns used were Luna Phenyl-hexyl (21.2  $\times$  150 mm), Phenomenex, packed with hexyl linked phenyl with TMS endcapping on 5  $\mu\text{m}$  silica gel or X-Bridge Prep OBD<sup>TM</sup>, C<sub>18</sub> (19  $\times$  50 mm; 5  $\mu\text{m}$ ) for reverse phase HPLC.

### 3.4.3 Gel Permeation Chromatography

Gel permeation chromatography was performed using Sephadex LH20 (Sigma-Aldrich) in a non-gradient of solvent system (MeOH or MeOH:MeCN). The gel was swelled in excess MeOH, at room temperature for 3 hours. It was then made into a slurry *via* stirring, poured into a column with a dimension of 60 cm (L)  $\times$  3.5 cm (D), and allowed to equilibrate for at least a day. For sample which has low solubility in MeOH, the column was conditioned using mobile phase containing appropriate percentage of MeCN and allowed to equilibrate for overnight prior to use. The sample was dissolved in a minimum volume of MeOH (or MeOH:MeCN) and loaded onto the gel. Elution was then carried out by gravity and the eluent was collected in test tube and dried *in vacuo*. After the chromatography, the column was regenerated *via* eluting with

MeOH (or MeOH:MeCN, according to the eluting solvent for the respective sample), three times the column volume.

### 3.5 Microwave Irradiation Experiments

All microwave irradiation experiments were carried out in a Discover SP microwave synthesizer (CEM Corporation). The reactions were carried out in heavy-walled Pyrex tubes (10 or 35 mL) equipped with a small magnetic stir bar and sealed with silicon caps fitted with a Teflon septum. The Pyrex tubes, magnetic stir bar, and silicon caps were obtained from CEM Corporation. The mixture was irradiated at the desired preselected temperature (e.g., 120 °C) with an irradiation power of 120 W. The temperature was measured using a built in vertically focused IR sensor on the outer surface of the tubes. After the irradiation period, gas jet cooling rapidly cools the reaction vessel to ambient temperature.

### 3.6 Synthesis of Stilbenes

**Synthesis of Stilbenes 1, 3, 5, 6, 8, 32, 34, 35, 36, 37, 38, 39, 41, 44, 46, 47, and 48 by Heck Coupling.** Aryl halide (0.22 mmol) was added to a flask containing a mixture of Pd<sub>2</sub>(dba)<sub>3</sub> (2.7 mg, 0.003 mmol) and Pd(*t*-Bu<sub>3</sub>P)<sub>2</sub> (3.1 mg, 0.006 mmol). The corresponding styrene (0.2 mmol), triethylamine (42 μL, 0.3 mmol), and dioxane (4 mL) were then added to the mixture. The reaction mixture was microwave irradiated (with the heating program starting at 120 W) at 120 °C for 30–60 min. The mixture was then filtered through a pad of silica gel, washed with 5% HCl (3 × 20 mL), extracted with CH<sub>2</sub>Cl<sub>2</sub> (3 × 20 mL), washed with H<sub>2</sub>O (3 × 20 mL), dried over Na<sub>2</sub>SO<sub>4</sub>, filtered, and the solvent removed under reduced pressure. The resulting residue was purified by

preparative radial chromatography (Chromatotron) over SiO<sub>2</sub> to yield the corresponding stilbenes.

**Synthesis of Stilbenes 2 and 4 from 1 and 3, respectively.** Hexamethyldisilazane (29  $\mu$ L, 0.14 mmol) was added dropwise to a solution of the corresponding 2-hydroxystilbene (**1** and **3**, 0.2 mmol) and LiClO<sub>4</sub> (10.6 mg, 0.1 mmol) in MeCN (5 mL). The reaction mixture was stirred at room temperature with TLC monitoring. The reaction mixture was extracted with CH<sub>2</sub>Cl<sub>2</sub> (3  $\times$  20 mL), and the combined organic layer was then washed with H<sub>2</sub>O, dried (Na<sub>2</sub>SO<sub>4</sub>), and concentrated under reduced pressure. The resulting residue was then fractionated by preparative radial chromatography to yield the corresponding stilbene.

**Synthesis of Stilbenes 7 and 12 from 5 and 6, respectively.** Triethylamine (67  $\mu$ L, 0.5 mmol) and acetic anhydride (47  $\mu$ L, 0.5 mmol) were added dropwise to a solution of the corresponding 2-aminostilbene (**5** and **6**, 0.2 mmol) in CH<sub>2</sub>Cl<sub>2</sub> (5 mL) at 0 °C. The reaction mixture was stirred at room temperature with TLC monitoring. Hydrochloric acid (5%) was added and the mixture extracted with CH<sub>2</sub>Cl<sub>2</sub> (3  $\times$  20 mL). The combined organic layer was then washed with H<sub>2</sub>O, dried (Na<sub>2</sub>SO<sub>4</sub>) and concentrated under reduced pressure. The resulting residue was then fractionated by preparative radial chromatography to yield the corresponding stilbene.

**Synthesis of Stilbenes 9 and 13 from 5 and 6, respectively.** K<sub>2</sub>CO<sub>3</sub> (0.28g, 2.0 mmol) in THF:H<sub>2</sub>O: 3:1 and methyl chloroformate (23  $\mu$ L, 0.3 mmol) were added dropwise to a solution of the corresponding 2-aminostilbene (**5** and **6**, 0.2 mmol) in CH<sub>2</sub>Cl<sub>2</sub> (5 mL). The reaction mixture was stirred at room temperature with TLC monitoring. Hydrochloric acid (5%) was added and the mixture extracted with CH<sub>2</sub>Cl<sub>2</sub> (3  $\times$  20 mL). The combined organic layer was then washed with H<sub>2</sub>O, dried (Na<sub>2</sub>SO<sub>4</sub>)

and concentrated under reduced pressure. The resulting residue was then fractionated by preparative radial chromatography to yield the corresponding stilbene.

**Synthesis of Stilbenes 10 and 14 from 5 and 16, respectively.** Pyridine (24  $\mu$ L, 0.3 mmol) and a solution of 4-toluenesulfonyl chloride (57.2 mg, 0.3 mmol) in  $\text{CH}_2\text{Cl}_2$  (5 mL) were added dropwise to a solution of the corresponding 2-aminostilbene (**5** and **6**, 0.2 mmol) in  $\text{CH}_2\text{Cl}_2$  (5 mL) at 0 °C. The reaction mixture was stirred at room temperature with TLC monitoring. Hydrochloric acid (5%) was added and the mixture extracted with  $\text{CH}_2\text{Cl}_2$  (3  $\times$  20 mL). The combined organic layer was then washed with  $\text{H}_2\text{O}$ , dried ( $\text{Na}_2\text{SO}_4$ ) and concentrated under reduced pressure. The resulting residue was then fractionated by preparative radial chromatography to yield the corresponding stilbene.

**Synthesis of Stilbenes 11 and 15 from 5 and 6, respectively.** Pyridine (24  $\mu$ L, 0.3 mmol) and a solution of 2-nitrobenzenesulfonyl chloride (66.5mg, 0.3 mmol) in  $\text{CH}_2\text{Cl}_2$  (5 mL) were added dropwise to a solution of the corresponding 2-aminostilbene **5** and **6**, 0.2 mmol) in  $\text{CH}_2\text{Cl}_2$  (5 mL) at 0 °C. The reaction mixture was stirred at room temperature with TLC monitoring. Hydrochloric acid (5%) was added and the mixture extracted with  $\text{CH}_2\text{Cl}_2$  (3  $\times$  20 mL). The combined organic layer was then washed with  $\text{H}_2\text{O}$ , dried ( $\text{Na}_2\text{SO}_4$ ) and concentrated under reduced pressure. The resulting residue was then fractionated by preparative radial chromatography to yield the corresponding stilbene.

**Reduction of 37 and 46, to Stilbenes 16 and 18, respectively.** Lithium aluminum hydride (38.0 mg, 1.0 mmol) in THF was added dropwise to a solution of the corresponding methylbenzoate (**37** and **46**, 0.2 mmol) in THF (5 mL). The reaction mixture was refluxed with TLC monitoring. The reaction mixture was cooled and cold distilled water was added. The mixture was then filtered through celite and the filtrate

was extracted with  $\text{CH}_2\text{Cl}_2$  ( $3 \times 20$  mL), the combined organic layer washed with  $\text{H}_2\text{O}$ , dried ( $\text{Na}_2\text{SO}_4$ ), and concentrated under reduced pressure. The resulting residue was then purified by preparative radial chromatography to yield the corresponding stilbene.

**Synthesis of Stilbenes 18 and 19 from 16 and 17, respectively.**

Hexamethyldisilazane ( $29 \mu\text{L}$ ,  $0.14$  mmol) was added dropwise to a solution of the corresponding 2-(hydroxymethyl)stilbene (**16** and **17**,  $0.2$  mmol) and  $\text{LiClO}_4$  ( $10.6$  mg,  $0.1$  mmol) in MeCN ( $5$  mL). The reaction mixture was stirred at room temperature with TLC monitoring. The reaction mixture was extracted with  $\text{CH}_2\text{Cl}_2$  ( $3 \times 20$  mL), and the combined organic layer was then washed with  $\text{H}_2\text{O}$ , dried ( $\text{Na}_2\text{SO}_4$ ), and concentrated under reduced pressure. The resulting residue was then fractionated by preparative radial chromatography to yield the corresponding stilbene.

**Synthesis of Stilbenes 20 and 25 from 49 and 50, respectively.** Pyridine ( $24 \mu\text{L}$ ,  $0.3$  mmol) and a solution of 2-nitrobenzenesulfonyl chloride ( $66.5$ mg,  $0.3$  mmol) in  $\text{CH}_2\text{Cl}_2$  ( $5$  mL) were added dropwise to a solution of the corresponding 2-(aminomethyl)stilbene (**49** and **50**,  $0.2$  mmol) in  $\text{CH}_2\text{Cl}_2$  ( $5$  mL) at  $0$  °C. The reaction mixture was stirred at room temperature with TLC monitoring. Hydrochloric acid (5%) was added and the mixture extracted with  $\text{CH}_2\text{Cl}_2$  ( $3 \times 20$  mL). The combined organic layer was then washed with  $\text{H}_2\text{O}$ , dried ( $\text{Na}_2\text{SO}_4$ ) and concentrated under reduced pressure. The resulting residue was then fractionated by preparative radial chromatography to yield the corresponding stilbene.

**Synthesis of Stilbenes 21 and 24 from 49 and 50, respectively.** Pyridine ( $24 \mu\text{L}$ ,  $0.3$  mmol) and a solution of 4-toluenesulfonyl chloride ( $57.2$  mg,  $0.3$  mmol) in  $\text{CH}_2\text{Cl}_2$  ( $5$  mL) were added dropwise to a solution of the corresponding 2-(aminomethyl)stilbene (**49** and **50**,  $0.2$  mmol) in  $\text{CH}_2\text{Cl}_2$  ( $5$  mL) at  $0$  °C. The reaction mixture was stirred at room temperature with TLC monitoring. Hydrochloric acid (5%) was added and the

mixture extracted with  $\text{CH}_2\text{Cl}_2$  ( $3 \times 20$  mL). The combined organic layer was then washed with  $\text{H}_2\text{O}$ , dried ( $\text{Na}_2\text{SO}_4$ ) and concentrated under reduced pressure. The resulting residue was then fractionated by preparative radial chromatography to yield the corresponding stilbene.

**Synthesis of Stilbenes 22 and 26 from 49 and 50, respectively.** Triethylamine (67  $\mu\text{L}$ , 0.5 mmol) and acetic anhydride (47  $\mu\text{L}$ , 0.5 mmol) were added dropwise to a solution of the corresponding 2-(aminomethyl)stilbene (**49** and **50**, 0.2 mmol) in  $\text{CH}_2\text{Cl}_2$  (5 mL) at 0 °C. The reaction mixture was stirred at room temperature with TLC monitoring. Hydrochloric acid (5%) was added and the mixture extracted with  $\text{CH}_2\text{Cl}_2$  ( $3 \times 20$  mL). The combined organic layer was then washed with  $\text{H}_2\text{O}$ , dried ( $\text{Na}_2\text{SO}_4$ ) and concentrated under reduced pressure. The resulting residue was then fractionated by preparative radial chromatography to yield the corresponding stilbene.

**Synthesis of Stilbenes 23 and 27 from 49 and 50, respectively.**  $\text{K}_2\text{CO}_3$  (0.28g, 2.0 mmol) in  $\text{THF}:\text{H}_2\text{O}$ : 3:1 and methyl chloroformate (23  $\mu\text{L}$ , 0.3 mmol) were added dropwise to a solution of the corresponding 2-(aminomethyl)stilbene (**49** and **50**, 0.2 mmol) in  $\text{CH}_2\text{Cl}_2$  (5 mL). The reaction mixture was stirred at room temperature with TLC monitoring. Hydrochloric acid (5%) was added and the mixture extracted with  $\text{CH}_2\text{Cl}_2$  ( $3 \times 20$  mL). The combined organic layer was then washed with  $\text{H}_2\text{O}$ , dried ( $\text{Na}_2\text{SO}_4$ ) and concentrated under reduced pressure. The resulting residue was then fractionated by preparative radial chromatography to yield the corresponding stilbene.

**Hydrolysis of 37 and 46, to Stilbenes 28 and 29, respectively.**  $\text{LiOH}$  (14.3 mg, 0.6 mmol) was added to a solution of the corresponding methylbenzoate (**37** and **46**, 0.2 mmol) in  $\text{THF}:\text{MeOH}:\text{H}_2\text{O}$  (4:1:1, 3 mL) at room temperature. The reaction mixture was microwave irradiated (with the heating program starting at 120 W) at 70 °C for 2 hours. The mixture was then neutralized with hydrochloric acid (5%) to pH 6 and

extracted with EtOAc ( $3 \times 20$  mL). The combined organic layer was then washed with H<sub>2</sub>O, dried (Na<sub>2</sub>SO<sub>4</sub>), and concentrated under reduced pressure to yield the corresponding stilbenes.

**Synthesis of Stilbenes 30 and 31 from 41 and 44, respectively.** A solution of the corresponding stilbene (**41** and **44**, 0.2 mmol) in THF was added to a suspension of methyltriphenylphosphonium bromide (85.7 mg, 0.24 mmol) and NaH (21.6 mg, 0.9 mmol) in THF (10 mL) at 0 °C under Ar. The reaction mixture was refluxed with TLC monitoring. The reaction was cooled in an ice bath and cold distilled water was slowly added. The mixture was then extracted with CH<sub>2</sub>Cl<sub>2</sub> ( $3 \times 20$  mL), and the combined organic layer was then washed with H<sub>2</sub>O, dried (Na<sub>2</sub>SO<sub>4</sub>) and concentrated under reduced pressure. The resulting residue was then fractionated by preparative radial chromatography to yield the corresponding stilbene.

**Synthesis of Stilbenes 33 and 40 from 1 and 3, respectively.** Triethylamine (84  $\mu$ L, 0.6 mmol) and acetic anhydride (57  $\mu$ L, 0.6 mmol) were added dropwise to a solution of 2-hydroxystilbene (**1** and **3**, 0.2 mmol) in CH<sub>2</sub>Cl<sub>2</sub> (5 mL) at 0 °C. The reaction mixture was stirred at room temperature with TLC monitoring. The reaction was quenched with 5% HCl. The reaction mixture was extracted with CH<sub>2</sub>Cl<sub>2</sub> ( $3 \times 20$  mL), and the combined organic layer was then washed with H<sub>2</sub>O, dried (Na<sub>2</sub>SO<sub>4</sub>) and concentrated under reduced pressure. The resulting residue was then fractionated by preparative radial chromatography to yield the corresponding stilbene.

**Synthesis of Stilbenes 42 and 45 from 41 and 44, respectively.** A mixture of the corresponding stilbene (**41** and **44**, 0.2 mmol), trimethylorthoformate (66  $\mu$ L, 0.6 mmol), and PTSA (1.9 mg, 0.01 mmol) in MeOH was microwave irradiated (with the heating program starting at 100 W) at 60 °C for 25 min. Triethylamine (1.4  $\mu$ L, 0.01 mmol) was added to neutralize the reaction mixture. The mixture was then extracted

with CH<sub>2</sub>Cl<sub>2</sub> (3 × 20 mL), and the combined organic layer was then washed with H<sub>2</sub>O, dried (Na<sub>2</sub>SO<sub>4</sub>) and concentrated under reduced pressure. The resulting residue was then fractionated by preparative radial chromatography to yield the corresponding stilbene.

**Synthesis of Stilbene 43 from 41.** Ethylene glycol (22 μL, 0.4 mmol) and PTSA (1.9 mg, 0.01 mmol) were added separately to a solution of the corresponding stilbene (**41**, 0.2 mmol) in toluene (5 mL) at room temperature. The reaction mixture was microwave irradiated (with the heating program starting at 120 W) at 100 °C for 45 min. NaOH (5%) was added and the mixture was extracted with CH<sub>2</sub>Cl<sub>2</sub> (3 × 20 mL). The combined organic layer was then washed with H<sub>2</sub>O, dried (Na<sub>2</sub>SO<sub>4</sub>) and concentrated under reduced pressure. The resulting residue was then fractionated by preparative radial chromatography to yield the corresponding stilbene.

**Reduction of 47 and 48, to Stilbenes 49 and 50, respectively.** Lithium aluminum hydride (38.0 mg, 1.0 mmol) in THF was added dropwise to a solution of the corresponding benzamide (**47** and **48**, 0.2 mmol) in THF (5 mL). The reaction mixture was refluxed with TLC monitoring. The reaction mixture was cooled in an ice bath and cold distilled water was slowly added. The mixture was then filtered through celite and the filtrate was extracted with CH<sub>2</sub>Cl<sub>2</sub> (3 × 20 mL), the combined organic layer washed with H<sub>2</sub>O, dried (Na<sub>2</sub>SO<sub>4</sub>), and concentrated under reduced pressure. The resulting residue was then purified by preparative radial chromatography to yield the corresponding stilbene.

*(E)*-2-(4-methoxystyryl)phenol (**1**).<sup>119</sup> Brown solid (38.5 mg, 85%); mp 120–122 °C (lit. 117–118 °C); <sup>1</sup>H NMR (CDCl<sub>3</sub>, 400 MHz) δ 3.83 (3H, s), 5.21 (1H, br s), 6.80 (1H, d, *J* = 7.6 Hz), 6.89 (2H, d, *J* = 8.8 Hz), 6.94 (1H, t, *J* = 7.6 Hz), 7.06 (1H, d, *J* = 16.4 Hz),

7.12 (1H, td,  $J = 7.6, 1.5$  Hz), 7.22 (1H, d,  $J = 16.4$  Hz), 7.46 (2H, d,  $J = 8.8$  Hz), 7.50 (1H, dd,  $J = 7.6, 1.5$  Hz);  $^{13}\text{C}$  NMR ( $\text{CDCl}_3$ , 100 MHz)  $\delta$  55.4, 114.2, 116.0, 121.0, 121.1, 125.1, 127.1, 127.8, 128.4, 129.8, 130.5, 153.0, 159.4; ESIMS  $m/z$  227  $[\text{M} + \text{H}]^+$  ( $\text{C}_{15}\text{H}_{14}\text{O}_2 + \text{H}$ ).

*(E)*-2-(4-methoxystyryl)phenoxy)trimethylsilane (**2**). Light yellowish solid (53.1 mg, 89%); mp 68–70 °C;  $^1\text{H}$  NMR ( $\text{CDCl}_3$ , 400 MHz)  $\delta$  0.33 (9H, s), 3.84 (3H, s), 6.86 (1H, d,  $J = 8.0$  Hz), 6.93 (2H, d,  $J = 8.8$  Hz), 7.00 (1H, t,  $J = 7.6$  Hz), 7.08 (1H, d,  $J = 16.6$  Hz), 7.14 (1H, t,  $J = 7.6$  Hz), 7.30 (1H, d,  $J = 16.6$  Hz), 7.48 (2H, d,  $J = 8.8$  Hz), 7.61 (1H, d,  $J = 7.6$  Hz);  $^{13}\text{C}$  NMR ( $\text{CDCl}_3$ , 100 MHz)  $\delta$  0.39, 55.2, 114.1, 119.9, 121.7, 121.9, 126.2, 127.5, 128.0, 128.2, 129.1, 130.7, 152.7, 159.1; HRMS (DART-TOF)  $m/z$ :  $[\text{M} + \text{H}]^+$  Calcd for  $\text{C}_{18}\text{H}_{23}\text{O}_2\text{Si}$  299.1467; Found 299.1469.

*(E)*-2-(3,4-dimethoxystyryl)phenol (**3**).<sup>120</sup> Yellowish oil (46.1 mg, 90%);  $^1\text{H}$  NMR ( $\text{CDCl}_3$ , 400 MHz)  $\delta$  3.85 (3H, s), 3.87 (3H, s), 5.26 (1H, br s), 6.80 (1H, d,  $J = 7.8$  Hz), 6.81 (1H, d,  $J = 8.2$  Hz), 6.91 (1H, t,  $J = 7.8$  Hz), 7.03 (1H, d,  $J = 8.2$  Hz), 7.05 (1H, d,  $J = 16.5$  Hz), 7.08 (1H, s), 7.09 (1H, t,  $J = 7.8$  Hz), 7.28 (1H, d,  $J = 16.5$  Hz), 7.51 (1H, d,  $J = 7.8$  Hz);  $^{13}\text{C}$  NMR ( $\text{CDCl}_3$ , 100 MHz)  $\delta$  55.9, 56.0, 108.9, 111.3, 116.1, 120.1, 121.0, 121.4, 125.0, 126.9, 128.5, 129.6, 131.1, 148.8, 149.1, 153.4; HRMS (DART-TOF)  $m/z$ :  $[\text{M} + \text{H}]^+$  Calcd for  $\text{C}_{16}\text{H}_{17}\text{O}_3$ , 257.1178; Found 257.1173.

*(E)*-2-(3,4-dimethoxystyryl)phenoxy)trimethylsilane (**4**). Colorless oil (57.2 mg, 87%); mp 73–75 °C  $^1\text{H}$  NMR ( $\text{CDCl}_3$ , 400 MHz)  $\delta$  0.34 (9H, s), 3.94 (3H, s), 3.97 (3H, s),

6.86 (1H, d,  $J = 8.0$  Hz), 6.90 (1H, d,  $J = 8.4$  Hz), 7.01 (1H, t,  $J = 8.0$  Hz), 7.07 (1H, dd,  $J = 8.4, 2.0$  Hz), 7.08 (1H, d,  $J = 16.4$  Hz), 7.12 (1H, d,  $J = 2.0$  Hz), 7.16 (1H, t,  $J = 8.0$  Hz), 7.31 (1H, d,  $J = 16.4$  Hz), 7.62 (1H, t,  $J = 8.0$  Hz);  $^{13}\text{C}$  NMR ( $\text{CDCl}_3$ , 100 MHz)  $\delta$  0.4, 55.7, 55.9, 108.6, 111.2, 119.7, 120.0, 121.7, 122.1, 126.1, 128.1, 128.3, 128.9, 131.1, 148.7, 149.1, 152.8; HRMS (DART-TOF)  $m/z$ :  $[\text{M} + \text{H}]^+$  Calcd for  $\text{C}_{19}\text{H}_{25}\text{O}_3\text{Si}$ , 329.1573; Found 329.1577.

*(E)*-2-(4-methoxystyryl)aniline (**5**).<sup>121</sup> Yellowish solid (31.5 mg, 70%); mp 108–110 °C;  $^1\text{H}$  NMR ( $\text{CDCl}_3$ , 400 MHz)  $\delta$  3.83 (3H, s), 6.71 (1H, d,  $J = 7.8$  Hz), 6.81 (1H, t,  $J = 7.8$  Hz), 6.90 (2H, d,  $J = 8.7$  Hz), 6.94 (1H, d,  $J = 16.0$  Hz), 7.03 (1H, d,  $J = 16.0$  Hz), 7.09 (1H, t,  $J = 7.8$  Hz), 7.39 (1H, d,  $J = 7.8$  Hz), 7.45 (2H, d,  $J = 8.7$  Hz);  $^{13}\text{C}$  NMR ( $\text{CDCl}_3$ , 100 MHz)  $\delta$  55.5, 114.2, 116.3, 119.3, 122.2, 124.3, 127.2, 127.8, 128.4, 130.0, 130.5, 143.9, 159.4; HRMS (DART-TOF)  $m/z$ :  $[\text{M} + \text{H}]^+$  Calcd for  $\text{C}_{15}\text{H}_{16}\text{NO}$ , 226.1232; Found 226.1235.

*(E)*-2-(3,4-dimethoxystyryl)aniline (**6**).<sup>96</sup> Yellowish solid (34.1 mg, 89%);  $^1\text{H}$  NMR ( $\text{CDCl}_3$ , 400 MHz)  $\delta$  3.89 (3H, s), 3.93 (3H, s), 6.71 (1H, d,  $J = 7.8$  Hz), 6.80 (1H, t,  $J = 7.8$  Hz), 6.85 (1H, d,  $J = 7.8$  Hz), 6.92 (1H, d,  $J = 16.0$  Hz), 7.02 (1H, d,  $J = 16.0$  Hz), 7.05 (2H, m), 7.09 (1H, d,  $J = 7.8$  Hz), and 7.38 (1H, d,  $J = 7.8$  Hz);  $^{13}\text{C}$  NMR ( $\text{CDCl}_3$ , 100 MHz)  $\delta$  56.0, 56.1, 108.9, 111.3, 116.4, 119.3, 119.8, 122.5, 124.2, 127.2, 128.5, 130.3, 130.9, 143.9, 149.0, and 149.2; HRMS (DART-TOF)  $m/z$ :  $[\text{M} + \text{H}]^+$  Calcd for  $\text{C}_{16}\text{H}_{18}\text{NO}_2$ , 256.1338; Found 256.1345.

(*E*)-*N*-(2-(4-methoxystyryl)phenyl)acetamide (**7**).<sup>122</sup> White solid, and subsequently, colorless block crystals from CH<sub>2</sub>Cl<sub>2</sub>; (37.4 mg, 70%); mp 123–125 °C; <sup>1</sup>H NMR (CDCl<sub>3</sub>, 400 MHz) δ 2.19 (3H, s), 3.82 (3H, s), 6.89 (2H, d, *J* = 8.4 Hz), 6.93 (1H, m), 6.98 (1H, d, *J* = 16.8 Hz), 7.15 (1H, t, *J* = 8.0 Hz), 7.24 (1H, t, *J* = 8.0 Hz), 7.42 (2H, d, *J* = 8.4 Hz), 7.49 (1H, d, *J* = 8.0 Hz), 7.76 (1H, d, *J* = 8.0 Hz); <sup>13</sup>C NMR (CDCl<sub>3</sub>, 100 MHz) δ 24.4, 55.5, 114.3, 121.3, 124.3, 125.7, 126.8, 128.1, 129.9, 130.7, 132.1, 134.5, 159.7, 168.7; ESIMS *m/z* 268 [M + H]<sup>+</sup>.

(*E*)-*tert*-butyl (2-(4-methoxystyryl)phenyl)carbamate (**8**). Yellowish oil, and subsequently, colorless needle crystals from *n*-hexane/CH<sub>2</sub>Cl<sub>2</sub>; (53.4 mg, 82%); mp 109–111 °C; <sup>1</sup>H NMR (CDCl<sub>3</sub>, 400 MHz) δ 1.52 (9H, s), 3.83 (3H, s), 6.42 (1H, br s), 6.91 (2H, d, *J* = 9.1 Hz), 6.92 (1H, d, *J* = 16.5 Hz), 7.01 (1H, d, *J* = 16.5 Hz), 7.09 (1H, t, *J* = 7.8 Hz), 7.25 (1H, t, *J* = 7.8 Hz), 7.46 (2H, d, *J* = 9.1 Hz), 7.47 (1H, m), 7.78 (1H, br d, *J* = 5.9 Hz); <sup>13</sup>C NMR (CDCl<sub>3</sub>, 100 MHz) δ 28.4, 55.5, 80.0, 114.3, 121.5, 124.3, 126.8, 128.0, 128.1, 130.0, 132.0, 135.3, 153.2, 159.7, 178.8; HRMS (DART-TOF) *m/z*: [M + H]<sup>+</sup> Calcd for C<sub>20</sub>H<sub>24</sub>NO<sub>3</sub>, 326.1756; Found 326.1759.

(*E*)-methyl (2-(4-methoxystyryl)phenyl)carbamate (**9**). Yellowish solid; (48.7 mg, 86%); mp 118–120 °C; <sup>1</sup>H NMR (CDCl<sub>3</sub>, 400 MHz) δ 3.76 (3H, s), 3.80 (3H, s), 6.71 (1H, br s), 6.88 (2H, d, *J* = 8.8 Hz), 6.91 (1H, d, *J* = 15.6 Hz), 7.00 (1H, d, *J* = 15.6 Hz), 7.11 (1H, t, *J* = 7.2 Hz), 7.24 (1H, t, *J* = 7.2 Hz), 7.42 (2H, d, *J* = 8.8 Hz), 7.48 (1H, d, *J* = 7.2 Hz), 7.74 (1H, br s); <sup>13</sup>C NMR (CDCl<sub>3</sub>, 100 MHz) δ 52.4, 55.2, 114.1, 120.9, 122.4, 124.6, 126.5, 127.8, 127.9, 129.7, 131.9, 134.5, 154.5, 159.5; HRMS (DART-TOF) *m/z*: [M + H]<sup>+</sup> Calcd for C<sub>17</sub>H<sub>18</sub>NO<sub>3</sub>, 284.1287; Found 284.1285.

*(E)-N-(2-(4-methoxystyryl)phenyl)-4-methylbenzenesulfonamide (10)*.<sup>123</sup> Yellowish oil (56.9 mg, 75%); <sup>1</sup>H NMR (CDCl<sub>3</sub>, 400 MHz) δ 2.29 (3H, s), 3.83 (3H, s), 6.63 (1H, br s), 6.65 (1H, d, *J* = 16.0 Hz), 6.72 (1H, d, *J* = 16.0 Hz), 6.86 (2H, d, *J* = 9.2 Hz), 7.15 (2H, d, *J* = 8.2 Hz), 7.20 (2H, m), 7.24 (2H, d, *J* = 9.2 Hz), 7.35 (1H, m), 7.44 (1H, m), 7.60 (2H, d, *J* = 8.2 Hz); <sup>13</sup>C NMR (CDCl<sub>3</sub>, 100 MHz) δ 21.6, 55.4, 126.5, 126.6, 127.1, 127.3, 128.0, 128.1, 129.6, 129.7, 131.9, 133.1, 133.5, 136.7, 144.0, 159.7; HRMS (DART-TOF) *m/z*: [M + H]<sup>+</sup> Calcd for C<sub>22</sub>H<sub>22</sub>NO<sub>3</sub>S, 380.1320; Found 380.1310.

*(E)-N-(2-(4-methoxystyryl)phenyl)-2-nitrobenzenesulfonamide (11)*. Yellowish oil (73.9 mg, 90%); <sup>1</sup>H NMR (CDCl<sub>3</sub>, 400 MHz) δ 3.81 (3H, s), 6.66 (1H, d, *J* = 16.5 Hz), 6.83 (2H, d, *J* = 9.2 Hz), 7.04 (1H, d, *J* = 16.5 Hz), 7.21 (2H, d, *J* = 9.2 Hz), 7.25 (1H, m), 7.34 (2H, m), 7.47 (3H, m), 7.54 (1H, m), 7.64 (1H, m); <sup>13</sup>C NMR (CDCl<sub>3</sub>, 100 MHz) δ 55.5, 128.0, 128.1, 128.2, 128.4, 129.5, 131.1, 131.7, 132.3, 132.6, 133.1, 133.8, 134.1, 134.9, 147.9, 159.8; HRMS (DART-TOF) *m/z*: [M + H]<sup>+</sup> Calcd for C<sub>21</sub>H<sub>19</sub>N<sub>2</sub>O<sub>5</sub>S, 411.1015; Found 411.1011.

*(E)-N-(2-(3,4-dimethoxystyryl)phenyl)acetamide (12)*.<sup>96</sup> White solid; (53.5 mg, 90%); mp 108–110 °C; <sup>1</sup>H NMR (CDCl<sub>3</sub>, 400 MHz) δ 2.15 (3H, s), 3.86 (3H, s), 3.88 (3H, s), 6.82 (1H, d, *J* = 8.7 Hz), 6.87 (1H, d, *J* = 16.5 Hz), 6.97 (1H, d, *J* = 16.5 Hz), 6.99 (1H, s), 7.01 (1H, d, *J* = 8.7 Hz), 7.14 (1H, d, *J* = 7.8 Hz), 7.21 (1H, d, *J* = 7.8 Hz), 7.47 (1H, d, *J* = 7.8 Hz), 7.70 (1H, d, *J* = 7.8 Hz); <sup>13</sup>C NMR (CDCl<sub>3</sub>, 100 MHz) δ 24.3, 56.0, 109.4, 111.3, 120.0, 121.8, 124.6, 125.7, 126.7, 128.1, 130.3, 130.9, 132.0, 134.6, 149.2, 149.3, 169.0; ESIMS *m/z* 298 [M + H]<sup>+</sup>.

*(E)*-methyl (2-(3,4-dimethoxystyryl)phenyl)carbamate (**13**). Yellowish oil; (43.9 mg, 70%);  $^1\text{H}$  NMR ( $\text{CDCl}_3$ , 400 MHz)  $\delta$  3.78 (3H, s), 3.88 (3H, s), 3.93 (3H, s), 6.71 (1H, br s), 6.85 (1H, d,  $J = 8.7$  Hz), 6.91 (1H, d,  $J = 16.0$  Hz), 7.01 (1H, d,  $J = 16.0$  Hz), 7.03 (1H, m), 7.04 (1H, m), 7.13 (1H, t,  $J = 7.5$  Hz), 7.27 (1H, t,  $J = 7.5$  Hz), 7.49 (1H, d,  $J = 7.5$  Hz), 7.76 (1H, br d,  $J = 6.4$  Hz);  $^{13}\text{C}$  NMR ( $\text{CDCl}_3$ , 100 MHz)  $\delta$  52.5, 56.0, 109.1, 111.3, 120.1, 121.3, 124.7, 126.9, 128.1, 129.3, 130.1, 132.6, 134.7, 149.2, 149.4, 154.5; HRMS (DART-TOF)  $m/z$ :  $[\text{M} + \text{H}]^+$  Calcd for  $\text{C}_{18}\text{H}_{20}\text{NO}_4$ , 314.1392; Found 314.1397.

*(E)*-*N*-(2-(3,4-dimethoxystyryl)phenyl)-4-methylbenzenesulfonamide (**14**). Yellowish solid, and subsequently, colorless block crystals from hexane/ $\text{CH}_2\text{Cl}_2$  (68.0 mg, 83%); mp 153–155 °C;  $^1\text{H}$  NMR ( $\text{CDCl}_3$ , 400 MHz)  $\delta$  2.26 (3H, s), 3.89 (3H, s), 3.91 (3H, s), 6.67 (1H, d,  $J = 16.0$  Hz), 6.76 (1H, d,  $J = 16.0$  Hz), 6.80 (1H, d,  $J = 8.2$  Hz), 6.88 (1H, dd,  $J = 8.2, 1.8$  Hz), 6.90 (1H, d,  $J = 1.8$  Hz), 7.04 (1H, br s), 7.12 (2H, d,  $J = 8.2$  Hz), 7.20 (1H, t,  $J = 7.4$  Hz), 7.22 (1H, t,  $J = 7.4$  Hz), 7.37 (1H, m), 7.45 (1H, m), 7.60 (2H, d,  $J = 8.2$  Hz);  $^{13}\text{C}$  NMR ( $\text{CDCl}_3$ , 100 MHz)  $\delta$  21.5, 55.9, 108.9, 111.1, 120.2, 120.6, 126.4, 126.5, 126.9, 127.1, 128.0, 129.6, 129.9, 132.1, 133.1, 133.3, 136.5, 145.7, 149.0, 149.3; HRMS (DART-TOF)  $m/z$ :  $[\text{M} + \text{H}]^+$  Calcd for  $\text{C}_{23}\text{H}_{24}\text{NO}_4\text{S}$ , 410.1426; Found 410.1422.

*(E)*-*N*-(2-(3,4-dimethoxystyryl)phenyl)-2-nitrobenzenesulfonamide (**15**). Yellowish oil (62.5 mg, 71%);  $^1\text{H}$  NMR ( $\text{CDCl}_3$ , 400 MHz)  $\delta$  3.89 (3H, s), 3.90 (3H, s), 6.66 (1H, d, 16.4 Hz), 6.80 (2H, m), 6.92 (1H, s), 7.08 (1H, d, 16.4 Hz), 7.26 (2H, m), 7.37 (1H, br s), 7.43 (1H, m), 7.49 (3H, m), 7.55 (1H, m), 7.66 (1H, m);  $^{13}\text{C}$  NMR ( $\text{CDCl}_3$ , 100

MHz)  $\delta$  55.9, 56.0, 108.2, 111.1, 120.4, 120.6, 125.2, 126.2, 128.1, 128.2, 131.2, 132.0, 132.3, 132.6, 133.8, 147.9, 149.3, 149.4; HRMS (DART-TOF)  $m/z$ :  $[M + H]^+$  Calcd for  $C_{22}H_{21}N_2O_6S$ , 441.1120; Found 441.1103.

*(E)*-(2-(4-methoxystyryl)phenyl)methanol (**16**).<sup>124</sup> White solid (38.4 mg, 80%); mp 142–143 °C (lit. 103 °C);  $^1H$  NMR ( $CDCl_3$ , 400 MHz)  $\delta$  3.83 (3H, s), 4.82 (2H, s), 6.90 (2H, d,  $J = 8.8$  Hz), 7.00 (1H, d,  $J = 16.0$  Hz), 7.25 (1H, t,  $J = 7.2$  Hz), 7.31 (1H, d,  $J = 16.0$  Hz), 7.32 (1H, t,  $J = 7.2$  Hz), 7.37 (1H, d,  $J = 7.2$  Hz), 7.47 (2H, d,  $J = 8.8$  Hz), 7.63 (1H, d,  $J = 7.2$  Hz);  $^{13}C$  NMR ( $CDCl_3$ , 100 MHz)  $\delta$  55.3, 63.7, 114.1, 123.1, 125.7, 127.3, 127.9, 128.3, 128.6, 130.2, 130.7, 136.6, 137.6, 159.4; HRMS (DART-TOF)  $m/z$ :  $[M + H]^+$  Calcd for  $C_{16}H_{17}O_2$ , 241.1229; Found 241.1233.

*(E)*-((2-(4-methoxystyryl)benzyl)oxy)trimethylsilane (**17**). Colorless oil (47.5 mg, 76%);  $^1H$  NMR ( $CDCl_3$ , 400 MHz)  $\delta$  0.17 (9H, s), 3.84 (3H, s), 4.81 (2H, s), 6.91 (2H, d,  $J = 8.7$  Hz), 6.97 (1H, d,  $J = 16.2$  Hz), 7.26 (3H, m), 7.41 (1H, d,  $J = 7.0$  Hz), 7.46 (2H, d,  $J = 8.7$  Hz), 7.59 (1H, d,  $J = 7.0$  Hz);  $^{13}C$  NMR ( $CDCl_3$ , 100 MHz)  $\delta$  -0.004, 55.7, 63.3, 114.5, 123.9, 125.8, 127.5, 127.9, 128.1, 128.2, 130.5, 130.8, 136.4, 138.0, 159.7; HRMS (DART-TOF)  $m/z$ :  $[M + H]^+$  Calcd for  $C_{19}H_{25}O_2Si$ , 313.1624; Found 313.1623.

*(E)*-(2-(3,4-dimethoxystyryl)phenyl)methanol (**18**). Light yellowish oil (43.3 mg, 80%);  $^1H$  NMR ( $CDCl_3$ , 400 MHz)  $\delta$  3.86 (3H, s), 3.90 (3H, s), 4.77 (2H, d,  $J = 3.6$  Hz), 6.82 (1H, d,  $J = 8.0$  Hz), 6.96 (1H, d,  $J = 16.0$  Hz), 7.04 (1H, s), 7.05 (1H, m), 7.22 (1H, t,  $J = 7.6$  Hz), 7.27 (1H, d,  $J = 16.0$  Hz), 7.29 (1H, m), 7.34 (1H, d,  $J = 7.6$  Hz), 7.60 (1H, d,

$J = 7.6$  Hz);  $^{13}\text{C}$  NMR ( $\text{CDCl}_3$ , 100 MHz)  $\delta$  55.8, 63.4, 109.1, 111.2, 119.8, 123.3, 125.7, 127.3, 128.1, 128.4, 130.4, 130.8, 136.4, 137.6, 148.97, 148.99; HRMS (DART-TOF)  $m/z$ :  $[\text{M} + \text{H}]^+$  Calcd for  $\text{C}_{17}\text{H}_{19}\text{O}_3$ , 271.1334; Found 271.1333.

*(E)-((2-(3,4-dimethoxystyryl)benzyl)oxy)trimethylsilane (19)*. Colorless oil (51.4 mg, 75%);  $^1\text{H}$  NMR ( $\text{CDCl}_3$ , 400 MHz)  $\delta$  0.06 (9H, s), 3.79 (3H, s), 3.83 (3H, s), 4.70 (2H, s), 6.76 (1H, d,  $J = 8.7$  Hz), 6.84 (1H, d,  $J = 16.1$  Hz), 6.95 (2H, m), 7.15 (3H, m), 7.28 (1H, d,  $J = 7.2$  Hz), 7.48 (1H, d,  $J = 7.2$  Hz);  $^{13}\text{C}$  NMR ( $\text{CDCl}_3$ , 100 MHz)  $\delta$  -0.004, 56.2, 56.3, 63.5, 109.4, 111.6, 120.2, 124.2, 125.9, 127.6, 128.0, 128.4, 130.8, 131.1, 136.5, 138.0, 149.3, 149.5; HRMS (DART-TOF)  $m/z$ :  $[\text{M} + \text{H}]^+$  Calcd for  $\text{C}_{20}\text{H}_{27}\text{O}_3\text{Si}$ , 343.1729; Found 343.1730.

*(E)-N-(2-(4-methoxystyryl)benzyl)-2-nitrobenzenesulfonamide (20)*. Yellowish oil; (53.5 mg, 63%);  $^1\text{H}$  NMR ( $\text{CDCl}_3$ , 400 MHz)  $\delta$  3.81 (3H, s), 4.39 (2H, d,  $J = 6.0$  Hz), 5.66 (1H, t,  $J = 6.0$  Hz), 6.83 (1H, d,  $J = 16.0$  Hz), 6.87 (2H, d,  $J = 8.8$  Hz), 7.12 (1H, d,  $J = 16.0$  Hz), 7.13 (1H, t,  $J = 7.6$  Hz), 7.19 (1H, d,  $J = 7.6$  Hz), 7.24 (1H, t,  $J = 7.6$  Hz), 7.36 (2H, d,  $J = 8.8$  Hz), 7.48 (1H, d,  $J = 7.6$  Hz), 7.58 (1H, td,  $J = 7.6, 2.0$  Hz), 7.62 (1H, td,  $J = 7.6, 2.0$  Hz), 7.72 (1H, dd,  $J = 7.6, 2.0$  Hz), 7.98 (1H, dd,  $J = 7.6, 2.0$  Hz);  $^{13}\text{C}$  NMR ( $\text{CDCl}_3$ , 100 MHz)  $\delta$  46.0, 55.3, 114.1, 122.2, 125.2, 126.0, 127.3, 127.9, 128.7, 129.7, 129.9, 130.9, 131.6, 132.2, 132.7, 133.3, 133.5, 137.1, 147.6, 159.5; HRMS (DART-TOF)  $m/z$ :  $[\text{M} + \text{H}]^+$  Calcd for  $\text{C}_{22}\text{H}_{21}\text{N}_2\text{O}_5\text{S}$ , 425.1171; Found 425.1175.

*(E)*-*N*-(2-(4-methoxystyryl)benzyl)-4-methylbenzenesulfonamide (**21**). White solid; (48.0 mg, 61%); <sup>1</sup>H NMR (CDCl<sub>3</sub>, 400 MHz) δ 2.43 (3H, s), 3.84 (3H, s), 4.17 (2H, s), 6.90 (2H, d, *J* = 8.8 Hz), 6.93 (1H, d, *J* = 16.4 Hz), 7.16 (2H, m), 7.18 (1H, d, *J* = 16.4 Hz), 7.28 (3H, m), 7.42 (2H, d, *J* = 8.8 Hz), 7.58 (1H, d, *J* = 7.6 Hz), 7.75 (2H, d, *J* = 8.4 Hz); <sup>13</sup>C NMR (CDCl<sub>3</sub>, 100MHz) δ 21.5, 45.3, 55.4, 114.2, 122.6, 125.8, 127.1, 127.3, 128.1, 128.6, 129.8, 129.9, 130.1, 131.1, 132.9, 136.7, 137.1, 143.5, 159.5; HRMS (DART-TOF) *m/z*: [M + H]<sup>+</sup> Calcd for C<sub>23</sub>H<sub>24</sub>NO<sub>3</sub>S, 394.1477; Found 394.1470.

*(E)*-*N*-(2-(4-methoxystyryl)benzyl)acetamide (**22**). Light yellowish solid; (48.4 mg, 86%); mp 130–133 °C; <sup>1</sup>H NMR (CDCl<sub>3</sub>, 400 MHz) δ 1.91 (3H, s), 3.80 (3H, s), 4.52 (2H, d, *J* = 5.6 Hz), 5.66 (1H, br s), 6.89 (2H, d, *J* = 8.8 Hz), 6.94 (1H, d, *J* = 16.0 Hz), 7.17 (1H, d, *J* = 16.0 Hz), (2H, m), 7.20 7.28 (1H, t, *J* = 7.2 Hz), 7.44 (2H, d, *J* = 8.8 Hz), 7.61 (1H, d, *J* = 7.2 Hz); <sup>13</sup>C NMR (CDCl<sub>3</sub>, 100 MHz) δ 23.0, 41.8, 55.2, 114.1, 122.8, 125.6, 127.2, 127.9, 128.1, 129.6, 129.9, 130.5, 134.9, 136.7, 159.4, 169.5; HRMS (DART-TOF) *m/z*: [M + H]<sup>+</sup> Calcd for C<sub>18</sub>H<sub>20</sub>NO<sub>2</sub>, 282.1494; Found 282.1492.

*(E)*-methyl 2-(4-methoxystyryl)benzylcarbamate (**23**). White solid; (42.8 mg, 72%); mp 122–124 °C; <sup>1</sup>H NMR (CDCl<sub>3</sub>, 400 MHz) δ 3.64 (3H, br s), 3.81 (3H, s), 4.50 (2H, d, *J* = 5.6 Hz), 4.93 (1H, br s), 6.89 (2H, d, *J* = 8.8 Hz), 6.95 (1H, d, *J* = 16.0 Hz), 7.24 (4H, m), 7.49 (2H, br d, *J* = 8.4 Hz), 7.61 (1H, d, *J* = 7.2 Hz); <sup>13</sup>C NMR (CDCl<sub>3</sub>, 100MHz) δ 43.4, 52.2, 55.3, 114.2, 123.0, 125.8, 127.4, 128.0, 128.2, 129.2, 130.1, 130.8, 135.2, 136.8, 156.8, 159.5; HRMS (DART-TOF) *m/z*: [M + H]<sup>+</sup> Calcd for C<sub>18</sub>H<sub>20</sub>NO<sub>3</sub>, 298.1443; Found 298.1437.

*(E)*-*N*-(2-(3,4-dimethoxystyryl)benzyl)-4-methylbenzenesulfonamide (**24**). White solid; (52.5 mg, 62%); <sup>1</sup>H NMR (CDCl<sub>3</sub>, 400 MHz) δ 2.37 (3H, s), 3.86 (3H, s), 3.92 (3H, s), 4.14 (2H, d, *J* = 6.4 Hz), 5.12 (1H, t, *J* = 6.4 Hz), 6.81 (1H, d, *J* = 8.4 Hz), 6.92 (1H, d, *J* = 16.4 Hz), 6.97 (1H, dd, *J* = 8.4, 2.0 Hz), 7.05 (1H, d, *J* = 2.0 Hz), 7.08 (1H, t, *J* = 7.6 Hz), 7.23 (4H, m), 7.37 (1H, d, *J* = 16.4 Hz), 7.57 (1H, d, *J* = 7.6 Hz), 7.70 (2H, d, *J* = 8.4 Hz); <sup>13</sup>C NMR (CDCl<sub>3</sub>, 100MHz) δ 21.3, 45.6, 55.7, 55.9, 108.7, 110.9, 120.4, 122.8, 125.4, 126.9, 127.0, 128.4, 129.5, 129.8, 130.3, 130.8, 132.6, 136.5, 136.9, 143.2, 148.9, 149.1; HRMS (DART-TOF) *m/z*: [M + H]<sup>+</sup> Calcd for C<sub>24</sub>H<sub>26</sub>NO<sub>4</sub>S, 424.1583; Found 424.1590.

*(E)*-*N*-(2-(3,4-dimethoxystyryl)benzyl)-2-nitrobenzenesulfonamide (**25**). Yellowish oil; (56.4 mg, 62%); <sup>1</sup>H NMR (CDCl<sub>3</sub>, 400 MHz) δ 3.89 (3H, s), 3.94 (3H, s), 4.38 (2H, d, *J* = 6.0 Hz), 5.64 (1H, t, *J* = 6.0 Hz), 6.83 (1H, d, *J* = 8.0 Hz), 6.88 (1H, d, *J* = 16.0 Hz), 6.97 (1H, dd, *J* = 8.0, 2.0 Hz), 7.14 (2H, m), 7.15 (1H, d, *J* = 2.0 Hz), 7.26 (1H, m), 7.27 (1H, d, *J* = 16.0 Hz), 7.53 (1H, d, *J* = 7.6 Hz), 7.63 (2H, m), 7.72 (1H, m), 8.01 (1H, m); <sup>13</sup>C NMR (CDCl<sub>3</sub>, 100 MHz) δ 46.2, 55.8, 55.9, 108.7, 111.0, 120.4, 122.6, 125.2, 125.7, 127.2, 128.8, 130.0, 130.2, 130.9, 131.5, 132.1, 132.6, 133.35, 133.40, 137.1, 147.7, 149.1; HRMS (DART-TOF) *m/z*: [M + H]<sup>+</sup> Calcd for C<sub>23</sub>H<sub>23</sub>N<sub>2</sub>O<sub>6</sub>S, 455.1277; Found 455.1272.

*(E)*-*N*-(2-(3,4-dimethoxystyryl)benzyl)acetamide (**26**). Yellowish oil; (42.3 mg, 68%); <sup>1</sup>H NMR (CDCl<sub>3</sub>, 400 MHz) δ 1.91 (3H, s), 3.87 (3H, s), 3.96 (3H, s), 4.55 (2H, d, *J* = 5.6 Hz), 5.96 (1H, br t, *J* = 5.2 Hz), 6.83 (1H, d, *J* = 8.4 Hz), 6.93 (1H, d, *J* = 15.6 Hz), 7.02 (1H, dd, *J* = 8.4, 1.6 Hz), 7.19 (4H, m), 7.29 (1H, t, *J* = 8.0 Hz), 7.63 (1H, d, *J* =

8.0 Hz);  $^{13}\text{C}$  NMR ( $\text{CDCl}_3$ , 100 MHz)  $\delta$  23.0, 41.8, 55.8, 55.9, 108.7, 111.0, 120.1, 123.1, 125.4, 127.2, 128.1, 129.6, 130.3, 130.5, 135.0, 136.6, 148.9, 149.1, 169.3; HRMS (DART-TOF)  $m/z$ :  $[\text{M} + \text{H}]^+$  Calcd for  $\text{C}_{19}\text{H}_{22}\text{NO}_3$ , 312.1600; Found 312.1599.

*(E)*-methyl 2-(3,4-dimethoxystyryl)benzylcarbamate (**27**). White solid; (41.9 mg, 64%); mp 113–115 °C;  $^1\text{H}$  NMR ( $\text{CDCl}_3$ , 400 MHz)  $\delta$  3.63 (3H, br s), 3.90 (3H, s), 3.98 (3H, br s), 4.53 (2H, d,  $J = 6.0$  Hz), 4.91 (1H, br s), 6.85 (1H, d,  $J = 8.4$  Hz), 6.95 (1H, d,  $J = 16.0$  Hz), 7.04 (1H, dd,  $J = 8.4, 2.0$  Hz), 7.25 (5H, m), 7.64 (1H, d,  $J = 7.6$  Hz);  $^{13}\text{C}$  NMR ( $\text{CDCl}_3$ , 100MHz)  $\delta$  43.5, 52.2, 55.9, 108.8, 111.1, 120.4, 123.2, 125.7, 127.4, 128.2, 129.3, 130.5, 130.8, 135.3, 136.7, 149.1, 149.2, 156.7; HRMS (DART-TOF)  $m/z$ :  $[\text{M} + \text{H}]^+$  Calcd for  $\text{C}_{19}\text{H}_{22}\text{NO}_4$ , 328.1549; Found 328.1555.

*(E)*-2-(4-methoxystyryl)benzoic acid (**28**). White solid; (48.8 mg, 96%);  $^1\text{H}$  NMR ( $\text{CDCl}_3$ , 400 MHz)  $\delta$  3.83 (3H, s), 6.89 (2H, d,  $J = 8.6$  Hz), 6.98 (1H, d,  $J = 16.2$  Hz), 7.29 (1H, t,  $J = 7.8$  Hz), 7.48 (2H, d,  $J = 8.6$  Hz), 7.51 (1H, m), 7.71 (1H, d,  $J = 7.8$  Hz), 7.88 (1H, d,  $J = 16.2$  Hz), 7.95 (1H, d,  $J = 7.8$  Hz);  $^{13}\text{C}$  NMR ( $\text{CDCl}_3$ , 100MHz)  $\delta$  55.2, 114.0, 125.5, 126.2, 126.7, 128.0, 130.1, 130.4, 131.1, 131.6, 138.2, 159.2, 172.4; HRMS (DART-TOF)  $m/z$ :  $[\text{M} + \text{H}]^+$  Calcd for  $\text{C}_{16}\text{H}_{15}\text{O}_3$ , 255.1021; Found 255.1028.

*(E)*-2-(3,4-dimethoxystyryl)benzoic acid (**29**). White solid; (55.7 mg, 98%);  $^1\text{H}$  NMR ( $\text{CDCl}_3$ , 400 MHz)  $\delta$  3.90 (3H, s), 3.94 (3H, s), 6.88 (1H, d,  $J = 8.4$  Hz), 6.97 (1H, d,  $J = 16.4$  Hz), 7.10 (1H, dd,  $J = 8.4, 2.0$  Hz), 7.12 (1H, d,  $J = 2.0$  Hz), 7.31 (1H, t,  $J = 7.6$  Hz), 7.51 (1H, t,  $J = 7.6$  Hz), 7.71 (1H, d,  $J = 7.6$  Hz), 7.99 (1H, d,  $J = 16.4$  Hz), 7.97

(1H, d,  $J = 7.6$  Hz);  $^{13}\text{C}$  NMR ( $\text{CDCl}_3$ , 100 MHz)  $\delta$  55.96, 56.01, 109.5, 111.4, 120.4, 126.0, 126.9, 127.0, 129.0, 131.0, 131.06, 131.11, 132.3, 139.5, 149.2, 170.2; HRMS (DART-TOF)  $m/z$ :  $[\text{M} + \text{H}]^+$  Calcd for  $\text{C}_{17}\text{H}_{17}\text{O}_4$ , 285.1127; Found 285.1120.

*(E)*-1-(4-methoxystyryl)-2-vinylbenzene (**30**). Colorless oil; (26.9 mg, 57%);  $^1\text{H}$  NMR ( $\text{CDCl}_3$ , 400 MHz)  $\delta$  3.79 (3H, s), 5.34 (1H, d,  $J = 10.8$  Hz), 5.63 (1H, d,  $J = 17.2$  Hz), 6.88 (2H, d,  $J = 8.4$  Hz), 6.91 (1H, d,  $J = 15.6$  Hz), 7.09 (1H, dd,  $J = 17.2, 10.8$  Hz), 7.23 (3H, m), 7.43 (2H, d,  $J = 8.4$  Hz), 7.44 (1H, d,  $J = 15.6$  Hz), 7.53 (1H, d,  $J = 7.2$  Hz);  $^{13}\text{C}$  NMR ( $\text{CDCl}_3$ , 100MHz)  $\delta$  55.5, 114.3, 116.5, 124.5, 126.2, 126.7, 127.5, 127.97, 128.00, 130.5, 130.7, 135.2, 136.0, 136.4, 159.5; HRMS (DART-TOF)  $m/z$ :  $[\text{M} + \text{H}]^+$  Calcd for  $\text{C}_{17}\text{H}_{17}\text{O}$ , 237.1279; Found 237.1282.

*(E)*-1,2-dimethoxy-4-(2-vinylstyryl)benzene (**31**). Colorless oil; (33.0 mg, 62%);  $^1\text{H}$  NMR ( $\text{CDCl}_3$ , 400 MHz)  $\delta$  3.90 (3H, s), 3.94 (3H, s), 5.37 (1H, dd,  $J = 11.2, 1.6$  Hz), 5.66 (1H, dd,  $J = 17.6, 1.6$  Hz), 6.86 (1H, d,  $J = 9.2$  Hz), 6.91 (1H, d,  $J = 16.0$  Hz), 7.05 (1H, s), 7.06 (1H, m), 7.10 (1H, dd,  $J = 18.0, 11.6$  Hz), 7.25 (3H, m), 7.47 (1H, d,  $J = 7.2$  Hz), 7.54 (1H, d,  $J = 7.2$  Hz);  $^{13}\text{C}$  NMR ( $\text{CDCl}_3$ , 100 MHz)  $\delta$  56.0, 56.1, 109.1, 111.4, 116.5, 120.0, 124.7, 126.3, 126.7, 127.5, 128.0, 130.8, 131.0, 135.2, 135.9, 136.3, 149.1, 149.2; HRMS (DART-TOF)  $m/z$ :  $[\text{M} + \text{H}]^+$  Calcd for  $\text{C}_{18}\text{H}_{19}\text{O}_2$ , 267.1385; Found 267.1382.

*(E)*-1-methoxy-2-(4-methoxystyryl)benzene (**32**).<sup>85</sup> White solid (42.8 mg, 89%); mp 80–82 °C;  $^1\text{H}$  NMR ( $\text{CDCl}_3$ , 400 MHz)  $\delta$  3.82 (3H, s), 3.88 (3H, s), 6.88 (2H, d,  $J = 8.6$

Hz), 6.95 (1H, t,  $J = 7.7$  Hz), 7.06 (1H, d,  $J = 16.8$  Hz), 7.22 (1H, br t,  $J = 7.7$  Hz), 7.25 (1H, d,  $J = 1.3$  Hz), 7.35 (1H, d,  $J = 16.8$  Hz), 7.47 (2H, d,  $J = 8.6$  Hz), 7.57 (1H, br d,  $J = 7.7$  Hz);  $^{13}\text{C}$  NMR ( $\text{CDCl}_3$ , 100 MHz)  $\delta$  55.4, 55.6, 111.0, 114.1, 120.8, 121.5, 126.2, 126.9, 127.8, 128.3, 128.7, 130.9, 156.8, 159.2; EIMS  $m/z$  240  $[\text{M}]^+$ , ( $\text{C}_{16}\text{H}_{16}\text{O}_2$ ).

*(E)*-2-(4-methoxystyryl)phenyl acetate (**33**).<sup>120</sup> White solid (32.7 mg, 61%); mp 70–71 °C (lit. 75.8 °C);  $^1\text{H}$  NMR ( $\text{CDCl}_3$ , 400 MHz)  $\delta$  2.36 (3H, s), 3.84 (3H, s), 6.89 (2H, d,  $J = 8.8$  Hz), 6.97 (1H, d,  $J = 16.3$  Hz), 7.06 (1H, d,  $J = 16.3$  Hz), 7.07 (1H, dd,  $J = 7.7$ , 2.0 Hz), 7.24 (2H, m), 7.42 (2H, d,  $J = 8.8$  Hz), 7.66, (1H, dd,  $J = 7.0$ , 2.0 Hz);  $^{13}\text{C}$  NMR ( $\text{CDCl}_3$ , 100 MHz)  $\delta$  21.1, 55.4, 114.3, 119.8, 122.8, 126.3, 126.4, 128.0, 128.1, 130.1, 130.4, 130.7, 148.1, 159.7, 169.5; ESIMS  $m/z$  269  $[\text{M} + \text{H}]^+$  ( $\text{C}_{17}\text{H}_{16}\text{O}_3 + \text{H}$ ).

*(E)*-2-(4-methoxystyryl)benzotrile (**34**). Light yellow solid (37.2 mg, 79%); mp 84–86 °C;  $^1\text{H}$  NMR ( $\text{CDCl}_3$ , 400 MHz)  $\delta$  3.83 (3H, s), 6.91 (1H, d,  $J = 8.6$  Hz), 7.02 (1H, d,  $J = 16.1$  Hz), 7.28 (1H, d,  $J = 7.7$  Hz), 7.31 (1H, d,  $J = 16.1$  Hz), 7.47 (2H, d,  $J = 8.6$  Hz), 7.51 (1H, t,  $J = 7.7$  Hz), 7.64 (1H, d,  $J = 7.7$  Hz), 7.75 (1H, d,  $J = 7.7$  Hz);  $^{13}\text{C}$  NMR ( $\text{CDCl}_3$ , 100 MHz)  $\delta$  55.4, 114.2, 122.19, 122.21, 125.89, 125.94, 126.7, 126.8, 128.2, 129.7, 131.8, 132.1, 136.8, 159.8; ESIMS  $m/z$  258  $[\text{M} + \text{Na}]^+$  ( $\text{C}_{16}\text{H}_{13}\text{NO} + \text{Na}$ ).

*(E)*-1-(4-methoxystyryl)-2-nitrobenzene (**35**). Yellow solid (37.6 mg, 73%); mp 66–68 °C;  $^1\text{H}$  NMR ( $\text{CDCl}_3$ , 400 MHz)  $\delta$  3.84 (3H, s), 6.92 (2H, d,  $J = 8.6$  Hz), 7.05 (1H, d,  $J = 16.1$  Hz), 7.36 (1H, t,  $J = 7.8$  Hz), 7.48 (3H, m), 7.57 (1H, t,  $J = 7.8$  Hz), 7.75 (1H, d,  $J = 7.8$  Hz), 7.93 (1H, d,  $J = 7.8$  Hz);  $^{13}\text{C}$  NMR ( $\text{CDCl}_3$ , 100 MHz)  $\delta$  55.4, 114.3, 121.1,

124.8, 127.5, 127.9, 128.5, 129.3, 133.0, 133.3, 133.5, 147.9, 160.1; ESIMS  $m/z$  278  
[M + Na]<sup>+</sup> (C<sub>15</sub>H<sub>13</sub>NO<sub>3</sub> + Na).

*(E)*-1-(4-methoxystyryl)-2-(trifluoromethyl)benzene (**36**). White solid (39.5 mg, 71%);  
mp 40–41 °C; <sup>1</sup>H NMR (CDCl<sub>3</sub>, 400 MHz) δ 3.83 (3H, s), 6.91 (2H, d,  $J$  = 8.7 Hz), 7.03  
(1H, d,  $J$  = 16.4 Hz), 7.31 (2H, m), 7.47 (2H, d,  $J$  = 8.7 Hz), 7.51 (1H, t,  $J$  = 7.7 Hz),  
7.64 (1H, d,  $J$  = 7.7 Hz), 7.76 (1H, d,  $J$  = 7.7 Hz); <sup>13</sup>C NMR (CDCl<sub>3</sub>, 100 MHz) δ 55.4,  
114.3, 122.3, 125.96, 126.02, 126.8, 126.9, 128.3, 129.8, 131.9, 132.2, 136.8, 159.9;  
ESIMS  $m/z$  279 [M + H]<sup>+</sup> (C<sub>16</sub>H<sub>13</sub>OF<sub>3</sub> + H).

*(E)*-methyl 2-(4-methoxystyryl)benzoate (**37**).<sup>125</sup> White solid; (52.1 mg, 97%); mp 77–78  
°C (lit. 80–81 °C); <sup>1</sup>H NMR (CDCl<sub>3</sub>, 400 MHz) δ 3.83 (3H, s), 3.92 (s, 3H), 6.90 (2H, d,  
 $J$  = 9.2 Hz), 6.97 (1H, d,  $J$  = 16.4 Hz), 7.29 (1H, t,  $J$  = 7.6 Hz), 7.47 (1H, t,  $J$  = 7.6 Hz),  
7.49 (2H, d,  $J$  = 9.2 Hz), 7.70 (1H, d,  $J$  = 7.6 Hz), 7.86 (1H, d,  $J$  = 16.4 Hz), 7.91 (1H,  
d,  $J$  = 7.6 Hz); <sup>13</sup>C NMR (CDCl<sub>3</sub>, 100MHz) δ 52.0, 55.3, 114.1, 125.2, 126.68, 126.71,  
128.1, 128.3, 130.2, 130.6, 131.0, 132.1, 139.5, 159.4, 168.0; ESIMS  $m/z$  269 [M + H]<sup>+</sup>  
(C<sub>17</sub>H<sub>16</sub>O<sub>3</sub> + H).

*(E)*-*N*-acetyl-2-(4-methoxystyryl)benzamide (**38**). Light yellowish oil and subsequently,  
colorless block in hexane/CH<sub>2</sub>Cl<sub>2</sub> (41.3 mg, 70%); mp 149–151 °C; <sup>1</sup>H NMR (CDCl<sub>3</sub>,  
400 MHz) δ 2.60 (3H, s), 3.83 (3H, s), 6.90 (2H, d,  $J$  = 8.8 Hz), 7.03 (1H, d,  $J$  = 16.2  
Hz), 7.32 (1H, d,  $J$  = 16.2 Hz), 7.32 (1H, t,  $J$  = 7.9 Hz), 7.44 (2H, d,  $J$  = 8.8 Hz), 7.49  
(1H, d,  $J$  = 7.9 Hz), 7.52 (1H, t,  $J$  = 7.9 Hz), 7.71 (1H, d,  $J$  = 7.9 Hz), 8.26 (1H, br s);

$^{13}\text{C}$  NMR ( $\text{CDCl}_3$ , 100MHz)  $\delta$  25.5, 55.3, 122.8, 126.9, 127.2, 127.7, 128.2, 129.6, 131.8, 132.6, 132.8, 137.0, 159.9, 167.7, 172.4; HRMS (DART-TOF)  $m/z$ :  $[\text{M} + \text{H}]^+$  Calcd for  $\text{C}_{18}\text{H}_{18}\text{NO}_3$ , 296.1287; Found 296.1283.

*(E)*-1,2-dimethoxy-4-(2-methoxystyryl)benzene (**39**).<sup>126</sup> Light yellowish oil and subsequently, colorless needles in hexane/ $\text{CH}_2\text{Cl}_2$  (49.2 mg, 91%); mp 102–104 °C (lit. 102–104 °C);  $^1\text{H}$  NMR ( $\text{CDCl}_3$ , 400 MHz)  $\delta$  3.88 (3H, s), 3.89 (3H, s), 3.94 (3H, s), 6.84 (1H, d,  $J = 8.0$  Hz), 6.89 (1H, d,  $J = 7.6$  Hz), 6.96 (1H, t,  $J = 7.6$  Hz), 7.05 (1H, d,  $J = 16.4$  Hz), 7.06 (1H, dd,  $J = 8.0, 2.0$  Hz), 7.22 (1H, t,  $J = 7.6$  Hz), 7.33 (1H, d,  $J = 16.4$  Hz), 7.57 (1H, d,  $J = 7.6$  Hz);  $^{13}\text{C}$  NMR ( $\text{CDCl}_3$ , 100 MHz)  $\delta$  55.5, 55.86, 55.88, 108.9, 110.9, 111.2, 119.9, 120.7, 121.5, 126.2, 126.6, 128.3, 128.9, 131.1, 148.7, 149.0, 156.7; EIMS  $m/z$  270  $[\text{M}]^+$ , ( $\text{C}_{17}\text{H}_{18}\text{O}_3$ ).

*(E)*-2-(3,4-dimethoxystyryl)phenyl acetate (**40**). White solid (38.8 mg, 65%); mp 80–82 °C;  $^1\text{H}$  NMR ( $\text{CDCl}_3$ , 400 MHz)  $\delta$  2.36 (3H, s), 3.89 (3H, s), 3.92 (3H, s), 6.86 (1H, d,  $J = 8.4$  Hz), 6.96 (1H, d,  $J = 16.0$  Hz), 7.02 (1H, d,  $J = 2.0$  Hz), 7.03 (1H, m), 7.04 (1H, m), 7.07 (1H, dd,  $J = 8.4, 2.0$  Hz), 7.23 (1H, t,  $J = 7.2$  Hz), 7.26 (1H, t,  $J = 7.2$  Hz), 7.65 (1H, d,  $J = 7.2$  Hz);  $^{13}\text{C}$  NMR ( $\text{CDCl}_3$ , 100 MHz)  $\delta$  20.9, 55.8, 55.9, 109.3, 111.2, 119.8, 120.1, 122.6, 126.2, 126.4, 128.0, 130.1, 130.3, 130.9, 148.0, 149.0, 149.2, 169.2; HRMS (DART-TOF)  $m/z$ :  $[\text{M} + \text{H}]^+$  Calcd for  $\text{C}_{18}\text{H}_{19}\text{O}_4$ , 299.1283; Found 299.1289.

*(E)*-2-(4-methoxystyryl)benzaldehyde (**41**).<sup>127</sup> Yellow solid (42.9 mg, 90%); mp 116–118 °C; <sup>1</sup>H NMR (CDCl<sub>3</sub>, 400 MHz) δ 3.84 (3H, s), 6.92 (2H, d, *J* = 8.8 Hz), 7.01 (1H, d, *J* = 16.2 Hz), 7.41 (1H, t, *J* = 7.8 Hz), 7.51 (2H, d, *J* = 8.8 Hz), 7.56 (1H, t, *J* = 7.8 Hz), 7.70 (1H, d, *J* = 7.8 Hz), 7.83 (1H, d, *J* = 7.8 Hz), 7.91 (1H, d, *J* = 16.2 Hz), 10.33 (1H, s); <sup>13</sup>C NMR (CDCl<sub>3</sub>, 100 MHz) δ 55.4, 114.2, 122.5, 127.0, 127.2, 128.3, 129.8, 132.2, 132.8, 133.7, 140.4, 159.9, 192.7; HRMS (DART-TOF) *m/z*: [M + H]<sup>+</sup> Calcd for C<sub>16</sub>H<sub>15</sub>O<sub>2</sub>, 239.1072; Found 239.1069.

*(E)*-1-(dimethoxymethyl)-2-(4-methoxystyryl)benzene (**42**). Yellowish oil (54.6 mg, 96%); <sup>1</sup>H NMR (CDCl<sub>3</sub>, 400 MHz) δ 3.33 (6H, s), 3.80 (3H, s), 5.59 (1H, s), 6.89 (2H, d, *J* = 8.8 Hz), 6.94 (1H, d, *J* = 16.2 Hz), 7.25 (1H, t, *J* = 7.7 Hz), 7.31 (1H, t, *J* = 7.7 Hz), 7.46 (2H, d, *J* = 8.8 Hz), 7.58 (1H, d, *J* = 7.7 Hz), 7.61 (1H, d, *J* = 7.7 Hz); <sup>13</sup>C NMR (CDCl<sub>3</sub>, 100 MHz) δ 53.0, 55.3, 101.7, 114.2, 123.7, 125.8, 126.8, 127.0, 128.0, 128.7, 130.4, 130.4, 134.6, 136.6, 159.4; HRMS (DART-TOF) *m/z*: [M + H]<sup>+</sup> Calcd for C<sub>18</sub>H<sub>21</sub>O<sub>3</sub>, 285.1491; Found 285.1496.

*(E)*-2-(2-(4-methoxystyryl)phenyl)-1,3-dioxolane (**43**). Yellowish oil (45.2 mg, 80%); <sup>1</sup>H NMR (CDCl<sub>3</sub>, 400 MHz) δ 3.80 (3H, s), 4.04 (2H, m), 4.15 (2H, m), 6.09 (1H, s), 6.88 (2H, d, *J* = 8.8 Hz), 6.96 (1H, d, *J* = 16.0 Hz), 7.26 (1H, t, *J* = 7.6 Hz), 7.34 (1H, t, *J* = 7.6 Hz), 7.40 (1H, d, *J* = 16.0 Hz), 7.45 (2H, d, *J* = 8.8 Hz), 7.59 (1H, d, *J* = 7.6 Hz), 7.60 (1H, d, *J* = 7.6 Hz); <sup>13</sup>C NMR (CDCl<sub>3</sub>, 100 MHz) δ 55.4, 65.4, 101.9, 114.1, 123.5, 126.0, 126.1, 127.1, 128.0, 129.2, 130.4, 130.9, 134.4, 137.0, 159.4; HRMS (DART-TOF) *m/z*: [M + H]<sup>+</sup> Calcd for C<sub>18</sub>H<sub>19</sub>O<sub>3</sub>, 283.1334; Found 283.1340.

*(E)*-2-(3,4-dimethoxystyryl)benzaldehyde (**44**). Yellow solid (51.0 mg, 95%); mp 125–127 °C; <sup>1</sup>H NMR (CDCl<sub>3</sub>, 400 MHz) δ 3.90 (3H, s), 3.95 (3H, s), 6.86 (1H, d, *J* = 8.0 Hz), 6.99 (1H, d, *J* = 16.0 Hz), 7.10 (1H, dd, *J* = 8.0, 2.4 Hz), 7.11 (1H, s), 7.40 (1H, t, *J* = 7.6 Hz), 7.55 (1H, t, *J* = 7.6 Hz), 7.69 (1H, d, *J* = 7.6 Hz), 7.81 (1H, d, *J* = 7.6 Hz), 7.91 (1H, d, *J* = 16.0 Hz), 10.31 (1H, s); <sup>13</sup>C NMR (CDCl<sub>3</sub>, 100 MHz) δ 55.99, 56.04, 109.2, 111.3, 120.7, 122.8, 127.1, 127.4, 130.1, 132.4, 132.8, 133.8, 134.0, 140.3, 149.3, 149.6, 192.9; HRMS (DART-TOF) *m/z*: [M + H]<sup>+</sup> Calcd for C<sub>17</sub>H<sub>17</sub>O<sub>3</sub>, 269.1178; Found 269.1170.

*(E)*-4-(2-(dimethoxymethyl)styryl)-1,2-dimethoxybenzene (**45**). Yellowish oil (59.1 mg, 94%); <sup>1</sup>H NMR (CDCl<sub>3</sub>, 400 MHz) δ 3.34 (6H, s), 3.88 (3H, s), 3.93 (3H, s), 5.60 (1H, s), 6.85 (1H, d, *J* = 8.4 Hz), 6.93 (1H, d, *J* = 16.0 Hz), 7.06 (1H, d, *J* = 2.0 Hz), 7.08 (1H, dd, *J* = 8.4, 2.0 Hz), 7.26 (1H, t, *J* = 7.6 Hz), 7.32 (1H, t, *J* = 7.6 Hz), 7.42 (1H, d, *J* = 16.0 Hz), 7.59 (1H, d, *J* = 7.6 Hz), 7.60 (1H, d, *J* = 7.6 Hz); <sup>13</sup>C NMR (CDCl<sub>3</sub>, 100 MHz) δ 53.2, 55.95, 55.99, 101.7, 109.4, 111.3, 119.9, 124.1, 125.9, 126.8, 127.0, 128.7, 130.7, 130.8, 134.6, 136.5, 149.0, 149.1; HRMS (DART-TOF) *m/z*: [M + H]<sup>+</sup> Calcd for C<sub>19</sub>H<sub>23</sub>O<sub>4</sub>, 315.1596; Found 315.1591.

*(E)*-methyl 2-(3,4-dimethoxystyryl)benzoate (**46**). Colorless oil; (54.9 mg, 92%); <sup>1</sup>H NMR (CDCl<sub>3</sub>, 400 MHz) δ 3.85 (3H, s), 3.88 (3H, s), 3.91 (3H, s), 6.81 (1H, d, *J* = 8.0 Hz), 6.94 (1H, d, *J* = 16.0 Hz), 7.07 (2H, m), 7.25 (1H, t, *J* = 7.6 Hz), 7.45 (1H, t, *J* = 7.6 Hz), 7.67 (1H, d, *J* = 7.6 Hz), 7.88 (1H, d, *J* = 16.0 Hz), 7.90 (1H, d, *J* = 7.6 Hz); <sup>13</sup>C NMR (CDCl<sub>3</sub>, 100 MHz) δ 51.7, 55.59, 55.62, 109.1, 111.0, 120.0, 125.2, 126.47,

126.53, 128.0, 130.3, 130.4, 131.0, 131.8, 139.1, 148.8, 148.9, 167.6; HRMS (DART-TOF)  $m/z$ :  $[M + H]^+$  Calcd for  $C_{18}H_{19}O_4$ , 299.1283; Found 299.1283.

*(E)*-2-(4-methoxystyryl)benzamide (**47**). White solid; (42.0 mg, 83%); mp 150–153 °C;  $^1H$  NMR ( $CDCl_3$ , 400 MHz)  $\delta$  3.83 (3H, s), 6.90 (2H, d,  $J = 8.8$  Hz), 7.02 (1H, d,  $J = 16.4$  Hz), 7.29 (1H, t,  $J = 7.6$  Hz), 7.41 (1H, d,  $J = 16.4$  Hz), 7.45 (1H, t,  $J = 7.6$  Hz), 7.46 (2H, d,  $J = 8.8$  Hz), 7.57 (1H, d,  $J = 7.6$  Hz), 7.68 (1H, d,  $J = 7.6$  Hz);  $^{13}C$  NMR ( $CDCl_3$ , 100MHz)  $\delta$  55.3, 114.1, 123.8, 126.2, 127.1, 127.3, 127.8, 128.1, 128.6, 128.8, 130.6, 131.1, 131.9, 134.1, 136.0, 159.6, 171.6; HRMS (DART-TOF)  $m/z$ :  $[M + H]^+$  Calcd for  $C_{16}H_{16}NO_2$ , 254.1181; Found 254.1184.

*(E)*-2-(3,4-dimethoxystyryl)benzamide (**48**). White solid; (48.7 mg, 86%); mp 180–182 °C;  $^1H$  NMR ( $CDCl_3$ , 400 MHz)  $\delta$  3.87 (3H, s), 3.90 (3H, s), 6.84 (1H, d,  $J = 8.8$  Hz), 6.99 (1H, d,  $J = 16.0$  Hz), 7.05 (2H, m), 7.26 (1H, t,  $J = 7.6$  Hz), 7.38 (1H, d,  $J = 16.0$  Hz), 7.42 (1H, t,  $J = 7.6$  Hz), 7.51 (1H, d,  $J = 7.6$  Hz), 7.67 (1H, d,  $J = 7.6$  Hz);  $^{13}C$  NMR ( $CDCl_3$ , 100 MHz)  $\delta$  55.7, 55.8, 109.1, 111.1, 120.1, 123.8, 126.0, 127.0, 127.6, 130.1, 130.5, 131.2, 133.9, 135.8, 148.9, 149.1, 172.1; HRMS (DART-TOF)  $m/z$ :  $[M + H]^+$  Calcd for  $C_{17}H_{18}NO_3$ , 284.1287; Found 284.1286.

*(E)*-(2-(4-methoxystyryl)phenyl)methanamine (**49**).<sup>128</sup> Yellowish solid; (53.4 mg, 82%); mp 90–92 °C (lit. 204–204 °C);  $^1H$  NMR ( $CDCl_3$ , 400 MHz)  $\delta$  3.82 (3H, s), 3.98 (2H, s), 6.90 (2H, d,  $J = 8.8$  Hz), 6.98 (1H, d,  $J = 16.1$  Hz), 7.27 (4H, m), 7.46 (2H, d,  $J = 8.8$  Hz), 7.60 (1H, d,  $J = 7.1$  Hz);  $^{13}C$  NMR ( $CDCl_3$ , 100 MHz)  $\delta$  44.3, 55.3, 114.1, 123.3,

125.8, 127.3, 127.5, 127.8, 128.1, 130.2, 130.5, 136.0, 140.2, 159.4; HRMS (DART-TOF)  $m/z$ :  $[M + H]^+$  Calcd for  $C_{16}H_{18}NO$ , 240.1388; Found 240.1392.

*(E)*-2-(3,4-dimethoxystyryl)phenylmethanamine (**50**). Yellowish solid; (32.3 mg, 60%); mp 108–110 °C;  $^1H$  NMR ( $CDCl_3$ , 400 MHz)  $\delta$  3.90 (3H, s), 3.94 (3H, s), 4.00 (2H, s), 6.87 (1H, d,  $J = 8.0$  Hz), 6.97 (1H, d,  $J = 16.0$  Hz), 7.07 (2H, m), 7.26 (1H, d,  $J = 16.0$  Hz), 7.28 (3H, m), 7.59 (1H, d,  $J = 6.8$  Hz);  $^{13}C$  NMR ( $CDCl_3$ , 100 MHz)  $\delta$  44.3, 55.87, 55.90, 109.1, 111.2, 119.8, 123.5, 125.9, 127.3, 127.5, 128.0, 130.5, 130.8, 135.9, 140.3, 149.0, 149.1; HRMS (DART-TOF)  $m/z$ :  $[M + H]^+$  Calcd for  $C_{17}H_{20}NO_2$ , 270.1494; Found 270.1491.

### 3.7 Cyclic Voltammetry

All cyclic voltammetry experiments were carried out in a divided cell fitted with a Teflon cell top and a nitrogen inlet. The electrodes used were a Pt electrode (1.6 mm diameter) as the working electrode, Pt as the counter electrode and Ag/AgNO<sub>3</sub> (0.01 M)/TEAP (0.1 M in MeCN) as the reference electrode.

### 3.8 General Procedure for Electrochemical Oxidation (Controlled Potential Electrolysis)

To the electrochemical cell containing 0.2 M LiClO<sub>4</sub> in 25 mL of MeCN was added the corresponding stilbene (ca. 0.2 mmol) under nitrogen or argon. Bulk electrolysis was carried out using a Pt gauze electrode (working electrode), Pt (counter electrode), and Ag/AgNO<sub>3</sub> (0.01 M)/TEAP (0.1 M in MeCN) (reference electrode), with stirring,

and the electrolysis was allowed to proceed until 0.9 – 1.0 F of charge had been transferred at the first anodic wave. The reaction mixture was then concentrated by evaporation under reduced pressure, and CH<sub>2</sub>Cl<sub>2</sub> (10 mL) was then added. The mixture was then poured into H<sub>2</sub>O and extracted with CH<sub>2</sub>Cl<sub>2</sub> (3 × 20 mL). The combined organic layer was then washed with H<sub>2</sub>O, dried (Na<sub>2</sub>SO<sub>4</sub>), and concentrated under reduced pressure, and the resulting residue was then fractionated by various chromatographic methods (preparative radial chromatography; HPLC; LH20) until pure compounds were obtained.

### 3.8.1 Anodic oxidation of **1** in MeCN/ 0.2 M LiClO<sub>4</sub>

Controlled potential electrolysis of **1** (+0.97 V, 1 F) yielded a mixture, which on preparative radial chromatography (SiO<sub>2</sub>, *n*-hexane:CH<sub>2</sub>Cl<sub>2</sub>, 1:1 to 100% CH<sub>2</sub>Cl<sub>2</sub>), followed by HPLC (X-Bridge Prep OBD<sup>TM</sup>, C<sub>18</sub> column, 20% H<sub>2</sub>O:MeCN to 100% MeCN in 7 min, 5 ml/min), and Sephadex LH20 (MeOH as mobile phase), gave **1aa** (12.4 mg, 25%), **1ab** (7.0 mg, 14%), **1ac** (9.5 mg, 19%), and **1ae** (11.0 mg, 22%).

*Bisbenzopyran (1aa)*. Light yellowish oil, and subsequently, colorless block crystals from *n*-hexane/CH<sub>2</sub>Cl<sub>2</sub>; mp 237–240 °C; UV (EtOH) λ<sub>max</sub> (log ε) 205 (4.75), 227 (4.40), and 281 (3.75) nm; IR (dry film) ν<sub>max</sub> 2054, 2020, 1943, 1889, 1786, 1611, 1514, 831, and 755 cm<sup>-1</sup>; <sup>1</sup>H NMR (CDCl<sub>3</sub>, 400 MHz) δ 3.33 (H-8a, H-8b, 2H, d, *J* = 9.8 Hz), 3.85 (OMe, 4a, 4b, 6H, s), 5.28 (H-7a, H-7b, 2H, d, *J* = 9.8 Hz), 5.99 (H-14a, H-14b, 2H, dd, *J* = 7.6, 1.2 Hz), 6.52 (H-13a, H-13b, 2H, td, *J* = 7.6, 1.2 Hz), 6.90 (H-3a, H-3b, H-5a, H-5b, H-11a, H-11b, 6H, m), 7.09 (H-12a, H-12b, 2H, td, *J* = 7.6, 1.2 Hz), and 7.19 (H-2a, H-2b, H-6a, H-6b, 4H, d, *J* = 8.6 Hz); <sup>13</sup>C NMR (CDCl<sub>3</sub>, 100 MHz) δ 40.6 (C-8a,

C-8b), 55.4 (OMe, 4a, 4b), 80.0 (C-7a, C-7b), 113.7 (C-3a, C-3b, C-5a, C-5b), 116.6 (C-11a, C-11b), 119.0 (C-9a, C-9b), 119.6 (C-13a, C-13b), 128.5 (C-12a, C-12b), 129.3 (C-2a, C-2b, C-6a, C-6b), 131.5 (C-1a, C-1b), 131.8 (C-14a, C-14b), 155.0 (C-10a, C-10b), and 159.8 (C-4a, C-4b); HRMS (ESI-TOF)  $m/z$ :  $[M + K]^+$  Calcd for  $C_{30}H_{26}O_4K$ , 489.1463; Found 489.1443.

*Bisbenzopyran (1ab)*. Light yellowish oil, and subsequently, colorless block crystals from MeOH/ $CH_2Cl_2$ ; mp 189–190 °C; UV (EtOH)  $\lambda_{max}$  (log  $\epsilon$ ) 232 (3.54), 256 (3.11), and 280 (2.84) nm; IR (dry film)  $\nu_{max}$  2055, 2020, 1943, 1891, 1791, 1611, 1514, 834, and 755  $cm^{-1}$ ;  $^1H$  NMR ( $CDCl_3$ , 400 MHz)  $\delta$  3.49 (H-8a, 1H, t,  $J = 10.8$  Hz), 3.71 (OMe, 4b, 3H, s), 3.86 (OMe, 4a, 3H, s), 3.90 (H-8b, 1H, dd,  $J = 10.8, 3.6$  Hz), 4.99 (H-7a, 1H, d,  $J = 10.8$  Hz), 6.19 (H-7b, 1H, d,  $J = 3.6$  Hz), 6.26 (H-14a, 1H, dd,  $J = 7.2, 1.1$  Hz), 6.51 (H-13a, 1H, td,  $J = 7.2, 1.1$  Hz), 6.68 (H-3b, H-5b, 2H, d,  $J = 8.9$  Hz), 6.83 (H-11b, 1H, d,  $J = 8.2$  Hz), 6.97 (H-3a, H-5a, 2H, d,  $J = 8.6$  Hz), 7.02 (H-2b, H-6b, 2H, d,  $J = 8.9$  Hz), 7.00 (H-11a, H-13b, 2H, m), 7.11 (H-12a, 1H, td,  $J = 7.2, 1.1$  Hz), 7.14 (H-12b, 1H, t,  $J = 8.2$  Hz), 7.35 (H-2a, H-6a, 2H, d,  $J = 8.6$  Hz), and 7.52 (H-14b, 1H, d,  $J = 8.2$  Hz);  $^{13}C$  NMR ( $CDCl_3$ , 100 MHz)  $\delta$  34.1 (C-8a), 41.7 (C-8b), 55.2 (OMe, 4b), 55.5 (OMe, 4a), 77.2 (C-7b), 80.9 (C-7a), 113.6 (C-3b, C-5b), 114.6 (C-3a, C-5a), 117.2 (C-11a), 117.6 (C-11b), 119.7 (C-13a), 120.5 (C-9b), 120.8 (C-13b), 122.4 (C-9a), 127.3 (C-14b), 127.7 (C-14a), 128.1 (C-2b, C-6b), 128.2 (C-12b), 128.5 (C-12a), 129.7 (C-2a, C-6a), 131.0 (C-1b), 132.8 (C-1a), 154.7 (C-10a), 155.5 (C-10b), 159.0 (C-4b), and 160.2 (C-4a); HRMS (ESI-TOF)  $m/z$ :  $[M + H]^+$  Calcd for  $C_{30}H_{27}O_4$ , 451.1904; Found 451.1894.

*Bisbenzofuran (Iac)*. Light yellowish oil, and subsequently, colorless block crystals from *n*-hexane/CH<sub>2</sub>Cl<sub>2</sub>; mp 132–134 °C; UV (EtOH)  $\lambda_{\max}$  (log  $\epsilon$ ) 208 (4.65), 227 (4.54), and 283 (3.98) nm; IR (dry film)  $\nu_{\max}$  2059, 2020, 1942, 1892, 1782, 1612, 1513, 828, and 753 cm<sup>-1</sup>; <sup>1</sup>H NMR (CDCl<sub>3</sub>, 400 MHz)  $\delta$  3.85 (OMe, 4a, 4b, 6H, s), 3.90 (H-8a, H-8b, 2H, d,  $J$  = 3.6 Hz), 5.44 (H-7a, H-7b, 2H, d,  $J$  = 3.6 Hz), 6.70 (H-3a, H-3b, H-5a, H-5b, 4H, d,  $J$  = 8.8 Hz), 6.75 (H-2a, H-2b, H-6a, H-6b, 4H, d,  $J$  = 8.8 Hz), 6.88 (H-13a, H-13b, 2H, m), 7.00 (H-11a, H-11b, 2H, d,  $J$  = 8.2 Hz), 7.06 (H-14a, H-14b, 2H, d,  $J$  = 8.2 Hz), and 7.26 (H-12a, H-12b, 2H, m); <sup>13</sup>C NMR (CDCl<sub>3</sub>, 100 MHz)  $\delta$  55.2 (C-8a, C-8b), 55.4 (OMe, 4a, 4b), 85.4 (C-7a, C-7b), 109.9 (C-11a, C-11b), 113.9 (C-3a, C-3b, C-5a, C-5b), 121.0 (C-13a, C-13b), 125.3 (C-14a, C-14b), 126.5 (C-2a, C-2b, C-6a, C-6b), 126.7 (C-9a, C-9b), 129.4 (C-12a, C-12b), 134.6 (C-1a, C-1b), 159.2 (C-4a, C-4b), and 160.5 (C-10a, C-10b); HRMS (ESI-TOF)  $m/z$ : [M + K]<sup>+</sup> Calcd for C<sub>30</sub>H<sub>26</sub>O<sub>4</sub>K, 489.1463; Found 489.1477.

*Benzofurano-benzopyran (Iae)*. Light yellowish oil, and subsequently, colorless needle crystals from MeOH/CH<sub>2</sub>Cl<sub>2</sub>; mp 154–156 °C; UV (EtOH)  $\lambda_{\max}$  (log  $\epsilon$ ) 202 (4.01), 225 (3.21), 240 (3.04), 255 (2.83), and 280 (2.52) nm; IR (dry film)  $\nu_{\max}$  2058, 2021, 1941, 1890, 1779, 1610, 1511, 827, and 751 cm<sup>-1</sup>; <sup>1</sup>H NMR (CDCl<sub>3</sub>, 400 MHz)  $\delta$  3.69 (OMe, 4a, 3H, s), 3.74 (H-8b, 1H, dd,  $J$  = 11.8, 0.9 Hz), 3.79 (OMe, 4b, 3H, s), 4.04 (H-8a, 1H, dd,  $J$  = 7.8, 0.9 Hz), 4.23 (H-7b, 1H, d,  $J$  = 11.8 Hz), 6.29 (H-14b, 1H, dd,  $J$  = 7.2, 1.3 Hz), 6.36 (H-7a, 1H, d,  $J$  = 7.8 Hz), 6.52 (H-12b, 1H, dd,  $J$  = 7.2, 1.3 Hz), 6.63 (H-3a, H-5a, H-11a, 3H, m), 6.78 (H-13a, 1H, t,  $J$  = 7.5 Hz), 6.93 (H-2a, H-6a, H-12a, H-3b, H-5b, H-11b, H-13b, 7H, m), 7.12 (H-14a, 1H, d,  $J$  = 7.5 Hz), and 7.45 (H-2b, H-6b, 2H, d,  $J$  = 8.6 Hz); <sup>13</sup>C NMR (CDCl<sub>3</sub>, 100 MHz)  $\delta$  44.8 (C-8a), 45.7 (C-8b), 53.6 (C-7b), 55.2 (OMe, 4a), 55.4 (OMe, 4b), 104.2 (C-7a), 109.2 (C-11a), 113.6 (C-3a, C-5a),

114.7 (C-3b, C-5b), 118.1 (C-11b), 121.2 (C-13a), 122.5 (C-13b), 123.3 (C-14a), 127.1 (C-9a), 127.6 (C-9b), 127.8 (C-12b), 128.3 (C-12a), 128.9 (C-2a, C-6a), 128.9 (C-2b, C-6b), 130.6 (C-14b), 134.9 (C-1b), 135.5 (C-1a), 152.0 (C-10b), 158.0 (C-4a), 158.6 (C-4b), and 158.8 (C-10a); HRMS (ESI-TOF)  $m/z$ :  $[M + K]^+$  Calcd for  $C_{30}H_{26}O_4K$ , 489.1463; Found 489.1452.

### 3.8.2 Anodic oxidation of **2** in MeCN/ 0.2 M LiClO<sub>4</sub>

Controlled potential electrolysis of **2** (+0.97 V, 1 F) yielded essentially the same compounds from the anodic oxidation of **1**, namely, **1aa** (12.2 mg, 27%), **1ab** (6.8 mg, 15%), **1ac** (9.0 mg, 20%), and **1ae** (9.0 mg, 20%).

### 3.8.3 Anodic oxidation of **3** in MeCN/ 0.2 M LiClO<sub>4</sub>

Controlled potential electrolysis of **3** (+0.95 V, 1 F) yielded a mixture, which on preparative radial chromatography (SiO<sub>2</sub>, hexanes:CH<sub>2</sub>Cl<sub>2</sub>, 2:1 to 3% MeOH:CH<sub>2</sub>Cl<sub>2</sub>), followed by Sephadex LH20 (20% MeCN:MeOH as mobile phase), gave **3aa** (10.7 mg, 21%), **3ac** (9.2 mg, 18%), **3ad** (8.7 mg, 17%), and **3af** (16.3 mg, 32%).

*Bisbenzopyran (3aa)*. Colorless oil, and subsequently, colorless block crystals from *n*-hexane/CH<sub>2</sub>Cl<sub>2</sub>; mp 250–252 °C; UV (EtOH)  $\lambda_{\max}$  (log  $\epsilon$ ) 212 (4.49), 229 (4.18), 279 (3.80), and 284 (3.81) nm; IR (dry film)  $\nu_{\max}$  1608, 1516, 1237, 1026, and 755 cm<sup>-1</sup>; <sup>1</sup>H NMR (CDCl<sub>3</sub>, 400 MHz)  $\delta$  3.35 (H-8a, H-8b, 2H, d,  $J$  = 9.2 Hz), 3.81 (OMe, 3a, 3b, 6H, s), 3.92 (OMe, 4a, 4b, 6H, s), 5.27 (H-7a, H-7b, 2H, d,  $J$  = 9.2 Hz), 6.02 (H-14a, H-14b, 2H, d,  $J$  = 7.6 Hz), 6.54 (H-13a, H-13b, 2H, t,  $J$  = 7.6 Hz), 6.82 (H-2a, H-2b, H-5a, H-5b, H-6a, H-6b, 6H, m), 6.93 (H-11a, H-11b, 2H, d,  $J$  = 7.6 Hz), and 7.11 (H-12a, H-12b, 2H, t,  $J$  = 7.6 Hz); <sup>13</sup>C NMR (CDCl<sub>3</sub>, 100 MHz)  $\delta$  40.5 (C-8a, C-8b), 55.9 (OMe,

3a, 3b), 56.0 (OMe, 4a, 4b), 80.1 (C-7a, C-7b), 110.7 (C-2a, C-2b), 110.8 (C-5a, C-5b), 116.5 (C-11a, C-11b), 118.9 (C-9a, C-9b), 119.6 (C-13a, C-13b), 120.6 (C-6a, C-6b), 128.5 (C-12a, C-12b), 131.6 (C-1a, C-1b), 131.7 (C-14a, C-14b), 148.8 (C-3a, C-3b), 149.1 (C-4a, C-4b), and 154.7 (C-10a, C-10b);

*Bisbenzofuran (3ac)*. Colorless oil; UV (EtOH)  $\lambda_{\max}$  (log  $\epsilon$ ) 212 (4.68), 232 (4.33), 283 (4.09), and 292 (3.91) nm; IR (dry film)  $\nu_{\max}$  1608, 1517, 1235, 1027, and 752  $\text{cm}^{-1}$ ;  $^1\text{H}$  NMR ( $\text{CDCl}_3$ , 400 MHz)  $\delta$  3.68 (OMe, 3a, 3b, 6H, s), 3.81 (OMe, 4a, 4b, 6H, s), 3.91 (H-8a, H-8b, 2H, d,  $J = 3.4$  Hz), 5.44 (H-7a, H-7b, 2H, d,  $J = 3.4$  Hz), 6.20 (H-2a, H-2b, 2H, d,  $J = 1.7$  Hz), 6.48 (H-6a, H-6b, 2H, dd,  $J = 8.3, 1.7$  Hz), 6.68 (H-5a, H-5b, 2H, d,  $J = 8.3$  Hz), 6.90 (H-13a, H-13b, 2H, t,  $J = 7.8$  Hz), 7.02 (H-11a, H-11b, 2H, d,  $J = 7.8$  Hz), 7.12 (H-14a, H-14b, 2H, d,  $J = 7.8$  Hz), and 7.27 (H-12a, H-12b, 2H, t,  $J = 7.8$  Hz);  $^{13}\text{C}$  NMR ( $\text{CDCl}_3$ , 100 MHz)  $\delta$  55.5 (C-8a, C-8b), 55.7 (OMe, 3a, 3b), 55.9 (OMe, 4a, 4b), 85.2 (C-7a, C-7b), 108.1 (C-2a, C-2b), 109.8 (C-11a, C-11b), 111.1 (C-5a, C-5b), 116.9 (C-6a, C-6b), 121.0 (C-13a, C-13b), 125.3 (C-14a, C-14b), 126.7 (C-9a, C-9b), 129.3 (C-12a, C-12b), 134.9 (C-1a, C-1b), 148.4 (C-4a, C-4b), 148.8 (C-3a, C-3b), and 160.5 (C-10a, C-10b); HRMS (DART-TOF)  $m/z$ :  $[\text{M} + \text{H}]^+$  Calcd for  $\text{C}_{32}\text{H}_{31}\text{O}_6$ , 511.2121; Found 511.2115.

*Bisbenzofuran (3ad)*. Colorless oil; UV (EtOH)  $\lambda_{\max}$  (log  $\epsilon$ ) 212 (4.74), 230 (4.45), 282 (4.18), and 289 (4.11) nm; IR (dry film)  $\nu_{\max}$  1594, 1517, 1233, 1026, and 752  $\text{cm}^{-1}$ ;  $^1\text{H}$  NMR ( $\text{CDCl}_3$ , 400 MHz)  $\delta$  3.68 (OMe, 3a, 3b, 6H, s), 3.81 (OMe, 4a, 4b, 6H, s), 3.99 (H-8a, H-8b, 2H, d,  $J = 6.9$  Hz), 5.36 (H-7a, H-7b, 2H, d,  $J = 3.4$  Hz), 6.76 (H-14a, H-14b, 2H, d,  $J = 7.8$  Hz), 6.78 (H-2a, H-2b, 2H, s), 6.82 (H-5a, H-5b, H-6a, H-6b, 4H, m), 6.84 (H-13a, H-13b, 2H, t,  $J = 7.8$  Hz), 6.88 (H-11a, H-11b, 2H, d,  $J = 7.8$  Hz), and

7.22 (H-12a, H-12b, 2H, t,  $J = 7.8$  Hz);  $^{13}\text{C}$  NMR ( $\text{CDCl}_3$ , 100 MHz)  $\delta$  53.1 (C-8a, C-8b), 56.0 (OMe, 3a, 3b), 56.0 (OMe, 4a, 4b), 86.6 (C-7a, C-7b), 109.2 (C-2a, C-2b), 109.8 (C-11a, C-11b), 111.2 (C-5a, C-5b), 119.0 (C-6a, C-6b), 121.1 (C-13a, C-13b), 124.9 (C-14a, C-14b), 127.1 (C-9a, C-9b), 129.3 (C-12a, C-12b), 133.8 (C-1a, C-1b), 149.3 (C-4a, C-4b), 149.4 (C-3a, C-3b), and 160.2 (C-10a, C-10b); HRMS (DART-TOF)  $m/z$ :  $[\text{M} + \text{H}]^+$  Calcd for  $\text{C}_{32}\text{H}_{31}\text{O}_6$ , 511.2121; Found 511.2115.

*Bridged oxocine (3af)*. Colourless oil; UV (EtOH)  $\lambda_{\text{max}}$  (log  $\epsilon$ ) 215 (4.88), 237 (4.50), 281 (4.31), and 288 (4.23) nm; IR (dry film)  $\nu_{\text{max}}$  3441, 1608, 1513, 1354, 1238, 1217, 1026, and 753  $\text{cm}^{-1}$ ;  $^1\text{H}$  NMR ( $\text{CDCl}_3$ , 400 MHz)  $\delta$  3.35 (H-8b, 1H, br s), 3.68 (OMe, 4a, 3H, s), 3.81 (H-8a, OMe, 3b, 4H, s), 3.82 (OMe, 4b, 3H, s), 3.89 (OMe, 3a, 3H, s), 4.48 (H-7b, 1H, d,  $J = 1.4$  Hz), 5.40 (OH, 1H, br s), 5.60 (H-7a, 1H, br t,  $J = 1.4$  Hz), 6.43 (H-5a, 1H, s), 6.60 (H-11a, 1H, dd,  $J = 7.8, 1.0$  Hz), 6.63 (H-6b, 1H, dd,  $J = 8.3, 1.8$  Hz), 6.64 (H-13a, 1H, td,  $J = 7.8, 1.0$  Hz), 6.68 (H-11b, 1H, dd,  $J = 7.8, 1.1$  Hz), 6.74 (H-2b, 1H, d,  $J = 1.8$  Hz), 6.79 (H-5b, 1H, d,  $J = 8.3$  Hz), 6.92 (H-14a, 1H, dd,  $J = 7.8, 1.0$  Hz), 6.95 (H-13b, 1H, td,  $J = 7.8, 1.1$  Hz), 6.96 (H-12a, 1H, td,  $J = 7.8, 1.0$  Hz), 6.99 (H-2a, 1H, s), 7.08 (H-12b, 1H, td,  $J = 7.8, 1.1$  Hz), and 7.43 (H-14b, 1H, dd,  $J = 7.8, 1.1$  Hz);  $^{13}\text{C}$  NMR ( $\text{CDCl}_3$ , 100 MHz)  $\delta$  30.1 (C-8a), 42.4 (C-8b), 55.8 (OMe, 4a), 55.9 (OMe, 3b), 55.9 (OMe, 4b), 56.0 (OMe, 3a), 56.1 (C-7b), 73.5 (C-7a), 111.1 (C-5b), 112.3 (C-2a), 112.5 (C-5a), 112.7 (C-2b), 115.0 (C-11a), 117.0 (C-11b), 120.6 (C-13a), 120.9 (C-12a), 121.5 (C-6b), 125.8 (C-9b), 127.4 (C-9a), 127.6 (C-13b), 127.9 (C-14a), 128.2 (C-12b), 128.8 (C-6a), 129.3 (C-1a), 129.3 (C-14b), 136.8 (C-1b), 147.7 (C-4b), 148.1 (C-3a), 148.9 (C-3b), 149.5 (C-4a), 152.2 (C-10b), and 153.8 (C-10a); HRMS (DART-TOF)  $m/z$ :  $[\text{M} + \text{H}]^+$  Calcd for  $\text{C}_{32}\text{H}_{31}\text{O}_6$ , 511.2121; Found 511.2119.

### 3.8.4 Anodic oxidation of **4** in MeCN/ 0.2 M LiClO<sub>4</sub>

Controlled potential electrolysis of **4** (+0.95 V, 1 F) yielded essentially the same compounds from the anodic oxidation of **3**, namely, **3aa** (9.7 mg, 19%), **3ac** (9.2 mg, 18%), **3ad** (9.2 mg, 18%), and **3af** (15.3 mg, 30%).

### 3.8.5 Anodic oxidation of **7** in MeCN/ 0.2 M LiClO<sub>4</sub>

Controlled potential electrolysis of **7** (+1.05 V, 1 F) yielded a mixture, which on preparative radial chromatography (SiO<sub>2</sub>, 100% CH<sub>2</sub>Cl<sub>2</sub> to 8% MeOH:CH<sub>2</sub>Cl<sub>2</sub>), gave **7ac** (18.6 mg, 35%) and **7ad** (3.2 mg, 6%).

*Bisindole (7ac)*.<sup>122</sup> Light yellowish oil; UV (EtOH)  $\lambda_{\max}$  (log  $\epsilon$ ) 212 (5.00), 228 (4.89), 251 (4.69), 279 (4.29), and 292 (4.13) nm; IR (dry film)  $\nu_{\max}$  1666, 1611, 1512, 1394, 1282, 1250, 1032, and 755 cm<sup>-1</sup>; <sup>1</sup>H NMR (CDCl<sub>3</sub>, 400 MHz)  $\delta$  1.86 (NCOMe, 6H, s), 3.48 (H-8a, H-8b, 2H, s), 3.69 (OMe, C-4a, C-4b, 6H, s), 4.66 (H-7a, H-7b, 2H, s), 6.44 (H-2a, H-2b, H-6a, H-6b, 4H, d,  $J$  = 8.7 Hz), 6.66 (H-3a, H-3b, H-5a, H-5b, 4H, d,  $J$  = 8.4 Hz), 7.24 (H-13a, H-13b, 2H, m), 7.25 (H-14a, H-14b, 2H, m), 7.47 (H-12a, H-12b, 2H, t,  $J$  = 8.0 Hz), and 8.45 (H-11a, H-11b, 2H, d,  $J$  = 8.2 Hz); <sup>13</sup>C NMR (CDCl<sub>3</sub>, 100 MHz)  $\delta$  23.7 (NCOMe), 55.3 (OMe, C-4a, C-4b), 56.7 (C-8a, C-8b), 64.1 (C-7a, C-7b), 114.5 (C-3a, C-3b, C-5a, C-5b), 117.7 (C-11a, C-11b), 124.9 (C-13a, C-13b), 125.3 (C-14a, C-14b), 125.7 (C-2a, C-2b, C-6a, C-6b), 129.4 (C-12a, C-12b), 130.1 (C-9a, C-9b), 133.9 (C-1a, C-1b), 143.9 (C-10a, C-10b), 159.1 (C-4a, C-4b) and 169.8 (NCOMe); HRMS (DART-TOF)  $m/z$ : [M + H]<sup>+</sup> Calcd for C<sub>34</sub>H<sub>33</sub>N<sub>2</sub>O<sub>4</sub>, 533.2440; Found 533.2450.

*Bisindole (7ad)*. Light yellowish oil, and subsequently, colorless block crystals from MeOH/CH<sub>2</sub>Cl<sub>2</sub>; mp 259–261 °C; UV (EtOH)  $\lambda_{\max}$  (log  $\epsilon$ ) 211 (4.25), 227 (4.13), 256 (3.95), 285 (3.54), and 293 (3.39) nm; IR (dry film)  $\nu_{\max}$  1665, 1611, 1512, 1392, 1281, 1250, 1031, and 754 cm<sup>-1</sup>; <sup>1</sup>H NMR (CDCl<sub>3</sub>, 400 MHz)  $\delta$  1.85 (NCOMe, 6H, s), 3.47 (H-8a, H-8b, 2H, s), 3.76 (OMe, C-4a, C-4b, 6H, s), 4.94 (H-7a, H-7b, 2H, s), 6.63 (H-14a, H-14b, 2H, br s), 6.82 (H-3a, H-3b, H-5a, H-5b, 4H, d,  $J$  = 8.4 Hz), 6.98 (H-13a, H-13b, 2H, m), 6.99 (H-2a, H-2b, H-6a, H-6b, 4H, d,  $J$  = 8.4 Hz), 7.31 (H-12a, H-12b, 2H, t,  $J$  = 8.0 Hz), and 8.26 (H-11a, H-11b, 2H, br d,  $J$  = 6.4 Hz); <sup>13</sup>C NMR (CDCl<sub>3</sub>, 100 MHz)  $\delta$  23.9 (NCOMe), 55.4 (OMe, C-4a, C-4b), 56.8 (C-8a, C-8b), 67.0 (C-7a, C-7b), 114.8 (C-3a, C-3b, C-5a, C-5b), 117.2 (C-11a, C-11b), 124.4 (C-13a, C-13b), 125.0 (C-14a, C-14b), 126.2 (C-2a, C-2b, C-6a, C-6b), 129.2 (C-12a, C-12b), 129.5 (C-9a, C-9b), 134.2 (C-1a, C-1b), 143.9 (C-10a, C-10b), 159.5 (C-4a, C-4b) and 169.0 (NCOMe); HRMS (DART-TOF) m/z: [M + H]<sup>+</sup> Calcd for C<sub>34</sub>H<sub>33</sub>N<sub>2</sub>O<sub>4</sub>, 533.2440; Found 533.2430.

### 3.8.6 Anodic oxidation of **8** in MeCN/ 0.2 M LiClO<sub>4</sub>

Controlled potential electrolysis of **8** (+1.04 V, 1 F) yielded a mixture, which on preparative radial chromatography (SiO<sub>2</sub>, *n*-hexane:CH<sub>2</sub>Cl<sub>2</sub>, 4:1 to 100% CH<sub>2</sub>Cl<sub>2</sub>), followed by HPLC (Luna Phenyl-Hexyl column, 15% H<sub>2</sub>O:MeCN, 10 ml/min), gave **8ac** (10.3 mg, 23%) and **8ag** (5.4 mg, 12%).

*Bisindole (8ac)*. Light yellowish solid; UV (EtOH)  $\lambda_{\max}$  (log  $\epsilon$ ) 212 (4.46), 227 (4.18), 253 (3.96), and 307 (3.58) nm; IR (dry film)  $\nu_{\max}$  3382, 1603, 1510, 1243, 1030, and 741 cm<sup>-1</sup>; <sup>1</sup>H NMR (CDCl<sub>3</sub>, 400 MHz)  $\delta$  3.69 (H-8a, H-8b, 2H, d,  $J$  = 2.3 Hz), 3.73 (OMe, C-4a, C-4b, 6H, s), 4.64 (H-7a, H-7b, 2H, d,  $J$  = 2.3 Hz), 6.66 (H-3a, H-3b, H-

5a, H-5b, 4H, d,  $J = 8.2$  Hz), 6.67 (H-13a, H-13b, 2H, t,  $J = 7.8$  Hz), 6.72 (H-11a, H-11b, 2H, d,  $J = 7.8$  Hz), 6.76 (H-2a, H-2b, H-6a, H-6b, 4H, d,  $J = 8.2$  Hz), 6.91 (H-14a, H-14b, 2H, d,  $J = 7.8$  Hz) and 7.12 (H-12a, H-12b, 2H, t,  $J = 7.8$  Hz);  $^{13}\text{C}$  NMR ( $\text{CDCl}_3$ , 100 MHz)  $\delta$  56.7 (C-8a, C-8b), 55.3 (OMe, C-4a, C-4b), 63.3 (C-7a, C-7b), 108.6 (C-11a, C-11b), 113.9 (C-3a, C-3b, C-5a, C-5b), 118.6 (C-13a, C-13b), 125.5 (C-14a, C-14b), 126.8 (C-2a, C-2b, C-6a, C-6b), 128.3 (C-9a, C-9b, C-12a, C-12b), 138.4 (C-1a, C-1b), 151.6 (C-10a, C-10b), and 158.6 (C-4a, C-4b); HRMS (DART-TOF)  $m/z$ :  $[\text{M} + \text{H}]^+$  Calcd for  $\text{C}_{30}\text{H}_{29}\text{N}_2\text{O}_2$ , 449.2229; Found 449.2236.

*Bisquinoline (8ag)*. Light yellowish solid; UV (EtOH)  $\lambda_{\text{max}}$  ( $\log \epsilon$ ) 211 (4.22), 227 (3.97), 249 (3.87), and 307 (3.50) nm; IR (dry film)  $\nu_{\text{max}}$  3378, 1606, 1511, 1244, 1034, and  $750\text{ cm}^{-1}$ ;  $^1\text{H}$  NMR ( $\text{CDCl}_3$ , 400 MHz)  $\delta$  3.39 (H-8a, H-8b, 2H, dd,  $J = 6.9, 2.8$  Hz), 3.82 (OMe, C-4a, C-4b, 6H, s), 4.60 (H-7a, H-7b, 2H, dd,  $J = 6.9, 2.8$  Hz), 6.46 (H-13a, H-13b, 2H, t,  $J = 7.8$  Hz), 6.49 (H-11a, H-11b, 2H, d,  $J = 7.8$  Hz), 6.63 (H-14a, H-14b, 2H, d,  $J = 7.8$  Hz), 6.92 (H-3a, H-3b, H-5a, H-5b, 4H, d,  $J = 8.7$  Hz), 6.95 (H-12a, H-12b, 2H, t,  $J = 7.8$  Hz), and 7.33 (H-2a, H-2b, H-6a, H-6b, 4H, d,  $J = 8.7$  Hz);  $^{13}\text{C}$  NMR ( $\text{CDCl}_3$ , 100 MHz)  $\delta$  43.0 (C-8a, C-8b), 55.4 (OMe, C-4a, C-4b), 61.1 (C-7a, C-7b), 144.3 (C-11a, C-11b), 114.6 (C-3a, C-3b, C-5a, C-5b), 117.8 (C-13a, C-13b), 125.0 (C-9a, C-9b), 126.7 (C-14a, C-14b), 127.1 (C-12a, C-12b), 129.0 (C-2a, C-2b, C-6a, C-6b), 136.4 (C-1a, C-1b), 144.3 (C-10a, C-10b), and 159.4 (C-4a, C-4b); HRMS (DART-TOF)  $m/z$ :  $[\text{M} + \text{H}]^+$  Calcd for  $\text{C}_{30}\text{H}_{29}\text{N}_2\text{O}_2$ , 449.2229; Found 449.2234.

### 3.8.7 Anodic oxidation of **9** in MeCN/ 0.2 M LiClO<sub>4</sub>

Controlled potential electrolysis of **9** (+0.96 V, 1 F) yielded a mixture, which on preparative radial chromatography (SiO<sub>2</sub>, *n*-hexane:CH<sub>2</sub>Cl<sub>2</sub>, 4:1 to 100% CH<sub>2</sub>Cl<sub>2</sub>), gave **9ac** (32.2 mg, 57%) bisquinoline **9ag** (12.4 mg, 22%).

*Bisindole (9ac)*. Light yellowish solid; UV (EtOH)  $\lambda_{\max}$  (log  $\epsilon$ ) 228 (4.47), 249 (4.24), and 285 (3.79) nm; IR (dry film)  $\nu_{\max}$  2955, 1707, 1511, 1440, 1384, 1247, 1033, and 752 cm<sup>-1</sup>; <sup>1</sup>H NMR (CDCl<sub>3</sub>, 400 MHz)  $\delta$  3.46 (H-8a, H-8b, 2H, s), 3.62 (CO<sub>2</sub>Me, 16a, 16b, 6H, br s), 3.70 (OMe, 4a, 4b, 6H, s), 4.90 (H-7a, H-7b, 2H, br s), 6.52 (H-2a, H-2b, H-6a, H-6b, 4H, br s), 6.65 (H-3a, H-3b, H-5a, H-5b, 4H, d,  $J = 8.5$  Hz), 7.12 (H-13a, H-13b, H-14a, H-14b, 4H, m), 7.41 (H-12a, H-12b, 2H, br t,  $J = 7.5$  Hz), and 8.10 (H-11a, H-11b, 2H, br s); <sup>13</sup>C NMR (CDCl<sub>3</sub>, 100 MHz)  $\delta$  52.8 (CO<sub>2</sub>Me, C-16a, C-16b), 52.7 (OMe, 4a, 4b), 55.8 (C-8a, C-8b), 63.3 (C-7a, C-7b), 113.9 (C-3a, C-3b, C-5a, C-5b), 115.4 (C-11a, C-11b), 123.5 (C-13a, C-13b), 125.3 (C-14a, C-14b), 125.8 (C-2a, C-2b, C-6a, C-6b), 129.1 (C-12a, C-12b), 130.0 (C-9a, C-9b), 135.1 (C-1a, C-1b), 143.5 (C-10a, C-10b), 153.5 (C-15a, C-15b), and 158.7 (C-4a, C-4b); HRMS (DART-TOF)  $m/z$ : [M + H]<sup>+</sup> Calcd for C<sub>34</sub>H<sub>33</sub>N<sub>2</sub>O<sub>6</sub>, 565.2339; Found 565.2348.

*Bisquinoline (9ag)*. Light yellowish solid, and subsequently, colorless block crystals from MeOH/CH<sub>2</sub>Cl<sub>2</sub>; mp 264–266 °C; UV (EtOH)  $\lambda_{\max}$  (log  $\epsilon$ ) 230 (4.30) and 274 (3.46) nm; IR (dry film)  $\nu_{\max}$  2949, 1693, 1439, 1328, 1249, 1022, and 751 cm<sup>-1</sup>; <sup>1</sup>H NMR (CDCl<sub>3</sub>, 400 MHz)  $\delta$  3.13 (H-8a, H-8b, 2H, dd,  $J = 4.5, 2.4$  Hz), 3.82 (CO<sub>2</sub>Me, 16a, 16b, 6H, s), 3.74 (OMe, 4a, 4b, 6H, s), 6.26 (H-7a, H-7b, 2H, dd,  $J = 4.5, 2.4$  Hz), 6.78 (H-3a, H-3b, H-5a, H-5b, 4H, d,  $J = 8.7$  Hz), 7.19 (H-2a, H-2b, H-6a, H-6b, 4H, d,  $J = 8.7$  Hz), 7.29 (H-11a, H-11b, H-12a, H-12b, H-13a, H-13b, 6H, m), and 7.71 (H-

14a, H-14b, 2H, m);  $^{13}\text{C}$  NMR ( $\text{CDCl}_3$ , 100 MHz)  $\delta$  48.5 (C-8a, C-8b), 55.4 ( $\text{CO}_2\text{Me}$ , 16a, 16b), 55.2 (OMe, 4a, 4b), 57.1 (C-7a, C-7b), 113.9 (C-3a, C-3b, C-5a, C-5b), 124.2 (C-14a, C-14b), 125.7 (C-13a, C-13b), 126.6 (C-11a, C-11b), 127.1 (C-12a, C-12b), 128.6 (C-2a, C-2b, C-6a, C-6b), 134.4 (C-1a, C-1b), 134.6 (C-9a, C-9b), 137.3 (C-10a, C-10b), 155.3 (C-15a, C-15b), and 158.9 (C-4a, C-4b); HRMS (DART-TOF)  $m/z$ :  $[\text{M} + \text{H}]^+$  Calcd for  $\text{C}_{34}\text{H}_{33}\text{N}_2\text{O}_6$ , 565.2339; Found 565.2349.

### 3.8.8 Anodic oxidation of **10** in MeCN/ 0.2 M $\text{LiClO}_4$

Controlled potential electrolysis of **10** (+1.04 V, 1 F) yielded a mixture, which on preparative radial chromatography ( $\text{SiO}_2$ , *n*-hexane: $\text{CH}_2\text{Cl}_2$ , 2:1 to 2% MeOH: $\text{CH}_2\text{Cl}_2$ ), gave **10ac** (39.4 mg, 52%), **10ag** (18.9 mg, 25%), and **10ah** (4.5 mg, 6%).

*Bisindole (10ac)*. Light yellowish oil and subsequent as colorless needle crystals from MeOH/ $\text{CH}_2\text{Cl}_2$ ; ; mp 182–184 °C; UV (EtOH)  $\lambda_{\text{max}}$  ( $\log \epsilon$ ) 212 (4.58), 226 (4.52), and 275 (3.99) nm; IR (dry film)  $\nu_{\text{max}}$  1611, 1513, 1357, 1248, 1168, 1032, and 753  $\text{cm}^{-1}$ ;  $^1\text{H}$  NMR ( $\text{CDCl}_3$ , 400 MHz)  $\delta$  1.86 (H-8a, H-8b, 2H, s), 2.11 (Me, 6H, s), 3.85 (OMe, C-4a, C-4b, 6H, s), 4.95 (H-7a, H-7b, 2H, s), 5.96 (H-14a, H-14b, 2H, dd,  $J = 7.4, 0.8$  Hz), 6.71 (H-3a', H-3b', H-5a', H-5b', 4H, d,  $J = 8.3$  Hz), 6.84 (H-13a, H-13b, 2H, td,  $J = 7.4, 0.8$  Hz), 6.84 (H-3a, H-3b, H-5a, H-5b, 4H, d,  $J = 8.7$  Hz), 6.99 (H-2a, H-2b, H-6a, H-6b, 4H, d,  $J = 8.7$  Hz), 7.27 (H-12a, H-12b, 2H, td,  $J = 7.4, 0.8$  Hz), 7.33 (H-2a', H-2b', H-6a', H-6b', 4H, d,  $J = 8.3$  Hz), and 7.71 (H-11a, H-11b, 2H, dd,  $J = 7.4, 0.8$  Hz);  $^{13}\text{C}$  NMR ( $\text{CDCl}_3$ , 100 MHz)  $\delta$  21.4 (Me), 54.9 (C-8a, C-8b), 55.4 (OMe, C-4a, C-4b), 70.7 (C-7a, C-7b), 114.2 (C-3a, C-3b, C-5a, C-5b), 115.8 (C-11a, C-11b), 122.9 (C-13a, C-13b), 126.6 (C-2a', C-2b', C-6a', C-6b'), 127.0 (C-2a, C-2b, C-6a, C-6b), 128.2 (C-

14a, C-14b), 129.1 (C-12a, C-12b), 129.4 (C-3a', C-3b', C-5a', C-5b'), 130.1 (C-9a, C-9b), 134.0 (C-1a, C-1b), 135.3 (C-1a', C-1b'), 142.4 (C-10a, C-10b), 143.7 (C-4a', C-4b'), and 159.6 (C-4a, C-4b); HRMS (DART-TOF)  $m/z$ :  $[M + H]^+$  Calcd for  $C_{44}H_{41}N_2O_6S_2$ , 757.2406; Found 757.2433.

*Bisquinoline (10ag)*. White solid, and subsequently, colorless block crystals from MeOH/CH<sub>2</sub>Cl<sub>2</sub>; mp 342–344 °C; UV (EtOH)  $\lambda_{max}$  (log  $\epsilon$ ) 210 (3.86) and 230 (3.50) nm; IR (dry film)  $\nu_{max}$  1610, 1512, 1346, 1251, 1162, 1031, and 753 cm<sup>-1</sup>; <sup>1</sup>H NMR (CDCl<sub>3</sub>, 400 MHz)  $\delta$  1.96 (H-8a, H-8b, 2H, dd,  $J = 4.8, 2.8$  Hz), 2.17 (Me, 6H, s), 3.77 (OMe, C-4a, C-4b, 6H, s), 5.88 (H-7a, H-7b, 2H, dd,  $J = 4.8, 2.8$  Hz), 6.69 (H-3a, H-3b, H-5a, H-5b, 4H, d,  $J = 8.7$  Hz), 6.78 (H-2a, H-2b, H-6a, H-6b, 4H, d,  $J = 8.7$  Hz), 6.85 (H-3a', H-3b', H-5a', H-5b', 4H, d,  $J = 8.7$  Hz), 7.16 (H-2a', H-2b', H-6a', H-6b', 4H, d,  $J = 8.7$  Hz), 7.34 (H-12a, H-12b, H-13a, H-13b, 4H, m), 7.44 (H-11a, H-11b, 2H, m) and 7.59 (H-14a, H-14b, 2H, m); <sup>13</sup>C NMR (CDCl<sub>3</sub>, 100 MHz)  $\delta$  21.6 (Me), 47.7 (C-8a, C-8b), 55.3 (OMe, C-4a, C-4b), 59.1 (C-7a, C-7b), 113.8 (C-3a, C-3b, C-5a, C-5b), 124.5 (C-11a, C-11b), 126.7 (C-2a', C-2b', C-6a', C-6b'), 127.5 (C-12a, C-12b), 128.0 (C-13a, C-13b), 128.1 (C-2a, C-2b, C-6a, C-6b), 129.4 (C-14a, C-14b), 129.6 (C-3a', C-3b', C-5a', C-5b'), 133.9 (C-1a, C-1b), 135.3 (C-9a, C-9b), 136.7 (C-1a', C-1b'), 136.9 (C-10a, C-10b), 143.5 (C-4a', C-4b') and 158.8 (C-4a, C-4b); HRMS (DART-TOF)  $m/z$ :  $[M + H]^+$  Calcd for  $C_{44}H_{41}N_2O_6S_2$ , 757.2406; Found 757.2397.

*Indole (10ah)*.<sup>123</sup> Light yellowish oil; UV (EtOH)  $\lambda_{max}$  (log  $\epsilon$ ) 211 (4.35), 224 (4.25), 245 (4.18), and 296 (3.82) nm; IR (dry film)  $\nu_{max}$  1612, 1506, 1370, 1249, 1174, 1035, and 748 cm<sup>-1</sup>; <sup>1</sup>H NMR (CDCl<sub>3</sub>, 400 MHz)  $\delta$  2.33 (Me, 3H, s), 3.85 (OMe, 3H, s), 6.99

(H-3, H-5, 2H, d,  $J = 8.7$  Hz), 7.21 (H-3', H-5', 2H, d,  $J = 8.2$  Hz), 7.26 (H-13, 1H, t,  $J = 8.2$  Hz), 7.34 (H-12, 1H, t,  $J = 8.2$  Hz), 7.51 (H-2, H-6, 2H, d,  $J = 8.7$  Hz), 7.62 (H-8, 1H, s), 7.73 (H-14, 1H, d,  $J = 8.2$  Hz), 7.79 (H-2', H-6', 2H, d,  $J = 8.2$  Hz) and 8.04 (H-11, 1H, d,  $J = 8.2$  Hz);  $^{13}\text{C}$  NMR ( $\text{CDCl}_3$ , 100 MHz)  $\delta$  21.7 (Me), 55.5 (OMe), 113.9 (C-11), 114.4 (C-3, C-5), 120.5 (C-14), 122.4 (C-7), 123.5 (C-13), 124.9 (C-12), 125.6 (C-1), 125.8 (C-8), 127.0 (C-2', C-6'), 129.1 (C-2, C-6), 129.6 (C-9), 130.0 (C-3', C-5'), 135.3 (C-1'), 135.6 (C-10), 145.0 (C-4') and 159.2 (C-4); HRMS (DART-TOF)  $m/z$ :  $[\text{M} + \text{H}]^+$  Calcd for  $\text{C}_{22}\text{H}_{20}\text{NO}_3\text{S}$ , 378.1164; Found 378.1163.

### 3.8.9 Anodic oxidation of **11** in MeCN/ 0.2 M LiClO<sub>4</sub>

Controlled potential electrolysis of **11** (+1.06 V, 1 F) yielded a mixture, which on preparative radial chromatography ( $\text{SiO}_2$ , *n*-hexane: $\text{CH}_2\text{Cl}_2$ , 2:1 to 2% MeOH: $\text{CH}_2\text{Cl}_2$ ), gave **11ac** (40.1 mg, 49%), **11ad** (17.2 mg, 21%), and **11ag** (10.6 mg, 13%).

*Bisindole (11ac)*. Light yellowish oil; UV (EtOH)  $\lambda_{\text{max}}$  (log  $\epsilon$ ) 212 (4.69), 228 (4.55), and 284 (3.97) nm; IR (dry film)  $\nu_{\text{max}}$  1611, 1538, 1513, 1371, 1249, 1175, 1030, 756, and 586  $\text{cm}^{-1}$ ;  $^1\text{H}$  NMR ( $\text{CDCl}_3$ , 400 MHz)  $\delta$  2.79 (H-8a, H-8b, 2H, s), 3.75 (OMe, C-4a, C-4b, 6H, s), 5.15 (H-7a, H-7b, 2H, s), 6.38 (H-14a, H-14b, 2H, d,  $J = 7.8$  Hz), 6.63 (H-3a, H-3b, H-5a, H-5b, 4H, d,  $J = 8.7$  Hz), 6.83 (H-2a, H-2b, H-6a, H-6b, 4H, d,  $J = 8.7$  Hz), 6.91 (H-13a, H-13b, 2H, t,  $J = 7.8$  Hz), 7.24 (H-3a', H-3b', 2H, m), 7.25 (H-5a', H-5b', 2H, m), 7.31 (H-12a, H-12b, 2H, m), 7.38 (H-4a', H-4b', 2H, t,  $J = 7.8$  Hz), 7.57 (H-11a, H-11b, 2H, d,  $J = 7.8$  Hz), and 7.59 (H-6a', H-6b', 2H, d,  $J = 7.8$  Hz);  $^{13}\text{C}$  NMR ( $\text{CDCl}_3$ , 100 MHz)  $\delta$  54.5 (C-8a, C-8b), 55.4 (OMe, C-4a, C-4b), 69.4 (C-7a, C-7b), 114.1 (C-3a, C-3b, C-5a, C-5b), 115.8 (C-11a, C-11b), 123.6 (C-13a, C-13b), 124.2 (C-

5a', C-5b'), 127.5 (C-14a, C-14b), 127.8 (C-2a, C-2b, C-6a, C-6b), 129.4 (C-9a, C-9b, C-12a, C-12b), 130.0 (C-6a', C-6b'), 131.3 (C-3a', C-3b'), 132.2 (C-1a', C-1b'), 132.8 (C-1a, C-1b), 133.8 (C-4a', C-4b'), 142.2 (C-10a, C-10b), 147.7 (C-2a', C-2b') and 159.5 (C-4a, C-4b); HRMS (DART-TOF) m/z: [M + H]<sup>+</sup> Calcd for C<sub>42</sub>H<sub>35</sub>N<sub>4</sub>O<sub>10</sub>S<sub>2</sub>, 819.1795; Found 819.1806.

*Bisindole (11ad)*. Light yellowish oil; UV (EtOH)  $\lambda_{\max}$  (log  $\epsilon$ ) 212 (4.74), 230 (4.59), and 284 (4.12) nm; IR (dry film)  $\nu_{\max}$  1611, 1543, 1513, 1371, 1250, 1176, 1030, 753, and 586 cm<sup>-1</sup>; <sup>1</sup>H NMR (CDCl<sub>3</sub>, 400 MHz)  $\delta$  3.45 (H-8a, H-8b, 2H, s), 3.71 (OMe, C-4a, C-4b, 6H, s), 5.34 (H-7a, H-7b, 2H, s), 6.62 (H-3a, H-3b, H-5a, H-5b, 4H, d,  $J$  = 8.7 Hz), 6.85 (H-14a, H-14b, 2H, d,  $J$  = 8.2 Hz), 6.92 (H-2a, H-2b, H-6a, H-6b, 4H, d,  $J$  = 8.7 Hz), 6.94 (H-13a, H-13b, 2H, t,  $J$  = 8.2 Hz), 7.23 (H-12a, H-12b, 2H, t,  $J$  = 8.2 Hz), 7.32 (H-5a', H-5b', 2H, m), 7.48 (H-3a', H-3b', H-4a', H-4b', 4H, m), 7.50 (H-11a, H-11b, 2H, d,  $J$  = 8.2 Hz) and 7.58 (H-6a', H-6b', 2H, d,  $J$  = 7.3 Hz); <sup>13</sup>C NMR (CDCl<sub>3</sub>, 100 MHz)  $\delta$  54.7 (C-8a, C-8b), 55.3 (OMe, C-4a, C-4b), 67.6 (C-7a, C-7b), 114.2 (C-3a, C-3b, C-5a, C-5b), 115.1 (C-11a, C-11b), 124.2 (C-13a, C-13b), 125.6 (C-14a, C-14b), 127.6 (C-2a, C-2b, C-6a, C-6b), 129.3 (C-12a, C-12b), 129.5 (C-9a, C-9b), 130.4 (C-6a', C-6b'), 131.7 (C-5a', C-5b'), 132.9 (C-1a', C-1b'), 133.2 (C-1a, C-1b), 133.5 (C-4a', C-4b'), 142.7 (C-10a, C-10b), 147.6 (C-2a', C-2b') and 159.4 (C-4a, C-4b); HRMS (DART-TOF) m/z: [M + H]<sup>+</sup> Calcd for C<sub>42</sub>H<sub>35</sub>N<sub>4</sub>O<sub>10</sub>S<sub>2</sub>, 819.1795; Found 819.1815.

*Bisquinoline (11ag)*. White solid, and subsequently, colorless block crystals from MeOH/CH<sub>2</sub>Cl<sub>2</sub>; mp 306–308 °C; UV (EtOH)  $\lambda_{\max}$  (log  $\epsilon$ ) 210 (4.54) and 228 (4.23) nm; IR (dry film)  $\nu_{\max}$  1608, 1531, 1513, 1365, 1349, 1261, 1174, 1024, 743, and 590 cm<sup>-1</sup>;

$^1\text{H}$  NMR ( $\text{CD}_2\text{Cl}_2$ , 400 MHz)  $\delta$  2.56 (H-8a, H-8b, 2H, dd,  $J = 4.6, 2.8$  Hz), 3.74 (OMe, C-4a, C-4b, 6H, s), 6.06 (H-7a, H-7b, 2H, dd,  $J = 4.6, 2.8$  Hz), 6.68 (H-3a, H-3b, H-5a, H-5b, 4H, d,  $J = 8.7$  Hz), 6.84 (H-2a, H-2b, H-6a, H-6b, 4H, d,  $J = 8.7$  Hz), 7.14 (H-3a', H-3b', H-6a', H-6b', 4H, m), 7.28 (H-5a', H-5b', 2H, d,  $J = 7.3$  Hz), 7.38 (H-4a', H-4b', 2H, m), 7.40 (H-13a, H-13b, 2H, m), 7.44 (H-12a, H-12b, 2H, td,  $J = 7.8, 1.4$  Hz), 7.56 (H-14a, H-14b, 2H, dd,  $J = 7.8, 1.4$  Hz) and 7.60 (H-11a, H-11b, 2H, d,  $J = 7.8$  Hz);  $^{13}\text{C}$  NMR ( $\text{CD}_2\text{Cl}_2$ , 100 MHz)  $\delta$  47.8 (C-8a, C-8b), 55.3 (OMe, C-4a, C-4b), 59.6 (C-7a, C-7b), 114.0 (C-3a, C-3b, C-5a, C-5b), 123.5 (C-5a', C-5b'), 125.8 (C-11a, C-11b), 127.8 (C-12a, C-12b), 128.0 (C-2a, C-2b, C-6a, C-6b, C-13a, C-13b), 128.3 (C-14a, C-14b), 130.6 (C-6a', C-6b'), 131.0 (C-3a', C-3b'), 131.3 (C-1a', C-1b'), 133.5 (C-1a, C-1b), 133.9 (C-4a', C-4b'), 134.4 (C-9a, C-9b), 136.5 (C-10a, C-10b), 147.3 (C-2a', C-2b') and 159.3 (C-4a, C-4b); HRMS (DART-TOF)  $m/z$ :  $[\text{M} + \text{H}]^+$  Calcd for  $\text{C}_{42}\text{H}_{35}\text{N}_4\text{O}_{10}\text{S}_2$ , 819.1795; Found 819.1799.

### 3.8.10 Anodic oxidation of **12** in MeCN/ 0.2 M LiClO<sub>4</sub>

Controlled potential electrolysis of **12** (+1.14 V, 1 F) yielded a mixture, which on preparative radial chromatography ( $\text{SiO}_2$ , *n*-hexane: $\text{CHCl}_3$ , 1:2 to 2% MeOH: $\text{CHCl}_3$ ), gave **12ac** (16.0 mg, 27%) and **12ai** (7.1 mg, 12%).

*Bisindole (12ac)*.<sup>96</sup> Light yellowish oil; UV (EtOH)  $\lambda_{\text{max}}$  (log  $\epsilon$ ) 212 (4.85), 238 (4.49), 282 (4.17), and 290 (4.09) nm; IR (dry film)  $\nu_{\text{max}}$  1667, 1597, 1515, 1392, 1256, 1026, and 752  $\text{cm}^{-1}$ ;  $^1\text{H}$  NMR ( $\text{CDCl}_3$ , 400 MHz)  $\delta$  1.88 (NCOMe, 6H, s), 3.51 (H-8a, H-8b, 2H, s), 3.59 (OMe, C-3a, C-3b, 6H, s), 3.74 (OMe, C-4a, C-4b, 6H, s), 4.66 (H-7a, H-7b, 2H, s), 5.80 (H-2a, H-2b, 2H, s), 6.22 (H-6a, H-6b, 2H, d,  $J = 8.7$  Hz), 6.60 (H-5a,

H-5b, 2H, d,  $J = 8.7$  Hz), 7.21 (H-13a, H-13b, 2H, t,  $J = 8.2$  Hz), 7.31 (H-14a, H-14b, 2H, d,  $J = 8.2$  Hz), 7.45 (H-12a, H-12b, 2H, t,  $J = 8.2$  Hz), and 8.47 (H-11a, H-11b, 2H, d,  $J = 8.2$  Hz);  $^{13}\text{C}$  NMR ( $\text{CDCl}_3$ , 100 MHz)  $\delta$  23.7 (NCOMe), 55.8 (OMe, C-3a, C-3b), 55.9 (OMe, C-4a, C-4b), 56.8 (C-8a, C-8b), 64.2 (C-7a, C-7b), 107.6 (C-2a, C-2b), 111.4 (C-5a, C-5b), 115.9 (C-6a, C-6b), 117.8 (C-11a, C-11b), 124.8 (C-13a, C-13b), 125.3 (C-14a, C-14b), 129.4 (C-12a, C-12b), 130.2 (C-9a, C-9b), 134.2 (C-1a, C-1b), 144.0 (C-10a, C-10b), 148.5 (C-4a, C-4b), 149.5 (C-3a, C-3b) and 169.9 (NCOMe); HRMS (DART-TOF)  $m/z$ :  $[\text{M} + \text{H}]^+$  Calcd for  $\text{C}_{36}\text{H}_{37}\text{N}_2\text{O}_6$ , 593.2652; Found 593.2656.

*Dihydroindole (12ai)*.<sup>122</sup> Light yellowish oil; UV (EtOH)  $\lambda_{\text{max}}$  ( $\log \epsilon$ ) 211 (4.16), 238 (3.71), 254 (3.69), 282 (3.43), and 290 (3.35) nm; IR (dry film)  $\nu_{\text{max}}$  1660, 1596, 1516, 1395, 1257, 1026, and 753  $\text{cm}^{-1}$ ;  $^1\text{H}$  NMR ( $\text{CDCl}_3$ , 400 MHz)  $\delta$  2.04 (NCOMe, 6H, s), 2.95 (H-8a, H-8b, 2H, d,  $J = 16.0$  Hz), 3.77 (H-8a, H-8b, 2H, m), 3.77 (OMe, C-3a, C-3b, 6H, s), 3.82 (OMe, C-4a, C-4b, 6H, s), 5.31 (H-7a, H-7b, 2H, d,  $J = 9.6$  Hz), 6.63 (H-2a, H-2b, 2H, s), 6.69 (H-6a, H-6b, 2H, d,  $J = 8.2$  Hz), 6.76 (H-5a, H-5b, 2H, d,  $J = 8.2$  Hz), 7.03 (H-13a, H-13b, 2H, t,  $J = 8.2$  Hz), 7.12 (H-14a, H-14b, 2H, d,  $J = 8.2$  Hz), 7.24 (H-12a, H-12b, 2H, t,  $J = 8.2$  Hz), and 8.29 (H-11a, H-11b, 2H, d,  $J = 8.2$  Hz);  $^{13}\text{C}$  NMR ( $\text{CDCl}_3$ , 100 MHz)  $\delta$  24.2 (NCOMe), 39.2 (C-8a, C-8b), 55.9 (OMe, C-3a, C-3b), 56.0 (OMe, C-4a, C-4b), 63.4 (C-7a, C-7b), 108.0 (C-2a, C-2b), 111.5 (C-5a, C-5b), 117.0 (C-11a, C-11b), 117.2 (C-6a, C-6b), 124.1 (C-13a, C-13b), 124.9 (C-14a, C-14b), 127.8 (C-12a, C-12b), 129.3 (C-9a, C-9b), 135.8 (C-1a, C-1b), 143.4 (C-10a, C-10b), 148.6 (C-4a, C-4b), 149.6 (C-3a, C-3b) and 169.7 (NCOMe); HRMS (DART-TOF)  $m/z$ :  $[\text{M} + \text{H}]^+$  Calcd for  $\text{C}_{18}\text{H}_{20}\text{NO}_3$ , 298.1443; Found 298.1452.

### 3.8.11 Anodic oxidation of **13** in MeCN/ 0.2 M LiClO<sub>4</sub>

Controlled potential electrolysis of **13** (+0.96 V, 1 F) yielded a mixture, which on preparative radial chromatography (SiO<sub>2</sub>, *n*-hexane:CH<sub>2</sub>Cl<sub>2</sub>, 4:1 to 100% CH<sub>2</sub>Cl<sub>2</sub>), gave **13ac** (41.9 mg, 67%), **13ag** (3.1 mg, 5%), and **13ah** (0.6 mg, 1%).

*Bisindole (13ac)*. Light yellowish solid, and subsequently, colorless block crystals from MeOH/CH<sub>2</sub>Cl<sub>2</sub>; mp 210–212 °C; UV (EtOH)  $\lambda_{\max}$  (log  $\epsilon$ ) 234 (4.06) and 285 (3.57) nm; IR (dry film)  $\nu_{\max}$  2935, 1709, 1516, 1441, 1385, 1256, 1025, and 756 cm<sup>-1</sup>; <sup>1</sup>H NMR (CDCl<sub>3</sub>, 400 MHz)  $\delta$  3.12 (H-8a, H-8b, 2H, dd,  $J$  = 4.8, 2.4 Hz), 3.70 (OMe, 3a, 3b, 6H, s), 3.72 (CO<sub>2</sub>Me, 16a, 16b, 12H, br s), 3.82 (OMe, 4a, 4b, 6H, s), 6.28 (H-7a, H-7b, 2H, dd,  $J$  = 4.8, 2.4 Hz), 6.64 (H-2a, H-2b, 2H, d,  $J$  = 1.6 Hz), 6.75 (H-5a, H-5b, 2H, d,  $J$  = 8.4 Hz), 6.89 (H-6a, H-6b, 2H, dd,  $J$  = 8.4, 1.6 Hz), 7.31 (H-11a, H-11b, H-12a, H-12b, H-13a, H-13b, 6H, m), and 7.76 (H-14a, H-14b, 2H, m); <sup>13</sup>C NMR (CDCl<sub>3</sub>, 100 MHz)  $\delta$  48.8 (C-8a, C-8b), 53.2 (CO<sub>2</sub>Me, C-16a, C-16b), 55.89 (OMe, 4a, 4b), 55.93 (OMe, 3a, 3b), 57.4 (C-7a, C-7b), 110.5 (C-2a, C-2b), 111.0 (C-5a, C-5b), 120.0 (C-6a, C-6b), 124.2 (C-14a, C-14b), 125.8 (C-13a, C-13b), 126.7 (C-11a, C-11b), 127.2 (C-12a, C-12b), 134.6 (C-9a, C-9b), 134.9 (C-1a, C-1b), 137.6 (C-10a, C-10b), 148.5 (C-4a, C-4b), 149.0 (C-3a, C-3b), and 155.3 (C-15a, C-15b); HRMS (DART-TOF)  $m/z$ : [M + H]<sup>+</sup> Calcd for C<sub>36</sub>H<sub>37</sub>N<sub>2</sub>O<sub>8</sub>, 625.2550; Found 625.2558.

*Bisquinoline (13ag)*. Light yellowish solid, and subsequently, colorless block crystals from MeOH/CH<sub>2</sub>Cl<sub>2</sub>; mp 251–253 °C; UV (EtOH)  $\lambda_{\max}$  (log  $\epsilon$ ) 233 (4.16), 273 (3.78), and 334 (3.19) nm; IR (dry film)  $\nu_{\max}$  2949, 1703, 1515, 1440, 1320, 1259, 1026, and 758 cm<sup>-1</sup>; <sup>1</sup>H NMR (CDCl<sub>3</sub>, 400 MHz)  $\delta$  3.12 (H-8a, H-8b, 2H, dd,  $J$  = 4.8, 2.4 Hz),

3.70 (OMe, 3a, 3b, 6H, s), 3.72 (CO<sub>2</sub>Me, 16a, 16b, 12H, br s), 3.82 (OMe, 4a, 4b, 6H, s), 6.28 (H-7a, H-7b, 2H, dd,  $J = 4.8, 2.4$  Hz), 6.64 (H-2a, H-2b, 2H, d,  $J = 1.6$  Hz), 6.75 (H-5a, H-5b, 2H, d,  $J = 8.4$  Hz), 6.89 (H-6a, H-6b, 2H, dd,  $J = 8.4, 1.6$  Hz), 7.31 (H-11a, H-11b, H-12a, H-12b, H-13a, H-13b, 6H, m), and 7.76 (H-14a, H-14b, 2H, m); <sup>13</sup>C NMR (CDCl<sub>3</sub>, 100 MHz)  $\delta$  48.8 (C-8a, C-8b), 53.2 (CO<sub>2</sub>Me, C-16a, C-16b), 55.89 (OMe, 4a, 4b), 55.93 (OMe, 3a, 3b), 57.4 (C-7a, C-7b), 110.5 (C-2a, C-2b), 111.0 (C-5a, C-5b), 120.0 (C-6a, C-6b), 124.2 (C-14a, C-14b), 125.8 (C-13a, C-13b), 126.7 (C-11a, C-11b), 127.2 (C-12a, C-12b), 134.6 (C-9a, C-9b), 134.9 (C-1a, C-1b), 137.6 (C-10a, C-10b), 148.5 (C-4a, C-4b), 149.0 (C-3a, C-3b), and 155.3 (C-15a, C-15b); HRMS (DART-TOF)  $m/z$ : [M + H]<sup>+</sup> Calcd for C<sub>36</sub>H<sub>37</sub>N<sub>2</sub>O<sub>8</sub>, 625.2550; Found 625.2550.

*Indole (13ah)*. Light yellowish solid; UV (EtOH)  $\lambda_{\max}$  (log  $\epsilon$ ) 223 (4.14) and 298 (3.81) nm; IR (dry film)  $\nu_{\max}$  2955, 1736, 1511, 1453, 1375, 1241 and 761 cm<sup>-1</sup>; <sup>1</sup>H NMR (CDCl<sub>3</sub>, 400 MHz)  $\delta$  3.95 (OMe, 4, 3H, s), 3.96 (OMe, 3, 3H, s), 4.08 (CO<sub>2</sub>Me, 16, 3H, s), 6.99 (H-5, 1H, d,  $J = 8.4$  Hz), 7.14 (H-2, 1H, d,  $J = 2.0$  Hz), 7.21 (H-6, 1H, dd,  $J = 8.4, 2.0$  Hz), 7.32 (H-13, 1H, t,  $J = 7.6$  Hz), 7.40 (H-12, 1H, t,  $J = 7.6$  Hz), 7.69 (H-8, 1H, s), 7.81 (H-14, 1H, d,  $J = 7.6$  Hz), and 8.25 (H-11, 1H, d,  $J = 7.6$  Hz); <sup>13</sup>C NMR (CDCl<sub>3</sub>, 100 MHz)  $\delta$  54.0 (CO<sub>2</sub>Me, C-16), 56.1 (OMe, 3, 4), 111.3 (C-2), 111.6 (C-5), 115.5 (C-11), 120.1 (C-14), 120.4 (C-6), 121.9 (C-8), 123.0 (C-7), 123.4 (C-13), 125.0 (C-12), 126.4 (C-1), 129.2 (C-9), 135.0 (C-10), 148.6 (C-4), 149.3 (C-3), and 152.0 (C-15); HRMS (DART-TOF)  $m/z$ : [M + H]<sup>+</sup> Calcd for C<sub>18</sub>H<sub>18</sub>NO<sub>4</sub>, 312.1236; Found 312.1230.

### 3.8.12 Anodic oxidation of **14** in MeCN/ 0.2 M LiClO<sub>4</sub>

Controlled potential electrolysis of **14** (+0.96 V, 1 F) yielded a mixture, which on preparative radial chromatography (SiO<sub>2</sub>, *n*-hexane:EtOAc, 4:1 to 100% EtOAc), gave **14ac** (44.1 mg, 54%) and **14af** (13.1 mg, 16%).

*Bisindole (14ac)*. Light yellowish oil, and subsequently, colorless block crystals from MeOH/MeCN; mp 154–156 °C; UV (EtOH)  $\lambda_{\max}$  (log  $\epsilon$ ) 222 (4.70) and 278 (4.26) nm; IR (dry film)  $\nu_{\max}$  2936, 1514, 1460, 1353, 1260, 1162, 1025, 676, and 569 cm<sup>-1</sup>; <sup>1</sup>H NMR (CDCl<sub>3</sub>, 400 MHz)  $\delta$  2.14 (Me, 4a', 4b', 6H, s), 2.20 (H-8a, H-8b, 2H, s), 3.65 (OMe, 3a, 3b, 6H, s), 3.91 (OMe, 4a, 4b, 6H, s), 5.09 (H-7a, H-7b, 2H, s), 6.09 (H-14a, H-14b, 2H, d,  $J = 7.8$  Hz), 6.40 (H-2a, H-2b, 2H, d,  $J = 1.2$  Hz), 6.74 (H-6a, H-6b, 2H, dd,  $J = 8.3, 1.2$  Hz), 6.78 (H-3a', H-5a', H-3b', H-5b', 4H, d,  $J = 8.1$  Hz), 6.81 (H-5a, H-5b, 2H, d,  $J = 8.3$  Hz), 6.86 (H-13a, H-13b, 2H, t,  $J = 7.8$  Hz), 7.27 (H-12a, H-12b, 2H, t,  $J = 7.8$  Hz), 7.36 (H-2a', H-6a', H-2b', H-6b', 4H, d,  $J = 8.1$  Hz), and 7.69 (H-11a, H-11b, 2H, d,  $J = 7.8$  Hz); <sup>13</sup>C NMR (CDCl<sub>3</sub>, 100 MHz)  $\delta$  21.2 (Me, 4a', 4b'), 54.7 (C-8a, C-8b), 55.6 (OMe, 3a, 3b), 56.1 (OMe, 4a, 4b), 70.5 (C-7a, C-7b), 108.6 (C-2a, C-2b), 111.1 (C-5a, C-5b), 115.3 (C-11a, C-11b), 118.3 (C-6a, C-6b), 122.9 (C-13a, C-13b), 126.8 (C-2a', C-6a', C-2b', C-6b'), 127.9 (C-14a, C-14b), 129.1 (C-12a, C-12b), 129.2 (C-3a', C-5a', C-3b', C-5b'), 130.1 (C-9a, C-9b), 134.0 (C-1a, C-1b), 135.5 (C-1a', C-1b'), 142.3 (C-10a, C-10b), 143.7 (C-4a', C-4b'), 149.0 (C-4a, C-4b), and 149.3 (C-3a, C-3b); HRMS (DART-TOF) *m/z*: [M + H]<sup>+</sup> Calcd for C<sub>46</sub>H<sub>45</sub>N<sub>2</sub>O<sub>8</sub>S<sub>2</sub>, 817.2617; Found 817.2646.

*Bridged azocine (14af)*. Light yellowish oil and subsequent as colorless block crystals from MeOH/CH<sub>2</sub>Cl<sub>2</sub>; mp 188–190 °C; UV (EtOH)  $\lambda_{\max}$  (log  $\epsilon$ ) 224 (3.90) and 279 (3.25) nm; IR (dry film)  $\nu_{\max}$  2938, 1511, 1327, 1261, 1156, 1026, 759, and 553 cm<sup>-1</sup>; <sup>1</sup>H NMR (CDCl<sub>3</sub>, 400 MHz)  $\delta$  2.31 (Me, 4b', 3H, s), 2.40 (Me, 4a', 3H, s), 3.40 (H-8b, 1H, br s), 3.70 (OMe, 4a, 3H, s), 3.87 (OMe, 3b, 4b, 6H, s), 3.88 (OMe, 3a, 3H, s), 4.30 (H-8a, 1H, d,  $J$  = 2.5 Hz), 4.45 (H-7b, 1H, d,  $J$  = 1.4 Hz), 6.29 (NH, 1H, br s), 6.31 (H-8a, 1H, d,  $J$  = 2.5 Hz), 6.39 (H-5a, 1H, s), 6.69 (H-11a, 1H, d,  $J$  = 7.9 Hz), 6.70 (H-2b, 1H, d,  $J$  = 1.9 Hz), 6.72 (H-14a, 1H, d,  $J$  = 7.9 Hz), 6.78 (H-6b, 1H, dd,  $J$  = 8.3, 1.9 Hz), 6.84 (H-13a, 1H, t,  $J$  = 7.9 Hz), 6.90 (H-5b, 1H, d,  $J$  = 8.3 Hz), 6.98 (H-3b', H-5b', 2H, d,  $J$  = 8.2 Hz), 7.00 (H-12a, 1H, m), 7.01 (H-12b, 1H, m), 7.07 (H-13b, 1H, m), 7.08 (H-2b', H-6b', 2H, d,  $J$  = 8.2 Hz), 7.09 (H-2a, 1H, s), 7.17 (H-11b, 1H, d,  $J$  = 8.1 Hz), 7.20 (H-3a', H-5a', 2H, d,  $J$  = 8.1 Hz), and 7.56 (H-2a', H-6a', H-14b, 3H, d,  $J$  = 8.1 Hz); <sup>13</sup>C NMR (CDCl<sub>3</sub>, 100 MHz)  $\delta$  21.4 (Me, 4b'), 21.6 (Me, 4a'), 31.2 (C-8a), 44.8 (C-8b), 55.7 (OMe), 55.8 (OMe), 55.9 (OMe), 55.9 (C-7a), 56.8 (C-7b), 111.3 (C-5b), 111.6 (C-2a), 112.3 (C-5a), 112.4 (C-2b), 119.0 (C-11b), 121.4 (C-6b), 123.3 (C-13b), 127.1 (C-11a), 127.2 (C-2b', C-6b'), 127.3 (C-1a, C-12b), 127.7 (C-2a', C-6a'), 127.9 (C-13a), 128.2 (C-6a), 128.7 (C-14a), 129.3 (C-12a, C-9b), 129.5 (C-3b', C-5b'), 129.8 (C-3a', C-5a'), 129.9 (C-14b), 134.7 (C-10a), 135.3 (C-10b), 136.3 (C-1a'), 136.4 (C-1b), 137.9 (C-1b'), 138.4 (C-9a), 143.4 (C-4b'), 143.8 (C-4a'), 147.8 (C-4b), 148.2 (C-3a), 149.0 (C-3b), and 149.3 (C-4a); HRMS (DART-TOF)  $m/z$ : [M + H]<sup>+</sup> Calcd for C<sub>46</sub>H<sub>45</sub>N<sub>2</sub>O<sub>8</sub>S<sub>2</sub>, 817.2617; Found 817.2598.

### 3.8.13 Anodic oxidation of **15** in MeCN/ 0.2 M LiClO<sub>4</sub>

Controlled potential electrolysis of **15** (+1.02 V, 1 F) yielded a mixture, which on preparative radial chromatography (SiO<sub>2</sub>, *n*-hexane:CH<sub>2</sub>Cl<sub>2</sub>, 1:2 to 3% MeOH:CH<sub>2</sub>Cl<sub>2</sub>), gave **15ac** (53.6 mg, 61%) and **15af** (7.9 mg, 9%).

*Bisindole (15ac)*. Light yellowish oil; UV (EtOH)  $\lambda_{\max}$  (log  $\epsilon$ ) 214 (4.83), 237 (4.55), and 281 (4.21) nm; IR (dry film)  $\nu_{\max}$  1594, 1544, 1517, 1370, 1261, 1173, 1026, 753, and 592 cm<sup>-1</sup>; <sup>1</sup>H NMR (CDCl<sub>3</sub>, 400 MHz)  $\delta$  3.22 (H-8a, H-8b, 2H, s), 3.63 (OMe, C-3a, C-3b, 6H, s), 3.79 (OMe, C-4a, C-4b, 6H, s), 5.24 (H-7a, H-7b, 2H, s), 6.35 (H-2a, H-2b, 2H, d,  $J$  = 1.5 Hz), 6.45 (H-6a, H-6b, 2H, dd,  $J$  = 8.2, 1.5 Hz), 6.53 (H-14a, H-14b, 2H, d,  $J$  = 7.8 Hz), 6.55 (H-5a, H-5b, 2H, d,  $J$  = 8.2 Hz), 6.91 (H-13a, H-13b, 2H, t,  $J$  = 7.8 Hz), 7.25 (H-5a', H-5b', 2H, t,  $J$  = 7.8 Hz), 7.29 (H-12a, H-12b, 2H, t,  $J$  = 7.8 Hz), 7.35 (H-3a', H-3b', 2H, d,  $J$  = 7.8 Hz), 7.42 (H-4a', H-4b', 2H, t,  $J$  = 7.8 Hz), 7.55 (H-6a', H-6b', 2H, d,  $J$  = 7.8 Hz) and 7.60 (H-11a, H-11b, 2H, d,  $J$  = 7.8 Hz); <sup>13</sup>C NMR (CDCl<sub>3</sub>, 100 MHz)  $\delta$  54.2 (C-8a, C-8b), 55.7 (OMe, C-3a, C-3b), 55.9 (OMe, C-4a, C-4b), 69.1 (C-7a, C-7b), 109.5 (C-2a, C-2b), 110.9 (C-5a, C-5b), 115.4 (C-11a, C-11b), 118.9 (C-6a, C-6b), 123.5 (C-13a, C-13b), 124.1 (C-3a', C-3b'), 126.8 (C-14a, C-14b), 129.1 (C-9a, C-9b), 129.2 (C-12a, C-12b), 130.0 (C-6a', C-6b'), 131.2 (C-5a', C-5b'), 132.4 (C-1a', C-1b'), 132.9 (C-1a, C-1b), 133.7 (C-4a', C-4b'), 142.4 (C-10a, C-10b), 147.5 (C-2a', C-2b'), 148.7 (C-3a, C-3b) and 148.8 (C-4a, C-4b); HRMS (DART-TOF)  $m/z$ : [M + H]<sup>+</sup> Calcd for C<sub>44</sub>H<sub>39</sub>N<sub>4</sub>O<sub>12</sub>S<sub>2</sub>, 879.2006; Found 879.2042.

*Bridged azocine (15af)*. Light yellowish oil. UV (EtOH)  $\lambda_{\max}$  (log  $\epsilon$ ) 216 (4.97), 238 (4.65) and 281 (4.24) nm; IR (dry film)  $\nu_{\max}$  3339, 1606, 1538, 1514, 1360, 1264, 1245, 1166, 1027, 753, and 581  $\text{cm}^{-1}$ ;  $^1\text{H}$  NMR ( $\text{CDCl}_3$ , 400 MHz)  $\delta$  3.50 (H-8b, 1H, s), 3.72 (OMe, C-3a, C-4a, 6H, s), 3.83 (OMe, C-3b, 3H, s), 3.86 (OMe, C-3a, 3H, s), 4.52 (H-7b, 1H, s), 4.59 (H-8a, 1H, d,  $J = 2.0$  Hz), 6.40 (H-7a, 1H, d,  $J = 2.0$  Hz), 6.45 (H-5a, 1H, s), 6.61 (H-11a, 1H, d,  $J = 7.8$  Hz), 6.64 (H-2b, 1H, s), 6.81 (H-6b, 1H, d,  $J = 8.7$  Hz), 6.82 (H-2a, 1H, s), 6.88 (H-5b, 1H, d,  $J = 8.7$  Hz), 6.88 (H-11b, 1H, d,  $J = 8.0$  Hz), 6.89 (H-12a, 1H, t,  $J = 7.8$  Hz), 6.92 (H-14a, 1H, d,  $J = 7.8$  Hz), 6.98 (H-13a, 1H, t,  $J = 7.8$  Hz), 7.05 (H-12b, 1H, t,  $J = 8.0$  Hz), 7.13 (NH, 1H, s), 7.19 (H-13b, 1H, t,  $J = 8.0$  Hz), 7.37 (H-6b', 1H, d,  $J = 7.8$  Hz), 7.38 (H-5b', 1H, t,  $J = 7.8$  Hz), 7.57 (H-5a', 1H, t,  $J = 7.8$  Hz), 7.63 (H-4b', 1H, t,  $J = 7.8$  Hz), 7.67 (H-14b, 1H, d,  $J = 8.0$  Hz), 7.70 (H-6a', 1H, d,  $J = 7.8$  Hz), 7.72 (H-4a', 1H, t,  $J = 7.8$  Hz), 7.78 (H-3b', 1H, d,  $J = 7.8$  Hz) and 7.89 (H-3a', 1H, d,  $J = 7.8$  Hz);  $^{13}\text{C}$  NMR ( $\text{CDCl}_3$ , 100 MHz)  $\delta$  31.3 (C-8a), 44.6 (C-8b), 55.8 (OMe, C-3a, C-4a), 55.9 (OMe, C-3b), 56.0 (OMe, C-4b), 56.9 (C-7b), 57.1 (C-7a), 111.4 (C-5b), 112.1 (C-2a), 112.3 (C-2b), 112.8 (C-5a), 120.5 (C-11b), 121.5 (C-6b), 124.4 (C-13b), 125.2 (C-3a'), 125.3 (C-3b'), 127.4 (C-12b), 127.7 (C-1a, C-11a), 127.9 (C-14a), 128.9 (C-13a), 128.9 (C-6a), 129.0 (C-6b'), 129.1 (C-12a), 130.0 (C-14b), 130.2 (C-9b), 132.1 (C-5b'), 132.3 (C-6a'), 132.6 (C-1a', C-5a'), 133.4 (C-4b'), 133.9 (C-4a'), 134.2 (C-1b'), 135.2 (C-10b), 135.3 (C-10a), 136.2 (C-1b), 139.2 (C-9a), 147.8 (C-3a), 147.8 (C-4b), 148.1 (C-2b'), 148.1 (C-2a'), 149.0 (C-3b) and 149.6 (C-4a); HRMS (DART-TOF)  $m/z$ :  $[\text{M} + \text{H}]^+$  Calcd for  $\text{C}_{44}\text{H}_{39}\text{N}_4\text{O}_{12}\text{S}_2$ , 879.2006; Found 879.2030.

### 3.8.14 Anodic oxidation of **16** in MeCN/ 0.2 M LiClO<sub>4</sub>

Controlled potential electrolysis of **16** (+1.09 V, 0.9 F) yielded a mixture, which on preparative radial chromatography (SiO<sub>2</sub>, *n*-hexane/CH<sub>2</sub>Cl<sub>2</sub>, 2/1 to 8% MeOH/CH<sub>2</sub>Cl<sub>2</sub>), gave **16ba** (13.9 mg, 29%) and **16bd** (7.7 mg, 16%).

*Bisbenzopyran (16ba)*: Light yellowish oil. UV (EtOH)  $\lambda_{\max}$  (log  $\epsilon$ ) 227 (4.09) and 272 (3.25) nm; IR (dry film)  $\nu_{\max}$  2934, 1510, 1246, 1034, and 739 cm<sup>-1</sup>; <sup>1</sup>H NMR (CDCl<sub>3</sub>, 400 MHz)  $\delta$  3.72 (OMe, 4a, 4b, 6H, s), 3.80 (H-8a, H-8b, 2H, s), 4.47 (H-15a, H-15b, 2H, d,  $J$  = 15.6 Hz), 4.79 (H-15a, H-15b, 2H, d,  $J$  = 15.6 Hz), 5.17 (H-7a, H-7b, 2H, s), 6.68 (H-3a, H-5a, H-3b, H-5b, 4H, d,  $J$  = 8.8 Hz), 6.81 (H-14a, H-14b, 2H, d,  $J$  = 7.2 Hz), 6.86 (H-11a, H-11b, 2H, d,  $J$  = 7.2 Hz), 6.91 (H-13a, H-13b, 2H, t,  $J$  = 7.2 Hz), 7.02 (H-12a, H-12b, 2H, t,  $J$  = 7.2 Hz), and 7.08 (H-2a, H-6a, H-2b, H-6b, 4H, d,  $J$  = 8.8 Hz); <sup>13</sup>C NMR (CDCl<sub>3</sub>, 100 MHz)  $\delta$  44.2 (C-8a, C-8b), 55.1 (OMe, 4a, 4b), 63.6 (C-15a, C-15b), 76.0 (C-7a, C-7b), 113.4 (C-3a, C-5a, C-3b, C-5b), 123.8 (C-11a, C-11b), 125.9 (C-12a, C-12b), 126.1 (C-14a, C-14b), 129.2 (C-2a, C-6a, C-2b, C-6b), 129.5 (C-13a, C-13b), 131.5 (C-1a, C-1b), 134.4 (C-9a, C-9b), 135.2 (C-10a, C-10b), and 158.8 (C-4a, C-4b); HRMS (DART-TOF)  $m/z$ : [M + H]<sup>+</sup> Calcd for C<sub>32</sub>H<sub>31</sub>O<sub>4</sub>, 479.2222; Found 479.2236.

*Benzopyrano-benzoxepine (16ad)*. Light yellowish oil. UV (EtOH)  $\lambda_{\max}$  (log  $\epsilon$ ) 223 (4.49), 236 (4.38) and 277 (3.74) nm; IR (dry film)  $\nu_{\max}$  2932, 1509, 1247, 1031, and 736 cm<sup>-1</sup>; <sup>1</sup>H NMR (CDCl<sub>3</sub>, 400 MHz)  $\delta$  3.58 (H-8a, 1H, br t,  $J$  = 3.6 Hz), 3.67 (OMe, 4b, 3H, s), 3.78 (OMe, 4a, 3H, s), 4.37 (H-8b, 1H, dd,  $J$  = 12.0, 3.6 Hz), 4.60 (H-15a, 1H, d,  $J$  = 15.2 Hz), 4.62 (H-7b, 1H, d,  $J$  = 12.0 Hz), 4.69 (H-15b, 1H, d,  $J$  = 14.8 Hz),

4.94 (H-15a, 1H, d,  $J = 15.2$  Hz), 5.15 (H-15b, 1H, d,  $J = 14.8$  Hz), 5.65 (H-7a, 1H, d,  $J = 3.6$  Hz), 6.58 (H-3b, H-5b, 2H, d,  $J = 8.8$  Hz), 6.72 (H-14b, 1H, d,  $J = 7.2$  Hz), 6.81 (H-13b, 1H, t,  $J = 7.2$  Hz), 6.88 (H-2b, H-6b, 2H, d,  $J = 8.8$  Hz), 6.89 (H-11a, H-12b, 2H, m), 6.90 (H-3a, H-5a, 2H, d,  $J = 8.8$  Hz), 6.92 (H-11b, 1H, m), 7.04 (H-12a, H-13a, 2H, m), 7.28 (H-14a, 1H, d,  $J = 6.0$  Hz), and 7.44 (H-2a, H-6a, 2H, d,  $J = 8.8$  Hz);  $^{13}\text{C}$  NMR ( $\text{CDCl}_3$ , 100 MHz)  $\delta$  40.4 (C-8a), 50.3 (C-8b), 52.2 (C-7b), 55.2 (OMe, 4b), 55.3 (OMe, 4a), 63.5 (C-15a), 70.1 (C-15b), 97.9 (C-7a), 113.5 (C-3b, C-5b), 114.7 (C-3a, C-5a), 123.9 (C-11a), 125.6 (C-12a), 125.9 (C-14a), 126.2 (C-12b), 126.6 (C-13a), 127.1 (C-13b), 128.5 (C-11b), 128.9 (C-2b, C-6b), 129.0 (C-2a, C-6a), 133.6 (C-9a), 134.0 (C-1a), 134.1 (C-14b), 134.2 (C-10a), 135.9 (C-1b), 137.9 (C-10b), 138.4 (C-9b), 157.8 (C-4b), and 158.5 (C-4a); HRMS (DART-TOF)  $m/z$ :  $[\text{M} + \text{H}]^+$  Calcd for  $\text{C}_{32}\text{H}_{31}\text{O}_4$ , 479.2222; Found 479.2230.

### 3.8.15 Anodic oxidation of **17** in MeCN/ 0.2 M LiClO<sub>4</sub>

Controlled potential electrolysis of **17** (+1.02 V, 0.9 F) yielded essentially the same compounds from the anodic oxidation of **16**: namely, **16ba** (12.0 mg, 25%) and **16bd** (7.2 mg, 15%).

### 3.8.16 Anodic oxidation of **18** in MeCN/ 0.2 M LiClO<sub>4</sub>

Controlled potential electrolysis of **18** (+0.96 V, 0.9 F) yielded a mixture, which on preparative radial chromatography ( $\text{SiO}_2$ , *n*-hexane/ $\text{CH}_2\text{Cl}_2$ , 4/1 to 8% MeOH/ $\text{CH}_2\text{Cl}_2$ ), gave **18be** (10.2 mg, 19%), **18bf** (6.2 mg, 12%), and **18bg** (4.7 mg, 9%).

*Tetralinylbenzopyran (18be)*. Light yellowish oil. UV (EtOH)  $\lambda_{\max}$  (log  $\epsilon$ ) 222 (4.61), 240 (4.34) and 279 (4.05) nm; IR (dry film)  $\nu_{\max}$  3515, 2935, 1511, 1463, 1255, 1237, 1026, and 730  $\text{cm}^{-1}$ ;  $^1\text{H}$  NMR ( $\text{CDCl}_3$ , 400 MHz)  $\delta$  3.27 (H-8a, 1H, dd,  $J = 11.6, 2.2$  Hz), 3.57 (OMe, 3b, 3H, s), 3.64 (OMe, 4a, 3H, s), 3.67 (H-15b, 2H, s), 3.76 (OMe, 4b, 3H, s), 3.95 (OMe, 3a, 3H, s), 3.95 (H-8b, 1H, t,  $J = 11.6$ ) 4.44 (H-7b, 1H, d,  $J = 11.6$ ), 4.75 (H-7a, 1H, d,  $J = 2.2$  Hz), 5.13 (H-15a, 2H, s), 6.13 (H-14a, 1H, d,  $J = 7.3$  Hz), 6.37 (H-5a, H-2b, 2H, m), 6.49 (H-6b, 1H, dd,  $J = 8.2, 1.9$  Hz), 6.60 (H-5b, 1H, d,  $J = 8.2$  Hz), 6.66 (H-13a, 1H, t,  $J = 7.3$  Hz), 6.93 (H-2a, 1H, s), 6.95 (H-11b, 1H, d,  $J = 7.4$  Hz), 6.99 (H-11a, 1H, d,  $J = 7.3$  Hz), 7.04 (H-12a, 1H, t,  $J = 7.3$  Hz), 7.14 (H-12b, 1H, t,  $J = 7.4$  Hz), 7.42 (H-13b, 1H, t,  $J = 7.4$  Hz), and 7.75 (H-14b, 1H, d,  $J = 7.4$  Hz);  $^{13}\text{C}$  NMR ( $\text{CDCl}_3$ , 100 MHz)  $\delta$  43.4 (C-8a), 45.6 (C-8b), 52.6 (C-7b), 55.65 (OMe, 4b), 55.75 (OMe, 3b), 55.9 (OMe, 4a), 56.0 (OMe, 3a), 62.5 (C-15b), 69.0 (C-15a), 74.8 (C-7a), 110.7 (C-5b), 112.0 (C-5a), 112.3 (C-2a), 112.4 (C-2b), 121.3 (C-6b), 123.7 (C-11a), 125.2 (C-13a), 126.5 (C-12b), 126.6 (C-12a), 127.6 (C-1a, C-13b), 128.1 (C-14b), 129.1 (C-11b), 130.2 (C-14a), 132.3 (C-6a), 134.2 (C-10a), 135.3 (C-9a), 137.4 (C-1b), 140.3 (C-10b), 140.7 (C-9b), 147.3 (C-4b), 147.9 (C-3a), 148.4 (C-3b), and 149.5 (C-4a); HRMS (DART-TOF)  $m/z$ :  $[\text{M} + \text{H}]^+$  Calcd for  $\text{C}_{34}\text{H}_{35}\text{O}_6$ , 539.2434; Found 539.2419.

*Indanyltetralin (18bf)*. Light yellowish oil. UV (EtOH)  $\lambda_{\max}$  (log  $\epsilon$ ) 222 (4.41), 276 (4.21) and 341 (3.94) nm; IR (dry film)  $\nu_{\max}$  3503, 2935, 1511, 1462, 1255, 1242, 1026, and 733  $\text{cm}^{-1}$ ;  $^1\text{H}$  NMR ( $\text{CDCl}_3$ , 400 MHz)  $\delta$  3.70 (OMe, 3b, 3H, s), 3.72 (OMe, 4a, 3H, s), 3.78 (H-15a, 1H, d,  $J = 22.3$  Hz), 3.92 (OMe, 4b, 3H, s), 3.94 (H-15a, 1H, d,  $J = 22.3$  Hz), 3.99 (OMe, 3a, 3H, s), 4.22 (H-7b, 1H, s), 4.68 (H-8b, 1H, s), 4.89 (H-15b, 2H, s), 6.52 (H-5a, 1H, s), 6.68 (H-5b, H-6b, 2H, m), 6.76 (H-14a, 1H, d,  $J = 7.4$  Hz),

6.82 (H-2b, 1H, s), 7.01 (H-2a, 1H, s), 7.05 (H-12a, H-13a, H-13b, H-14b, 4H, m), 7.17 (H-12b, 1H, t,  $J = 7.6$  Hz), 7.38 (H-11b, 1H, d,  $J = 7.6$  Hz), and 7.45 (H-11a, 1H, d,  $J = 7.4$  Hz);  $^{13}\text{C}$  NMR ( $\text{CDCl}_3$ , 100 MHz)  $\delta$  36.3 (C-15a), 42.7 (C-8b), 53.1 (C-7b), 55.76 (OMe, 3b), 55.82 (OMe, 4b), 55.9 (OMe, 4a), 56.1 (OMe, 3a), 63.7 (C-15b), 106.8 (C-2a), 111.2 (C-5b), 111.5 (C-2b), 113.3 (C-5a), 119.3 (C-14a), 119.8 (C-6b), 123.6 (C-11a), 124.5 (C-12a), 125.9 (C-1a), 126.4 (C-13a), 126.9 (C-12b), 128.5 (C-14b), 128.6 (C-13b), 129.2 (C-11b), 129.3 (C-6a), 137.5 (C-8a), 137.7 (C-10b), 138.1 (C-1b), 139.7 (C-7a), 141.1 (C-9b), 143.0 (C-10a), 144.8 (C-9a), 147.6 (C-4b), 148.0 (C-3a), 148.5 (C-3b), and 148.7 (C-4a); HRMS (DART-TOF)  $m/z$ :  $[\text{M} + \text{H}]^+$  Calcd for  $\text{C}_{34}\text{H}_{33}\text{O}_5$ , 521.2328; Found 521.2336.

*Indanylbenzopyranotetralin (18bg)*. Yellowish oil. UV (EtOH)  $\lambda_{\text{max}}$  (log  $\epsilon$ ) 219 (4.21), 234 (4.01) and 281 (3.69) nm; IR (dry film)  $\nu_{\text{max}}$  2933, 1511, 1461, 1252, 1228, 1028, and 738  $\text{cm}^{-1}$ ;  $^1\text{H}$  NMR ( $\text{CDCl}_3$ , 400 MHz)  $\delta$  2.95 (H-8b, 1H, d,  $J = 11.2$  Hz), 2.99 (H-15a, 1H, dd,  $J = 15.6, 10.8$  Hz), 3.59 (OMe, 4a, H-15a, 4H, m), 3.66 (OMe, 3b, 3H, s), 3.75 (H-7a, 1H, t,  $J = 11.2$  Hz), 3.86 (OMe, 4b, 3H, s), 3.92 (OMe, 3a, 3H, s), 3.98 (H-7b, 1H, d,  $J = 11.2$  Hz), 5.38 (H-15b, 2H, s), 6.01 (H-14b, 1H, d,  $J = 7.2$  Hz), 6.29 (H-5a, 1H, s), 6.35 (H-2b, 1H, d,  $J = 1.2$  Hz), 6.42 (H-6b, 1H, dd,  $J = 8.4, 1.2$  Hz), 6.57 (H-14a, 1H, d,  $J = 7.6$  Hz), 6.68 (H-5b, 1H, d,  $J = 8.4$  Hz), 6.81 (H-2a, H-13b, 2H, m), 6.88 (H-13a, 1H, t,  $J = 7.6$  Hz), 7.15 (H-12a, 1H, t,  $J = 7.6$  Hz), 7.16 (H-11b, 1H, d,  $J = 7.2$  Hz), 7.21 (H-12b, 1H, t,  $J = 7.2$  Hz), and 7.22 (H-11a, 1H, d,  $J = 7.6$  Hz);  $^{13}\text{C}$  NMR ( $\text{CDCl}_3$ , 100 MHz)  $\delta$  39.7 (C-15a), 47.7 (C-8b), 50.60 (C-7a), 50.62 (C-7b), 55.8 (OMe, 4b), 55.9 (OMe, 4a, 3b), 56.0 (OMe, 3a), 65.7 (C-15b), 83.2 (C-8a), 110.6 (C-5b), 111.0 (C-2a), 112.4 (C-5a), 113.1 (C-2b), 122.5 (C-6b), 123.7 (C-11b), 124.7 (C-11a), 125.2 (C-14a), 125.8 (C-13b), 126.6 (C-13a), 126.9 (C-12b), 127.9 (C-12a), 129.67 (C-1a),

129.69 (C-6a), 130.9 (C-14b), 134.1 (C-10b), 134.7 (C-9b), 136.4 (C-1b), 140.6 (C-10a), 146.7 (C-9a), 147.5 (C-4b), 147.6 (C-4a), 148.1 (C-3a), and 148.5 (C-3b); HRMS (DART-TOF)  $m/z$ :  $[M + H]^+$  Calcd for  $C_{34}H_{33}O_5$ , 521.2328; Found 521.2341.

### 3.8.17 Anodic oxidation of **19** in MeCN/ 0.2 M LiClO<sub>4</sub>

Controlled potential electrolysis of **19** (+0.96 V, 0.9 F) yielded essentially the same compounds from the anodic oxidation of **18**: namely, **18be** (10.2 mg, 19%), **18bf** (6.2 mg, 12%), and **18bg** (4.7 mg, 9%).

### 3.8.18 Anodic oxidation of **20** in MeCN/ 0.2 M LiClO<sub>4</sub>

Controlled potential electrolysis of **20** (+1.01 V, 1.0 F) yielded a mixture, which on preparative radial chromatography (SiO<sub>2</sub>, *n*-hexane/CH<sub>2</sub>Cl<sub>2</sub>, 1/1 to 8% MeOH/CH<sub>2</sub>Cl<sub>2</sub>), gave **20ba** (21.2 mg, 25%), **20be** (8.5 mg, 10%), **20bh** (16.9 mg, 20%), and **20bi** (7.9 mg, 12%).

*Bisisoquinoline (20ba)*. Yellowish oil. UV (EtOH)  $\lambda_{max}$  (log  $\epsilon$ ) 223 (4.65) and 283 (3.82) nm; IR (dry film)  $\nu_{max}$  2933, 1541, 1512, 1371, 1249, 1165, 1033, 731, and 581  $cm^{-1}$ ; <sup>1</sup>H NMR (CDCl<sub>3</sub>, 400 MHz)  $\delta$  3.30 (H-8a, H-8b, 2H, s), 3.60 (OMe, 4a, 4b, 6H, s), 4.92 (H-15a, H-15b, 2H, d,  $J = 15.8$  Hz), 5.12 (H-15a, H-15b, 2H, d,  $J = 15.8$  Hz), 5.86 (H-14a, H-14b, 2H, d,  $J = 7.4$  Hz), 6.17 (H-7a, H-7b, 2H, s), 6.44 (H-3a, H-3b, H-5a, H-5b, 4H, d,  $J = 8.8$  Hz), 6.67 (H-13a, H-13b, 2H, t,  $J = 7.4$  Hz), 6.88 (H-2a, H-2b, H-6a, H-6b, 4H, d,  $J = 8.8$  Hz), 7.07 (H-12a, H-12b, 2H, t,  $J = 7.4$  Hz), 7.19 (H-11a, H-11b, 2H, d,  $J = 7.4$  Hz), 7.33 (H-5a', H-5b', 2H, m), 7.47 (H-3a', H-3b', H-4a', H-4b',

4H, m), and 7.86 (H-6a', H-6b', 2H, d,  $J = 7.7$  Hz);  $^{13}\text{C}$  NMR ( $\text{CDCl}_3$ , 100 MHz)  $\delta$  45.6 (C-15a, C-15b), 50.3 (C-8a, C-8b), 55.1 (OMe, 4a, 4b), 57.0 (C-7a, C-7b), 113.4 (C-3a, C-3b, C-5a, C-5b), 123.4 (C-3a', C-3b'), 125.9 (C-11a, C-11b), 126.3 (C-13a, C-13b), 127.1 (C-12a, C-12b), 128.0 (C-2a, C-2b, C-6a, C-6b), 131.0 (C-14a, C-14b), 131.2 (C-10a, C-10b), 131.29 (C-6a', C-6b'), 131.3 (C-5a', C-5b'), 131.4 (C-1a, C-1b), 132.6 (C-1a', C-1b'), 132.7 (C-9a, C-9b), 133.5 (C-4a', C-4b'), 147.8 (C-2a', C-2b'), and 158.3 (C-4a, C-4b); HRMS (DART-TOF)  $m/z$ :  $[\text{M} + \text{H}]^+$  Calcd for  $\text{C}_{44}\text{H}_{39}\text{N}_4\text{O}_{10}\text{S}_2$ , 847.2108; Found 847.2124.

*Tetralinylisoquinoline (20be)*. Brownish oil. UV (EtOH)  $\lambda_{\text{max}}$  (log  $\epsilon$ ) 222 (4.57) and 279 (3.84) nm; IR (dry film)  $\nu_{\text{max}}$  3340, 2836, 1541, 1510, 1354, 1247, 1164, 1035, 736, and 582  $\text{cm}^{-1}$ ;  $^1\text{H}$  NMR ( $\text{CDCl}_3$ , 400 MHz)  $\delta$  3.58 (H-8a, 1H, br t,  $J = 7.0$  Hz), 3.65 (H-15b, 1H, m), 3.69 (OMe, 4b, 3H, s), 3.77 (OMe, 3a, 3H, s), 3.81 (H-15b, 1H, m), 3.99 (H-8b, 1H, br t,  $J = 6.4$  Hz), 4.34 (H-7b, 1H, d,  $J = 5.8$  Hz), 4.57 (H-15a, 1H, d,  $J = 16.8$  Hz), 4.76 (H-15a, 1H, d,  $J = 16.8$  Hz), 4.84 (NH, 1H, br t,  $J = 5.9$  Hz), 5.34 (H-7a, 1H, d,  $J = 7.4$  Hz), 6.30 (H-14a, 1H, d,  $J = 7.7$  Hz), 6.49 (H-13a, 1H, m), 6.50 (H-3b, H-5b, 2H, d,  $J = 8.8$  Hz), 6.58 (H-2b, H-6b, 2H, d,  $J = 8.8$  Hz), 6.77 (H-4a, 1H, dd,  $J = 8.4, 2.5$  Hz), 6.83 (H-5a, 1H, d,  $J = 8.4$  Hz), 6.84 (H-12a, 1H, t,  $J = 7.7$  Hz), 6.89 (H-11a, 1H, d,  $J = 7.7$  Hz), 6.96 (H-11b, 1H, dd,  $J = 7.6, 1.0$  Hz), 7.09 (H-12b, 1H, td,  $J = 7.6, 1.0$  Hz), 7.22 (H-2a, 1H, d,  $J = 2.5$  Hz), 7.26 (H-13b, 1H, m), 7.34 (H-14b, 1H, dd,  $J = 7.6, 1.0$  Hz), 7.35 (H-5a', 1H, td,  $J = 7.9, 1.3$  Hz), 7.44 (H-3a', 1H, dd,  $J = 7.9, 1.3$  Hz), 7.51 (H-4a', 1H, td,  $J = 7.9, 1.3$  Hz), 7.61 (H-6a', 1H, m), 7.62 (H-5b', 1H, td,  $J = 7.7, 1.4$  Hz), 7.69 (H-4b', 1H, td,  $J = 7.7, 1.4$  Hz), 7.81 (H-3b', 1H, dd,  $J = 7.7, 1.4$  Hz), and 7.92 (H-6b', 1H, dd,  $J = 7.7, 1.4$  Hz);  $^{13}\text{C}$  NMR ( $\text{CDCl}_3$ , 100 MHz)  $\delta$  42.4 (C-8a), 44.6 (C-15b), 44.9 (C-15a), 45.7 (C-8b), 47.6 (C-7b), 53.7 (C-7a), 55.20 (OMe, 4b), 55.24 (OMe, 3a),

111.5 (C-2a), 113.3 (C-3b, C-5b), 115.2 (C-4a), 123.9 (C-3a'), 125.3 (C-3b'), 125.7 (C-12a), 125.9 (C-11a), 126.3 (C-13a), 127.0 (C-12b), 127.6 (C-14b), 128.6 (C-14a), 128.7 (C-13b), 129.5 (C-11b), 130.0 (C-2b, C-6b), 131.0 (C-6a'), 131.1 (C-5a), 131.2 (C-6b'), 131.5 (C-5a'), 132.2 (C-6a), 132.5 (C-1a'), 132.7 (C-5b'), 133.0 (C-10a), 133.1 (C-1b'), 133.28 (C-10b), 133.33 (C-4a'), 133.6 (C-4b'), 134.6 (C-1a), 134.7 (C-9a), 136.7 (C-1b), 142.7 (C-9b), 147.5 (C-2a'), 148.0 (C-2b'), 157.7 (C-4b), and 158.8 (C-3a); HRMS (DART-TOF)  $m/z$ :  $[M + H]^+$  Calcd for  $C_{44}H_{39}N_4O_{10}S_2$ , 847.2108; Found 847.2133.

*Dihydroisoquinoline (20bh)*. Brownish oil. UV (EtOH)  $\lambda_{\max}$  (log  $\epsilon$ ) 223 (4.71) and 279 (4.08) nm; IR (dry film)  $\nu_{\max}$  3339, 2837, 1539, 1510, 1357, 1247, 1167, 1031, 732, and 577  $\text{cm}^{-1}$ ;  $^1\text{H}$  NMR ( $\text{CDCl}_3$ , 400 MHz)  $\delta$  3.49 (H-15b, 1H, br s), 3.67 (OMe, 4b, 3H, s), 3.73 (OMe, 4a, 3H, s), 4.09 (H-15b, 1H, br s), 4.47 (H-7b, 1H, d,  $J = 11.8$  Hz), 4.49 (H-15a, 1H, d,  $J = 14.9$  Hz), 4.79 (H-15a, 1H, d,  $J = 14.9$  Hz), 5.05 (NH, 1H, br s), 5.09 (H-8b, 1H, d,  $J = 11.8$  Hz), 6.55 (H-3b, H-5b, 2H, d,  $J = 8.6$  Hz), 6.72 (H-2b, H-6b, 2H, d,  $J = 8.6$  Hz), 6.75 (H-3a, H-5a, 2H, d,  $J = 8.6$  Hz), 6.84 (H-11b, 1H, m), 6.86 (H-7a, 1H, s), 6.91 (H-6a', 1H, br d,  $J = 5.6$  Hz), 7.03 (H-12b, 1H, t,  $J = 7.6$  Hz), 7.05 (H-11a, 1H, d,  $J = 7.4$  Hz), 7.09 (H-12a, 1H, t,  $J = 7.4$  Hz), 7.20 (H-13a, 1H, t,  $J = 7.4$  Hz), 7.25 (H-2a, H-6a, H-13b, 3H, m), 7.33 (H-5a', 1H, br t,  $J = 7.2$  Hz), 7.49 (H-14a, H-3a', H-4a', 3H, m), 7.68 (H-5b', 1H, t,  $J = 7.7$  Hz), 7.71 (H-14b, 1H, m), 7.74 (H-4b', 1H, t,  $J = 7.7$  Hz), 7.85 (H-3b', 1H, d,  $J = 7.7$  Hz), and 8.02 (H-6b', 1H, br d,  $J = 7.4$  Hz);  $^{13}\text{C}$  NMR ( $\text{CDCl}_3$ , 100 MHz)  $\delta$  43.4 (C-8b), 44.6 (C-15b), 47.7 (C-15a), 54.8 (C-7b), 55.1 (OMe, 4b), 55.2 (OMe, 4a), 113.2 (C-3b, C-5b), 114.1 (C-3a, C-5a), 122.2 (C-14a), 124.0 (C-3a'), 125.3 (C-3b'), 125.8 (C-11a), 125.9 (C-8a), 126.0 (C-7a), 127.2 (C-13b), 127.8 (C-12a), 128.2 (C-13a), 128.5 (C-11b), 128.6 (C-12b), 129.0 (C-10a, C-14b), 129.3 (C-2a, C-6a), 129.6 (C-6a'), 130.1 (C-2b, C-6b), 131.1 (C-6b'), 131.3 (C-9a), 131.8 (C-5a'),

132.1 (C-1a'), 132.7 (C-5b'), 133.1 (C-1b'), 133.4 (C-4a'), 133.8 (C-4b'), 134.1 (C-10b), 134.3 (C-1b), 135.1 (C-1a), 140.2 (C-9b), 147.8 (C-2a'), 148.2 (C-2b'), 157.8 (C-4a), and 157.9 (C-4b); HRMS (DART-TOF)  $m/z$ :  $[M + H]^+$  Calcd for  $C_{44}H_{39}N_4O_{10}S_2$ , 847.2108; Found 847.2118.

*Isoquinoline (20bi)*. Brownish oil. UV (EtOH)  $\lambda_{max}$  (log  $\epsilon$ ) 223 (4.56), 279 (3.76), and 318 (3.50) nm; IR (dry film)  $\nu_{max}$  3073, 2837, 1539, 1508, 1337, 1247, 1160, 1030, 756, and 584  $cm^{-1}$ ;  $^1H$  NMR ( $CDCl_3$ , 400 MHz)  $\delta$  3.59 (OMe, 4a, 3H, s), 3.70 (OMe, 4b, 3H, s), 3.77 (H-15b, 1H, br dd,  $J = 12.2, 5.5$  Hz), 4.01 (H-15b, 1H, dd,  $J = 13.6, 6.5$  Hz), 4.82 (H-7b, 1H, d,  $J = 11.7$  Hz), 5.39 (NH, 1H, br t,  $J = 6.0$  Hz), 5.72 (H-8b, 1H, d,  $J = 11.7$  Hz), 6.50 (H-3a, H-5a, 2H, d,  $J = 8.3$  Hz), 6.65 (H-3b, H-5b, 2H, d,  $J = 8.3$  Hz), 6.94 (H-2a, H-6a, H-11a, 3H, m), 6.96 (H-2b, H-6b, 2H, m), 7.01 (H-12b, 1H, t,  $J = 7.6$  Hz), 7.16 (H-13b, 1H, t,  $J = 7.6$  Hz), 7.48 (H-12a, 1H, t,  $J = 8.4$  Hz), 7.51 (H-14b, 1H, d,  $J = 7.6$  Hz), 7.62 (H-13a, 1H, t,  $J = 8.4$  Hz), 7.64 (H-5b', 1H, t,  $J = 7.8$  Hz), 7.72 (H-4b', 1H, t,  $J = 7.8$  Hz), 7.83 (H-11a, 1H, d,  $J = 8.4$  Hz), 7.86 (H-3b', 1H, d,  $J = 7.8$  Hz), 7.97 (H-6b', 1H, d,  $J = 7.8$  Hz), 8.19 (H-14a, 1H, d,  $J = 8.4$  Hz), 8.51 (H-7a, 1H, s), and 8.96 (H-15a, 1H, s);  $^{13}C$  NMR ( $CDCl_3$ , 100 MHz)  $\delta$  43.7 (C-8b), 44.8 (C-15b), 55.09 (OMe, 4a), 55.1 (OMe, 4b), 55.8 (C-7b), 113.5 (C-3b, C-5b), 113.6 (C-3a, C-5a), 122.8 (C-14a), 125.3 (C-3b'), 126.7 (C-12a), 126.8 (C-12b), 128.06 (C-10a), 128.1 (C-11a), 128.5 (C-13b), 129.1 (C-11b), 129.5 (C-14b), 129.6 (C-2a, C-6a), 130.0 (C-2b, C-6b), 130.5 (C-13a), 131.3 (C-6b'), 132.2 (C-8a), 132.6 (C-5b'), 133.2 (C-1b'), 133.7 (C-4b'), 133.8 (C-10b), 134.4 (C-1a), 134.5 (C-9a), 134.8 (C-1b), 140.9 (C-9b), 144.2 (C-7a), 148.2 (C-2b'), 151.0 (C-15a), 157.7 (C-4a), and 157.9 (C-4b); HRMS (DART-TOF)  $m/z$ :  $[M + H]^+$  Calcd for  $C_{38}H_{34}N_3O_6S$ , 660.2168; Found 660.2183.

### 3.8.19 Anodic oxidation of **21** in MeCN/ 0.2 M LiClO<sub>4</sub>

Controlled potential electrolysis of **21** (+0.99 V, 1.0 F) yielded a mixture, which on preparative radial chromatography (SiO<sub>2</sub>, *n*-hexane/EtOAc, 4/1 to 2% MeOH/EtOAc), gave **21ba** (18.8 mg, 24%) and **21bi** (17.0 mg, 27%).

*Bisisoquinoline (21ba)*. Yellowish oil. UV (EtOH)  $\lambda_{\max}$  (log  $\epsilon$ ) 227 (4.62), 275 (3.59), and 283 (3.46) nm; IR (dry film)  $\nu_{\max}$  1610, 1513, 1333, 1250, 1160, 1037, 748, and 559 cm<sup>-1</sup>; <sup>1</sup>H NMR (CDCl<sub>3</sub>, 400 MHz)  $\delta$  2.32 (Me, 4a', 4b', 6H, s), 3.36 (H-8a, H-8b, 2H, s), 3.67 (OMe, 4a, 4b, 6H, s), 4.39 (H-15a, H-15b, 2H, d,  $J$  = 15.6 Hz), 4.96 (H-15a, H-15b, 2H, d,  $J$  = 15.6 Hz), 5.81 (H-14a, H-14b, 2H, d,  $J$  = 8.0 Hz), 6.05 (H-7a, H-7b, 2H, s), 6.53 (H-3a, H-3b, H-5a, H-5b, 4H, d,  $J$  = 8.8 Hz), 6.59 (H-13a, H-13b, 2H, t,  $J$  = 8.0 Hz), 6.86 (H-2a, H-2b, H-6a, H-6b, 4H, d,  $J$  = 8.8 Hz), 7.01 (H-11a, H-11b, H-12a, H-12b, 4H, m), 7.07 (H-3a', H-3b', H-5a', H-5b', 4H, d,  $J$  = 8.4 Hz), and 7.60 (H-2a', H-2b', H-6a', H-6b', 4H, d,  $J$  = 8.4 Hz); <sup>13</sup>C NMR (CDCl<sub>3</sub>, 100 MHz)  $\delta$  21.5 (Me, 4a', 4b'), 44.7 (C-15a, C-15b), 50.3 (C-8a, C-8b), 55.2 (OMe, 4a, 4b), 57.5 (C-7a, C-7b), 113.5 (C-3a, C-3b, C-5a, C-5b), 125.5 (C-11a, C-11b), 126.0 (C-13a, C-13b), 126.7 (C-12a, C-12b), 127.5 (C-2a', C-2b', C-6a', C-6b'), 128.5 (C-2a, C-2b, C-6a, C-6b), 129.4 (C-3a', C-3b', C-5a', C-5b'), 131.2 (C-10a, C-10b), 131.3 (C-14a, C-14b), 131.9 (C-1a, C-1b), 133.3 (C-9a, C-9b), 136.3 (C-1a', C-1b'), 143.2 (C-4a', C-4b'), 158.4 (C-4a, C-4b); HRMS (DART-TOF)  $m/z$ : [M + H]<sup>+</sup> Calcd for C<sub>46</sub>H<sub>45</sub>N<sub>2</sub>O<sub>6</sub>S<sub>2</sub>, 785.2719; Found 785.2724.

*Isoquinoline (21bi)*. Yellowish oil. UV (EtOH)  $\lambda_{\max}$  (log  $\epsilon$ ) 226 (4.81), 278 (3.91), 288 (3.82), 314 (3.67), and 326 (3.77) nm; IR (dry film)  $\nu_{\max}$  3208, 2836, 1608, 1510, 1328,

1249, 1158, 1035, 754, and 552  $\text{cm}^{-1}$ ;  $^1\text{H}$  NMR ( $\text{CDCl}_3$ , 400 MHz)  $\delta$  2.45 (Me, 4b', 3H, s), 3.61 (OMe, 4b, 3H, s), 3.72 (OMe, 4a, 3H, s), 3.83 (H-15b, 2H, m), 4.05 (NH, 1H, br s), 4.81 (H-7b, 1H, d,  $J = 12.0$  Hz), 5.66 (H-8b, 1H, d,  $J = 12.0$  Hz), 6.53 (H-3b, H-5b, 2H, d,  $J = 8.8$  Hz), 6.65 (H-3a, H-5a, 2H, d,  $J = 8.8$  Hz), 6.88 (H-2a, H-6a, H-14b, 3H, m), 6.94 (H-2b, H-6b, 2H, d,  $J = 8.8$  Hz), 7.01 (H-13b, 1H, t,  $J = 8.0$  Hz), 7.16 (H-12b, 1H, t,  $J = 8.0$  Hz), 7.33 (H-3b', H-5b', 2H, d,  $J = 8.4$  Hz), 7.49 (H-12a, H-11b, 2H, m), 7.62 (H-13a, 1H, t,  $J = 8.4$  Hz), 7.74 (H-2b', H-6b', 2H, d,  $J = 8.4$  Hz), 7.83 (H-11a, 1H, d,  $J = 8.4$  Hz), 8.12 (H-14a, 1H, d,  $J = 8.4$  Hz), 8.53 (H-7a, 1H, s), and 8.95 (H-15a, 1H, s);  $^{13}\text{C}$  NMR ( $\text{CDCl}_3$ , 100 MHz)  $\delta$  21.7 (Me, 4b'), 43.7 (C-8b), 44.5 (C-15b), 55.16 (OMe, 4b), 55.24 (OMe, 4a), 55.8 (C-7b), 113.6 (C-3a, C-5a), 113.7 (C-3b, C-5b), 122.8 (C-14a), 126.8 (C-12a), 126.9 (C-13b), 127.4 (C-2b', C-6b'), 128.18 (C-10a), 128.23 (C-11a), 128.5 (C-12b), 129.4 (C-11b), 129.6 (C-2b, C-6b), 129.7 (C-14b), 129.9 (C-3b', C-5b'), 130.2 (C-2a, C-6a), 130.6 (C-13a), 132.2 (C-8a), 134.2 (C-9b), 134.4 (C-1b), 134.6 (C-9a), 135.0 (C-1a), 136.5 (C-1b'), 141.0 (C-10b), 143.8 (C-4b'), 144.1 (C-7a), 151.1 (C-15a), 157.8 (C-4b), and 158.0 (C-4a); HRMS (DART-TOF)  $m/z$ :  $[\text{M} + \text{H}]^+$  Calcd for  $\text{C}_{39}\text{H}_{37}\text{N}_2\text{O}_4\text{S}$ , 629.2474; Found 629.2479.

### 3.8.20 Anodic oxidation of **22** in MeCN/ 0.2 M LiClO<sub>4</sub>

Controlled potential electrolysis of **22** (+1.02 V, 1.0 F) yielded a mixture, which on preparative radial chromatography ( $\text{SiO}_2$ , *n*-hexane/ $\text{CH}_2\text{Cl}_2$ , 1/2 to 5% MeOH/ $\text{CH}_2\text{Cl}_2$ ), gave **22bb** (9.5 mg, 17%) and **22bi** (7.2 mg, 14%).

*Bisisoquinoline (22ba)*. Yellowish oil. UV (EtOH)  $\lambda_{\text{max}}$  (log  $\epsilon$ ) 225 (4.39) and 272 (3.53) nm; IR (dry film)  $\nu_{\text{max}}$  2933, 1635, 1510, 1404, 1247, 1032, and 731  $\text{cm}^{-1}$ ;  $^1\text{H}$

NMR (CDCl<sub>3</sub>, 400 MHz)  $\delta$  2.20 (NCOMe, 17a, 3H, s), 2.44 (NCOMe, 17b, 3H, s), 3.06 (H-8a, 1H, dd,  $J = 10.0, 1.5$  Hz), 3.40 (H-8b, 1H, d,  $J = 10.0$  Hz), 3.67 (OMe, 4a, 3H, s), 3.70 (OMe, 4b, 3H, s), 4.45 (H-15b, 1H, d,  $J = 16.4$  Hz), 4.83 (H-15b, 1H, d,  $J = 16.4$  Hz), 4.97 (H-15a, 2H, s), 5.77 (H-7a, 1H, br d,  $J = 1.5$  Hz), 5.92 (H-14a, 1H, d,  $J = 7.5$  Hz), 5.99 (H-14b, 1H, d,  $J = 7.4$  Hz), 6.64 (H-7b, 1H, s), 6.66 (H-3a, H-5a, 2H, d,  $J = 8.6$  Hz), 6.69 (H-3b, H-5b, 2H, d,  $J = 8.7$  Hz), 6.71 (H-13a, 1H, m), 6.74 (H-13b, 1H, t,  $J = 7.4$  Hz), 6.89 (H-2a, H-6a, 2H, d,  $J = 8.6$  Hz), 6.96 (H-2b, H-6b, 11b, 3H, m), 7.05 (H-12b, 1H, t,  $J = 7.4$  Hz), 7.10 (H-12a, 1H, t,  $J = 7.5$  Hz), and 7.22 (H-11a, 1H, d,  $J = 7.5$  Hz); <sup>13</sup>C NMR (CDCl<sub>3</sub>, 100 MHz)  $\delta$  22.35 (C-17a), 22.39 (C-17b), 45.1 (C-15a), 45.3 (C-8b), 45.6 (C-15b), 51.1 (C-7b), 51.9 (C-8a), 55.1 (OMe, 4a), 55.2 (OMe, 4b), 58.3 (C-7a), 113.8 (C-3a, C-5a), 113.9 (C-3b, C-5b), 125.5 (C-11b), 126.0 (C-13a), 126.1 (C-13b), 126.3 (C-11a), 126.8 (C-12b), 127.0 (C-2a, C-6a), 127.1 (C-12a), 128.2 (C-2b, C-6b), 130.5 (C-14a), 130.7 (C-1b), 130.8 (C-10b), 131.1 (C-14b), 132.5 (C-10a), 133.2 (C-9a), 133.5 (C-1a), 134.1 (C-9b), 158.4 (C-4a), 158.6 (C-4b), 170.9 (C-16b), and 172.1 (C-16a); HRMS (DART-TOF)  $m/z$ : [M + H]<sup>+</sup> Calcd for C<sub>36</sub>H<sub>37</sub>N<sub>2</sub>O<sub>4</sub>, 561.2753; Found 561.2736.

*Isoquinoline (22bi)*. Light yellowish oil. UV (EtOH)  $\lambda_{\max}$  (log  $\epsilon$ ) 221 (3.09) and 285 (3.09) nm; IR (dry film)  $\nu_{\max}$  3203, 2935, 1660, 1509, 1246, 1028, and 751 cm<sup>-1</sup>; <sup>1</sup>H NMR (CDCl<sub>3</sub>, 400 MHz)  $\delta$  1.74 (NHCOMe, 17b, 3H, s), 3.61 (OMe, 4b, 3H, s), 3.72 (OMe, 4a, 3H, s), 4.15 (H-15b, 1H, d,  $J = 14.2$  Hz), 4.52 (NH, 1H, br s), 4.68 (H-15b, 1H, dd,  $J = 14.2, 6.5$  Hz), 4.86 (H-7b, 1H, d,  $J = 11.7$  Hz), 5.70 (H-8b, 1H, d,  $J = 11.7$  Hz), 6.55 (H-3b, H-5b, 2H, d,  $J = 7.8$  Hz), 6.68 (H-3a, H-5a, 2H, d,  $J = 7.8$  Hz), 6.89 (H-2a, H-6a, 2H, d,  $J = 7.8$  Hz), 6.95 (H-2b, H-6b, 2H, d,  $J = 7.8$  Hz), 7.08 (H-11b, H-12b, 2H, br s), 7.16 (H-13b, 1H, t,  $J = 7.7$  Hz), 7.48 (H-14b, 1H, d,  $J = 7.7$  Hz), 7.50 (H-

12a, 1H, t,  $J = 8.0$  Hz), 7.60 (H-13a, 1H, t,  $J = 8.0$  Hz), 7.86 (H-11a, 1H, d,  $J = 8.0$  Hz), 7.93 (H-14a, 1H, d,  $J = 8.0$  Hz), 8.56 (H-7a, 1H, s), and 8.99 (H-15a, 1H, s);  $^{13}\text{C}$  NMR ( $\text{CDCl}_3$ , 100 MHz)  $\delta$  22.8 (C-17b), 40.3 (C-15b), 43.6 (C-8b), 55.09 (OMe, 4b), 55.13 (OMe, 4a), 55.6 (C-7b), 113.5 (C-3a, C-5a), 113.8 (C-3b, C-5b), 122.4 (C-14a), 126.8 (C-12a), 126.9 (C-12b), 127.8 (C-13b), 128.1 (C-10a), 128.3 (C-11a), 129.0 (C-14b), 129.3 (C-11b), 129.5 (C-2b, C-6b), 130.3 (C-2a, C-6a), 130.7 (C-13a), 132.4 (C-8a), 134.3 (C-1b), 134.6 (C-9a), 135.4 (C-1a), 136.1 (C-10b), 140.2 (C-9b), 143.5 (C-7a), 150.9 (C-15a), 157.7 (C-4a), 157.9 (C-4b), and 169.7 (C-16b); HRMS (DART-TOF)  $m/z$ :  $[\text{M} + \text{H}]^+$  Calcd for  $\text{C}_{34}\text{H}_{33}\text{N}_2\text{O}_3$ , 517.2491; Found 517.2491.

### 3.8.21 Anodic oxidation of **23** in MeCN/ 0.2 M LiClO<sub>4</sub>

Controlled potential electrolysis of **23** (+0.99 V, 1.0 F) yielded a mixture, which on preparative radial chromatography ( $\text{SiO}_2$ , *n*-hexane/EtOAc, 4/1 to 100% EtOAc), gave **23bi** (8.0 mg, 14%).

*Isoquinoline* (**23bi**). Yellowish oil. UV (EtOH)  $\lambda_{\text{max}}$  ( $\log \epsilon$ ) 225 (4.76), 278 (3.99), 288 (3.92), 314 (3.78), and 327 (3.84) nm; IR (dry film)  $\nu_{\text{max}}$  3336, 2954, 1709, 1510, 1247, 1178, 1034, 752  $\text{cm}^{-1}$ ;  $^1\text{H}$  NMR ( $\text{CDCl}_3$ , 400 MHz)  $\delta$  3.61 (OMe, 4b, 3H, s), 3.67 (NHCO<sub>2</sub>Me, 3H, s), 3.72 (OMe, 4a, 3H, s), 4.09 (H-15b, NH, 2H, m), 4.43 (H-15b, 1H, dd,  $J = 14.4, 6.8$  Hz), 4.85 (H-7b, 1H, d,  $J = 12.0$  Hz), 5.67 (H-8b, 1H, br d,  $J = 11.2$  Hz), 6.54 (H-3b, H-5b, 2H, d,  $J = 8.4$  Hz), 6.66 (H-3a, H-5a, 2H, d,  $J = 8.4$  Hz), 6.87 (H-2a, H-6a, 2H, d,  $J = 8.4$  Hz), 6.95 (H-2b, H-6b, 2H, br d,  $J = 8.0$  Hz), 7.10 (H-11b, H-12b, 2H, m), 7.15 (H-13b, 1H, m), 7.47 (H-14b, 1H, m), 7.48 (H-12a, 1H, t,  $J = 8.0$  Hz), 7.58 (H-13a, 1H, t,  $J = 8.0$  Hz), 7.85 (H-11a, 1H, d,  $J = 8.0$  Hz), 7.95 (H-14a, 1H,

br d,  $J = 8.4$  Hz), 8.56 (H-7a, 1H, s), and 8.99 (H-15a, 1H, s);  $^{13}\text{C}$  NMR ( $\text{CDCl}_3$ , 100 MHz)  $\delta$  41.8 (C-15b), 43.7 (C-8b), 52.3 ( $\text{NHCO}_2\text{Me}$ ), 55.2 (OMe, 4a, 4b), 55.6 (C-7b), 113.5 (C-3a, C-5a), 113.8 (C-3b, C-5b), 122.4 (C-14a), 126.7 (C-12a), 126.9 (C-12b), 127.8 (C-13b), 128.2 (C-10a), 128.4 (C-11a), 128.7 (C-11b), 129.1 (C-14b), 129.6 (C-2b, C-6b), 130.1 (C-2a, C-6a), 130.5 (C-13a), 132.3 (C-8a), 134.58 (C-1b), 134.61 (C-9a), 135.2 (C-1a), 136.3 (C-10b), 140.2 (C-9b), 143.9 (C-7a), 151.1 (C-15a), 157.1 (C-16b), 157.8 (C-4b), and 157.9 (C-4a); HRMS (DART-TOF)  $m/z$ :  $[\text{M} + \text{H}]^+$  Calcd for  $\text{C}_{34}\text{H}_{33}\text{N}_2\text{O}_4$ , 533.2440; Found 533.2438.

### 3.8.22 Anodic oxidation of 24 in MeCN/ 0.2 M LiClO<sub>4</sub>

Controlled potential electrolysis of **24** (+0.90 V, 1.0 F) yielded a mixture, which on preparative radial chromatography ( $\text{SiO}_2$ , *n*-hexane/ $\text{CH}_2\text{Cl}_2$ , 1/1 to 5% MeOH/ $\text{CH}_2\text{Cl}_2$ ), gave **24ba** (21.2 mg, 25%).

*Bisisoquinoline (24ba)*. Yellowish oil. UV (EtOH)  $\lambda_{\text{max}}$  ( $\log \epsilon$ ) 227 (4.51), 279 (3.72), and 286 (3.65) nm; IR (dry film)  $\nu_{\text{max}}$  1595, 1517, 1332, 1257, 1027, 753, and 555  $\text{cm}^{-1}$ ;  $^1\text{H}$  NMR ( $\text{CDCl}_3$ , 400 MHz)  $\delta$  2.33 (Me, 4a', 4b', 6H, s), 3.40 (H-8a, H-8b, 2H, s), 3.60 (OMe, 3a, 3b, 6H, s), 3.72 (OMe, 4a, 4b, 6H, s), 4.44 (H-15a, H-15b, 2H, d,  $J = 15.6$  Hz), 5.03 (H-15a, H-15b, 2H, d,  $J = 15.6$  Hz), 5.87 (H-14a, H-14b, 2H, d,  $J = 7.6$  Hz), 6.15 (H-7a, H-7b, 2H, s), 6.34 (H-6a, H-6b, 2H, dd,  $J = 8.4, 1.8$  Hz), 6.42 (H-5a, H-5b, 2H, d,  $J = 8.4$  Hz), 6.61 (H-13a, H-13b, 2H, t,  $J = 7.6$  Hz), 6.64 (H-2a, H-2b, 2H, d,  $J = 1.8$  Hz), 7.00 (H-12a, H-12b, 2H, t,  $J = 7.6$  Hz), 7.04 (H-11a, H-11b, 2H, d,  $J = 7.6$  Hz), 7.09 (H-3a', H-3b', H-5a', H-5b', 4H, d,  $J = 8.1$  Hz), and 7.62 (H-2a', H-2b', H-6a', H-6b', 4H, d,  $J = 8.1$  Hz);  $^{13}\text{C}$  NMR ( $\text{CDCl}_3$ , 100 MHz)  $\delta$  21.4 (Me, 4a', 4b'), 44.9 (C-15a,

C-15b), 50.5 (C-8a, C-8b), 55.6 (OMe, 3a, 3b), 55.7 (OMe, 4a, 4b), 57.4 (C-7a, C-7b), 110.4 (C-5a, C-5b), 110.6 (C-2a, C-2b), 119.0 (C-6a, C-6b), 125.3 (C-11a, C-11b), 126.1 (C-13a, C-13b), 126.7 (C-12a, C-12b), 127.4 (C-2a', C-2b', C-6a', C-6b'), 129.3 (C-2a', C-2b', C-6a', C-6b'), 131.0 (C-10a, C-10b), 131.3 (C-14a, C-14b), 132.5 (C-1a, C-1b), 133.2 (C-9a, C-9b), 136.2 (C-1a', C-1b'), 143.2 (C-4a', C-4b'), 147.6 (C-4a, C-4b), and 148.4 (C-3a, C-3b); HRMS (DART-TOF)  $m/z$ :  $[M + H]^+$  Calcd for  $C_{48}H_{49}N_2O_8S_2$ , 845.2930; Found 845.2938.

### 3.8.23 Anodic oxidation of stilbenes **25**, **26**, and **27** in MeCN/ 0.2 M LiClO<sub>4</sub>

Controlled potential electrolysis of **25** (+1.01 V, 1.0 F), **26** (+1.01 V, 1.0 F), and **27** (+0.87 V, 1.0 F) yielded a complex mixture of insoluble polymeric products.

### 3.8.24 Anodic oxidation of **28** in MeCN/ 0.2 M LiClO<sub>4</sub>

Controlled potential electrolysis of **28** (+1.04 V, 1.0 F) yielded a mixture, which on preparative radial chromatography (SiO<sub>2</sub>, *n*-hexane/CH<sub>2</sub>Cl<sub>2</sub>, 1/1 to 5% MeOH/CH<sub>2</sub>Cl<sub>2</sub>), gave **28ba** (14.7 mg, 29%), **28bb** (12.2 mg, 24%), and **28bc** (9.1 mg, 18%).

*Bis- $\delta$ -lactone (28ba)*. Colorless oil and, subsequently, colorless block crystals from CH<sub>2</sub>Cl<sub>2</sub>/MeOH; mp 173–175 °C; UV (EtOH)  $\lambda_{\max}$  (log  $\epsilon$ ) 229 (4.57), 284 (3.68), and 294 (3.41) nm; IR (dry film)  $\nu_{\max}$  1716, 1607, 1513, 1251, 1236, 1030, and 749 cm<sup>-1</sup>; <sup>1</sup>H NMR (CDCl<sub>3</sub>, 400 MHz)  $\delta$  3.71 (OMe, 4a, 4b, 6H, s), 3.80 (H-8a, H-8b, 2H, s), 6.16 (H-14a, H-14b, 2H, d,  $J = 7.5$  Hz), 6.21 (H-7a, H-7b, 2H, s), 6.75 (H-3a, H-5a, H-3b, H-5b, 4H, d,  $J = 8.7$  Hz), 7.07 (H-13a, H-13b, 2H, t,  $J = 7.5$  Hz), 7.15 (H-2a, H-6a, H-2b,

H-6b, 2H, d,  $J = 8.7$  Hz), 7.24 (H-12a, H-12b, 2H, t,  $J = 7.5$  Hz), and 8.04 (H-11a, H-11b, 2H, d,  $J = 7.5$  Hz);  $^{13}\text{C}$  NMR ( $\text{CDCl}_3$ , 100 MHz)  $\delta$  45.4 (C-8a, C-8b), 55.2 (OMe, 4a, 4b), 79.6 (C-7a, C-7b), 114.1 (C-3a, C-5a, C-3b, C-5b), 124.8 (C-10a, C-10b), 127.2 (C-2a, C-6a, C-2b, C-6b), 128.3 (C-12a, C-12b), 129.59 (C-14a, C-14b), 129.62 (C-1a, C-1b), 129.8 (C-11a, C-11b), 133.5 (C-13a, C-13b), 137.9 (C-9a, C-9b), 159.3 (C-4a, C-4b), and 164.2 (C-15a, C-15b); HRMS (DART-TOF)  $m/z$ :  $[\text{M} + \text{H}]^+$  Calcd for  $\text{C}_{32}\text{H}_{27}\text{O}_6$ , 507.1808; Found 507.1826.

*Bis- $\delta$ -lactone (28bb)*. Colorless oil and, subsequently, colorless block crystals from  $\text{CH}_2\text{Cl}_2/\text{MeOH}$ ; mp 151–153 °C; UV (EtOH)  $\lambda_{\text{max}}$  ( $\log \epsilon$ ) 228 (4.62), 283 (3.79), and 295 (3.37) nm; IR (dry film)  $\nu_{\text{max}}$  1725, 1609, 1514, 1252, 1031, and 758  $\text{cm}^{-1}$ ;  $^1\text{H}$  NMR ( $\text{CDCl}_3$ , 400 MHz)  $\delta$  3.49 (H-8b, 1H, t,  $J = 3.6$  Hz), 3.60 (H-8a, 1H, d,  $J = 3.6$  Hz), 3.65 (OMe, 4a, 3H, s), 3.89 (OMe, 4b, 3H, s), 5.95 (H-7a, 1H, s), 6.03 (H-7b, 1H, d,  $J = 3.6$  Hz), 6.32 (H-14b, 1H, d,  $J = 7.7$  Hz), 6.59 (H-3a, H-5a, 2H, d,  $J = 8.8$  Hz), 6.73 (H-2a, H-6a, 2H, d,  $J = 8.8$  Hz), 6.89 (H-14a, 1H, d,  $J = 7.7$  Hz), 7.04 (H-3b, H-5b, 2H, d,  $J = 8.8$  Hz), 7.31 (H-12a, 1H, t,  $J = 7.7$  Hz), 7.35 (H-13b, 1H, t,  $J = 7.7$  Hz), 7.44 (H-13a, 1H, t,  $J = 7.7$  Hz), 7.50 (H-12b, 1H, t,  $J = 7.7$  Hz), 7.54 (H-2b, H-6b, 2H, d,  $J = 8.8$  Hz), 7.87 (H-11a, 1H, d,  $J = 7.7$  Hz), and 8.28 (H-11b, 1H, d,  $J = 7.7$  Hz);  $^{13}\text{C}$  NMR ( $\text{CDCl}_3$ , 100 MHz)  $\delta$  41.9 (C-8a), 48.7 (C-8b), 55.1 (OMe, 4a), 55.5 (OMe, 4b), 78.7 (C-7a), 81.2 (C-7b), 113.7 (C-3a, C-5a), 114.6 (C-3b, C-5b), 125.2 (C-10b), 126.4 (C-2b, C-6b), 126.5 (C-2a, C-6a), 128.0 (C-14a, C-14b), 128.2 (C-12a), 128.6 (C-1b), 129.0 (C-12b), 129.2 (C-11a), 130.7 (C-1a), 131.3 (C-11b), 133.4 (C-13b), 134.2 (C-13a), 139.0 (C-9b), 139.1 (C-9a), 158.9 (C-4a), 159.6 (C-4b), 163.4 (C-15a), and 164.9 (C-15b); HRMS (DART-TOF)  $m/z$ :  $[\text{M} + \text{H}]^+$  Calcd for  $\text{C}_{32}\text{H}_{27}\text{O}_6$ , 507.1808; Found 507.1814.

*Bis- $\delta$ -lactone (28bc)*. Colorless oil and, subsequently, colorless block crystals from CH<sub>2</sub>Cl<sub>2</sub>/MeOH; mp 144–146 °C; UV (EtOH)  $\lambda_{\text{max}}$  (log  $\epsilon$ ) 228 (4.12), 283 (3.26), and 295 (2.98) nm; IR (dry film)  $\nu_{\text{max}}$  1721, 1608, 1514, 1253, 1238, 1080, and 759 cm<sup>-1</sup>; <sup>1</sup>H NMR (CDCl<sub>3</sub>, 400 MHz)  $\delta$  3.57 (H-8a, H-8b, 2H, s), 3.67 (OMe, 4a, 4b, 6H, s), 5.67 (H-7a, H-7b, 2H, s), 6.66 (H-3a, H-5a, H-3b, H-5b, 4H, d,  $J = 8.8$  Hz), 6.91 (H-2a, H-6a, H-2b, H-6b, 2H, d,  $J = 8.7$  Hz), 7.45 (H-12a, H-12b, 2H, td,  $J = 7.6, 1.0$  Hz), 7.56 (H-14a, H-14b, 2H, dd,  $J = 7.6, 1.0$  Hz), 7.61 (H-13a, H-13b, 2H, td,  $J = 7.6, 1.0$  Hz), and 8.13 (H-11a, H-11b, 2H, dd,  $J = 7.6, 1.0$  Hz); <sup>13</sup>C NMR (CDCl<sub>3</sub>, 100 MHz)  $\delta$  45.7 (C-8a, C-8b), 55.2 (OMe, 4a, 4b), 78.7 (C-7a, C-7b), 113.9 (C-3a, C-5a, C-3b, C-5b), 125.1 (C-10a, C-10b), 126.9 (C-2a, C-6a, C-2b, C-6b), 129.0 (C-12a, C-12b), 129.6 (C-1a, C-1b), 129.9 (C-14a, C-14b), 130.7 (C-11a, C-11b), 134.3 (C-13a, C-13b), 138.1 (C-9a, C-9b), 159.1 (C-4a, C-4b), and 164.3 (C-15a, C-15b); HRMS (DART-TOF)  $m/z$ : [M + H]<sup>+</sup> Calcd for C<sub>32</sub>H<sub>27</sub>O<sub>6</sub>, 507.1808; Found 507.1820.

### 3.8.25 Anodic oxidation of **29** in MeCN/ 0.2 M LiClO<sub>4</sub>

Controlled potential electrolysis of **29** (+0.98 V, 1.0 F) yielded a mixture, which on preparative radial chromatography (SiO<sub>2</sub>, *n*-hexane/CH<sub>2</sub>Cl<sub>2</sub>, 1/1 to 5% MeOH/CH<sub>2</sub>Cl<sub>2</sub>), gave **29ba** (11.9 mg, 21%), **29bb** (9.6 mg, 17%), **29bc** (9.1 mg, 16%), and **29bj** (3.4 mg, 6%).

*Bis- $\delta$ -lactone (29ba)*. Colorless oil; UV (EtOH)  $\lambda_{\text{max}}$  (log  $\epsilon$ ) 233 (4.36) and 283 (3.74) nm; IR (dry film)  $\nu_{\text{max}}$  1718, 1604, 1517, 1245, 1025, and 749 cm<sup>-1</sup>; <sup>1</sup>H NMR (CDCl<sub>3</sub>, 400 MHz)  $\delta$  3.76 (OMe, 3a, 3b, 6H, s), 3.79 (OMe, 4a, 4b, 6H, s), 3.82 (H-8a, H-8b, 2H, s), 6.19 (H-14a, H-14b, 2H, d,  $J = 7.6$  Hz), 6.20 (H-7a, H-7b, 2H, s), 6.72 (H-2a, H-

2b, H-5a, H-5b, H-6a, H-6b, 6H, m), 7.10 (H-13a, H-13b, 2H, t,  $J = 7.6$  Hz), 7.26 (H-12a, H-12b, 2H, t,  $J = 7.6$  Hz), and 8.05 (H-11a, H-11b, 2H, d,  $J = 7.6$  Hz);  $^{13}\text{C}$  NMR ( $\text{CDCl}_3$ , 100 MHz)  $\delta$  45.2 (C-8a, C-8b), 55.8 (OMe, 4a, 4b), 55.9 (OMe, 3a, 3b), 79.6 (C-7a, C-7b), 109.4 (C-2a, C-2b), 111.0 (C-5a, C-5b), 118.5 (C-6a, C-6b), 124.9 (C-10a, C-10b), 128.3 (C-12a, C-12b), 129.6 (C-14a, C-14b), 129.8 (C-11a, C-11b), 130.0 (C-1a, C-1b), 133.5 (C-13a, C-13b), 138.0 (C-9a, C-9b), 148.8 (C-4a, C-4b), 149.0 (C-3a, C-3b), and 164.2 (C-15a, C-15b); HRMS (DART-TOF)  $m/z$ :  $[\text{M} + \text{H}]^+$  Calcd for  $\text{C}_{34}\text{H}_{31}\text{O}_8$ , 567.2019; Found 567.2026.

*Bis- $\delta$ -lactone (29bb)*. Colorless oil; UV (EtOH)  $\lambda_{\text{max}}$  ( $\log \epsilon$ ) 233 (4.35) and 282 (3.79) nm; IR (dry film)  $\nu_{\text{max}}$  1724, 1604, 1517, 1255, 1241, 1025, and 752  $\text{cm}^{-1}$ ;  $^1\text{H}$  NMR ( $\text{CDCl}_3$ , 400 MHz)  $\delta$  3.52 (H-8b, 1H, t,  $J = 3.6$  Hz), 3.63 (OMe, 3a, 3H, s), 3.68 (H-8a, 1H, d,  $J = 3.6$  Hz), 3.72 (OMe, 4a, 3H, s), 3.84 (OMe, 3b, 3H, s), 3.96 (OMe, 4b, 3H, s), 6.02 (H-7a, 1H, s), 6.05 (H-7b, 1H, d,  $J = 3.6$  Hz), 6.27 (H-14b, 1H, d,  $J = 7.6$  Hz), 6.32 (H-6a, 1H, m), 6.33 (H-2a, 1H, s), 6.52 (H-5a, 1H, d,  $J = 8.4$  Hz), 6.97 (H-14a, 1H, d,  $J = 7.6$  Hz), 7.03 (H-5b, 1H, d,  $J = 8.8$  Hz), 7.15 (H-2b, 1H, s), 7.16 (H-6b, 1H, m), 7.34 (H-12a, 1H, t,  $J = 7.6$  Hz), 7.35 (H-13b, 1H, t,  $J = 7.6$  Hz), 7.49 (H-13a, 1H, t,  $J = 7.6$  Hz), 7.50 (H-12b, 1H, t,  $J = 7.6$  Hz), 7.86 (H-11a, 1H, d,  $J = 7.6$  Hz), and 8.29 (H-11b, 1H, d,  $J = 7.6$  Hz);  $^{13}\text{C}$  NMR ( $\text{CDCl}_3$ , 100 MHz)  $\delta$  41.7 (C-8a), 48.5 (C-8b), 55.66 (OMe, 3a), 55.71 (OMe, 4a), 55.05 (OMe, 3b), 55.11 (OMe, 4b), 78.6 (C-7a), 81.0 (C-7b), 108.4 (C-2b), 108.8 (C-2a), 110.6 (C-5a), 111.7 (C-5b), 117.4 (C-6b), 117.5 (C-6a), 125.2 (C-10b), 126.6 (C-10a), 127.9 (C-14a), 128.0 (C-14b), 128.3 (C-12a), 129.0 (C-12b), 129.2 (C-1b), 129.3 (C-11a), 131.1 (C-1a), 131.3 (C-11b), 133.5 (C-13b), 134.3 (C-13a), 138.8 (C-9b), 139.0 (C-9a), 148.4 (C-4a), 148.85 (C-3a), 148.90 (C-4b), 149.6

(C-3b), 163.3 (C-15a), and 164.8 (C-15b); HRMS (DART-TOF)  $m/z$ :  $[M + H]^+$  Calcd for  $C_{34}H_{31}O_8$ , 567.2019; Found 567.2029.

*Bis- $\delta$ -lactone (29bc)*. Colorless oil; UV (EtOH)  $\lambda_{\max}$  ( $\log \epsilon$ ) 232 (4.00) and 284 (3.45) nm; IR (dry film)  $\nu_{\max}$  1720, 1604, 1517, 1256, 1236, 1025, and 753  $\text{cm}^{-1}$ ;  $^1\text{H}$  NMR ( $\text{CDCl}_3$ , 400 MHz)  $\delta$  3.62 (H-8a, H-8b, 2H, s), 3.70 (OMe, 3a, 3b, 6H, s), 3.75 (OMe, 4a, 4b, 6H, s), 5.67 (H-7a, H-7b, 2H, s), 6.50 (H-6a, H-6b, 2H, dd,  $J = 8.4, 1.9$  Hz), 6.55 (H-2a, H-2b, 2H, d,  $J = 1.9$  Hz), 6.61 (H-5a, H-5b, 2H, d,  $J = 8.4$  Hz), 7.47 (H-12a, H-12b, 2H, t,  $J = 7.6$  Hz), 7.59 (H-14a, H-14b, 2H, d,  $J = 7.6$  Hz), 7.64 (H-13a, H-13b, 2H, t,  $J = 7.6$  Hz), and 8.13 (H-11a, H-11b, 2H, d,  $J = 7.6$  Hz);  $^{13}\text{C}$  NMR ( $\text{CDCl}_3$ , 100 MHz)  $\delta$  45.4 (C-8a, C-8b), 55.77 (OMe, 4a, 4b), 55.84 (OMe, 3a, 3b), 78.7 (C-7a, C-7b), 109.3 (C-2a, C-2b), 110.8 (C-5a, C-5b), 118.3 (C-6a, C-6b), 125.1 (C-10a, C-10b), 129.0 (C-12a, C-12b), 129.9 (C-14a, C-14b), 130.0 (C-1a, C-1b), 130.7 (C-11a, C-11b), 134.3 (C-13a, C-13b), 138.2 (C-9a, C-9b), 148.6 (C-4a, C-4b), 148.9 (C-3a, C-3b), and 164.3 (C-15a, C-15b); HRMS (DART-TOF)  $m/z$ :  $[M + H]^+$  Calcd for  $C_{34}H_{31}O_8$ , 567.2019; Found 567.2022.

*$\delta$ -Lactone (29bj)*. Colorless oil; UV (EtOH)  $\lambda_{\max}$  ( $\log \epsilon$ ) 233 (4.11) and 281 (3.50) nm; IR (dry film)  $\nu_{\max}$  1721, 1605, 1518, 1268, 1240, 1026, and 770  $\text{cm}^{-1}$ ;  $^1\text{H}$  NMR ( $\text{CDCl}_3$ , 400 MHz)  $\delta$  3.12 (H-8, 1H, dd,  $J = 16.4, 3.0$  Hz), 3.37 (H-8, 1H, dd,  $J = 16.4, 12.1$  Hz), 3.90 (OMe, 4, 3H, s), 3.92 (OMe, 3, 2H, s), 5.51 (H-7, 1H, dd,  $J = 12.1, 3.0$  Hz), 6.88 (H-5, 1H, d,  $J = 8.2$  Hz), 6.99 (H-6, 1H, dd,  $J = 8.2, 1.8$  Hz), 7.04 (H-2, 1H, d,  $J = 1.8$  Hz), 7.29 (H-14, 1H, d,  $J = 7.7$  Hz), 7.44 (H-12, 1H, t,  $J = 7.7$  Hz), 7.58 (H-12, 1H, t,  $J = 7.7$  Hz), and 8.16 (H-11, 1H, d,  $J = 7.7$  Hz);  $^{13}\text{C}$  NMR ( $\text{CDCl}_3$ , 100 MHz)  $\delta$  35.6 (C-

8), 55.98 (OMe), 56.00 (OMe), 80.0 (C-7), 109.4 (C-2), 111.0 (C-5), 118.7 (C-6), 125.2 (C-10), 127.3 (C-14), 127.9 (C-12), 130.5 (C-11), 131.1 (C-1), 133.9 (C-13), 139.0 (C-9), 149.2 (C-3), 149.3 (C-4), and 165.5 (C-15); HRMS (DART-TOF)  $m/z$ :  $[M + H]^+$  Calcd for  $C_{17}H_{17}O_4$ , 285.1127; Found 285.1120.

### 3.8.26 Anodic oxidation of **30** in MeCN/ 0.2 M LiClO<sub>4</sub>

Controlled potential electrolysis of **30** (+0.99 V, 1.0 F) yielded a mixture, which on preparative radial chromatography (SiO<sub>2</sub>, *n*-hexane/CH<sub>2</sub>Cl<sub>2</sub>, 2/1 to 5% MeOH/CH<sub>2</sub>Cl<sub>2</sub>), followed by HPLC (Luna Phenyl-Hexyl column, 10% H<sub>2</sub>O/MeCN, 10 mL/min), gave **30ba** (12.7 mg, 27%), **30bk** (3.2 mg, 6%), **30bm** (7.3 mg, 15%), and **30bn** (5.9 mg, 12%).

*Bisdihydronaphthalene (30ba)*. Colorless oil. UV (EtOH)  $\lambda_{max}$  (log  $\epsilon$ ) 227 (4.54), 271 (4.08), and 285 (3.91) nm; IR (dry film)  $\nu_{max}$  1607, 1507, 1244, 1175, 1033, and 750  $cm^{-1}$ ; <sup>1</sup>H NMR (CDCl<sub>3</sub>, 400 MHz)  $\delta$  3.16 (H-8a, H-8b, 2H, s), 3.60 (H-7a, H-7b, 2H, d,  $J = 6.0$  Hz), 3.67 (OMe, 4a, 4b, 6H, s), 6.01 (H-16a, H-16b, 2H, dd,  $J = 9.5, 6.0$  Hz), 6.62 (H-3a, H-3b, H-5a, H-5b, 4H, d,  $J = 8.8$  Hz), 6.67 (H-2a, H-2b, H-6a, H-6b, 4H, d,  $J = 8.8$  Hz), 6.68 (H-14a, H-14b, H-15a, H-15b, 4H, m), 6.99 (H-13a, H-13b, 2H, m), and 7.16 (H-11a, H-11b, H-12a, H-12b, 4H, m); <sup>13</sup>C NMR (CDCl<sub>3</sub>, 100 MHz)  $\delta$  39.7 (C-7a, C-7b), 52.2 (C-8a, C-8b), 55.1 (OMe, 4a, 4b), 113.8 (C-3a, C-3b, C-5a, C-5b), 125.7 (C-11a, C-11b), 126.7 (C-12a, C-12b), 126.9 (C-14a, C-14b), 127.5 (C-13a, C-13b), 128.2 (C-2a, C-2b, C-6a, C-6b), 130.0 (C-15a, C-15b), 130.1 (C-16a, C-16b), 133.8 (C-9a, C-9b), 134.0 (C-10a, C-10b), 135.9 (C-1a, C-1b), and 158.0 (C-4a, C-4b); HRMS (DART-TOF)  $m/z$ :  $[M + H]^+$  Calcd for  $C_{34}H_{31}O_2$ , 471.2324; Found 471.2322.

*Doubly-bridged-dibenzofused-cyclononane (30bk)*. Colorless oil. UV (EtOH)  $\lambda_{\max}$  (log  $\epsilon$ ) 226 (4.26), 267 (3.72), 286 (3.54), and 311 (3.12) nm; IR (dry film)  $\nu_{\max}$  3305, 1655, 1609, 1248, 1179, 1034, and 754  $\text{cm}^{-1}$ ;  $^1\text{H}$  NMR ( $\text{CDCl}_3$ , 400 MHz)  $\delta$  1.49 (NHCOMe, 3H, s), 1.62 (H-16b, 1H, m), 2.18 (H-16b, 1H, dd,  $J = 15.6, 10.4$  Hz), 2.52 (H-7b, 1H, ddd,  $J = 10.4, 4.0, 1.6$  Hz), 2.75 (H-7a, 1H, br t,  $J = 3.2$  Hz), 2.81 (H-16a, 1H, dt,  $J = 8.4, 3.2$  Hz), 3.30 (H-8b, 1H, dd,  $J = 9.6, 1.6$  Hz), 3.66 (OMe, 15b, 4H, m), 3.68 (OMe, 8a, 4H, m), 4.52 (NH, 1H, d,  $J = 9.2$  Hz), 5.31 (H-15a, 1H, d,  $J = 9.2$  Hz), 6.19 (H-2b, H-6b, 2H, d,  $J = 8.8$  Hz), 6.50 (H-3b, H-5b, 2H, d,  $J = 8.8$  Hz), 6.64 (H-3a, H-5a, 2H, d,  $J = 8.4$  Hz), 6.80 (H-14b, 1H, d,  $J = 7.6$  Hz), 6.86 (H-2a, H-6a, 2H, d,  $J = 8.4$  Hz), 7.08 (H-12a, 1H, br s), 7.15 (H-13b, 1H, t,  $J = 7.6$  Hz), 7.31 (H-11a, H-11b, H-12b, 3H, m), and 7.45 (H-13a, H-14a, 2H, m);  $^{13}\text{C}$  NMR ( $\text{CDCl}_3$ , 100 MHz)  $\delta$  23.3 (NHCOMe), 30.9 (C-16b), 39.2 (C-7a), 40.5 (C-8a), 41.6 (C-7b), 42.0 (C-15b), 45.1 (C-16a), 48.1 (C-15a), 52.6 (C-8b), 55.1 (OMe), 55.3 (OMe), 113.0 (C-3b, C-5b), 113.6 (C-3a, C-5a), 125.9 (C-11b), 126.9 (C-13b), 127.3 (C-12a), 127.6 (C-12b), 128.5 (C-13a), 128.6 (C-14b), 128.7 (C-2b, C-6b), 129.4 (C-2a, C-6a), 129.9 (C-14a), 130.6 (C-11a), 135.6 (C-1a), 135.8 (C-10a), 139.4 (C-9b), 140.0 (C-1b), 140.3 (C-9a), 141.3 (C-10b), 157.5 (C-4a, C-4b), and 168.5 (NHCOMe); HRMS (DART-TOF)  $m/z$ :  $[\text{M} + \text{H}]^+$  Calcd for  $\text{C}_{36}\text{H}_{36}\text{NO}_3$ , 530.2695; Found 530.2699.

*Tetraaryltetrahydrofuran (30bm)*. Colorless oil. UV (EtOH)  $\lambda_{\max}$  (log  $\epsilon$ ) 229 (4.58), 254 (3.99), 276 (3.42), and 284 (3.31) nm; IR (dry film)  $\nu_{\max}$  1612, 1511, 1247, 1172, 1032, and 771  $\text{cm}^{-1}$ ;  $^1\text{H}$  NMR ( $\text{CDCl}_3$ , 400 MHz)  $\delta$  3.78 (OMe, 4a, 4b, 6H, s), 4.08 (H-8a, H-8b, 2H, dd,  $J = 6.0, 2.8$  Hz), 4.93 (H-16a, H-16b, 2H, dd,  $J = 11.2, 1.6$  Hz), 5.08 (H-16a, H-16b, 2H, dd,  $J = 17.6, 1.6$  Hz), 5.38 (H-7a, H-7b, 2H, dd,  $J = 6.0, 2.8$  Hz), 6.33 (H-15a, H-15b, 2H, dd,  $J = 17.6, 11.2$  Hz), 6.82 (H-3a, H-3b, H-5a, H-5b, 4H, d,  $J = 8.8$

Hz), 7.10 (H-12a, H-12b, 2H, t,  $J = 7.6$  Hz), 7.17 (H-11a, H-11b, 2H, d,  $J = 7.6$  Hz), 7.21 (H-2a, H-2b, H-6a, H-6b, 4H, d,  $J = 8.8$  Hz), 7.22 (H-13a, H-13b, 2H, t,  $J = 7.6$  Hz), and 7.49 (H-14a, H-14b, 2H, d,  $J = 7.6$  Hz);  $^{13}\text{C}$  NMR ( $\text{CDCl}_3$ , 100 MHz)  $\delta$  55.3 (OMe, 4a, 4b), 58.5 (C-8a, C-8b), 87.8 (C-7a, C-7b), 113.8 (C-3a, C-3b, C-5a, C-5b), 116.7 (C-16a, C-16b), 126.5 (C-14a, C-14b), 126.7 (C-12a, C-12b), 126.8 (C-2a, C-2b, C-6a, C-6b), 127.0 (C-11a, C-11b), 127.9 (C-13a, C-13b), 133.6 (C-1a, C-1b), 134.8 (C-15a, C-15b), 135.3 (C-9a, C-9b), 138.8 (C-10a, C-10b), and 159.1 (C-4a, C-4b); HRMS (DART-TOF)  $m/z$ :  $[\text{M} + \text{H}]^+$  Calcd for  $\text{C}_{34}\text{H}_{33}\text{O}_3$ , 489.2430; Found 489.2437.

*Tetraaryltetrahydrofuran (30bn)*. Colorless oil. UV (EtOH)  $\lambda_{\text{max}}$  (log  $\epsilon$ ) 228 (4.71), 254 (4.11), 276 (3.59), and 283 (3.47) nm; IR (dry film)  $\nu_{\text{max}}$  1612, 1512, 1248, 1175, 1033, and 772  $\text{cm}^{-1}$ ;  $^1\text{H}$  NMR ( $\text{CDCl}_3$ , 400 MHz)  $\delta$  3.79 (OMe, 4a, 4b, 6H, s), 4.16 (H-8a, H-8b, 2H, dd,  $J = 4.8, 1.6$  Hz), 5.04 (H-16a, H-16b, 2H, dd,  $J = 10.8, 1.2$  Hz), 5.25 (H-16a, H-16b, 2H, dd,  $J = 17.6, 1.2$  Hz), 5.59 (H-7a, H-7b, 2H, dd,  $J = 4.8, 1.6$  Hz), 6.58 (H-15a, H-15b, 2H, dd,  $J = 17.6, 10.8$  Hz), 6.86 (H-3a, H-3b, H-5a, H-5b, 4H, d,  $J = 8.8$  Hz), 7.08 (H-12a, H-12b, H-13a, H-13b, H-14a, H-14b, 6H, m), 7.17 (H-11a, H-11b, 2H, m), and 7.35 (H-2a, H-2b, H-6a, H-6b, 4H, d,  $J = 8.8$  Hz);  $^{13}\text{C}$  NMR ( $\text{CDCl}_3$ , 100 MHz)  $\delta$  51.9 (C-8a, C-8b), 55.2 (OMe, 4a, 4b), 84.9 (C-7a, C-7b), 113.8 (C-3a, C-3b, C-5a, C-5b), 116.5 (C-16a, C-16b), 126.3 (C-11a, C-11b), 126.6 (C-13a, C-13b), 127.1 (C-12a, C-12b), 127.5 (C-2a, C-2b, C-6a, C-6b), 128.0 (C-14a, C-14b), 133.9 (C-1a, C-1b), 134.6 (C-15a, C-15b), 135.5 (C-9a, C-9b), 138.6 (C-10a, C-10b), and 159.0 (C-4a, C-4b); HRMS (DART-TOF)  $m/z$ :  $[\text{M} + \text{H}]^+$  Calcd for  $\text{C}_{34}\text{H}_{33}\text{O}_3$ , 489.2430; Found 489.2438.

### 3.8.27 Anodic oxidation of **31** in MeCN/ 0.2 M LiClO<sub>4</sub>

Controlled potential electrolysis of **31** (+0.87 V, 1.0 F) yielded a mixture, which on preparative radial chromatography (SiO<sub>2</sub>, *n*-hexane/CH<sub>2</sub>Cl<sub>2</sub>, 1/1 to 5% MeOH/CH<sub>2</sub>Cl<sub>2</sub>), gave **31bp** (14.9 mg, 28%) and **31bq** (7.4 mg, 14%) and

*Dihydrochrysene (31bp)*. Light yellowish oil. UV (EtOH)  $\lambda_{\max}$  (log  $\epsilon$ ) 227 (4.68), 235 (4.70), 265 (4.55), 273 (4.55), 290 (4.06), and 328 (4.15) nm; IR (dry film)  $\nu_{\max}$  1605, 1513, 1504, 1246, 1140, 1027, and 752 cm<sup>-1</sup>; <sup>1</sup>H NMR (CDCl<sub>3</sub>, 400 MHz)  $\delta$  3.54 (OMe, 3b, 3H, s), 3.72 (OMe, 4b, 3H, s), 3.77 (OMe, 4a, 3H, s), 4.05 (OMe, 3a, 3H, s), 4.15 (H-7b, 1H, s), 5.30 (H-8b, 1H, s), 5.65 (H-16b, 1H, dd,  $J$  = 11.2, 1.6 Hz), 5.92 (H-16b, 1H, dd,  $J$  = 17.6, 1.6 Hz), 6.49 (H-14b, 1H, d,  $J$  = 7.6 Hz), 6.54 (H-5a, 1H, s), 6.61 (H-5b, 1H, d,  $J$  = 8.4 Hz), 6.64 (H-2b, 1H, d,  $J$  = 2.0), 6.67 (H-6b, 1H, dd,  $J$  = 8.4, 2.0 Hz), 6.82 (H-13b, 1H, t,  $J$  = 7.6 Hz), 7.10 (H-12b, 1H, t,  $J$  = 7.6 Hz), 7.29 (H-13a, 1H, t,  $J$  = 7.6 Hz), 7.33 (H-12a, 1H, t,  $J$  = 7.6 Hz), 7.50 (H-2a, 1H, s), 7.57 (H-11b, 1H, d,  $J$  = 7.6 Hz), 7.64 (H-14a, 1H, d,  $J$  = 7.6), 7.69 (H-15b, 1H, dd,  $J$  = 17.6, 11.2 Hz), 7.78 (H-11a, 1H, d,  $J$  = 7.6 Hz), 7.89 (H-15a, 1H, d,  $J$  = 8.8 Hz), and 8.05 (H-16a, 1H, d,  $J$  = 8.8 Hz); <sup>13</sup>C NMR (CDCl<sub>3</sub>, 100 MHz)  $\delta$  44.4 (C-8b), 51.0 (C-7b), 55.5 (OMe, 3b), 55.8 (OMe, 4a, 4b), 56.2 (OMe, 3a), 107.5 (C-2a), 110.8 (C-2b), 111.2 (C-5b), 113.0 (C-5a), 117.2 (C-16b), 119.3 (C-6b), 121.4 (C-16a), 123.8 (C-14a), 125.4 (C-12a), 126.7 (C-12b), 126.8 (C-13a), 126.9 (C-11b), 127.2 (C-1a), 128.0 (C-13b), 128.1 (C-14b), 128.3 (C-15a), 128.5 (C-11a), 129.1 (C-6a), 130.9 (C-8a), 132.5 (C-7a), 132.9 (C-9a), 133.2 (C-10a), 135.4 (C-15b), 135.9 (C-10b), 137.6 (C-1b), 140.1 (C-9b), 147.5 (C-4b), 148.58 (C-3b), 148.64 (C-3a), and 149.2 (C-4a); HRMS (DART-TOF)  $m/z$ : [M + H]<sup>+</sup> Calcd for C<sub>36</sub>H<sub>33</sub>O<sub>4</sub>, 529.2379; Found 529.2370.

*Tetrahydrochrysene (31bq)*. Light yellowish oil. UV (EtOH)  $\lambda_{\max}$  (log  $\epsilon$ ) 225 (4.62), 241 (4.34) and 284 (4.06) nm; IR (dry film)  $\nu_{\max}$  1607, 1510, 1250, 1233, 1139, 1027, and 752  $\text{cm}^{-1}$ ;  $^1\text{H}$  NMR ( $\text{CDCl}_3$ , 400 MHz)  $\delta$  3.31 (H-8a, 1H, dd,  $J = 11.2, 6.0$  Hz), 3.56 (OMe, 3b, 3H, s), 3.64 (OMe, 4a, 3H, s), 3.75 (OMe, 4b, 3H, s), 3.90 (H-8b, 1H, t,  $J = 11.2$  Hz), 3.94 (OMe, 3a, 3H, s), 4.06 (H-7a, 1H, dt,  $J = 6.0, 2.8$  Hz), 4.31 (H-7b, 1H, d,  $J = 11.2$  Hz), 4.61 (H-16b, 1H, dd,  $J = 17.2, 2.0$  Hz), 4.63 (H-16a, 1H, dd,  $J = 10.8, 2.0$  Hz), 5.91 (H-15b, 1H, dd,  $J = 17.2, 10.8$  Hz), 5.96 (H-16a, 1H, d,  $J = 9.6$  Hz), 6.24 (H-2b, 1H, d,  $J = 2.4$ ), 6.30 (H-14a, 1H, d,  $J = 7.6$  Hz), 6.36 (H-5a, 1H, s), 6.38 (H-6b, 1H, dd,  $J = 8.4, 2.4$  Hz), 6.51 (H-15a, 1H, dd,  $J = 9.6, 3.2$  Hz), 6.56 (H-5b, 1H, d,  $J = 8.4$  Hz), 6.66 (H-13a, 1H, t,  $J = 7.6$  Hz), 6.76 (H-2a, 1H, s), 6.83 (H-11b, 1H, d,  $J = 7.6$  Hz), 6.91 (H-11a, 1H, d,  $J = 7.6$  Hz), 6.96 (H-12a, 1H, t,  $J = 7.6$  Hz), 6.99 (H-12b, 1H, t,  $J = 7.6$  Hz), 7.28 (H-13b, 1H, t,  $J = 7.6$  Hz), and 7.52 (H-14b, 1H, d,  $J = 7.6$  Hz);  $^{13}\text{C}$  NMR ( $\text{CDCl}_3$ , 100 MHz)  $\delta$  41.0 (C-7a), 42.0 (C-8b), 44.3 (C-8a), 52.2 (C-7b), 55.7 (OMe, 3b), 55.8 (OMe, 4b), 56.0 (OMe, 4a), 56.1 (OMe, 3a), 110.66 (C-5b), 110.75 (C-2a), 112.4 (C-5a, C-2b), 115.7 (C-16b), 121.1 (C-6b), 125.80 (C-11a), 125.83 (C-12b), 126.2 (C-13a), 126.3 (C-15a), 126.4 (C-11b), 126.6 (C-12a), 126.9 (C-13b, C-14b), 129.5 (C-14a), 130.8 (C-1a), 131.6 (C-6a), 132.9 (C-10a), 133.5 (C-16a), 134.9 (C-15b), 136.0 (C-9a), 137.9 (C-1b), 140.0 (C-10b), 140.9 (C-9b), 147.2 (C-4b), 147.7 (C-4a), 148.2 (C-3a, C-3b); HRMS (DART-TOF)  $m/z$ :  $[\text{M} + \text{H}]^+$  Calcd for  $\text{C}_{36}\text{H}_{35}\text{O}_4$ , 531.2535; Found 531.2540.

### 3.8.28 Anodic oxidation of **32** in MeCN/ 0.2 M LiClO<sub>4</sub>

Controlled potential electrolysis of **32** was reported previously by Hong.<sup>85</sup>

### 3.8.29 Anodic oxidation of **33** in MeCN/ 0.2 M LiClO<sub>4</sub>

Controlled potential electrolysis of **33** at the potential peak (+0.87 V, 1 F) yielded a mixture, which on preparative radial chromatography (SiO<sub>2</sub>, *n*-hexane:CH<sub>2</sub>Cl<sub>2</sub>, 2:1 to 100% CH<sub>2</sub>Cl<sub>2</sub>) resulted in the isolation of the stereoisomeric tetraaryltetrahydrofurans **33bm** (15.4 mg, 30%), **33bn** (12.9 mg, 25%), and dehydrotetralin **33ca** (5.0 mg, 10%).

*Tetraaryltetrahydrofuran (33bm)*. Light yellowish oil; UV (EtOH)  $\lambda_{\max}$  (log  $\epsilon$ ) 228 (4.84), 255 (3.97), and 277 (3.95) nm; IR (dry film)  $\nu_{\max}$  2054, 2019, 1922, 1887, 1764, 1612, 1513, 829, and 755 cm<sup>-1</sup>; <sup>1</sup>H NMR (CDCl<sub>3</sub>, 400 MHz)  $\delta$  1.97 (COMe, 16a, 16b, 6H, s), 3.77 (OMe, 4a, 4b, 6H, s), 3.98 (H-8a, H-8b, 2H, dd,  $J$  = 5.9, 2.8 Hz), 5.36 (H-7a, H-7b, 2H, dd,  $J$  = 5.9, 2.8 Hz), 6.83 (H-3a, H-5a, H-3b, H-5b, 4H, d,  $J$  = 8.6 Hz), 6.94 (H-11a, H-11b, 2H, dd,  $J$  = 7.4, 1.7 Hz), 7.16 (H-12a, H-13a, H-12b, H-13b, 4H, m), 7.23 (H-2a, H-6a, H-2b, H-6b, 4H, d,  $J$  = 8.6 Hz), and 7.36 (H-14a, H-14b, 2H, dd,  $J$  = 7.4, 1.7 Hz); <sup>13</sup>C NMR (CDCl<sub>3</sub>, 100 MHz)  $\delta$  20.7 (C-16a, C-16b), 55.3 (OMe, 4a, 4b), 56.6 (C-8a, C-8b), 86.0 (C-7a, C-7b), 113.9 (C-3a, C-5a, C-3b, C-5b), 123.1 (C-11a, C-11b), 126.2 (C-13a, C-13b), 126.8 (C-2a, C-6a, C-2b, C-6b), 127.8 (C-12a, C-12b), 128.6 (C-14a, C-14b), 129.9 (C-9a, C-9b), 133.6 (C-1a, C-1b), 149.0 (C-10a, C-10b), 159.1 (C-4a, C-4b), and 168.7 (C-15a, C-15b); HRMS (ESI-TOF)  $m/z$ : [M + K]<sup>+</sup> Calcd for C<sub>34</sub>H<sub>32</sub>O<sub>7</sub>K, 591.1780; Found 591.1796.

*Tetraaryltetrahydrofuran (33bn)*. Light yellowish oil and subsequently as colorless block crystals from MeOH/CH<sub>2</sub>Cl<sub>2</sub>; mp 144–146 °C; UV (EtOH)  $\lambda_{\max}$  (log  $\epsilon$ ) 228 (4.52), 253 (3.80), and 277 (3.66) nm; IR (dry film)  $\nu_{\max}$  2318, 2037, 1888, 1758, 1612, 1513, 830, and 755 cm<sup>-1</sup>; <sup>1</sup>H NMR (CDCl<sub>3</sub>, 400 MHz)  $\delta$  2.04 (COMe, 16a, 16b, 6H, s), 3.78

(OMe, 4a, 4b, 6H, s), 3.94 (H-8a, H-8b, 2H, br d,  $J = 4.6$  Hz), 5.51 (H-7a, H-7b, 2H, br d,  $J = 4.6$  Hz), 6.86 (H-3a, H-5a, H-3b, H-5b, 4H, d,  $J = 8.6$  Hz), 6.88 (H-11a, H-11b, 2H, d,  $J = 7.3$  Hz), 7.05 (H-13a, H-13b, t,  $J = 7.3$  Hz) 7.15 (H-14a, H-14b, 2H, d,  $J = 7.3, 1.7$  Hz), 7.16 (H-12a, H-12b, 2H, t,  $J = 7.3$  Hz), and 7.31 (H-2a, H-6a, H-2b, H-6b, 4H, d,  $J = 8.6$  Hz);  $^{13}\text{C}$  NMR ( $\text{CDCl}_3$ , 100 MHz)  $\delta$  20.6 (C-16a, C-16b), 55.3 (OMe, 4a, 4b), 48.6 (C-8a, C-8b), 83.5 (C-7a, C-7b), 113.8 (C-3a, C-5a, C-3b, C-5b), 121.9 (C-11a, C-11b), 125.8 (C-13a, C-13b), 127.7 (C-2a, C-6a, C-2b, C-6b), 127.8 (C-12a, C-12b), 128.8 (C-14a, C-14b), 130.1 (C-9a, C-9b), 133.3 (C-1a, C-1b), 149.3 (C-10a, C-10b), 159.1 (C-4a, C-4b), and 169.0 (C-15a, C-15b); HRMS (ESI-TOF)  $m/z$ :  $[\text{M} + \text{K}]^+$  Calcd for  $\text{C}_{34}\text{H}_{32}\text{O}_7\text{K}$ , 591.1780; Found 591.1796.

*Dehydrotetralin (33ca)*. Light yellowish oil; UV (EtOH)  $\lambda_{\text{max}}$  (log  $\epsilon$ ) 230 (4.04), 285 (3.45), 298 (3.43) nm; IR (dry film)  $\nu_{\text{max}}$  2413, 2288, 2047, 1920, 1886, 1761, 1609, 1510, 756  $\text{cm}^{-1}$ ;  $^1\text{H}$  NMR ( $\text{CDCl}_3$ , 400 MHz)  $\delta$  1.76 (COMe, 16b, 3H, s), 2.30 (COMe, 16a, 3H, s), 3.70 (OMe, 4a, 3H, s), 3.75 (OMe, 4b, 3H, s), 4.07 (H-7b, 1H, s), 4.30 (H-8b, 1H, s), 6.48 (H-5a, 1H, d,  $J = 2.3$  Hz), 6.78 (H-3a, 1H, dd,  $J = 8.8, 2.3$  Hz), 6.79 (H-3b, H-5b, 2H, d,  $J = 8.8$  Hz), 6.90 (H-11a, 1H, d,  $J = 8.0$  Hz), 6.92 (H-7a, 1H, s), 7.00 (H-12a, H-14a, H-11b, H-12b, 4H, m), 7.12 (H-2b, H-6b, 2H, d,  $J = 8.8$  Hz), 7.16 (H-13a, H-13b, H-14b, 3H, m), and 7.22 (H-2a, 1H, d,  $J = 8.8$  Hz);  $^{13}\text{C}$  NMR ( $\text{CDCl}_3$ , 100 MHz)  $\delta$  20.1 (C-16a), 20.8 (C-16b), 44.6 (C-8b), 50.7 (C-7b), 54.9 (OMe, 4a), 55.0 (OMe, 4b), 112.5 (C-3a), 113.7 (C-3b, C-5b), 114.8 (C-5a), 122.4 (C-11b), 122.6 (C-11a), 125.7 (C-12a), 125.9 (C-12b), 126.5 (C-1a), 127.4 (C-13b), 127.8 (C-2a, C-14b), 128.2 (C-13a), 128.3 (C-2b, C-6b), 129.0 (C-7a), 129.8 (C-14a), 132.0 (C-9b), 133.89 (C-9a), 133.94 (C-8a), 136.3 (C-6a), 137.3 (C-1b), 147.6 (C-10a, C-10b), 158.0 (C-4b),

159.5 (C-4a), 169.1 (C-15a), and 169.3 (C-15b); HRMS (ESI-TOF)  $m/z$ :  $[M + K]^+$   
Calcd for  $C_{34}H_{30}O_6K$ , 573.1674; Found 573.1687.

### 3.8.30 Anodic oxidation of **34** in MeCN/ 0.2 M LiClO<sub>4</sub>

Controlled potential electrolysis of **34** (+1.20 V, 1.0 F) yielded a mixture, which on preparative radial chromatography (SiO<sub>2</sub>, *n*-hexane/CH<sub>2</sub>Cl<sub>2</sub>, 2/1 to 5% MeOH/CH<sub>2</sub>Cl<sub>2</sub>), followed by HPLC (Luna Phenyl-Hexyl column, 10% H<sub>2</sub>O:MeCN, 10 ml/min), gave **34bm** (16.1 mg, 33%), **34bn** (13.1 mg, 27%), and **34ca** (2.3 mg, 5%).

*Tetraaryltetrahydrofuran (34bm)*. Light yellowish oil; UV (EtOH)  $\lambda_{max}$  (log  $\epsilon$ ) 206 (4.67), 229 (4.49), and 277 (3.70) nm; IR (dry film)  $\nu_{max}$  2225 (CN), 1613, 1514, 1250, 1032, 830, and 761 cm<sup>-1</sup>; <sup>1</sup>H NMR (CDCl<sub>3</sub>, 400 MHz)  $\delta$  3.78 (OMe, 4a, 4b, 6H, s), 4.29 (H-8a, H-8b, 2H, dd,  $J = 6.3, 2.7$  Hz), 5.42 (H-7a, H-7b, 2H, dd,  $J = 6.3, 2.7$  Hz), 6.85 (H-3a, H-3b, H-5a, H-5b, 4H, d,  $J = 8.6$  Hz), 7.25 (H-2a, H-2b, H-6a, H-6b, 4H, d,  $J = 8.6$  Hz), 7.27 (H-12a, H-12b, 2H, t,  $J = 7.7$  Hz), 7.40 (H-11a, H-11b, 2H, d,  $J = 7.7$  Hz), 7.64 (H-13a, H-13b, 2H, t,  $J = 7.7$  Hz), and 7.81 (H-14a, H-14b, 2H, d,  $J = 7.7$  Hz); <sup>13</sup>C NMR (CDCl<sub>3</sub>, 100 MHz)  $\delta$  55.3 (OMe, 4a, 4b), 60.7 (C-8a, C-8b), 87.8 (C-7a, C-7b), 113.6 (C-10a, C-10b), 114.2 (C-3a, C-3b, C-5a, C-5b), 117.3 (C-15a, C-15b), 127.3 (C-2a, C-2b, C-6a, C-6b), 127.6 (C-14a, C-14b), 128.1 (C-12a, C-12b), 131.5 (C-1a, C-1b), 133.1 (C-11a, C-11b), 133.6 (C-13a, C-13b), 140.7 (C-9a, C-9b), and 159.7 (C-4a, C-4b); HRMS (ESI-TOF)  $m/z$ :  $[M + H]^+$  Calcd for  $C_{32}H_{27}N_2O_3$ , 487.2022; Found 487.2034.

*Tetraaryltetrahydrofuran (34bn)*. Light yellowish oil; UV (EtOH)  $\lambda_{\max}$  (log  $\epsilon$ ) 204 (4.69), 227 (4.37), and 276 (3.26) nm; IR (dry film)  $\nu_{\max}$  2224 (CN), 1612, 1515, 1256, 832, and 765  $\text{cm}^{-1}$ ;  $^1\text{H}$  NMR ( $\text{CDCl}_3$ , 400 MHz)  $\delta$  3.78 (OMe, 4a, 4b, 6H, s), 4.53 (H-8a, H-8b, 2H, br d,  $J = 2.8$  Hz), 5.57 (H-7a, H-7b, 2H, br s), 6.88 (H-3a, H-3b, H-5a, H-5b, 4H, d,  $J = 8.6$  Hz), 7.22 (H-12a, H-12b, 2H, t,  $J = 7.7$  Hz), 7.23 (H-14a, H-14b, 2H, d,  $J = 7.7$  Hz), 7.37 (H-2a, H-2b, H-6a, H-6b, 4H, d,  $J = 8.6$  Hz), 7.42 (H-13a, H-13b, 2H, t,  $J = 7.7$  Hz), and 7.43 (H-11a, H-11b, 2H, d,  $J = 7.7$  Hz);  $^{13}\text{C}$  NMR ( $\text{CDCl}_3$ , 100 MHz)  $\delta$  55.4 (OMe, 4a, 4b, C-8a, C-8b), 84.5 (C-7a, C-7b), 114.2 (C-3a, C-3b, C-5a, C-5b), 114.6 (C-10a, C-10b), 117.2 (C-15a, C-15b), 127.6 (C-12a, C-12b, C-14a, C-14b), 127.9 (C-2a, C-2b, C-6a, C-6b), 131.9 (C-13a, C-13b), 132.3 (C-11a, C-11b), 133.2 (C-1a, C-1b), 141.2 (C-9a, C-9b), and 159.6 (C-4a, C-4b); HRMS (ESI-TOF)  $m/z$ :  $[\text{M} + \text{H}]^+$  Calcd for  $\text{C}_{32}\text{H}_{27}\text{N}_2\text{O}_3$ , 487.2022; Found 487.2029.

*Dehydrotetralin (34ca)*. Light yellowish oil; UV (EtOH)  $\lambda_{\max}$  (log  $\epsilon$ ) 228 (3.90) and 281 (3.24) nm; IR (dry film)  $\nu_{\max}$  2223 (CN), 2054, 1944, 1609, 1510, 1250, 1034, and 759  $\text{cm}^{-1}$ ;  $^1\text{H}$  NMR ( $\text{CDCl}_3$ , 400 MHz)  $\delta$  3.72 (OMe, 3H, s), 3.77 (OMe, 3H, s), 4.30 (H-7b, 1H, d,  $J = 2.4$  Hz), 4.55 (H-8b, 1H, d,  $J = 2.4$  Hz), 6.51 (H-5a, 1H, d,  $J = 2.8$  Hz), 6.84 (H-3b, H-5b, 2H, d,  $J = 8.8$  Hz), 6.85 (H-3a, 1H, dd,  $J = 8.4, 2.8$  Hz), 6.91 (H-14a, 1H, d,  $J = 7.6$  Hz), 7.28 (H-12a, 1H, t,  $J = 7.6$  Hz), 7.25 (H-12b, 1H, m), 7.26 (H-2b, H-6b, 2H, d,  $J = 8.8$  Hz), 7.29 (H-7a, 1H, s), 7.38 (H-13a, 1H, t,  $J = 7.6$  Hz), 7.39 (H-2a, 1H, d,  $J = 8.4$  Hz), 7.40 (H-13b, 1H, t,  $J = 7.6$  Hz), 7.46 (H-14b, 1H, d,  $J = 7.6$  Hz), 7.57 (H-11a, 1H, d,  $J = 7.6$  Hz), and 7.64 (H-11b, 1H, d,  $J = 7.6$  Hz);  $^{13}\text{C}$  NMR ( $\text{CDCl}_3$ , 100 MHz)  $\delta$  51.2 (C-8b), 51.9 (C-7b), 55.2 (OMe, 4a, 4b), 110.8 (C-10a), 112.0 (C-10b), 113.0 (C-3a), 114.0 (C-3b, C-5b), 115.2 (C-5a), 118.5 (C-15b), 118.9 (C-15a), 126.5 (C-1a), 127.4 (C-12a), 127.5 (C-12b), 127.8 (C-14a), 128.7 (C-14b), 128.9 (C-2a),

129.1 (C-2b, C-6b), 130.6 (C-8a), 132.0 (C-7a), 132.6 (C-13a), 133.3 (C-13b), 133.4 (C-11b), 133.8 (C-11a), 134.7 (C-1b), 135.9 (C-6a), 144.56 (C-9b), 144.61 (C-9a), 158.4 (C-4b), and 160.5 (C-4a); HRMS (ESI-TOF)  $m/z$ :  $[M + H]^+$  Calcd for  $C_{32}H_{24}N_2O_2Na$ , 491.1736; Found 491.1741.

### 3.8.31 Anodic oxidation of **35** in MeCN/ 0.2 M LiClO<sub>4</sub>

Controlled potential electrolysis of **35** (+1.08 V, 1.0 F) yielded a mixture, which on preparative radial chromatography (SiO<sub>2</sub>, *n*-hexane/CH<sub>2</sub>Cl<sub>2</sub>, 2/1 to 10% MeOH/CH<sub>2</sub>Cl<sub>2</sub>), followed by HPLC (Luna Phenyl-Hexyl column, 15% H<sub>2</sub>O:MeCN, 10 ml/min) and Sephadex LH20 (30% MeCN/MeOH as mobile phase), gave **35bm** (10.5 mg, 20%) and **35bn** (10.5 mg, 20%).

*Tetraaryltetrahydrofuran (35bm)*. Yellowish oil; UV (EtOH)  $\lambda_{max}$  (log  $\epsilon$ ) 206 (4.66), 227 (4.57), and 275 (4.47) nm; IR (dry film)  $\nu_{max}$  2054, 2022, 1926, 1889, 1609, 1514, 1348 (NO<sub>2</sub>), 828 and 753 cm<sup>-1</sup>; <sup>1</sup>H NMR (CDCl<sub>3</sub>, 400 MHz)  $\delta$  3.79 (OMe, 4a, 4b, 6H, s), 4.60 (H-8a, H-8b, 2H, dd,  $J = 5.9, 2.6$  Hz), 5.34 (H-7a, H-7b, 2H, dd,  $J = 5.9, 2.6$  Hz), 6.84 (H-3a, H-3b, H-5a, H-5b, 4H, d,  $J = 8.7$  Hz), 7.19 (H-2a, H-2b, H-6a, H-6b, 4H, d,  $J = 8.7$  Hz), 7.33 (H-12a, H-12b, 2H, t,  $J = 7.7$  Hz), 7.53 (H-11a, H-11b, 2H, d,  $J = 7.7$  Hz), 7.63 (H-13a, H-13b, 2H, t,  $J = 7.7$  Hz), and 7.82 (H-14a, H-14b, 2H, d,  $J = 7.7$  Hz); <sup>13</sup>C NMR (CDCl<sub>3</sub>, 100 MHz)  $\delta$  54.8 (OMe, 4a, 4b), 54.9 (C-8a, C-8b), 87.7 (C-7a, C-7b), 113.6 (C-3a, C-3b, C-5a, C-5b), 123.8 (C-11a, C-11b), 126.6 (C-2a, C-2b, C-6a, C-6b), 127.6 (C-12a, C-12b), 128.4 (C-14a, C-14b), 130.9 (C-1a, C-1b), 131.0 (C-9a, C-9b), 132.5 (C-13a, C-13b), 150.5 (C-10a, C-10b), and 159.1 (C-4a, C-4b); HRMS (ESI-TOF)  $m/z$ :  $[M + H]^+$  Calcd for  $C_{30}H_{27}N_2O_7$ , 527.1813; Found 527.1819.

*Tetraaryltetrahydrofuran (35bn)*. Yellowish oil; UV (EtOH)  $\lambda_{\max}$  (log  $\epsilon$ ) 202 (4.05), 227 (3.77), and 276 (3.65) nm; IR (dry film)  $\nu_{\max}$  2066, 1923, 1606, 1511, 1345 (NO<sub>2</sub>), 853, and 753 cm<sup>-1</sup>; <sup>1</sup>H NMR (CDCl<sub>3</sub>, 400 MHz)  $\delta$  3.78 (OMe, 4a, 4b, 6H, s), 4.76 (H-8a, H-8b, 2H, d,  $J$  = 4.5 Hz), 5.57 (H-7a, H-7b, 2H, d,  $J$  = 4.5 Hz), 6.86 (H-3a, H-3b, H-5a, H-5b, 4H, d,  $J$  = 8.6 Hz), 7.29 (H-12a, H-12b, 2H, t,  $J$  = 7.8 Hz), 7.32 (H-2a, H-2b, H-6a, H-6b, 4H, d,  $J$  = 8.6 Hz), 7.33 (H-14a, H-14b, 2H, d,  $J$  = 7.8 Hz), 7.42 (H-13a, H-13b, 2H, t,  $J$  = 7.8 Hz), and 7.62 (H-11a, H-11b, 2H, d,  $J$  = 7.8 Hz); <sup>13</sup>C NMR (CDCl<sub>3</sub>, 100 MHz)  $\delta$  51.1 (C-8a, C-8b), 55.4 (OMe, 4a, 4b), 84.9 (C-7a, C-7b), 114.2 (C-3a, C-3b, C-5a, C-5b), 124.9 (C-11a, C-11b), 127.8 (C-2a, C-2b, C-6a, C-6b), 128.1 (C-12a, C-12b), 129.5 (C-14a, C-14b), 132.1 (C-1a, C-1b), 132.2 (C-13a, C-13b), 132.3 (C-9a, C-9b), 150.8 (C-10a, C-10b), and 159.5 (C-4a, C-4b); HRMS (ESI-TOF)  $m/z$ : [M + H]<sup>+</sup> Calcd for C<sub>30</sub>H<sub>27</sub>N<sub>2</sub>O<sub>7</sub>, 527.1813; Found 527.1827.

### 3.8.32 Anodic oxidation of 36 in MeCN/ 0.2 M LiClO<sub>4</sub>

Controlled potential electrolysis of **36** (+1.15 V, 1.0 F) yielded a mixture, which on preparative radial chromatography (SiO<sub>2</sub>, *n*-hexane/CH<sub>2</sub>Cl<sub>2</sub>, 2/1 to 8% MeOH/CH<sub>2</sub>Cl<sub>2</sub>), followed by HPLC (Luna Phenyl-Hexyl column, 12% H<sub>2</sub>O:MeCN, 10 ml/min) and Sephadex LH20 (20% MeCN/MeOH as mobile phase), gave **36bm** (17.2 mg, 30%), **36bn** (17.2 mg, 30%), and **36ca** (5.5 mg, 10%).

*Tetraaryltetrahydrofuran (36bm)*. Light yellowish oil, and subsequently as colorless block crystals from hexanes/CH<sub>2</sub>Cl<sub>2</sub>; mp 160–161 °C; UV (EtOH)  $\lambda_{\max}$  (log  $\epsilon$ ) 209 (3.84), 229 (3.84), 265 (2.98), and 272 (2.97) nm; IR (dry film)  $\nu_{\max}$  2058, 2022, 1978, 1947, 1886, 1613, 1514, 829, 769, and 670 cm<sup>-1</sup>; <sup>1</sup>H NMR (CDCl<sub>3</sub>, 400 MHz)  $\delta$  3.78

(OMe, 4a, 4b, 6H, s), 4.07 (H-8a, H-8b, 2H, dd,  $J = 5.4, 1.8$  Hz), 5.47 (H-7a, H-7b, 2H, dd,  $J = 5.4, 1.8$  Hz), 6.83 (H-3a, H-3b, H-5a, H-5b, 4H, d,  $J = 8.6$  Hz), 7.21 (H-2a, H-2b, H-6a, H-6b, 4H, d,  $J = 8.6$  Hz), 7.26 (H-12a, H-12b, 2H, t,  $J = 7.7$  Hz), 7.42 (H-11a, H-11b, 2H, d,  $J = 7.7$  Hz), 7.59 (H-13a, H-13b, 2H, t,  $J = 7.7$  Hz), and 7.79 (H-14a, H-14b, 2H, d,  $J = 7.7$  Hz);  $^{13}\text{C}$  NMR ( $\text{CDCl}_3$ , 100 MHz)  $\delta$  55.3 (OMe, 4a, 4b), 59.9 (C-8a, C-8b), 89.5 (C-7a, C-7b), 113.8 (C-3a, C-3b, C-5a, C-5b), 125.7 (C-11a, C-11b), 126.8 (C-12a, C-12b), 126.9 (C-2a, C-2b, C-6a, C-6b), 127.4 ( $\text{CF}_3$ , 10a, 10b), 129.1 (C-10a, C-10b), 129.4 (C-14a, C-14b), 132.1 (C-13a, C-13b), 132.6 (C-1a, C-1b), 138.1 (C-9a, C-9b), and 159.3 (C-4a, C-4b); HRMS (ESI-TOF)  $m/z$ :  $[\text{M} + \text{H}]^+$  Calcd for  $\text{C}_{32}\text{H}_{27}\text{F}_6\text{O}_3$ , 573.1859; Found 573.1833.

*Tetraaryltetrahydrofuran (36bn)*. Light yellowish oil; UV (EtOH)  $\lambda_{\text{max}}$  (log  $\epsilon$ ) 208 (3.82), 227 (3.57), 256 (2.81), 261 (2.81), and 272 (2.76) nm; IR (dry film)  $\nu_{\text{max}}$  2056, 1947, 1885, 1613, 1514, 831, 767, and 668  $\text{cm}^{-1}$ ;  $^1\text{H}$  NMR ( $\text{CDCl}_3$ , 400 MHz)  $\delta$  3.78 (OMe, 4a, 4b, 6H, s), 4.34 (H-8a, H-8b, 2H, br d,  $J = 3.9$  Hz), 5.63 (H-7a, H-7b, 2H, br d,  $J = 3.9$  Hz), 6.87 (H-3a, H-3b, H-5a, H-5b, 4H, d,  $J = 8.6$  Hz), 7.25 (H-12a, H-12b, 2H, t,  $J = 7.7$  Hz), 7.33 (H-2a, H-2b, H-6a, H-6b, 4H, d,  $J = 8.6$  Hz), 7.37 (H-13a, H-13b, H-14a, H-14b, 4H, m), and 7.48 (H-11a, H-11b, 2H, d,  $J = 7.7$  Hz);  $^{13}\text{C}$  NMR ( $\text{CDCl}_3$ , 100 MHz)  $\delta$  52.3 (C-8a, C-8b), 55.3 (OMe, 4a, 4b), 84.5 (C-7a, C-7b), 113.9 (C-3a, C-3b, C-5a, C-5b), 122.7 ( $\text{CF}_3$ , 10a, 10b), 125.4 (C-10a, C-10b), 126.2 (C-11a, C-11b), 127.1 (C-12a, C-12b), 127.6 (C-2a, C-2b, C-6a, C-6b), 129.5 (C-14a, C-14b), 131.4 (C-13a, C-13b), 133.0 (C-1a, C-1b), 137.2 (C-9a, C-9b), and 159.3 (C-4a, C-4b); HRMS (ESI-TOF)  $m/z$ :  $[\text{M} + \text{H}]^+$  Calcd for  $\text{C}_{32}\text{H}_{27}\text{F}_6\text{O}_3$ , 573.1859; Found 573.1848.

*Dehydrotetralin (36ca)*. Light yellowish oil; UV (EtOH)  $\lambda_{\max}$  (log  $\epsilon$ ) 210 (4.61), 226 (4.60), and 296 (4.28) nm; IR (dry film)  $\nu_{\max}$  2063, 1972, 1941, 1885, 1605, 1510, 821, and 766  $\text{cm}^{-1}$ ;  $^1\text{H}$  NMR ( $\text{CDCl}_3$ , 400 MHz)  $\delta$  3.74 (OMe, 4a, 3H, s), 3.79 (OMe, 4b, 3H, s), 4.21 (H-7b, 1H, s), 4.39 (H-8b, 1H, s), 6.56 (H-5a, 1H, d,  $J = 2.5$  Hz), 6.59 (H-14a, 1H, m), 6.74 (H-7a, 1H, s), 6.82 (H-3b, H-5b, 2H, d,  $J = 8.6$  Hz), 6.85 (H-3a, 1H, dd,  $J = 8.2, 2.5$  Hz), 7.09 (H-2b, H-6b, 2H, d,  $J = 8.6$  Hz), 7.20 (H-13a, 1H, m), 7.23 (H-12a, H-12b, 2H, m), 7.28 (H-2a, 1H, m), 7.31 (H-13b, 1H, t,  $J = 7.7$  Hz), 7.41 (H-14b, 1H, d,  $J = 7.7$  Hz), 7.53 (H-11a, 1H, m), and 7.56 (H-11b, 1H, m);  $^{13}\text{C}$  NMR ( $\text{CDCl}_3$ , 100 MHz)  $\delta$  48.4 (C-8b), 51.4 (C-7b), 55.3 (OMe, 4a, 4b), 112.9 (C-3a), 113.8 (C-3b, C-5b), 115.6 (C-5a), 122.6 (C-10a), 123.1 (C-10b), 125.7 (C-11a), 126.2 (C-11b), 126.9 (C-12a), 127.0 (C-12b), 127.2 (C-1a), 127.6 ( $\text{CF}_3$ , 10a), 128.0 ( $\text{CF}_3$ , 10b), 128.3 (C-2a), 129.2 (C-2b, C-6b), 129.3 (C-7a), 130.0 (C-14b), 130.8 (C-14a), 130.9 (C-13a), 132.0 (C-13b), 134.5 (C-8a), 136.5 (C-6a), 136.8 (C-1b), 140.5 (C-9a), 141.0 (C-9b), 158.3 (C-4b), and 160.1 (C-4a); HRMS (ESI-TOF)  $m/z$ :  $[\text{M} + \text{H}]^+$  Calcd for  $\text{C}_{32}\text{H}_{27}\text{F}_6\text{O}_2$ , 555.1753; Found 555.1769.

### 3.8.33 Anodic oxidation of 37 in MeCN/ 0.2 M LiClO<sub>4</sub>

Controlled potential electrolysis of **37** (+1.20 V, 1.0 F) yielded a mixture, which on preparative radial chromatography ( $\text{SiO}_2$ , *n*-hexane/ $\text{CH}_2\text{Cl}_2$ , 4/1 to 5% MeOH/ $\text{CH}_2\text{Cl}_2$ ), followed by HPLC (Luna Phenyl-Hexyl column, 8%  $\text{H}_2\text{O}$ :MeCN, 10 ml/min), gave **37bn** (2.8 mg, 5%), **37ca** (10.7 mg, 20%), and **37cc** (2.7 mg, 5%).

*Tetraaryltetrahydrofuran (37bn)*. Light yellowish oil; UV (EtOH)  $\lambda_{\max}$  (log  $\epsilon$ ) 203 (4.13), 228 (3.72), 257 (3.16), and 280 (2.94) nm; IR (dry film)  $\nu_{\max}$  2051, 1944, 1911,

1891, 1721 (CO<sub>2</sub>Me), 1612, 1514, 828, and 755 cm<sup>-1</sup>; <sup>1</sup>H NMR (CDCl<sub>3</sub>, 400 MHz) δ 3.58 (CO<sub>2</sub>Me, 16a, 16b, 6H, s), 3.78 (OMe, 4a, 4b, 6H, s), 5.13 (H-8a, H-8b, 2H, d, *J* = 4.1 Hz), 5.57 (H-7a, H-7b, 2H, d, *J* = 4.1 Hz), 6.86 (H-3a, H-3b, H-5a, H-5b, 4H, d, *J* = 8.6 Hz), 7.12 (H-12a, H-12b, 2H, t, *J* = 7.7 Hz), 7.19 (H-14a, H-14b, 2H, d, *J* = 7.7 Hz), 7.27 (H-13a, H-13b, 2H, t, *J* = 7.7 Hz), 7.39 (H-2a, H-2b, H-6a, H-6b, 4H, d, *J* = 8.6 Hz), and 7.57 (H-11a, H-11b, 2H, d, *J* = 7.7 Hz); <sup>13</sup>C NMR (CDCl<sub>3</sub>, 100 MHz) δ 51.6 (C-8a, C-8b), 51.9 (C-16a, C-16b), 55.3 (OMe, 4a, 4b), 84.6 (C-7a, C-7b), 113.8 (C-3a, C-3b, C-5a, C-5b), 126.3 (C-12a, C-12b), 128.0 (C-2a, C-2b, C-6a, C-6b), 128.8 (C-14a, C-14b), 130.4 (C-11a, C-11b), 131.2 (C-13a, C-13b), 131.3 (C-10a, C-10b), 133.7 (C-1a, C-1b), 139.2 (C-9a, C-9b), 159.1 (C-4a, C-4b), and 168.0 (C-15a, C-15b); HRMS (ESI-TOF) *m/z*: [M + H]<sup>+</sup> Calcd for C<sub>34</sub>H<sub>32</sub>O<sub>7</sub>K, 591.1780; Found 591.1770.

*Naphthalene (37ca)*. Light yellowish oil, and subsequently as colorless block crystals from hexanes/CH<sub>2</sub>Cl<sub>2</sub>; mp 71–74 °C; UV (EtOH) λ<sub>max</sub> (log ε) 205 (4.12), 232 (3.71), 295 (3.00), and 340 (2.32) nm; IR (dry film) ν<sub>max</sub> 2059, 2019, 1946, 1915, 1723 (CO<sub>2</sub>Me), 1622, 1515, 842, and 753 cm<sup>-1</sup>; <sup>1</sup>H NMR (CDCl<sub>3</sub>, 400 MHz) δ 3.61 (CO<sub>2</sub>Me, 16a, 3H, s), 3.62 (CO<sub>2</sub>Me, 16b, 3H, s), 3.69 (OMe, 4a, 3H, s), 3.74 (OMe, 4b, 3H, s), 6.72 (H-2b, H-6b, 2H, d, *J* = 8.6 Hz), 6.92 (H-5a, 1H, d, *J* = 2.3 Hz), 6.98 (H-12b, 1H, m), 7.05 (H-13a, 1H, m), 7.05 (H-3b, H-5b, 2H, m), 7.09 (H-12b, 1H, m), 7.13 (H-3a, 1H, dd, *J* = 9.0, 2.3 Hz), 7.19 (H-12a, 1H, t, *J* = 7.3 Hz), 7.25 (H-13b, 1H, t, *J* = 7.7 Hz), 7.29 (H-14a, 1H, d, *J* = 7.3 Hz), 7.49 (H-11b, 1H, d, *J* = 7.7 Hz), 7.66 (H-7a, 1H, s), 7.67 (H-11a, 1H, d, *J* = 7.3 Hz), and 7.78 (H-14a, 1H, d, *J* = 9.0 Hz); <sup>13</sup>C NMR (CDCl<sub>3</sub>, 100 MHz) δ 51.7 (C-16a), 51.9 (C-16b), 55.1 (OMe, 4a), 55.3 (OMe, 4b), 105.6 (C-5a), 113.0 (C-2b), 113.1 (C-6b), 118.2 (C-3a), 126.3 (C-12b), 126.7 (C-12a), 127.0 (C-7a), 128.4 (C-1a), 129.3 (C-11b), 129.4 (C-11a), 129.8 (C-2a), 130.6 (C-13a), 130.7 (C-8a,

C-8b), 130.8 (C-13b), 131.7 (C-1b), 131.8 (C-3b), 132.2 (C-14a), 132.3 (C-5b), 133.3 (C-14b), 133.6 (C-6a), 136.0 (C-7b), 136.5 (C-10b), 138.1 (C-9a), 142.2 (C-9b), 143.0 (C-10a), 157.8 (C-4a), 158.1 (C-4b), 167.4 (C-15b), and 168.1 (C-15a); HRMS (ESI-TOF)  $m/z$ :  $[M + H]^+$  Calcd for  $C_{34}H_{29}O_6$ , 533.1959; Found 533.1980.

*Diene (37cc)*. Light yellowish oil; UV (EtOH)  $\lambda_{max}$  (log  $\epsilon$ ) 203 (4.11), 230 (3.42), 257 (3.10), and 340 (3.15) nm; IR (dry film)  $\nu_{max}$  2058, 2021, 1948, 1891, 1726 (CO<sub>2</sub>Me), 1604, 1508, 827, and 757 cm<sup>-1</sup>; <sup>1</sup>H NMR (CDCl<sub>3</sub>, 400 MHz)  $\delta$  3.66 (OMe, 4a, 4b, 6H, s), 3.75 (CO<sub>2</sub>Me, 16a, 16b, 6H, s), 5.96 (H-7a, H-7b, 2H, s), 6.52 (H-2a, H-2b, H-3a, H-3b, H-5a, H-5b, H-6a, H-6b, 8H, s), 7.43 (H-14a, H-14b, 2H, d,  $J = 7.7$  Hz), 7.48 (H-12a, H-12b, 2H, t,  $J = 7.7$  Hz), 7.58 (H-13a, H-13b, 2H, t,  $J = 7.7$  Hz), and 8.03 (H-11a, H-11b, 2H, d,  $J = 7.7$  Hz); <sup>13</sup>C NMR (CDCl<sub>3</sub>, 100 MHz)  $\delta$  52.1 (C-16a, C-16b), 55.2 (OMe, 4a, 4b), 113.4 (C-3a, C-3b, C-5a, C-5b), 127.6 (C-12a, C-12b), 128.7 (C-7a, C-7b), 130.1 (C-1a, C-1b), 130.4 (C-2a, C-2b, C-6a, C-6b), 130.6 (C-11a, C-11b), 131.7 (C-10a, C-10b), 132.3 (C-14a, C-14b), 133.0 (C-13a, C-13b), 141.2 (C-9a, C-9b), 142.6 (C-8a, C-8b), 158.1 (C-4a, C-4b), and 167.4 (C-15a, C-15b); HRMS (ESI-TOF)  $m/z$ :  $[M + H]^+$  Calcd for  $C_{34}H_{31}O_6$ , 535.2115; Found 535.2123.

### 3.8.34 Anodic oxidation of 38 in MeCN/ 0.2 M LiClO<sub>4</sub>

Controlled potential electrolysis of **38** (+1.25 V, 1.0 F) yielded a mixture, which on preparative radial chromatography (SiO<sub>2</sub>, *n*-hexane/CH<sub>2</sub>Cl<sub>2</sub>, 2/1 to 10% MeOH/CH<sub>2</sub>Cl<sub>2</sub>), followed by HPLC (Luna Phenyl-Hexyl column, 12% H<sub>2</sub>O:MeCN, 10 ml/min), gave **38bm** (12.1 mg, 20%), **38bm + 38bn** (24.3 mg, 40%, **38bm:38bn**, 1:1.2), and **38cd** (5.5 mg, 10%).

*Tetraaryltetrahydrofuran (38bm)*. Light yellowish oil. UV (EtOH)  $\lambda_{\max}$  (log  $\epsilon$ ) 228 (4.54), 276 (3.78), and 283 (3.73) nm; IR (dry film)  $\nu_{\max}$  3265, 2837, 1717, 1694, 1675, 1512, 1246, 1176, 1022, 828, and 752  $\text{cm}^{-1}$ ;  $^1\text{H}$  NMR ( $\text{CDCl}_3$ , 400 MHz)  $\delta$  2.33 (Me, 17a, 17b, 6H, s) 3.77 (OMe, 4a, 4b, 6H, s), 4.73 (H-8a, H-8b, 2H, dd,  $J = 5.2, 2.2$  Hz), 5.19 (H-7a, H-7b, 2H, dd,  $J = 5.2, 2.2$  Hz), 6.81 (H-2a, H-2b, H-6a, H-6b, 4H, d,  $J = 8.7$  Hz), 7.16 (H-11a, H-11b, 2H, d,  $J = 7.8$  Hz), 7.22 (H-3a, H-3b, H-5a, H-5b, 4H, d,  $J = 8.7$  Hz), 7.23 (H-12a, H-12b, 2H, m), 7.56 (H-13a, H-13b, 2H, t,  $J = 7.8$  Hz), 7.72 (NH, 2H, br s), and 7.89 (H-14a, H-14b, 2H, d,  $J = 7.8$  Hz);  $^{13}\text{C}$  NMR ( $\text{CDCl}_3$ , 100 MHz)  $\delta$  25.2 (C-17a, C-17b), 54.7 (C-8a, C-8b), 55.2 (OMe, 4a, 4b), 88.4 (C-7a, C-7b), 113.8 (C-3a, C-3b, C-5a, C-5b), 126.6 (C-11a, C-11b), 127.0 (C-12a, C-12b), 127.9 (C-2a, C-2b, C-6a, C-6b), 128.0 (C-14a, C-14b), 131.86 (C-13a, C-13b), 131.88 (C-1a, C-1b), 135.9 (C-9a, C-9b), 136.0 (C-10a, C-10b), 159.7 (C-4a, C-4b), 167.7 (C-15a, C-15b), and 172.2 (C-16a, C-16b); HRMS (DART-TOF)  $m/z$ :  $[\text{M} + \text{H}]^+$  Calcd for  $\text{C}_{36}\text{H}_{35}\text{N}_2\text{O}_7$ , 607.2444; Found 607.2450.

*Mixture of 38bm and 38bn*. light yellowish oil. *Tetraaryltetrahydrofuran (38bn)*.  $^1\text{H}$  NMR ( $\text{CDCl}_3$ , 400 MHz)  $\delta$  2.33 (Me, 17a, 17b, 6H, s) 3.78 (OMe, 4a, 4b, 6H, s), 4.73 (H-8a, H-8b, 2H, dd,  $J = 4.4, 1.0$  Hz), 5.52 (H-7a, H-7b, 2H, dd,  $J = 4.4, 1.0$  Hz), 6.85 (H-2a, H-2b, H-6a, H-6b, 4H, d,  $J = 8.7$  Hz), 7.18 (H-3a, H-3b, H-5a, H-5b, 4H, d,  $J = 8.7$  Hz), 7.24 (H-11a, H-11b, H-12a, H-12b, H-14a, H-14b, 6H)\*, 7.56 (H-13a, H-13b, 2H, t,  $J = 7.6$  Hz), and 7.98 (NH, 2H, br s);  $^{13}\text{C}$  NMR ( $\text{CDCl}_3$ , 100 MHz)  $\delta$  25.2 (C-17a, C-17b), 51.9 (C-8a, C-8b), 55.3 (OMe, 4a, 4b), 84.7 (C-7a, C-7b), 114.0 (C-3a, C-3b, C-5a, C-5b), 126.5 (C-11a, C-11b), 127.5 (C-12a, C-12b), 127.6 (C-2a, C-2b, C-6a, C-6b), 129.0 (C-14a, C-14b), 130.8 (C-13a, C-13b), 132.7 (C-1a, C-1b), 136.3 (C-9a, C-9b), 136.5 (C-10a, C-10b), 159.3 (C-4a, C-4b), 168.0 (C-15a, C-15b), and 172.0 (C-16a,

C-16b); HRMS (DART-TOF)  $m/z$ :  $[M + H]^+$  Calcd for  $C_{36}H_{35}N_2O_7$ , 607.2444; Found 607.2454. \*overlapped signals

*Isocoumarin N-acetylbenzamide (38cd)*: Light yellowish oil and subsequently, colorless block crystals from MeOH/CH<sub>2</sub>Cl<sub>2</sub>; mp 177–179 °C; UV (EtOH)  $\lambda_{\max}$  (log  $\epsilon$ ) 232 (4.50), 278 (3.82), and 328 (3.49) nm; IR (dry film)  $\nu_{\max}$  3284, 2836, 1716, 1695, 1508, 1246, 1176, 1019, and 748 cm<sup>-1</sup>; <sup>1</sup>H NMR (CDCl<sub>3</sub>, 400 MHz)  $\delta$  2.49 (Me, 17b, 3H, s), 3.70 (OMe, 4b, 3H, s), 3.74 (OMe, 4a, 3H, s), 4.26 (H-7b, 1H, d,  $J = 12.0$  Hz), 5.97 (H-8b, 1H, d,  $J = 12.0$  Hz), 6.55 (H-2b, H-3b, H-5b, H-6b, 4H, m), 6.77 (H-3a, H-5a, 2H, d,  $J = 8.8$  Hz), 7.07 (NH, 1H, br s), 7.12 (H-2a, H-6a, 2H, d,  $J = 8.8$  Hz), 7.22 (H-7a, H-11b, H-12b, 3H, m), 7.44 (H-12a, H-13b, 2H, m), 7.61 (H-14b, 1H, d,  $J = 7.6$  Hz), 7.67 (H-13a, 1H, t,  $J = 7.6$  Hz), 8.25 (H-11a, 1H, d,  $J = 7.6$  Hz), and 8.45 (H-11a, 1H, d,  $J = 7.6$  Hz); <sup>13</sup>C NMR (CDCl<sub>3</sub>, 100 MHz)  $\delta$  25.5 (C-17b), 41.3 (C-8b), 55.1 (OMe, 4b, C-7b), 55.3 (OMe, 4b), 113.4 (C-3b, C-5b), 114.4 (C-3a, C-5a), 117.6 (C-8a), 121.4 (C-10a), 124.4 (C-14a), 126.6 (C-12b), 127.3 (C-11b), 128.3 (C-12a), 129.0 (C-2a, C-6a), 129.2 (C-14b), 129.8 (C-11a), 130.7 (C-2b, C-6b), 132.2 (C-13b), 134.1 (C-1a), 134.6 (C-10b), 135.2 (C-13a), 137.0 (C-9a), 141.8 (C-9b), 145.7 (C-7a), 158.2 (C-4a), 158.3 (C-4b), 162.1 (C-15a), 167.9 (C-15b), and 172.0 (C-16b); HRMS (DART-TOF)  $m/z$ :  $[M + H]^+$  Calcd for  $C_{34}H_{30}NO_6$ , 548.2073; Found 548.2068.

### 3.8.35 Anodic oxidation of 39 in MeCN/ 0.2 M LiClO<sub>4</sub>

Controlled potential electrolysis of 7 at the potential peak (+0.90 V, 1 F) yielded the dehydrotetralin **39ca** (28.0 mg, 52%), purified by preparative radial chromatography (SiO<sub>2</sub>, *n*-hexane:CH<sub>2</sub>Cl<sub>2</sub>, 4:1 to 5% MeOH:CH<sub>2</sub>Cl<sub>2</sub>).

*Dehydrotetralin (39ca)*. Light yellowish oil. UV (EtOH)  $\lambda_{\max}$  (log  $\epsilon$ ) 225 (4.64), 248 (4.45), 280 (4.23), and 317 (4.18) nm; IR (dry film)  $\nu_{\max}$  2935, 1509, 1461, 1234, 1025, and 732  $\text{cm}^{-1}$ ;  $^1\text{H}$  NMR ( $\text{CDCl}_3$ , 400 MHz)  $\delta$  3.46 (OMe, 10a, 3H, s), 3.71 (OMe, 4a, 3H, s), 3.83 (OMe, 4b, 3H, s), 3.86 (OMe, 3b, 3H, s), 3.90 (OMe, 10b, 3H, s), 3.93 (OMe, 3a, 3H, s), 4.17 (H-7b, 1H, d,  $J = 1.6$  Hz), 4.74 (H-8b, 1H, d,  $J = 1.6$  Hz), 6.46 (H-5a, 1H, s), 6.60 (H-6b, 1H, dd,  $J = 8.2, 1.8$  Hz), 6.70 (H-11a, 1H, d,  $J = 7.5$  Hz), 6.72 (H-13b, 1H, t,  $J = 7.6$  Hz), 6.74 (H-5b, 1H, d,  $J = 8.2$  Hz), 6.75 (H-13a, 1H, t,  $J = 7.5$  Hz), 6.82 (H-2a, 1H, s), 6.83 (H-11a, 1H, d,  $J = 7.6$  Hz), 6.93 (H-7a, 1H, s), 7.02 (H-14a, 1H, d,  $J = 7.5$  Hz), 7.05 (H-2b, 1H, d,  $J = 1.8$  Hz), 7.07 (H-12a, 1H, m), 7.09 (H-12b, 1H, m), and 7.15 (H-14b, 1H, d,  $J = 7.6$  Hz);  $^{13}\text{C}$  NMR ( $\text{CDCl}_3$ , 100 MHz)  $\delta$  45.2 (C-8b), 50.1 (C-7b), 55.26 (OMe, 10a), 55.34 (OMe, 10b), 55.65 (OMe, 3b), 55.70 (OMe, 4a), 55.87 (OMe, 4b), 55.93 (OMe, 3a), 109.8 (C-2a), 110.3 (C-11b), 110.6 (C-5b), 111.1 (C-11a), 111.7 (C-2b), 112.9 (C-5a), 119.9 (C-6b), 120.30 (C-13a), 120.35 (C-13b), 127.1 (C-12b), 127.4 (C-6a), 127.7 (C-1a), 128.0 (C-12a), 128.4 (C-14b), 128.5 (C-7a), 129.6 (C-14a), 129.9 (C-9b), 131.2 (C-9a), 134.8 (C-8a), 138.7 (C-1b), 147.1 (C-4b), 147.6 (C-3a), 148.3 (C-4a), 148.4 (C-3b), 156.9 (C-10b), and 157.4 (C-10a); HRMS (DART-TOF)  $m/z$ :  $[\text{M} + \text{H}]^+$  Calcd for  $\text{C}_{34}\text{H}_{35}\text{O}_6$ , 539.2434; Found 539.2435.

### 3.8.36 Anodic oxidation of 40 in MeCN/ 0.2 M LiClO<sub>4</sub>

Controlled potential electrolysis of **40** at the potential peak (+0.99 V, 1 F) yielded the dehydrotetralin **40ca** (35.7 mg, 60%), purified by preparative radial chromatography ( $\text{SiO}_2$ , *n*-hexane: $\text{CH}_2\text{Cl}_2$ , 4:1 to 5% MeOH: $\text{CH}_2\text{Cl}_2$ ).

*Dehydrotetralin (40ca)*. Light yellowish oil. UV (EtOH)  $\lambda_{\max}$  (log  $\epsilon$ ) 234 (4.39), 289 (3.96) and 318 (4.04) nm; IR (dry film)  $\nu_{\max}$  2936, 1756, 1510, 1463, 1193, 1026, and 732  $\text{cm}^{-1}$ ;  $^1\text{H}$  NMR ( $\text{CDCl}_3$ , 400 MHz)  $\delta$  1.70 (COMe, 16a, 3H, s), 2.28 (COMe, 16b, 3H, s), 3.74 (OMe, 4a, 3H, s), 3.79 (OMe, 3b, 3H, s), 3.83 (OMe, 4b, 3H, s), 3.94 (OMe, 3a, 3H, s), 4.04 (H-7b, 1H, s), 4.33 (H-8b, 1H, s), 6.47 (H-5a, 1H, s), 6.73 (H-6b, 1H, dd,  $J = 8.3, 1.8$  Hz), 6.77 (H-5b, 1H, d,  $J = 8.3$  Hz), 6.80 (H-2b, 1H, d,  $J = 1.8$  Hz), 6.82 (H-2a, 1H, s), 6.83 (H-7a, 1H, s), 6.90 (H-11a, 1H, d,  $J = 7.8$  Hz), 6.98 (H-12a, H-11b, 2H, m), 7.02 (H-14a, H-12b, 2H, m), and 7.17 (H-12a, H-12b, H-13b, 3H, m);  $^{13}\text{C}$  NMR ( $\text{CDCl}_3$ , 100 MHz)  $\delta$  20.2 (C-16a), 21.1 (C-16b), 44.7 (C-8b), 50.7 (C-7b), 55.8 (OMe, 4a, 3b), 55.9 (OMe, 4b), 56.0 (OMe, 3a), 110.0 (C-2a), 111.2 (C-2b), 111.3 (C-5b), 112.8 (C-5a), 119.5 (C-6b), 122.6 (C-11a), 122.9 (C-11b), 126.0 (C-13a), 126.2 (C-1a), 126.3 (C-13b), 127.5 (C-6a), 127.7 (C-12b), 128.3 (C-14b), 128.4 (C-12a), 128.8 (C-7a), 130.4 (C-14a), 133.8 (C-9b), 134.2 (C-9a), 134.4 (C-8a), 138.5 (C-1b), 147.7 (C-10b), 147.8 (C-10a), 147.9 (C-4b), 148.0 (C-3a), 149.0 (C-3b), 149.1 (C-4a), 169.5 (C-15a), and 169.6 (C-15b); HRMS (DART-TOF)  $m/z$ :  $[\text{M} + \text{H}]^+$  Calcd for  $\text{C}_{36}\text{H}_{35}\text{O}_8$ , 595.2332; Found 595.2331.

### 3.8.37 Anodic oxidation of **41** in MeCN/ 0.2 M LiClO<sub>4</sub>

Controlled potential electrolysis of **41** (+1.10 V, 1.0 F) yielded a mixture, which on preparative radial chromatography ( $\text{SiO}_2$ , *n*-hexane/ $\text{CH}_2\text{Cl}_2$ , 2/1 to 10% MeOH/ $\text{CH}_2\text{Cl}_2$ ) gave **41ce** (3.2 mg, 7%), **41cf** (11.3 mg, 23%), **41cg** (4.9 mg, 10%), and **41bm** (11.8 mg, 24%).

*Fused indanylnaphthalene (41ce)*. Light yellowish oil and subsequently, colorless needle crystals from MeOH/CH<sub>2</sub>Cl<sub>2</sub>; mp 181–183 °C; UV (EtOH)  $\lambda_{\max}$  (log  $\epsilon$ ) 216 (4.49), 261 (4.50), 270 (4.48), and 319 (3.88) nm; IR (dry film)  $\nu_{\max}$  2836, 1693, 1620, 1513, 1463, 1245, 1231, 1173, 1031, and 753 cm<sup>-1</sup>; <sup>1</sup>H NMR (CDCl<sub>3</sub>, 400 MHz)  $\delta$  3.71 (OMe, 4a, 3H, s), 3.76 (OMe, 4b, 3H, s), 4.28 (H-15a, 1H, s), 6.07 (H-14a, 1H, d,  $J$  = 7.8 Hz), 6.76 (H-3b, H-5b, 2H, m), 6.88 (H-5a, 1H, d,  $J$  = 2.5 Hz), 6.95 (H-13a, 1H, t,  $J$  = 7.8 Hz), 6.99 (H-2b, 1H, m), 7.02 (H-6b, 1H, m), 7.17 (H-12a, 1H, t,  $J$  = 7.8 Hz), 7.27 (H-3a, 1H, dd,  $J$  = 9.0, 2.5 Hz), 7.31 (H-14b, 1H, d,  $J$  = 7.6 Hz), 7.44 (H-12b, 1H, t,  $J$  = 7.6 Hz), 7.54 (H-13b, 1H, t,  $J$  = 7.6 Hz), 7.58 (H-11a, 1H, d,  $J$  = 7.8 Hz), 7.91 (H-11b, 1H, d,  $J$  = 7.6 Hz), 8.05 (H-2a, 1H, d,  $J$  = 9.0 Hz), and 9.81 (H-15b, 1H, s); <sup>13</sup>C NMR (CDCl<sub>3</sub>, 100 MHz)  $\delta$  35.8 (C-15a), 55.1 (OMe, 4a), 55.2 (OMe, 4b), 106.6 (C-5a), 113.2 (C-5b), 113.7 (C-3b), 119.1 (C-3a), 121.7 (C-14a), 124.7 (C-11a), 125.8 (C-2a), 125.9 (C-1a, C-12a), 126.6 (C-13a), 127.1 (C-11b), 128.0 (C-12b), 130.7 (C-1b), 130.9 (C-8b), 131.3 (C-2b), 131.9 (C-14b), 132.1 (C-6b), 133.3 (C-6a), 133.7 (C-13b), 133.9 (C-10b), 135.3 (C-8a), 138.0 (C-7b), 140.1 (C-7a), 142.5 (C-9a), 143.4 (C-10a), 144.2 (C-9b), 157.9 (C-4a), 158.2 (C-4b), and 191.8 (C-15b); HRMS (DART-TOF)  $m/z$ : [M + H]<sup>+</sup> Calcd for C<sub>32</sub>H<sub>25</sub>O<sub>3</sub>, 457.1804; Found 457.1793.

*Fused indanylbenzopyran aldehyde (41cf)*. Light yellowish oil and subsequently, colorless block crystals from MeOH/CH<sub>2</sub>Cl<sub>2</sub>; mp 202–204 °C; UV (EtOH)  $\lambda_{\max}$  (log  $\epsilon$ ) 234 (4.12) and 275 (3.36) nm; IR (dry film)  $\nu_{\max}$  3415, 2836, 1720, 1607, 1509, 1247, 1177, 1026, and 752 cm<sup>-1</sup>; <sup>1</sup>H NMR (CDCl<sub>3</sub>, 400 MHz)  $\delta$  3.51 (OH, 15a, 1H, br d,  $J$  = 3.2 Hz), 3.67 (OMe, 4a, 3H, s), 3.74 (OMe, 4b, 3H, s), 3.99 (H-7b, 1H, d,  $J$  = 8.8 Hz), 4.85 (H-8b, 1H, d,  $J$  = 8.8 Hz), 5.65 (H-15b, 1H, s), 5.93 (H-15a, 1H, br d,  $J$  = 3.2 Hz), 6.39 (H-14b, 1H, d,  $J$  = 7.5 Hz), 6.51 (H-2a, H-3a, H-5a, H-6a, 4H, m), 6.58 (H-14a,

1H, d,  $J = 7.6$  Hz), 6.62 (H-3b, H-5b, 2H, d,  $J = 8.7$  Hz), 6.89 (H-13a, 1H, t,  $J = 7.6$  Hz), 6.93 (H-2b, H-6b, 2H, d,  $J = 8.7$  Hz), 6.98 (H-13b, 1H, t,  $J = 7.5$  Hz), 7.17 (H-12a, 1H, t,  $J = 7.6$  Hz), 7.20 (H-12b, 1H, t,  $J = 7.5$  Hz), 7.27 (H-11a, 1H, d,  $J = 7.6$  Hz), 7.44 (H-11b, 1H, d,  $J = 7.5$  Hz), and 9.31 (H-7a, 1H, s);  $^{13}\text{C}$  NMR ( $\text{CDCl}_3$ , 100 MHz)  $\delta$  51.9 (C-8b), 52.9 (C-7b), 55.1 (OMe, 4a), 55.3 (OMe, 4b), 63.5 (C-8a), 72.6 (C-15b), 91.9 (C-15a), 112.9 (C-3a, C-5a), 113.7 (C-3b, C-5b), 125.3 (C-11b), 127.1 (C-9a, C-14b), 127.2 (C-11a), 127.4 (C-12b), 127.9 (C-12a), 128.0 (C-13a), 128.6 (C-13b), 129.1 (C-2b, C-6b), 130.45 (C-2a, C-6a), 130.52 (C-14a), 134.4 (C-1a), 134.9 (C-10a), 135.9 (C-1b), 138.4 (C-10b), 147.3 (C-9b), 157.7 (C-4b), 157.9 (C-4a), and 197.6 (C-7a); HRMS (DART-TOF)  $m/z$ :  $[\text{M} + \text{H}]^+$  Calcd for  $\text{C}_{32}\text{H}_{29}\text{O}_5$ , 493.2015; Found 493.2013.

*Fused indanylbzopyran aldehyde (41cg)*. Light yellowish oil. UV (EtOH)  $\lambda_{\text{max}}$  (log  $\epsilon$ ) 232 (4.23) and 275 (3.60) nm; IR (dry film)  $\nu_{\text{max}}$  3393, 2836, 1714, 1607, 1511, 1249, 1031, and 752  $\text{cm}^{-1}$ ;  $^1\text{H}$  NMR ( $\text{CDCl}_3$ , 400 MHz)  $\delta$  2.96 (OH, 15a, 1H, br d,  $J = 9.8$  Hz), 3.73 (OMe, 4a, 3H, s), 3.82 (OMe, 4b, 3H, s), 4.15 (H-7b, 1H, d,  $J = 9.8$  Hz), 4.44 (H-8b, 1H, d,  $J = 9.8$  Hz), 5.75 (H-15a, 1H, br d,  $J = 9.8$  Hz), 6.01 (H-14b, 1H, d,  $J = 7.6$  Hz), 6.27 (H-15b, 1H, s), 6.66 (H-3a, H-5a, 2H, d,  $J = 8.8$  Hz), 6.75 (H-2a, H-6a, 2H, d,  $J = 8.8$  Hz), 6.84 (H-13b, 1H, t,  $J = 7.6$  Hz), 6.95 (H-3b, H-5b, 2H, d,  $J = 8.7$  Hz), 7.19 (H-12b, 1H, t,  $J = 7.6$  Hz), 7.25 (H-12a, 1H, t,  $J = 7.7$  Hz), 7.33 (H-11a, 1H, d,  $J = 7.7$  Hz), 7.38 (H-2b, H-6b, 2H, d,  $J = 8.7$  Hz), 7.44 (H-13a, 1H, t,  $J = 7.7$  Hz), 7.51 (H-11b, 1H, d,  $J = 7.6$  Hz), 7.67 (H-14a, 1H, d,  $J = 7.7$  Hz), and 9.22 (H-7a, 1H, s);  $^{13}\text{C}$  NMR ( $\text{CDCl}_3$ , 100 MHz)  $\delta$  52.2 (C-7b), 55.2 (OMe, 4a), 55.3 (OMe, 4b), 62.0 (C-8b), 63.1 (C-8a), 78.2 (C-15b), 89.1 (C-15a), 113.6 (C-3a, C-5a), 114.3 (C-3b, C-5b), 124.0 (C-11b), 125.6 (C-11a), 127.3 (C-14b), 127.5 (C-12b, C-13b), 127.6 (C-12a), 128.3 (C-14a), 129.2 (C-13a), 129.9 (C-2b, C-6b), 130.1 (C-2a, C-6a), 133.8 (C-1a, C-

9a), 134.4 (C-1b), 137.6 (C-10a), 138.4 (C-10b), 140.8 (C-9b), 158.4 (C-4a), 158.6 (C-4b), and 199.1 (C-7a); HRMS (DART-TOF)  $m/z$ :  $[M + H]^+$  Calcd for  $C_{32}H_{29}O_5$ , 493.2015; Found 493.2014.

*Tetraaryltetrahydrofuran (41bm)*. Light yellowish oil. UV (EtOH)  $\lambda_{\max}$  ( $\log \epsilon$ ) 229 (4.44), 255 (4.05), and 301 (3.48) nm; IR (dry film)  $\nu_{\max}$  2836, 1689, 1511, 1246, 1175, 1029, 828, and 753  $\text{cm}^{-1}$ ;  $^1\text{H}$  NMR ( $\text{CDCl}_3$ , 400 MHz)  $\delta$  3.77 (OMe, 4a, 4b, 6H, s), 5.23 (H-8a, H-8b, 2H, dd,  $J = 6.2, 2.6$  Hz), 5.41 (H-7a, H-7b, 2H, dd,  $J = 6.2, 2.6$  Hz), 6.82 (H-2a, H-2b, H-6a, H-6b, 4H, d,  $J = 8.7$  Hz), 7.21 (H-3a, H-3b, H-5a, H-5b, 4H, d,  $J = 8.7$  Hz), 7.32 (H-12a, H-12b, 2H, t,  $J = 7.8$  Hz), 7.58 (H-11a, H-11b, 2H, d,  $J = 7.8$  Hz), 7.59 (H-13a, H-13b, 2H, t,  $J = 7.8$  Hz), 7.82 (H-14a, H-14b, 2H, d,  $J = 7.8$  Hz), and 9.66 (H-15a, H-15b, 2H, s);  $^{13}\text{C}$  NMR ( $\text{CDCl}_3$ , 100 MHz)  $\delta$  54.6 (C-8a, C-8b), 55.2 (OMe, 4a, 4b), 88.5 (C-7a, C-7b), 113.9 (C-3a, C-3b, C-5a, C-5b), 127.2 (C-2a, C-2b, C-6a, C-6b), 127.4 (C-12a, C-12b), 128.0 (C-14a, C-14b), 132.1 (C-1a, C-1b), 132.4 (C-11a, C-11b), 134.2 (C-13a, C-13b), 134.7 (C-9a, C-9b), 139.7 (C-10a, C-10b), 159.4 (C-4a, C-4b), and 191.5 (C-15a, C-15b); HRMS (DART-TOF)  $m/z$ :  $[M + H]^+$  Calcd for  $C_{32}H_{29}O_5$ , 493.2015; Found 493.2019.

### 3.8.38 Anodic oxidation of 42 in MeCN/ 0.2 M LiClO<sub>4</sub>

Controlled potential electrolysis of **42** (+1.07 V, 1.0 F) yielded a mixture, which on preparative radial chromatography ( $\text{SiO}_2$ , *n*-hexane/ $\text{CH}_2\text{Cl}_2$ , 2/1 to 10% MeOH/ $\text{CH}_2\text{Cl}_2$ ) gave **41ce** (3.7 mg, 8%), **41cf** (12.3 mg, 25%), **41cg** (6.9 mg, 14%), **41bm** (11.3 mg, 23%), and **42cf** (8.6 mg, 17%).

*Fused indanylbenzopyran aldehyde (42cf)*. Light yellowish oil. UV (EtOH)  $\lambda_{\max}$  ( $\log \epsilon$ ) 231 (4.24) and 275 (3.62) nm; IR (dry film)  $\nu_{\max}$  2834, 1720, 1608, 1509, 1248, 1177, 1033, and 754  $\text{cm}^{-1}$ ;  $^1\text{H}$  NMR ( $\text{CDCl}_3$ , 400 MHz)  $\delta$  3.69 (OMe, 4b, 3H, s), 3.71 (OMe, 16a, 3H, s), 3.74 (OMe, 4a, 3H, s), 3.99 (H-7b, 1H, d,  $J = 9.6$  Hz), 4.85 (H-8b, 1H, d,  $J = 9.6$  Hz), 5.48 (H-15b, 1H, s), 5.50 (H-15a, 1H, s), 6.36 (H-14b, 1H, d,  $J = 7.8$  Hz), 6.47 (H-14a, 1H, d,  $J = 7.7$  Hz), 6.55 (H-3b, H-5b, 2H, d,  $J = 8.8$  Hz), 6.59 (H-2b, H-6b, 2H, d,  $J = 8.8$  Hz), 6.61 (H-3a, H-5a, 2H, d,  $J = 8.8$  Hz), 6.81 (H-13a, 1H, t,  $J = 7.7$  Hz), 6.90 (H-2a, H-6a, 2H, d,  $J = 8.8$  Hz), 6.96 (H-13b, 1H, t,  $J = 7.8$  Hz), 7.13 (H-12a, 1H, t,  $J = 7.7$  Hz), 7.19 (H-12b, 1H, t,  $J = 7.8$  Hz), 7.21 (H-11a, 1H, d,  $J = 7.7$  Hz), 7.45 (H-11b, 1H, d,  $J = 7.8$  Hz), and 9.29 (H-7a, 1H, s);  $^{13}\text{C}$  NMR ( $\text{CDCl}_3$ , 100 MHz)  $\delta$  51.6 (C-8b), 53.3 (C-7b), 55.2 (OMe, 4b), 55.3 (OMe, 4a), 55.9 (OMe, 16a), 63.6 (C-8a), 72.7 (C-15b), 98.5 (C-15a), 113.0 (C-3b, C-5b), 113.6 (C-3a, C-5a), 125.2 (C-11b), 127.0 (C-9a), 127.1 (C-12b), 127.3 (C-11a, C-14b), 127.75 (C-12a), 127.81 (C-13a), 128.5 (C-13b), 129.0 (C-2a, C-6a), 130.2 (C-2b, C-6b), 130.6 (C-14a), 134.2 (C-10a), 135.0 (C-1b), 136.0 (C-1a), 138.2 (C-10b), 147.5 (C-9b), 157.6 (C-4a), 157.8 (C-4b), and 197.5 (C-7a); HRMS (DART-TOF)  $m/z$ :  $[\text{M} + \text{H}]^+$  Calcd for  $\text{C}_{33}\text{H}_{31}\text{O}_5$ , 507.2172; Found 507.2175.

### 3.8.39 Anodic oxidation of 43 in MeCN/ 0.2 M LiClO<sub>4</sub>

Controlled potential electrolysis of **43** (+1.08 V, 1.0 F) yielded a mixture, which on preparative radial chromatography ( $\text{SiO}_2$ , *n*-hexane/ $\text{CH}_2\text{Cl}_2$ , 2/1 to 10% MeOH/ $\text{CH}_2\text{Cl}_2$ ) gave **41ce** (2.7 mg, 6%), **41cf** (11.8 mg, 24%), **41cg** (6.4 mg, 13%), **41bm** (9.9 mg, 20%), and **43ch** (2.2 mg, 5%).

*Indenyl benzaldehyde (43ch)*. Light yellowish oil. UV (EtOH)  $\lambda_{\max}$  (log  $\epsilon$ ) 231 (4.19) and 286 (3.80) nm; IR (dry film)  $\nu_{\max}$  2836, 1686, 1608, 1510, 1248, 1178, 1034, and 758  $\text{cm}^{-1}$ ;  $^1\text{H}$  NMR ( $\text{CDCl}_3$ , 400 MHz)  $\delta$  3.69 (OMe, 4a, 3H, s), 3.83 (OMe, 4b, 3H, s), 4.51 (H-7b, 1H, d,  $J = 5.8$  Hz), 4.80 (H-8b, 1H, d,  $J = 5.8$  Hz), 6.28 (H-2a, H-6a, 2H, d,  $J = 8.7$  Hz), 6.51 (H-3a, H-5a, 2H, d,  $J = 8.7$  Hz), 6.56 (H-15b, 1H, s), 6.59 (H-14b, 1H, d,  $J = 7.4$  Hz), 6.87 (H-3b, H-5b, 2H, d,  $J = 8.7$  Hz), 7.05 (H-13b, 1H, t,  $J = 7.4$  Hz), 7.21 (H-2b, H-6b, 2H, d,  $J = 8.7$  Hz), 7.31 (H-12b, 1H, t,  $J = 7.4$  Hz), 7.37 (H-11b, 1H, d,  $J = 7.4$  Hz), 7.43 (H-12a, 1H, t,  $J = 7.5$  Hz), 7.52 (H-14a, 1H, d,  $J = 7.5$  Hz), 7.66 (H-13a, 1H, t,  $J = 7.5$  Hz), 7.89 (H-11a, 1H, d,  $J = 7.5$  Hz), and 8.90 (H-15a, 1H, s);  $^{13}\text{C}$  NMR ( $\text{CDCl}_3$ , 100 MHz)  $\delta$  50.0 (C-7b), 55.2 (OMe, 4a), 55.3 (OMe, 4b), 56.4 (C-8b), 113.5 (C-3a, C-5a), 113.7 (C-3b, C-5b), 121.7 (C-11b), 124.8 (C-14b), 125.3 (C-13b), 127.4 (C-12a, C-12b), 128.0 (C-11a), 129.47 (C-2b, C-6b), 129.52 (C-2a, C-6a, C-14a), 130.6 (C-1a), 133.1 (C-13a), 134.8 (C-1b), 135.0 (C-10a), 135.8 (C-15b), 140.0 (C-9a), 144.3 (C-10b), 145.2 (C-9b), 146.1 (C-8a), 158.1 (C-4b), 158.7 (C-4a), and 192.6 (C-15a); HRMS (DART-TOF)  $m/z$ :  $[\text{M} + \text{H}]^+$  Calcd for  $\text{C}_{31}\text{H}_{27}\text{O}_3$ , 447.1960; Found 447.1968.

#### 3.8.40 Anodic oxidation of 44 in MeCN/ 0.2 M LiClO<sub>4</sub>

Controlled potential electrolysis of **44** (+1.10 V, 1.0 F) yielded a mixture, which on preparative radial chromatography ( $\text{SiO}_2$ , *n*-hexane/ $\text{CH}_2\text{Cl}_2$ , 2/1 to 10% MeOH/ $\text{CH}_2\text{Cl}_2$ ) gave **44ci** (10.3 mg, 20%).

*Fused benzofluorene-dibenzoannulene (44ci)*. Light yellowish oil and subsequently, colorless block crystals from MeOH/CH<sub>2</sub>Cl<sub>2</sub>; mp 195–197 °C; UV (EtOH)  $\lambda_{\max}$  (log  $\epsilon$ ) 210 (4.43), 233 (4.27), 281 (4.40), 290 (4.42), 301 (4.24), and 335 (3.59) nm; IR (dry film)  $\nu_{\max}$  3508, 2834, 1505, 1487, 1257, 1240, 1202, 1159, 1133, 1027, and 747 cm<sup>-1</sup>; <sup>1</sup>H NMR (CDCl<sub>3</sub>, 400 MHz)  $\delta$  2.51 (OH, 15b, 1H, d,  $J$  = 2.8 Hz), 3.77 (OMe, 3b, 3H, s), 3.85 (OMe, 4a, 3H, s), 3.99 (OMe, 4b, 3H, s), 4.11 (OMe, 3a, 3H, s), 4.14 (H-15a, 1H, d,  $J$  = 21.9 Hz), 4.34 (H-15a, 1H, d,  $J$  = 21.9 Hz), 5.71 (H-15b, 1H, d,  $J$  = 2.8 Hz), 6.97 (H-14a, 1H, d,  $J$  = 7.8 Hz), 7.06 (H-13a, 1H, t,  $J$  = 7.8 Hz), 7.15 (H-2b, 1H, s), 7.18 (H-13b, 1H, t,  $J$  = 7.8 Hz), 7.21 (H-12a, 1H, t,  $J$  = 7.8 Hz), 7.32 (H-2a, 1H, s), 7.34 (H-5b, 1H, s), 7.43 (H-12b, 1H, t,  $J$  = 7.8 Hz), 7.58 (H-5b, 1H, s), 7.59 (H-11a, H-14b, 2H, m), 7.74 (H-11b, 1H, d,  $J$  = 7.8 Hz); <sup>13</sup>C NMR (CDCl<sub>3</sub>, 100 MHz)  $\delta$  36.2 (C-15a), 55.8 (OMe, 4a), 55.9 (OMe, 4b), 55.96 (OMe, 3b), 56.01 (OMe, 3a), 70.1 (C-15b), 103.1 (C-2a), 103.3 (C-5b), 107.7 (C-5a), 115.2 (C-2b), 119.5 (C-11b), 123.36 (C-14b), 123.43 (C-1b), 124.5 (C-11a), 125.3 (C-13b), 125.7 (C-12a), 125.8 (C-6a), 126.0 (C-13a), 126.6 (C-1a), 128.1 (C-12b), 130.1 (C-8b), 131.7 (C-9b), 131.9 (C-14b), 133.3 (C-7b), 134.7 (C-8a), 139.7 (C-7a), 140.3 (C-6b), 143.2 (C-9a), 143.6 (C-10a), 146.0 (C-3b), 146.4 (C-10b), 149.0 (C-4b), 149.2 (C-4a), and 149.8 (C-3a); HRMS (DART-TOF)  $m/z$ : [M + H]<sup>+</sup> Calcd for C<sub>34</sub>H<sub>29</sub>O<sub>5</sub>, 517.2015; Found 517.2005.

### 3.8.41 Anodic oxidation of 45 in MeCN/ 0.2 M LiClO<sub>4</sub>

Controlled potential electrolysis of **45** (+1.10 V, 1.0 F) yielded a mixture, which on preparative radial chromatography (SiO<sub>2</sub>, *n*-hexane/CH<sub>2</sub>Cl<sub>2</sub>, 2/1 to 10% MeOH/CH<sub>2</sub>Cl<sub>2</sub>) gave **44ci** (15.5 mg, 30%).

**Conversion of 3af to the tosylate derivative (103).** Triethylamine (21  $\mu$ L, 0.15 mmol) and a solution of 4-toluenesulfonyl chloride (28.6 mg, 0.15 mmol) in  $\text{CH}_2\text{Cl}_2$  (5 ml) were added dropwise to a solution of **3af** (51.1 mg, 0.1 mmol) in  $\text{CH}_2\text{Cl}_2$  (5 ml) at 0 °C. The reaction mixture was stirred at room temperature with TLC monitoring. Hydrochloric acid (5%) was added and the mixture extracted with  $\text{CH}_2\text{Cl}_2$  (3  $\times$  20 ml). The combined organic layer was then washed with  $\text{H}_2\text{O}$ , dried ( $\text{Na}_2\text{SO}_4$ ) and concentrated under reduced pressure. The resulting residue was then fractionated by preparative radial chromatography to yield the tosylate derivative.

*Bridged oxocine (103).* Light yellowish oil;  $^1\text{H}$  NMR ( $\text{CDCl}_3$ , 400 MHz)  $\delta$  2.43 (Me, 4a', s), 3.28 (H-8b, 1H, s), 3.71 (OMe, 4a, 3H, s), 3.83 (OMe, 3b, 3H, s), 3.89 (OMe, 3a, 3H, s), 3.96 (OMe, 4b, 3H, s), 4.01 (H-8a, 1H, s), 4.46 (H-7b, 1H, s), 5.41 (H-7a, 1H, s), 6.42 (H-5a, 1H, s), 6.65 (H-11b, 1H, d,  $J = 7.8$  Hz), 6.67 (H-2b, 1H, s), 6.68 (H-6b, 1H, d,  $J = 7.9$  Hz), 6.83 (H-5b, 1H, d,  $J = 7.9$  Hz), 6.87 (H-11a, 1H, d,  $J = 7.9$  Hz), 6.91 (H-14a, 1H, d,  $J = 7.9$  Hz), 6.92 (H-13a, 1H, t,  $J = 7.9$  Hz), 6.95 (H-2a, 1H, s), 6.97 (H-13b, 1H, t,  $J = 7.8$  Hz), 7.02 (H-12a, 1H, t,  $J = 7.9$  Hz), 7.10 (H-12b, 1H, t,  $J = 7.9$  Hz), 7.23 (H-3a', H-5a', 2H, d,  $J = 8.0$  Hz), 7.43 (H-14b, 1H, d,  $J = 7.8$  Hz), and 7.62 (H-2a', H-6a', 2H, d,  $J = 8.0$  Hz);  $^{13}\text{C}$  NMR ( $\text{CDCl}_3$ , 100 MHz)  $\delta$  21.7 (Me, 4a'), 30.2 (C-8a), 42.3 (C-8b), 55.8 (OMe, 4a), 55.9 (OMe, 3b), 55.9 (OMe, 4b), 56.0 (OMe, 3a), 56.4 (C-7b), 73.9 (C-7a), 111.3 (C-5b), 112.2 (C-2a), 112.5 (C-5a), 112.4 (C-2b), 117.1 (C-11b), 121.0 (C-13b), 121.1 (C-11a), 121.4 (C-6b), 125.7 (C-9b), 126.9 (C-13a), 127.6 (C-12a), 128.3 (C-12b), 128.3 (C-2a', C-6a'), 128.6 (C-6a), 128.9 (C-1a), 129.0 (C-14a), 129.1 (C-14b), 129.8 (C-3a', C-5a'), 133.1 (C-1a'), 134.3 (C-9a), 136.4 (C-1b), 145.3 (C-4a'), 147.8 (C-4b), 148.1 (C-3a), 148.4 (C-10a), 149.0 (C-3b), 149.6 (C-4a), and

152.3 (C-10b); HRMS (DART-TOF)  $m/z$ :  $[M + H]^+$  Calcd for  $C_{39}H_{37}O_8S$ , 665.2209; Found 665.2208.

**Conversion of 3af to the acetate derivative (104).** Triethylamine (42  $\mu$ L, 0.3 mmol) and a solution of acetic anhydride (28  $\mu$ L, 0.3 mmol) in  $CH_2Cl_2$  (5 ml) were added dropwise to a solution of **3af** (51.1 mg, 0.1 mmol) in  $CH_2Cl_2$  (5 ml) at 0 °C. The reaction mixture was stirred at room temperature with TLC monitoring. Hydrochloric acid (5%) was added and the mixture extracted with  $CH_2Cl_2$  (3  $\times$  20 ml). The combined organic layer was then washed with  $H_2O$ , dried ( $Na_2SO_4$ ) and concentrated under reduced pressure. The resulting residue was then fractionated by preparative radial chromatography to yield the acetate derivative.

*Bridged oxocine (104).* Colorless oil;  $^1H$  NMR ( $CDCl_3$ , 400 MHz)  $\delta$  1.83 (COMe, 16a, 3H, s), 3.33 (H-8b, 1H, br s), 3.64 (H-8a, 1H, br s), 3.69 (OMe, 4a, 3H, s), 3.85 (OMe, 3b, 3H, s), 3.86 (OMe, 4b, 3H, s), 3.95 (OMe, 3a, 3H, s), 4.43 (H-7b, 1H, d,  $J = 1.7$  Hz), 5.40 (H-7a, 1H, t,  $J = 1.7$  Hz), 6.38 (H-5a, 1H, s), 6.56 (H-6b, 1H, dd,  $J = 8.3, 2.0$  Hz), 6.70 (H-2b, 1H, d,  $J = 2.0$  Hz), 6.74 (H-11b, 1H, dd,  $J = 7.8, 1.6$  Hz), 6.80 (H-5b, 1H, d,  $J = 8.3$  Hz), 6.90 (H-11a, 1H, dd,  $J = 7.8, 1.6$  Hz), 6.92 (H-13b, 1H, td,  $J = 7.8, 1.6$  Hz), 6.97 (H-2a, 1H, s), 7.02 (H-13a, 1H, td,  $J = 7.8, 1.6$  Hz), 7.10 (H-12b, 1H, td,  $J = 7.8, 1.6$  Hz), 7.15 (H-12a, 1H, td,  $J = 7.8, 1.6$  Hz), 7.33 (H-14b, 1H, dd,  $J = 7.8, 1.6$  Hz), and 7.37 (H-14a, 1H, dd,  $J = 7.8, 1.6$  Hz);  $^{13}C$  NMR ( $CDCl_3$ , 100 MHz)  $\delta$  20.4 (COMe, C-16a), 30.0 (C-8a), 43.1 (C-8b), 55.8 (OMe, 4a), 55.9 (OMe, 3a), 56.0 (OMe, 3b, 4b), 56.2 (C-7b), 73.8 (C-7a), 111.2 (C-5b), 111.8 (C-2a), 112.6 (C-2b), 112.7 (C-5a), 117.0 (C-11b), 120.9 (C-13b), 121.4 (C-6b), 122.2 (C-11a), 125.2 (C-9b), 126.3 (C-13a),

127.7 (C-12a), 128.3 (C-12b), 128.4 (C-6a), 128.5 (C-14a), 129.1 (C-1a), 129.5 (C-14b), 133.1 (C-9a), 137.0 (C-1b), 148.0 (C-4b), 148.2 (C-3a), 148.9 (C-3b), 149.1 (C-10a), 149.6 (C-4a), 151.8 (C-10b), and 169.3 (C-15a); HRMS (DART-TOF)  $m/z$ :  $[M + H]^+$  Calcd for  $C_{34}H_{33}O_7$ , 553.2226; Found 553.2219.

**Conversion of 3af to the *p*-bromobenzoate derivative (105).** Triethylamine (21  $\mu$ L, 0.15 mmol) and a solution of *p*-bromobenzoate chloride (32.9 mg, 0.15 mmol) in  $CH_2Cl_2$  (5 ml) were added dropwise to a solution of **3af** (51.1 mg, 0.1 mmol) in  $CH_2Cl_2$  (5 ml) at 0 °C. The reaction mixture was stirred at room temperature with TLC monitoring. Hydrochloric acid (5%) was added and the mixture extracted with  $CH_2Cl_2$  (3  $\times$  20 ml). The combined organic layer was then washed with  $H_2O$ , dried ( $Na_2SO_4$ ) and concentrated under reduced pressure. The resulting residue was then fractionated by preparative radial chromatography (Chromatotron) to yield the acetate derivative.

*Bridged oxocine (105)*. Light yellowish oil;  $^1H$  NMR ( $CDCl_3$ , 400 MHz)  $\delta$  3.37 (H-8b, 1H, br s), 3.62 (OMe, 3b, 3H, s), 3.63 (OMe, 4a, 3H, s), 3.71 (OMe, 4b, 3H, s), 3.74 (H-8a, 1H, br s), 3.91 (OMe, 3a, 3H, s), 4.38 (H-7b, 1H, d,  $J = 2.0$  Hz), 5.43 (H-7a, 1H, t,  $J = 2.0$  Hz), 6.30 (H-5a, 1H, s), 6.34 (H-6b, 1H, dd,  $J = 8.4, 1.6$  Hz), 6.37 (H-5b, 1H, d,  $J = 8.4$  Hz), 6.48 (H-2b, 1H, d,  $J = 1.6$  Hz), 6.73 (H-11b, 1H, dd,  $J = 7.6, 1.6$  Hz), 6.91 (H-2a, 1H, s), 6.94 (H-13b, 1H, td,  $J = 7.6, 1.6$  Hz), 7.01 (H-11a, 1H, dd,  $J = 7.6, 1.6$  Hz), 7.04 (H-13a, 1H, td,  $J = 7.6, 1.6$  Hz), 7.11 (H-12b, 1H, td,  $J = 7.6, 1.6$  Hz), 7.20 (H-12a, 1H, td,  $J = 7.6, 1.6$  Hz), 7.29 (H-14a, 1H, dd,  $J = 7.6, 1.6$  Hz), 7.37 (H-14b, 1H, dd,  $J = 7.6, 1.6$  Hz), 7.58 (H-3a', H-5a', 2H, d,  $J = 8.8$  Hz), and 7.79 (H-2a', H-6a', 2H, d,  $J = 8.8$  Hz);  $^{13}C$  NMR ( $CDCl_3$ , 100 MHz)  $\delta$  30.2 (C-8a), 42.9 (C-8b), 55.6 (OMe,

3b), 55.76 (OMe, 4b), 55.82 (OMe, 4a), 56.0 (OMe, 3a), 56.2 (C-7b), 74.1 (C-7a), 110.6 (C-5b), 111.8 (C-2a), 112.0 (C-2b), 112.6 (C-5a), 117.1 (C-11b), 121.1 (C-6b, C-13b), 122.1 (C-11a), 125.4 (C-9b), 126.6 (C-13a), 127.87 (C-1a'), 127.95 (C-12a), 128.4 (C-12b), 128.59 (C-14a), 128.64 (C-6a), 128.9 (C-1a), 129.0 (C-4a'), 129.5 (C-14b), 131.4 (C-2a', C-6a'), 131.9 (C-3a', C-5a'), 133.5 (C-9a), 136.4 (C-1b), 147.5 (C-4b), 148.2 (C-3a), 148.8 (C-3b), 149.2 (C-10a), 149.6 (C-4a), 152.0 (C-10b), and 164.3 (C-15a); HRMS (DART-TOF) m/z:  $[M + H]^+$  Calcd for  $C_{39}H_{34}BrO_7$ , 693.1488; Found 693.1463.

**Removal of *N*-acetyl protecting group.** A solution of the *N*-acetyl derivative (0.01 mmol) in a mixture of MeOH (1.6 mL), H<sub>2</sub>O (0.2 mL), and conc. HCl (0.1 mL) was refluxed with TLC monitoring. Upon completion, the reaction mixture was diluted with water and K<sub>2</sub>CO<sub>3</sub> was added to neutralize the solution. The reaction mixture was then extracted with EtOAc and the combined organic layer was then washed with H<sub>2</sub>O, dried (Na<sub>2</sub>SO<sub>4</sub>) and concentrated under reduced pressure. The resulting residue was then fractionated by preparative radial chromatography to yield the corresponding deprotected compound.

**Removal of *N*-CO<sub>2</sub>Me protecting group.** To a solution of the carbamate derivative (0.01 mmol) in a mixture MeOH (2 mL) and THF (1 mL) was added 5N NaOH (0.5 mmol, 50 equivs) at room temperature. The reaction mixture was refluxed with TLC monitoring. Upon completion, the reaction mixture was extracted with CH<sub>2</sub>Cl<sub>2</sub> and the combined organic layer was then washed with H<sub>2</sub>O, dried (Na<sub>2</sub>SO<sub>4</sub>) and concentrated under reduced pressure. The resulting residue was then fractionated by preparative radial chromatography to yield the corresponding deprotected compound.

**Removal of *N*-tosyl protecting group.** To a solution of the *N*-tosyl derivative (0.01 mmol) in toluene (2 mL) was added sodium bis(2-methoxyethoxy)aluminium dihydride (8  $\mu$ L, 0.04 mmol) in toluene (1 mL) at room temperature. The reaction mixture was refluxed with TLC monitoring. Upon completion, the reaction mixture was quenched with 5% HCl (1 mL) and stirred for 1 h at room temperature. After filtration through Celite, the filtrate was extracted three times with 5% HCl. The combined aqueous layer was basified with Na<sub>2</sub>CO<sub>3</sub> and was extracted with EtOAc, dried (Na<sub>2</sub>SO<sub>4</sub>) and concentrated under reduced pressure. The resulting residue was then fractionated by preparative radial chromatography to yield the corresponding deprotected compound.

**Removal of *N*-nosyl protecting group.** To a suspension of the *N*-nosyl derivative (0.01 mmol) and K<sub>2</sub>CO<sub>3</sub> (4.1 mg, 0.03 mmol) in DMF, was added PhSH (2  $\mu$ L, 0.02 mmol) at room temperature. The mixture was stirred at room temperature with TLC monitoring. Upon completion, the reaction mixture was extracted with EtOAc and the combined organic layer was then washed with H<sub>2</sub>O, dried (Na<sub>2</sub>SO<sub>4</sub>) and concentrated under reduced pressure. The resulting residue was then fractionated by preparative radial chromatography to yield the corresponding deprotected compound. (Removal of the *N*-nosyl groups from the bridged azocine **15af** was partially successful with removal of one of the nosyl groups, giving azocine **108**. Attempted removal of the remaining nosyl group in **108** led to decomposition of the compound.)

*Bisindole (107)*. Light yellowish solid;  $^1\text{H}$  NMR ( $\text{CDCl}_3$ , 400 MHz)  $\delta$  3.74 (2H, d,  $J = 6.8$  Hz), 3.80 (6H, s), 4.67 (2H, d,  $J = 6.8$  Hz), 6.65 (4H, m), 6.70 (2H, d,  $J = 7.6$  Hz), 6.83 (4H, d,  $J = 8.8$  Hz), 7.08 (2H, t,  $J = 7.6$  Hz), and 7.17 (4H, d,  $J = 8.8$  Hz);  $^{13}\text{C}\{^1\text{H}\}$  NMR ( $\text{CDCl}_3$ , 100 MHz)  $\delta$  54.1, 55.3, 65.1, 108.7, 113.9, 118.7, 124.8, 127.4, 128.0, 129.0, 136.9, 151.1, and 159.0; HRMS (DART-TOF)  $m/z$ :  $[\text{M} + \text{H}]^+$  Calcd for  $\text{C}_{30}\text{H}_{29}\text{N}_2\text{O}_2$ , 449.2229; Found 449.2233  $[\text{M} + \text{H}]^+$ .

*Bridged azocine (108)*. Light yellowish solid;  $^1\text{H}$  NMR ( $\text{CDCl}_3$ , 600 MHz)  $\delta$  3.24 (1H, br s), 3.69 (3H, s), 3.85 (3H, s), 3.87 (3H, s), 3.96 (3H, s), 4.20 (1H, br d,  $J = 1.6$  Hz), 4.47 (1H, br s), 4.64 (1H, br s), 6.42 (1H, s), 6.46 (1H, d,  $J = 7.6$  Hz), 6.70 (1H, d,  $J = 1.9$  Hz), 6.73 (1H, dd,  $J = 8.2, 1.9$  Hz), 6.74 (1H, d,  $J = 7.4$  Hz), 6.78 (1H, s), 6.83 (1H, t,  $J = 7.4$  Hz), 6.86 (1H, d,  $J = 8.2$  Hz), 6.95 (1H, t,  $J = 7.6$  Hz), 7.02 (3H, m), 7.15 (1H, br s), 7.41 (1H, d,  $J = 7.6$  Hz), 7.62 (1H, td,  $J = 7.8, 1.0$  Hz), 7.73 (1H, td,  $J = 7.8, 1.0$  Hz), 7.83 (1H, dd,  $J = 7.8, 1.0$  Hz), and 7.89 (1H, dd,  $J = 7.8, 1.0$  Hz);  $^{13}\text{C}\{^1\text{H}\}$  NMR ( $\text{CDCl}_3$ , 150 MHz)  $\delta$  30.9, 44.8, 52.8, 55.8, 55.9, 56.0, 57.8, 110.6, 111.3, 112.4, 113.1, 115.6, 118.7, 121.5, 125.4, 125.67, 125.70, 127.0, 127.48, 127.54, 128.1, 129.1, 129.4, 131.8, 132.7, 133.1, 133.4, 133.6, 133.8, 137.5, 140.4, 142.3, 147.6, 148.1, 148.2, 148.6, and 148.9; HRMS (DART-TOF)  $m/z$ :  $[\text{M} + \text{H}]^+$  Calcd for  $\text{C}_{38}\text{H}_{36}\text{N}_3\text{O}_8\text{S}$ , 694.2223; Found 694.2233.

## REFERENCES

- (1) Yan, M., Kawamata, Y., & Baran, P. S. (2018). Synthetic organic electrochemistry: Calling all engineers. *Angewandte Chemie International Edition*, *57*, 4149–4155.
- (2) Moeller, K. D. (2000). Synthetic applications of anodic electrochemistry. *Tetrahedron*, *56*, 9527–9554.
- (3) Yoshida, J., Kataoka, K., Horcajada, R., & Nagaki, A. (2008). Modern strategies in electroorganic synthesis. *Chemical Reviews*, *108*, 2265–2299.
- (4) Yan, M., Kawamata, Y., & Baran, P. S. (2017). Synthetic organic electrochemical methods since 2000: On the verge of a renaissance. *Chemical Reviews*, *117*, 13230–13319.
- (5) Wiebe, A., Gieshoff, T., Möhle, S., Rodrigo, E., Zirbes, M., & Waldvogel, S. R. (2018). Electrifying organic synthesis. *Angewandte Chemie International Edition*, *57*, 5594–5619.
- (6) Horn, E. J., Rosen, B. R., & Baran, P. S. (2016). Synthetic organic electrochemistry: An enabling and innately sustainable method. *ACS Central Science*, *2*, 302–308.
- (7) Francke, R., & Little, R. D. (2014). Redox catalysis in organic electrosynthesis: Basic principles and recent developments. *Chemical Society Reviews*, *43*, 2492.
- (8) Möhle, S., Zirbes, M., Rodrigo, E., Gieshoff, T., Wiebe, A., & Waldvogel, S. R. (2018). Modern electrochemical aspects for the synthesis of value-added organic products. *Angewandte Chemie International Edition*, *57*, 6018–6041.
- (9) Lund, H. (2002). A century of organic electrochemistry. *Journal of The Electrochemical Society*, *149*, S21–S33.
- (10) Little, R. D., & Moeller, K. D. (2018). Introduction: Electrochemistry: Technology, synthesis, energy, and materials. *Chemical Reviews*, *118*, 4483–4484.
- (11) Horn, E. J., Rosen, B. R., Chen, Y., Tang, J., Chen, K., Eastgate, M. D., & Baran, P. S. (2016). Scalable and sustainable electrochemical allylic C–H oxidation. *Nature*, *533*, 77–81.

- (12) O'Brien, A. G., Maruyama, A., Inokuma, Y., Fujita, M., Baran, P. S., & Blackmond, D. G. (2014). Radical C–H functionalization of heteroarenes under electrochemical control. *Angewandte Chemie International Edition*, *53*, 11868–11871.
- (13) Merchant, R. R., Oberg, K. M., Lin, Y., Novak, A. J. E., Felding, J., & Baran, P. S. (2018). Divergent synthesis of pyrone diterpenes via radical cross coupling. *Journal of the American Chemical Society*, *140*, 7462–7465.
- (14) Xu, H. C., & Moeller, K. D. (2010). Intramolecular anodic olefin coupling reactions and the synthesis of cyclic amines. *Journal of the American Chemical Society*, *132*, 2839–2844.
- (15) Lipp, A., Ferenc, D., Gütz, C., Geffe, M., Vierengel, N., Schollmeyer, D., ... Opatz, T. (2018). A regio- and diastereoselective anodic aryl-aryl coupling in the biomimetic total synthesis of (–)-thebaine. *Angewandte Chemie International Edition*, *57*, 11055–11059.
- (16) Li, L.-J., Jiang, Y.-Y., Lam, C. M., Zeng, C.-C., Hu, L.-M., & Little, R. D. (2015). Aromatic C–H bond functionalization induced by electrochemically in situ generated tris(*p*-bromophenyl)aminium radical cation: Cationic chain reactions of electron-rich aromatics with enamides. *The Journal of Organic Chemistry*, *80*, 11021–11030.
- (17) Lu, N., Zhang, N., Zeng, C.-C., Hu, L.-M., Yoo, S. J., & Little, R. D. (2015). Electrochemically induced ring-opening/friedel–crafts arylation of chalcone epoxides catalyzed by a triarylimidazole redox mediator. *The Journal of Organic Chemistry*, *80*, 781–789.
- (18) Kolbe, H. (1847). Beobachtungen über die oxydirende wirkung des sauerstoffs, wenn derselbe mit hülfe einer elektrischen säule entwickelt wird. *Journal Für Praktische Chemie*, *41*, 137–139.
- (19) Tafel, J., & Hahl, H. (1907). Vollständige reduktion des benzylacetessigesters. *Berichte Der Deutschen Chemischen Gesellschaft*, *40*, 3312–3318.
- (20) Simons, J. H. (1949). Production of fluorocarbons. *Journal of The Electrochemical Society*, *95*, 47–52.
- (21) Danly, D. E. (1984). Development and commercialization of the Monsanto electrochemical adiponitrile process. *Journal of The Electrochemical Society*, *131*, 435C–442C.
- (22) Frontana-Uribe, B. A., Little, R. D., Ibanez, J. G., Palma, A., & Vasquez-Medrano, R. (2010). Organic electrosynthesis: A promising green methodology in organic chemistry. *Green Chemistry*, *12*, 2099–2119.

- (23) Sperry, J. B., & Wright, D. L. (2006). The application of cathodic reductions and anodic oxidations in the synthesis of complex molecules. *Chemical Society Reviews*, 35, 605–621.
- (24) Schäfer, H. J. (1981). Anodic and cathodic CC-bond formation. *Angewandte Chemie International Edition in English*, 20, 911–934.
- (25) Seo, E. T., Nelson, R. F., Fritsch, J. M., Marcoux, L. S., Leedy, D. W., & Adams, R. N. (1966). Anodic oxidation pathways of aromatic amines. Electrochemical and electron paramagnetic resonance studies. *Journal of the American Chemical Society*, 88, 3498–3503.
- (26) Steckhan, E. (1987). Organic syntheses with electrochemically regenerable redox systems. *Topics in Current Chemistry*, 142, 1–69.
- (27) Schmittel, M., & Burghart, A. (1997). Understanding reactivity patterns of radical cations. *Angewandte Chemie International Edition in English*, 36, 2550–2589.
- (28) Hammerich, O., & Speiser, B. (Eds.). (2016). *Organic electrochemistry, fifth edition: Revised and expanded* (5th ed.). Boca Raton, FL: CRC Press.
- (29) Llorente, M. J., Nguyen, B. H., Kubiak, C. P., & Moeller, K. D. (2016). Paired electrolysis in the simultaneous production of synthetic intermediates and substrates. *Journal of the American Chemical Society*, 138, 15110–15113.
- (30) Waldvogel, S. R., Lips, S., Selt, M., Riehl, B., & Kampf, C. J. (2018). Electrochemical arylation reaction. *Chemical Reviews*, 118, 6706–6765.
- (31) Burgbacher, G., & Schäfer, H. J. (1979). Kinetics of the anodic dimerization of 4,4'-dimethoxystilbene by the rotating ring-disk electrode. *Journal of the American Chemical Society*, 101, 7590–7593.
- (32) Ebersson, L., & Parker, V. D. (1970). Anodic oxidation of aryl-olefins. II. Acetoxylation of anisylethylenes. *Acta Chemica Scandinavica*, 24, 3553–3562.
- (33) Halas, S. M., Okyne, K., & Fry, A. J. (2003). Anodic oxidation of stilbenes bearing electron-withdrawing ring substituents. *Electrochimica Acta*, 48, 1837–1844.
- (34) Parker, V. D., & Ebersson, L. (1969). Anode potential controlled mechanisms of oxidation of aryl olefins. *Journal of the Chemical Society D: Chemical Communications*, 340.
- (35) Steckhan, E. (1978). Spectroelectrochemical studies of olefins. 3. The dimerization mechanism of the 4,4'-dimethoxystilbene cation radical in the

- absence and presence of methanol. *Journal of the American Chemical Society*, *100*, 3526–3533.
- (36) Walsh, F. C., & Wills, R. G. A. (2010). The continuing development of Magnéli phase titanium sub-oxides and Ebonex® electrodes. *Electrochimica Acta*, *55*, 6342–6351.
- (37) Trasatti, S. (2000). Electrocatalysis: Understanding the success of DSA®. *Electrochimica Acta*, *45*, 2377–2385.
- (38) Waldvogel, S. R., Mentizi, S., & Kirste, A. (2012). Boron-doped diamond electrodes for electroorganic chemistry. *Topics in Current Chemistry*, *320*, 1–32.
- (39) Lund, H., & Hammerich, O. (Eds.). (2001). *Organic electrochemistry, fourth edition: Revised and expanded* (4th ed.). New York: Marcel Dekker, Inc.
- (40) Corey, E. J., & Sauers, R. R. (1959). The synthesis of pentacyclosqualene (8,8'-cycloöncerene) and the  $\alpha$ - and  $\beta$ -onoceradienes 1. *Journal of the American Chemical Society*, *81*, 1739–1743.
- (41) Matzeit, A., Schäfer, H. J., & Amatore, C. (1995). Radical tandem cyclizations by anodic decarboxylation of carboxylic acids. *Synthesis*, *1995*, 1432–1444.
- (42) Brecht-Forster, A., Fitremann, J., & Renaud, P. (2002). Synthesis of ( $\pm$ )-nephromopsinic, (-)-phaseolinic, and (-)-dihydropertusaric acids. *Helvetica Chimica Acta*, *85*, 3965–3974.
- (43) Le Blanc, M. (1900). Über einen versuch zur demonstration des elektrolytischen lösungsdruckes. *Zeitschrift Für Elektrotechnik Und Elektrochemie*, *7*, 287–290.
- (44) Semmelhack, M. F., Chou, C. S., & Cortes, D. A. (1983). Nitroxyl-mediated electrooxidation of alcohols to aldehydes and ketones. *Journal of the American Chemical Society*, *105*, 4492–4494.
- (45) Steckhan, E. (1986). Indirect electroorganic syntheses—A modern chapter of organic electrochemistry. *Angewandte Chemie International Edition in English*, *25*, 683–701.
- (46) Park, Y. S., & Little, R. D. (2008). Redox electron-transfer reactions: electrochemically mediated rearrangement, mechanism, and a total synthesis of daucene. *The Journal of Organic Chemistry*, *73*, 6807–6815.
- (47) Shono, T., Hamaguchi, H., & Matsumura, Y. (1975). Electroorganic chemistry. XX. Anodic oxidation of carbamates. *Journal of the American Chemical Society*, *97*, 4264–4268.

- (48) Shono, Tatsuya. (1984). Electroorganic chemistry in organic synthesis. *Tetrahedron*, 40, 811–850.
- (49) Libendi, S. S., Demizu, Y., Matsumura, Y., & Onomura, O. (2008). High regioselectivity in electrochemical  $\alpha$ -methoxylation of *N*-protected cyclic amines. *Tetrahedron*, 64, 3935–3942.
- (50) Onomura, O. (2012). Anodic selective functionalization of cyclic amine derivatives. *Heterocycles*, 85, 2111–2133.
- (51) Yoshida, J., Murata, T., & Isoe, S. (1986). Electrochemical oxidation of organosilicon compounds I. Oxidative cleavage of carbon-silicon bond in allylsilanes and benzylsilanes. *Tetrahedron Letters*, 27, 3373–3376.
- (52) Suga, S., Nagaki, A., Tsutsui, Y., & Yoshida, J. (2003). “*N*-acyliminium ion pool” as a heterodiene in [4 + 2] cycloaddition reaction. *Organic Letters*, 5, 945–947.
- (53) Suga, S., Nishida, T., Yamada, D., Nagaki, A., & Yoshida, J. (2004). Three-component coupling based on the “cation pool” method. *Journal of the American Chemical Society*, 126, 14338–14339.
- (54) Suga, S., Okajima, M., & Yoshida, J. (2001). Reaction of an electrogenerated ‘iminium cation pool’ with organometallic reagents. direct oxidative  $\alpha$ -alkylation and -arylation of amine derivatives. *Tetrahedron Letters*, 42, 2173–2176.
- (55) Suga, S., Tsutsui, Y., Nagaki, A., & Yoshida, J. (2005). Cycloaddition of “*N*-acyliminium ion pools” with carbon–carbon multiple bonds. *Bulletin of the Chemical Society of Japan*, 78, 1206–1217.
- (56) Suga, S., Yamada, D., & Yoshida, J. (2010). Cationic three-component coupling involving an optically active enamine derivative. From time integration to space integration of reactions. *Chemistry Letters*, 39, 404–406.
- (57) Yoshida, J., Suga, S., Suzuki, S., Kinomura, N., Yamamoto, A., & Fujiwara, K. (1999). Direct oxidative carbon–carbon bond formation using the “cation pool” method. 1. Generation of iminium cation pools and their reaction with carbon nucleophiles. *Journal of the American Chemical Society*, 121, 9546–9549.
- (58) Suga, S., Suzuki, S., Yamamoto, A., & Yoshida, J. (2000). Electrooxidative generation and accumulation of alkoxy-carbenium ions and their reactions with carbon nucleophiles. *Journal of the American Chemical Society*, 122, 10244–10245.

- (59) Nokami, T., Watanabe, T., Musya, N., Morofuji, T., Tahara, K., Tobe, Y., & Yoshida, J. (2011). Direct dendronization of polystyrenes using dendritic diarylcarbenium ion pools. *Chemical Communications*, 47, 5575–5577.
- (60) Okajima, M., Soga, K., Watanabe, T., Terao, K., Nokami, T., Suga, S., & Yoshida, J. (2009). Generation of diarylcarbenium ion pools via electrochemical C–H bond dissociation. *Bulletin of the Chemical Society of Japan*, 82, 594–599.
- (61) Okajima, M., Soga, K., Nokami, T., Suga, S., & Yoshida, J. (2006). Oxidative generation of diarylcarbenium ion pools. *Organic Letters*, 8, 5005–5007.
- (62) Terao, K., Watanabe, T., Suehiro, T., Nokami, T., & Yoshida, J. (2010). A new highly sterically demanding silyl (TEDAMS) group. Synthesis by multiple substitution of tris(diphenylmethyl)silane with diarylcarbenium ions. *Tetrahedron Letters*, 51, 4107–4109.
- (63) Nokami, T., Soma, R., Yamamoto, Y., Kamei, T., Itami, K., & Yoshida, J.-I. (2007). Generation of pyridyl coordinated organosilicon cation pool by oxidative Si–Si bond dissociation. *Beilstein Journal of Organic Chemistry*, 3, 1–5.
- (64) Kataoka, K., Hagiwara, Y., Midorikawa, K., Suga, S., & Yoshida, J. (2008). Practical electrochemical iodination of aromatic compounds. *Organic Process Research & Development*, 12, 1130–1136.
- (65) Midorikawa, K., Suga, S., & Yoshida, J. (2006). Selective monoiodination of aromatic compounds with electrochemically generated  $I^+$  using micromixing. *Chemical Communications*, 2006, 3794–3796.
- (66) Ashikari, Y., Nokami, T., & Yoshida, J. (2011). Integrated electrochemical–chemical oxidation mediated by alkoxyulfonium ions. *Journal of the American Chemical Society*, 133, 11840–11843.
- (67) Ashikari, Y., Shimizu, A., Nokami, T., & Yoshida, J. (2013). Halogen and chalcogen cation pools stabilized by DMSO. Versatile reagents for alkene difunctionalization. *Journal of the American Chemical Society*, 135, 16070–16073.
- (68) Nokami, T., Shibuya, A., Tsuyama, H., Suga, S., Bowers, A. A., Crich, D., & Yoshida, J. (2007). Electrochemical generation of glycosyl triflate pools. *Journal of the American Chemical Society*, 129, 10922–10928.
- (69) Saito, K., Saigusa, Y., Nokami, T., & Yoshida, J. (2011). Electrochemically generated  $ArS(ArSSAr)^+B(C_6F_5)_4^-$  as an activator of thioglycosides for glycosylation. *Chemistry Letters*, 40, 678–679.

- (70) Suzuki, S., Matsumoto, K., Kawamura, K., Suga, S., & Yoshida, J. (2004). Generation of alkoxy-carbenium ion pools from thioacetals and applications to glycosylation chemistry. *Organic Letters*, 6, 3755–3758.
- (71) Yoshida, J., & Suga, S. (2002). Basic concepts of “cation pool” and “cation flow” methods and their applications in conventional and combinatorial organic synthesis. *Chemistry - A European Journal*, 8, 2650–2658.
- (72) Moeller, K. D. (2009). Intramolecular anodic olefin coupling reactions: Using radical cation intermediates to trigger new umpolung reactions. *Synlett*, 8, 1208–1218.
- (73) Sutterer, A., & Moeller, K. D. (2000). Reversing the polarity of enol ethers: An anodic route to tetrahydrofuran and tetrahydropyran rings. *Journal of the American Chemical Society*, 122, 5636–5637.
- (74) Wu, H., & Moeller, K. D. (2007). Anodic coupling reactions: A sequential cyclization route to the arteannuin ring skeleton. *Organic Letters*, 9, 4599–4602.
- (75) Duan, S., & Moeller, K. D. (2001). Anodic coupling reactions: Probing the stereochemistry of tetrahydrofuran formation. A short, convenient synthesis of linalool oxide. *Organic Letters*, 3, 2685–2688.
- (76) Liu, B., Duan, S., Sutterer, A. C., & Moeller, K. D. (2002). Oxidative cyclization based on reversing the polarity of enol ethers and ketene dithioacetals. Construction of a tetrahydrofuran ring and application to the synthesis of (+)-nemorensic acid. *Journal of the American Chemical Society*, 124, 10101–10111.
- (77) Mihelcic, J., & Moeller, K. D. (2004). Oxidative cyclizations: The asymmetric synthesis of (–)-alliacol A. *Journal of the American Chemical Society*, 126, 9106–9111.
- (78) Liu, B., & Moeller, K. D. (2001). Anodic oxidation reactions: the total synthesis of (+)-nemorensic acid. *Tetrahedron Letters*, 42, 7163–7165.
- (79) Xu, H.-C., Brandt, J. D., & Moeller, K. D. (2008). Anodic cyclization reactions and the synthesis of (–)-crobarbatic acid. *Tetrahedron Letters*, 49, 3868–3871.
- (80) Hughes, C. C., Miller, A. K., & Trauner, D. (2005). An electrochemical approach to the guanacastepenes. *Organic Letters*, 7, 3425–3428.
- (81) Miller, A. K., Hughes, C. C., Kennedy-Smith, J. J., Gradl, S. N., & Trauner, D. (2006). Total synthesis of (–)-heptemerone B and (–)-guanacastepene E. *Journal of the American Chemical Society*, 128, 17057–17062.

- (82) Sperry, J. B., & Wright, D. L. (2005). Synthesis of the hamigeran skeleton through an electro-oxidative coupling reaction. *Tetrahedron Letters*, *46*, 411–414.
- (83) Wright, D. L., Whitehead, C. R., Sessions, E. H., Ghiviriga, I., & Frey, D. A. (1999). Studies on inducers of nerve growth factor: Synthesis of the cyathin core. *Organic Letters*, *1*, 1535–1538.
- (84) Rosen, B. R., Werner, E. W., O'Brien, A. G., & Baran, P. S. (2014). Total synthesis of dixiamycin B by electrochemical oxidation. *Journal of the American Chemical Society*, *136*, 5571–5574.
- (85) Hong, F. J., Low, Y. Y., Chong, K. W., Thomas, N. F., & Kam, T. S. (2014). Biomimetic oxidative dimerization of anodically generated stilbene radical cations: Effect of aromatic substitution on product distribution and reaction pathways. *Journal of Organic Chemistry*, *79*, 4528–4543.
- (86) Ziegler, C. B., & Heck, R. F. (1978). Palladium-catalyzed vinylic substitution with highly activated aryl halides. *The Journal of Organic Chemistry*, *43*, 2941–2946.
- (87) Littke, A. F., & Fu, G. C. (2001). A versatile catalyst for heck reactions of aryl chlorides and aryl bromides under mild conditions. *Journal of the American Chemical Society*, *123*, 6989–7000.
- (88) Hills, I. D., & Fu, G. C. (2004). Elucidating reactivity differences in palladium-catalyzed coupling processes: The chemistry of palladium hydrides. *Journal of the American Chemical Society*, *126*, 13178–13179.
- (89) Pagar, V. V., Tseng, C.-C., & Liu, R.-S. (2014). Gold-catalyzed oxa-povarov reactions for the synthesis of highly substituted dihydrobenzopyrans from diaryloxymethylarenes and olefins. *Chemistry - A European Journal*, *20*, 10519–10526.
- (90) Juhász, L., Szilágyi, L., Antus, S., Visy, J., Zsila, F., & Simonyi, M. (2002). New insight into the mechanism of hypervalent iodine oxidation of flavanones. *Tetrahedron*, *58*, 4261–4265.
- (91) Lim, K. H., Low, Y. Y., Tan, G. H., Kam, T. S., & Lim, T. M. (2008). Kopsine and danuphylline alkaloids from *Kopsia*. Biomimetic partial synthesis of danuphylline B. *Helvetica Chimica Acta*, *91*, 1559–1566.
- (92) Kam, T.-S., Lim, T.-M., & Tan, G.-H. (2001). Electrochemical oxidation of aspidofractinine-type alkaloids: Formation of kopsine, kopsidine, kopsinitarine and bisindole derivatives. *Journal of the Chemical Society, Perkin Transactions I*, 1594–1604.

- (93) Kam, T. S., Lim, T. M., & Choo, Y. M. (1999). Structure and biomimetic, electrochemically-mediated semisynthesis of the novel pentacyclic indole danuphylline. *Tetrahedron*, *55*, 1457–1468.
- (94) Tan, G. H., Lim, T. M., & Kam, T. S. (1995). Electrochemical Oxidation of Aspidofractinine-Type Indole Alkaloids. A facile, electrochemically-mediated conversion of kopsingine to kopsidines A, B, C, and kopsinganol. *Tetrahedron Letters*, *36*, 1327–1330.
- (95) Kam, T.-S., Lim, T.-M., & Tan, G.-H. (1999). Unprecedented cyanation and cyanomethylation following ring closure versus dimer formation during anodic oxidation of the aspidofractinine alkaloid kopsamine. *Heterocycles*, *51*, 249–253.
- (96) Thomas, N. F., Velu, S. S., Weber, J. F. F., Lee, K. C., Hadi, A. H. A., Richomme, P., ... Awang, K. (2004). A tandem highly stereoselective FeCl<sub>3</sub>-promoted synthesis of a bisindoline: synthetic utility of radical cations in heterocyclic construction. *Tetrahedron*, *60*, 11733–11742.
- (97) Smith, C. D., Gavriilyuk, J. I., Lough, A. J., & Batey, R. A. (2010). Lewis acid catalyzed three-component hetero-diels-alder (Povarov) reaction of *N*-arylimines with strained norbornene-derived dienophiles. *Journal of Organic Chemistry*, *75*, 702–715.
- (98) Snyder, S. A., Zografos, A. L., & Lin, Y. (2007). Total synthesis of resveratrol-based natural products: A chemoselective solution. *Angewandte Chemie International Edition*, *46*, 8186–8191.
- (99) Chong, K. W., Hong, F. J., Thomas, N. F., Low, Y. Y., & Kam, T. S. (2017). Electrochemically mediated oxidative transformations of substituted 4-methoxystilbenes: Effect of ortho-substituted nucleophilic groups. *The Journal of Organic Chemistry*, *82*, 6172–6191.
- (100) Galli, C., Illuminati, G., Mandolini, L., & Tamborra, P. (1977). Ring-closure reactions. 7. Kinetics and activation parameters of lactone formation in the range of 3- to 23-membered rings. *Journal of the American Chemical Society*, *99*, 2591–2597.
- (101) Illuminati, G., & Mandolini, L. (1981). Ring closure reactions of bifunctional chain molecules. *Accounts of Chemical Research*, *14*, 95–102.
- (102) Casadei, M. A., Galli, C., & Mandolini, L. (1984). Ring-closure reactions. 22. Kinetics of cyclization of diethyl ( $\omega$ -bromoalkyl)malonates in the range of 4- to 21-membered rings. Role of ring strain. *Journal of the American Chemical Society*, *106*, 1051–1056.

- (103) Martí-Centelles, V., Pandey, M. D., Burguete, M. I., & Luis, S. V. (2015). Macrocyclization reactions: The importance of conformational, configurational, and template-induced preorganization. *Chemical Reviews*, *115*, 8736–8834.
- (104) Barnes, E. C., Jumpathong, J., Lumyong, S., Voigt, K., & Hertweck, C. (2016). Daldionin, an unprecedented binaphthyl derivative, and diverse polyketide congeners from a fungal orchid endophyte. *Chemistry - A European Journal*, *22*, 4551–4555.
- (105) Chen, H. D., Ding, Y. Q., Yang, S. P., Li, X. C., Wang, X. J., Zhang, H. Y., ... Yue, J. M. (2012). Morusalbanol A, a neuro-protective diels-alder adduct with an unprecedented architecture from *Morus alba*. *Tetrahedron*, *68*, 6054–6058.
- (106) Yao, H., Song, L., Liu, Y., & Tong, R. (2014). Cascade michael addition/cycloketalization of cyclic 1,3-dicarbonyl compounds: Important role of the tethered alcohol of  $\alpha,\beta$ -unsaturated carbonyl compounds on reaction rate and regioselectivity. *The Journal of Organic Chemistry*, *79*, 8774–8785.
- (107) Tedesco, R., Youngman, M. K., Wilson, S. R., & Katzenellenbogen, J. A. (2001). Synthesis and evaluation of hexahydrochrysene and tetrahydrobenzofluorene ligands for the estrogen receptor. *Bioorganic & Medicinal Chemistry Letters*, *11*, 1281–1284.
- (108) Fukai, M., Tsukada, M., Miki, K., Suzuki, T., Sugita, T., Kinoshita, K., ... Koyama, K. (2012). Hypoxylonols C–F, benzo[j]fluoranthenes from *Hypoxylon truncatum*. *Journal of Natural Products*, *75*, 22–25.
- (109) Park, J. E., Cuong, T. D., Hung, T. M., Lee, I., Na, M., Kim, J. C., ... Min, B. S. (2011). Alkaloids from *Chelidonium majus* and their inhibitory effects on LPS-induced NO production in RAW264.7 cells. *Bioorganic & Medicinal Chemistry Letters*, *21*(23), 6960–6963.
- (110) aynes, R. K., Ho, W.-Y., Chan, H.-W., Fugmann, B., Stetter, J., Croft, S. L., ... Robinson, B. L. (2004). Highly antimalaria-active artemisinin derivatives: Biological activity does not correlate with chemical reactivity. *Angewandte Chemie International Edition*, *43*, 1381–1385.
- (111) Yu, S. Y., Zhang, H., Gao, Y., Mo, L., Wang, S., & Yao, Z. J. (2013). Asymmetric cascade annulation based on enantioselective oxa-diels-alder cycloaddition of in situ generated isochromenyliums by cooperative binary catalysis of Pd(OAc)<sub>2</sub> and (*S*)-trip. *Journal of the American Chemical Society*, *135*, 11402–11407.

- (112) Williams, D. E., Bottriell, H., Davies, J., Tietjen, I., Brockman, M. A., & Andersen, R. J. (2015). Unciaphenol, an Oxygenated Analogue of the Bergman cyclization product of uncialamycin exhibits anti-HIV activity. *Organic Letters*, *17*, 5304–5307.
- (113) Yang, X. W., Li, S. M., Feng, L., Shen, Y. H., Tian, J. M., Zeng, H. W., ... Zhang, W. D. (2008). Abiesanol A, a novel biflavanol with unique six connective hexacyclic rings isolated from *Abies georgei*. *Tetrahedron Letters*, *49*, 3042–3044.
- (114) Yang, G.-Y., Miao, M.-M., Wang, Y., Liu, C.-B., Shen, Q.-P., Zhang, F.-M., ... Yang, X.-D. (2015). Flavonoids from the leaves of sun cured tobacco and their anti-tobacco mosaic virus activity. *Heterocycles*, *91*, 1198–1203.
- (115) Li, W., Li, S., Higai, K., Sasaki, T., Asada, Y., Ohshima, S., & Koike, K. (2013). Evaluation of licorice flavonoids as protein tyrosine phosphatase 1B inhibitors. *Bioorganic and Medicinal Chemistry Letters*, *23*, 5836–5839.
- (116) Lankri, D., Mostinski, Y., & Tselikhovsky, D. (2017). Palladium-catalyzed cascade assembly of tricyclic spiroethers from diene-alcohol precursors. *The Journal of Organic Chemistry*, *82*, 9452–9463.
- (117) Obata, T., Suzuki, S., Nakagawa, A., Kajihara, R., Noguchi, K., & Saito, A. (2016). Gold-catalyzed domino synthesis of functionalized benzofurans and tetracyclic isochromans via formal carboalkoxylation. *Organic Letters*, *18*, 4136–4139.
- (118) Chen, G.-G., Wei, J.-Q., Yang, X., & Yao, Z.-J. (2016). Convenient one-step synthesis of benzo[*c*]phenanthridines by three-component reactions of isochromenylium tetrafluoroborates and stilbenes in acetonitrile. *Organic Letters*, *18*, 1502–1505.
- (119) Lion, C. J., Matthews, C. S., Stevens, M. F. G., & Westwell, A. D. (2005). Synthesis, antitumor evaluation, and apoptosis-inducing activity of hydroxylated (*E*)-stilbenes. *Journal of Medicinal Chemistry*, *48*, 1292–1295.
- (120) Nogami, K., & Kurosawa, K. (1974). The reactions of 2-hydroxystilbenes with lead tetraacetate and manganese acetate. *Bulletin of the Chemical Society of Japan*, *47*, 505–506.
- (121) Ortgies, S., & Breder, A. (2015). Selenium-catalyzed oxidative C(sp<sup>2</sup>)-H amination of alkenes exemplified in the expedient synthesis of (aza-)indoles. *Organic Letters*, *17*, 2748–2751.

- (122) Ahmad, K., Thomas, N. F., Mukhtar, M. R., Noorbacha, I., Faizal Weber, J.-F., Nafiah, M. A., ... Awang, K. (2009). A FeCl<sub>3</sub>-promoted highly atropodiastereoselective cascade reaction: synthetic utility of radical cations in indolostilbene construction. *Tetrahedron*, *65*, 1504–1516.
- (123) Jang, Y. H., & Youn, S. W. (2014). Metal-free C–H amination for indole synthesis. *Organic Letters*, *16*, 3720–3723.
- (124) Shahzad, S. A., & Wirth, T. (2009). Fast synthesis of benzofluorenes by selenium-mediated carbocyclizations. *Angewandte Chemie International Edition*, *48*, 2588–2591.
- (125) Shahzad, S. A., Vivant, C., & Wirth, T. (2010). Selenium-mediated synthesis of biaryls through rearrangement. *Organic Letters*, *12*, 1364–1367.
- (126) Mikstacka, R., Wierzchowski, M., Dutkiewicz, Z., Gielara-Korzańska, A., Korzański, A., Teubert, A., ... Baer-Dubowska, W. (2014). 3,4,2'-Trimethoxy-*trans*-stilbene – a potent CYP1B1 inhibitor. *MedChemComm*, *5*, 496–501.
- (127) Bryan, C. S., & Lautens, M. (2010). A tandem catalytic approach to methyleneindenes: mechanistic insights into *gem*-dibromoolefin reactivity<sup>†</sup>. *Organic Letters*, *12*, 2754–2757.
- (128) Remy, D. C., Van Saun, W. A., Engelhardt, E. L., Torchiana, M. Lou, & Stone, C. A. (1975). Antiarrhythmic agents. 2-, 3-, and 4-substituted benzylamines. *Journal of Medicinal Chemistry*, *18*, 142–148.

## LIST OF PUBLICATIONS AND PAPERS PRESENTED

### Publications:

- (1) **Chong, K. W.**, Thomas, N. F., Low, Y. Y., & Kam, T. S. (2018). Reactivity of anodically generated 4-methoxystilbene cation radicals: The influence of ortho-substituted hydroxymethyl, aminomethyl, and carboxylic acid groups. *The Journal of Organic Chemistry*, 83, 15087–15100.
- (2) **Chong, K. W.**, Hong, F. J., Thomas, N. F., Low, Y. Y., & Kam, T. S. (2017). Electrochemically mediated oxidative transformations of substituted 4-methoxystilbenes: Effect of ortho-substituted nucleophilic groups. *The Journal of Organic Chemistry*, 82, 6172–6191.
- (3) Hong, F. J., Low, Y. Y., **Chong, K. W.**, Thomas, N. F., & Kam, T. S. (2014). Biomimetic oxidative dimerization of anodically generated stilbene radical cations: Effect of aromatic substitution on product distribution and reaction pathways. *Journal of Organic Chemistry*, 79, 4528–4543.

### Conference:

- (1) **Chong, K. W.**, Hong, F. J., Low, Y. Y., & Kam, T. S. (2014). Oxidative coupling and cyclization reactions of electrochemically generated stilbene cation radicals. *International Conference on Chemistry and Environmental Science Research*, Parkroyal Penang Resort, Penang, Malaysia. (Poster award)

## APPENDIX

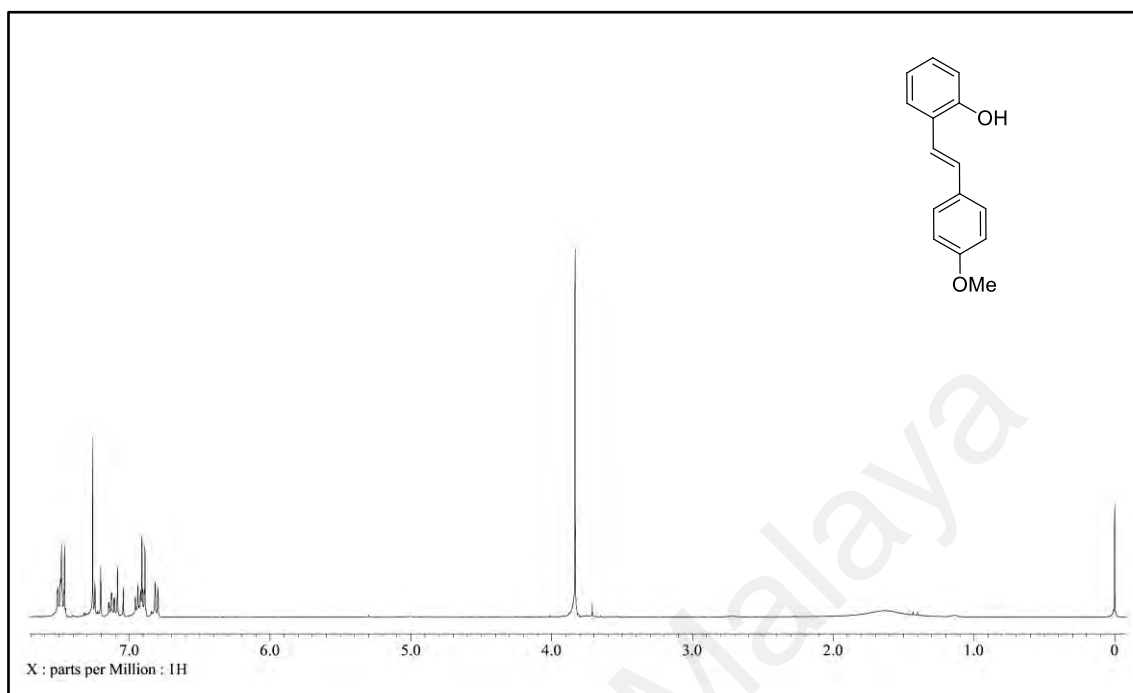


**Figure A1:**  $^1\text{H}$  NMR ( $\text{CDCl}_3$ , 400 MHz) spectrum of stilbene 1

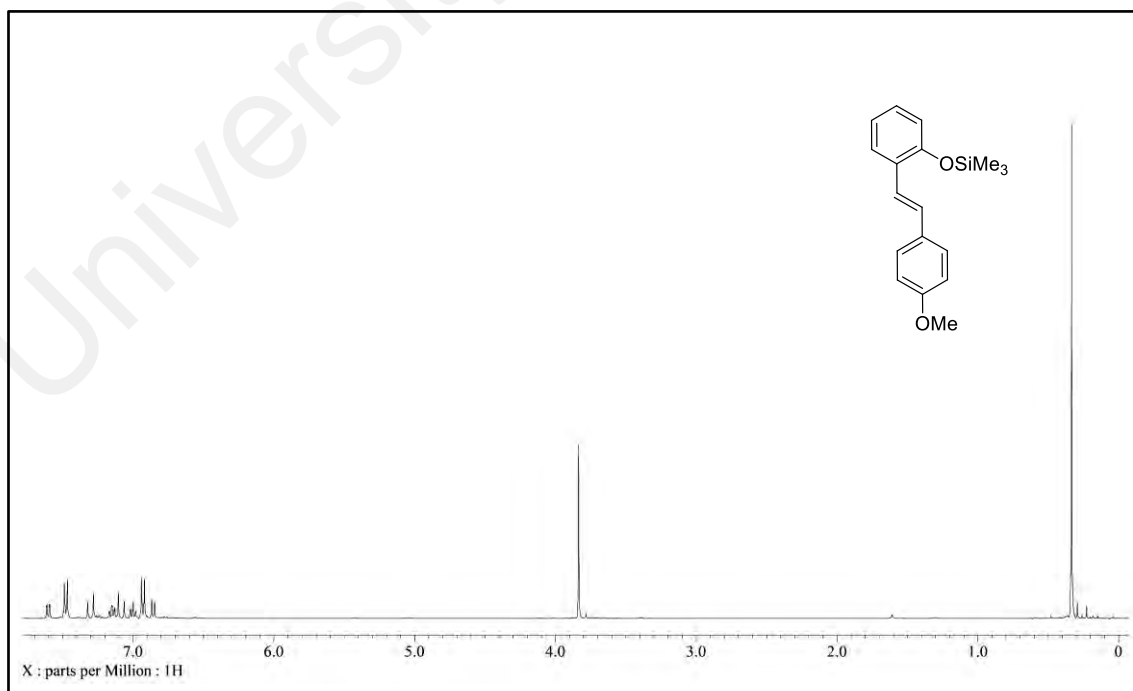


**Figure A2:**  $^1\text{H}$  NMR ( $\text{CDCl}_3$ , 400 MHz) spectrum of stilbene 2

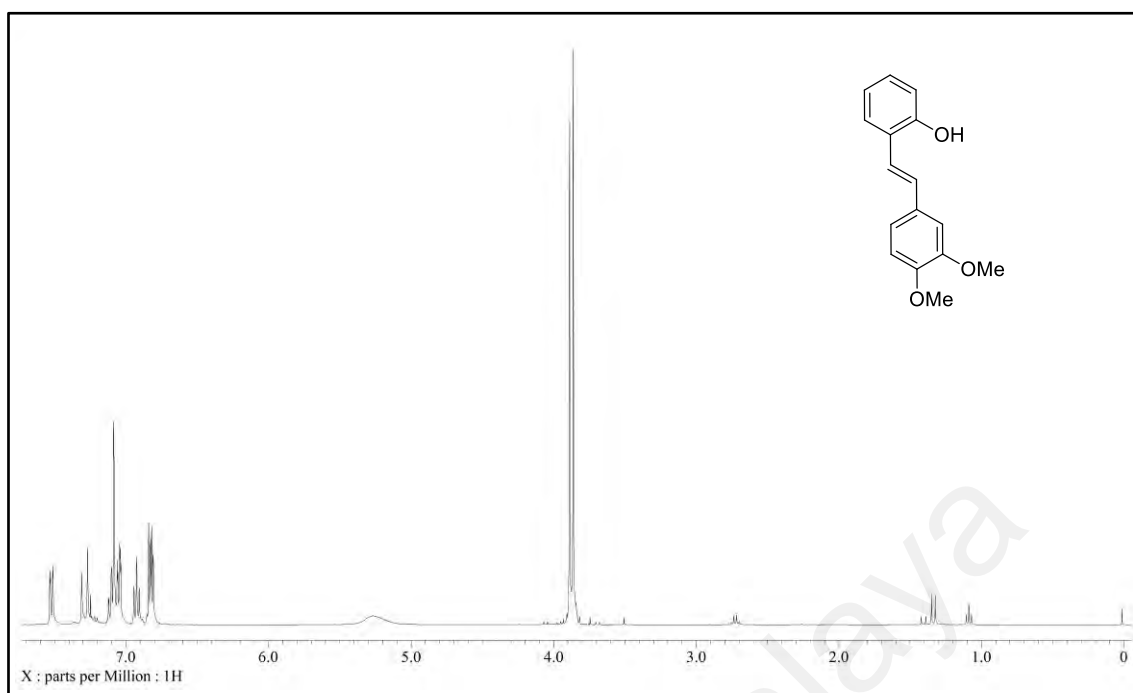


**Figure A3:** <sup>1</sup>H NMR (CDCl<sub>3</sub>, 400 MHz) spectrum of stilbene 3

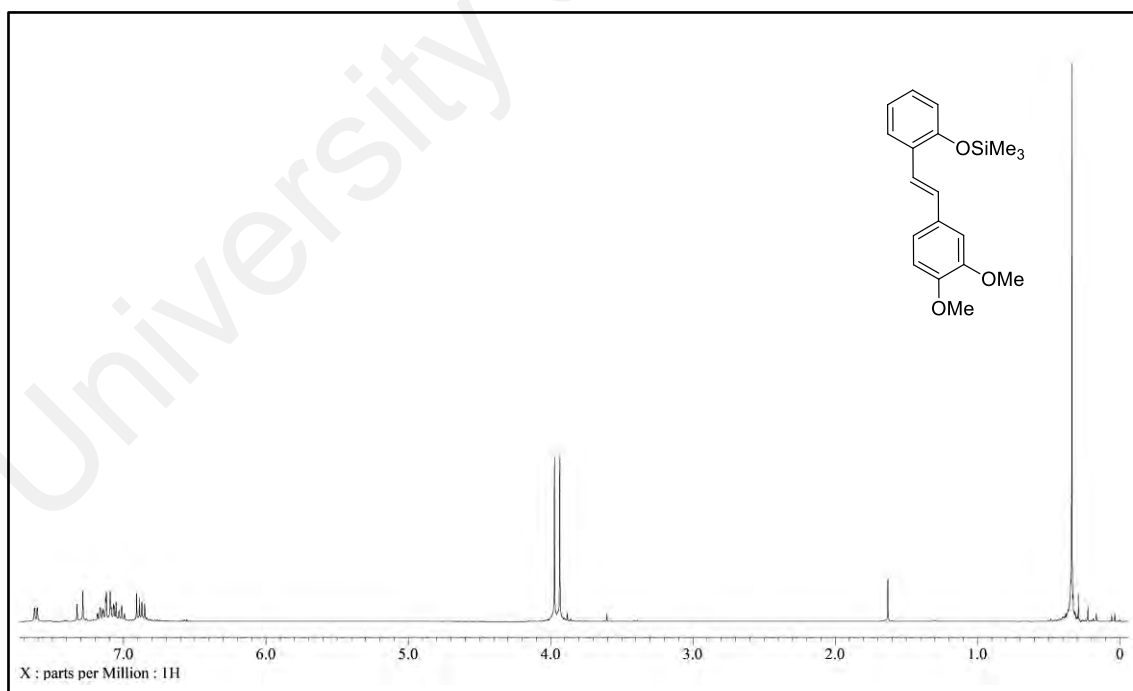


**Figure A4:** <sup>1</sup>H NMR (CDCl<sub>3</sub>, 400 MHz) spectrum of stilbene 4